



HAL
open science

Reconstruction of multi-phase fluid flow history and tectonic evolution in a Variscan granite (Velence Mts., Hungary)

Zsolt Benkó

► **To cite this version:**

Zsolt Benkó. Reconstruction of multi-phase fluid flow history and tectonic evolution in a Variscan granite (Velence Mts., Hungary). Earth Sciences. Université Henri Poincaré - Nancy 1, 2008. English. NNT : 2008NAN10116 . tel-01748468

HAL Id: tel-01748468

<https://hal.univ-lorraine.fr/tel-01748468>

Submitted on 29 Mar 2018

HAL is a multi-disciplinary open access archive for the deposit and dissemination of scientific research documents, whether they are published or not. The documents may come from teaching and research institutions in France or abroad, or from public or private research centers.

L'archive ouverte pluridisciplinaire **HAL**, est destinée au dépôt et à la diffusion de documents scientifiques de niveau recherche, publiés ou non, émanant des établissements d'enseignement et de recherche français ou étrangers, des laboratoires publics ou privés.



AVERTISSEMENT

Ce document est le fruit d'un long travail approuvé par le jury de soutenance et mis à disposition de l'ensemble de la communauté universitaire élargie.

Il est soumis à la propriété intellectuelle de l'auteur. Ceci implique une obligation de citation et de référencement lors de l'utilisation de ce document.

D'autre part, toute contrefaçon, plagiat, reproduction illicite encourt une poursuite pénale.

Contact : ddoc-theses-contact@univ-lorraine.fr

LIENS

Code de la Propriété Intellectuelle. articles L 122. 4

Code de la Propriété Intellectuelle. articles L 335.2- L 335.10

http://www.cfcopies.com/V2/leg/leg_droi.php

<http://www.culture.gouv.fr/culture/infos-pratiques/droits/protection.htm>



**RECONSTRUCTION OF MULTI-PHASE FLUID FLOW HISTORY AND
TECTONIC EVOLUTION IN A VARISCAN GRANITE INTRUSION
(VELENCE MTS., HUNGARY)**

Doctoral thesis

ZSOLT BENKÓ

Department of Mineralogy, Eötvös Loránd University, Budapest

PhD School in Earth Sciences

Head: Prof. Miklós Monostori

Geology-Geophysics PhD Programme

Head: Prof. Miklós Monostori

and

Université Henry Poincaré, Nancy 1, Faculté des Sciences & Techniques

U.F.R. Sciences & Techniques de la Matière et des Procédés

Ecole Doctorale RP2E

Département de Formation Doctorale Géosciences

Supervisors

Ferenc Molnár

Professor, Department of Mineralogy, ELTE University

Marc Lespinasse

Professor, Henri Poincaré University, Nancy 1

2008

CONTENTS

| | | |
|---------|------------------------------------------------------------------------------------------------------------------------------------------------------------------------------|----|
| 1. | INTRODUCTION | 4 |
| 2. | GEOLOGICAL SETTING OF THE VELENCE MOUNTAINS | 7 |
| 2.1 | REGIONAL GEOLOGY | 8 |
| 2.2 | MAJOR GEOLOGICAL FORMATIONS OF THE VELENCE MOUNTAINS | 11 |
| 2.2.1 | Variscan granite (Velence Granite Formation)..... | 11 |
| 2.2.2 | Early Palaeozoic Slate (Lovas Slate Formation) | 13 |
| 2.2.3 | Cretaceous igneous rocks (Budakeszi Picrite Formation) | 14 |
| 2.2.4 | Palaeogene igneous rocks (Nadap Andesite Formation) | 14 |
| 2.3 | GENERAL GEOLOGY OF THE SZABADBATTYÁN AREA | 15 |
| 2.4 | HYDROTHERMAL SYSTEMS IN THE VELENCE MTS..... | 16 |
| 2.4.1 | Mineralization of the granite and the shale..... | 18 |
| 2.4.2 | Hydrothermal processes related to the igneous activity of the Palaeogene age | 19 |
| 2.4.3 | Hydrothermal mineralization of Palaeogene age in the Variscan granite | 21 |
| 2.5 | HYDROTHERMAL MINERALIZATION OF THE SZABADBATTYÁN AREA | 22 |
| 3. | THEORETICAL BACKGROUND AND APPLIED METHODS | 23 |
| 3.1 | FLUID INCLUSION PLANES | 24 |
| 3.2 | FLUID INCLUSION STUDIES: PRINCIPLES AND METHODS..... | 28 |
| 3.3 | METHODS OF ANALYSIS OF HYDROTHERMAL VEIN NETWORKS, JOINTS, FRACTURES..... | 31 |
| 3.4 | FRACTAL ANALYSIS OF HYDROTHERMAL VEINS | 33 |
| 3.5 | CLAY MINERAL STUDIES: SAMPLE PREPARATION, METHODOLOGY | 35 |
| 3.6 | RADIATIVE AND STABLE ISOTOPE STUDIES | 37 |
| 4. | RESULTS | 39 |
| 4.1 | DELINEATION AND CHARACTERIZATION OF SUPERIMPOSING HYDROTHERMAL PROCESSES ON THE BASIS OF CLAY MINERALOGY IN THE ARGILLIC ALTERATION ZONES OF THE VELENCE GRANITE | 39 |
| 4.1.1 | The aim of the clay mineral studies and previous studies | 40 |
| 4.1.2 | Argillic alteration in and around the andesite dikes of Palaeogene age and hydrothermal breccias hosted by the granite around the quartz-barite hydrothermal veins .. | 41 |
| 4.1.3 | Argillic alteration around the quartz-fluorite-base metal veins and regional argillic alteration of granite | 44 |
| 4.1.4 | Temperature conditions during the formation of the clay mineral assemblages | 53 |
| 4.2 | AGE, ORIGIN AND TEMPERATURE OF HYDROTHERMAL FLUID FLOW EVENTS IN THE VELENCE MTS..... | 54 |
| | <i>K-Ar analyses</i> | 54 |
| 4.2.1 | K-Ar analyses | 56 |
| 4.2.1.1 | K-Ar ages for rock forming minerals | 56 |
| 4.2.1.2 | K-Ar ages measured on hydrothermal minerals | 63 |
| 4.2.1.3 | Interpretation of K-Ar radiometric age data from the aspect of the extent of superimposing hydrothermal events that affected the granite intrusion | 65 |
| 4.2.2 | Pb isotope studies: age and genetical relationships of the quartz-fluorite-base metal veins and their geotectonical connections..... | 66 |
| 4.2.3 | Sulphur isotope analysis: temperature estimation for the formation of the quartz- fluorite-base metal veins | 69 |
| 4.3 | FLUID INCLUSION STUDIES | 70 |

| | | |
|-------|------------------------------------------------------------------------------------------------------------------------------------|-----|
| 4.3.1 | Type I FIA: Carbonic-aqueous fluid inclusion assemblages trapped from an inhomogeneous fluid (Photoplate 1/A.) | 73 |
| 4.3.2 | Type II and Type III FIA: Aqueous fluid inclusion assemblages trapped from homogeneous parent fluid | 74 |
| 4.3.3 | Type IV FIA: Aqueous fluid inclusion assemblages, trapped from inhomogeneous fluid | 75 |
| 4.3.4 | Interpretation of the fluid inclusion analysis | 80 |
| 4.3.5 | Proving vertical movements in the granite by means of fluid inclusion studies ... | 84 |
| 4.4 | ANALYSIS OF THE STRUCTURAL ELEMENTS OF THE GRANITE AND THE ANDESITE DIKES.. | 86 |
| 4.4.1 | The Székesfehérvár area | 88 |
| 4.4.2 | Pákozd area | 89 |
| 4.4.3 | The Nadap-Sukoró area | 90 |
| 4.4.4 | The Nadap area | 92 |
| 4.4.5 | Palaeogene Volcanic Unit..... | 93 |
| 4.4.6 | Relationships between FIP orientations, fluid inclusion petrography and microthermometry | 94 |
| 4.5 | STATISTICAL ANALYSIS OF PALAEOGENE HYDROTHERMAL VEIN ARRAYS: FRACTAL ANALYSIS AND PERMEABILITY CALCULATION | 99 |
| 4.5.1 | Fractal analysis | 99 |
| 4.5.2 | Permeabilities calculated from the geometrical data of the veins | 101 |
| 4.6 | FIP STATISTICAL PARAMETERS: AVERAGE LENGTH, LENGTH DENSITY, NUMBER DENSITY | 102 |
| 4.6.1 | Iso-Fracture density map of the Nadap area and comparison of statistical parameters | 106 |
| 5. | DISCUSSION | 109 |
| 5.1 | VARISCAN TECTONISM AND ITS CONSEQUENCES ON THE FORMATION OF THE INITIAL FRACTURE SYSTEM OF THE GRANITE | 109 |
| 5.2 | REGIONAL TRIASSIC FLUID FLOW IN THE GRANITE: GENETIC MODEL AND STRUCTURAL CONTROL | 110 |
| 5.2.1 | Radiometric age constraints | 111 |
| 5.2.2 | Model for the Triassic fluid mobilization processes in the Velence Mts. | 113 |
| 5.2.3 | Geotectonical considerations | 114 |
| 5.2.4 | Structural control of the Triassic fluid flow: uplift of the granite and its effect on the fracture evolution on the granite | 117 |
| 5.3 | EVOLUTION OF THE FRACTURE SYSTEM OF THE GRANITE RELATED TO THE PALAEOGENE MAGMATIC-HYDROTHERMAL PROCESSES | 119 |
| 5.3.1 | Reopening of FIP in the illitic Palaeogene alteration zones and thermal propagation of the fracture network | 119 |
| 5.3.2 | Fracture formation and evolution: thermal reopening versus mechanical fracture formation | 121 |
| 5.4 | POST-PALAEOGENE STRUCTURAL EVENTS | 125 |
| 5.5 | STATISTICAL ANALYSIS OF THE FRACTURE SYSTEMS AT DIFFERENT SCALES: PRACTICAL APPLICABILITY | 126 |
| 6. | SUMMARY | 128 |
| 7. | ACKNOWLEDGEMENT | 132 |
| 8. | REFERENCES | 133 |

1. INTRODUCTION

INTRODUCTION

Les principaux chenaux favorisant les écoulements fluides de subsurface dans les roches cristallines sont les microfissures. Elles drainent les fluides durant les processus hydrothermaux et peuvent être des réservoirs non négligeables de CH ou eau. De ce fait, leur présence est problématique sur un site potentiel de stockage de substances radioactives ce qui rend nécessaire leur analyse ainsi que celle des fissures fossiles. Par le passé, les études étaient surtout focalisées sur les systèmes de veines ou fractures ouvertes, failles et diaclases.

Durant les 10 dernières années, d'avantage de travaux se sont focalisés sur les microfissures cicatrisées ou ouvertes car elles apparaissent comme étant les témoins des principales circulations de fluides à l'instar des fractures macroscopiques.

Dans les systèmes plutoniques et volcaniques altérés, la reconstruction des processus tectoniques et hydrothermaux associés est rendu difficile par le fait que les témoins sont souvent masqués par l'altération.

Une nouvelle approche a été développée durant ces dernières années; elle est basée sur l'utilisation des plans d'Inclusions Fluides. La formation des plans d'IF est contrôlée par les événements tectoniques ce qui permet d'obtenir des relations entre processus d'altération, porosité de microfissures et tenseur de contraintes.

Ce travail est focalisé sur la région des Monts Velence (partie Ouest du bassin des Carpates, Hongrie) qui ont un substratum composé de granites hercyniens et d'intrusions volcaniques andésitiques. Les circulations fluides hydrothermales y sont à l'origine d'une forte altération des granites et basaltes.

Les différentes phases d'altérations hydrothermales Hercyniennes et Alpines sont parfaitement distinguables (MOLNAR et al. 1995 ; MOLNAR 1996; 1997). Ce travail a pour objectif de caractériser les relations entre événements structuraux et processus hydrothermaux en utilisant la méthode des plans d'IF ; les données seront compilées pour en déduire la chronologie des événements hydrothermaux à différentes échelles.

Ces travaux ont été complétés par des études minéralogiques et isotopiques (K-Ar datations, Pb, S isotope).

L'ensemble des résultats a permis de reconstituer l'évolution des monts Velence.

Cette approche s'est révélée très pertinente et pourra être étendue à d'autres problèmes de géologie économique, d'hydrogéologie et environnementaux.

Principal flow channels of hydrothermal fluids and groundwaters in crystalline rocks are the microcracks (μm -mm scale) and fissures (cm-m scale). Subsurface fluids depending on their character can be interesting for the geologists from different aspects. Depletion of the classical sedimentary rock hosted hydrocarbon reservoirs has increasingly turned the attention to the exploitability of gas and oil reservoirs with primary fracture related porosity and permeability in crystalline rocks (GAUTHIER et al. 2000). In magmatic and metamorphic rocks, hydrothermal fluid flow is constrained by fissures and microfractures: importance of these features in formation of hydrothermal ore deposits is widely known (GILLESPIE et al. 1999, ESSARAJ et al. 2001, NEX et al. 2001, VALLANCE et al. 2001; BOIRON et al. 2003). In the last decades, planning and designation of nuclear waste deposits has also attracted specific attention. Impermeability, homogeneity or at least knowledge of hydraulic properties of the rock unit selected for storing the nuclear waste materials is essential (BENKÓ et al., 2008; SZABÓ et al. 2008; POROS et al. 2008). Beyond the listed examples – from hydrogeological point of view – analysis of the fracture systems of water reservoirs is equally important since at many dry areas fractured rocks are the primary water reservoirs.

Earlier studies of fracture systems focused mostly on the large scale, well visible joints, faults and mineralised veins which can easily be surveyed on the field (GILLESPIE et al. 1999, 2001; ROBERTS et al. 1998). However, several processes and phenomenon are not interpretable by investigation of the macroscopic fractures only (e.g. intense fluid flow is a macroscopically homogeneous rock body). In the past few decades, more and more attention has turned to the open and healed microcracks and to their relationships to fracture systems of other magnitudes. It has been proved that analysis of these microfractures has primary importance in evaluation of the permeability of the rock and it also contributes to the reconstruction of the tectonic history of the investigated area. Moreover, some specific microfractures entrap small portions of the fluids which migrated in the open space at the time of their formation, which enables us to determine the physical and chemical conditions during the microfracture-driven fluid flow. Such fractures are called the fluid inclusion planes (hereinafter FIP). Formation of FIP is evidently tectonically controlled, while microthermometric analysis of the entrapped fluid inclusions may help to

determine the pressure-temperature-composition conditions of the fluid flow through the microfractures. Studying of FIP therefore enables us to reconstruct the tectonic history during the fluid flow in crystalline rocks in which otherwise it is very difficult to make such reconstruction due to the lack of either any stratigraphic layering or the absence of other markers used in structural evaluation. An additional advantage of the method is that the analysis does not demand the presence of large rock exposures because the measurements can be done on an oriented hand specimen or drillcore.

The subject of this work is the analysis of the relationship between fracture systems on different scales in a relatively homogeneous granite body and the temporal and spatial relationship of hydrothermal fluid percolation of different ages which interacted with the granite body. The selected area is the Velence Mountains in Western Hungary, which was affected by both the Variscan and Alpean orogeny. Owing to their special geotectonical position, the Velence Mts. and its region was involved in the whole Alpine cycle from the rift phase until the collision. Selection of this area for studies is also supported by the occurrence of sufficient amount of large outcrops. Also, earlier studies by MOLNÁR et al. (1995); MOLNÁR (1996, 2004) proved that the granite was affected by several high temperature fluid flow events and that these fluid migration events are easily distinguishable by means of fluid inclusion studies.

Understanding of fracture evolution in the frame of the tectonic history of the granite required field observations on fractures and tectonic phenomenon's and characterization of their correlation with microfracture properties as well as more accurate knowledge of the age of alteration resulted from the fluid/rock interaction. Geochemistry, mineralogy and physical conditions of the fracture forming hydrothermal systems were also necessary to be determined. Therefore studies on clay mineralogy of altered zones, K-Ar radiometric age dating, as well as lead and sulphur isotope analysis have also been carried out in addition to the fluid inclusion studies. In the knowledge of these general characteristics, it was possible to describe and compare the macroscopic and microscopic features related to the main hydrothermal processes (Variscan and Alpean). On the basis of regional knowledge gained by studies mentioned, a small representative area was selected for detailed investigation.

This work was also supported by the fractal analysis of the mineralised veins, and the correlation of the fractal properties with other mineralogical characters and structural parameters.

Geometrical and statistical analysis of the fracture systems in different magnitudes also supported evaluation of the paleo-porosity of the granite. An important question of the work was – in addition to the how and when the fractures formed – how the hydrothermal and other old fractures influenced the formation of the current fracture network of the granite.

The results of various analyses altogether facilitated the determination of age and geologic connections of some hydrothermal formations. Results also made it possible to correlate the tectonic evolution of the Velence Mts. in regional context. Beyond the new local and regional geological knowledge, the work also conveys new methodological approach for studies of fracture systems. This knowledge may be useful in the economic geology, reservoir geology, and hydrogeology or even in environmental geology.

2. GEOLOGICAL SETTING OF THE VELENCE MOUNTAINS

CONTEXTE GEOLOGIQUE

Les monts Velence sont localisés dans la partie centrale du bassin des Carpates au Nord du linéament Périadriatic – Balaton (PAL). Les monts Velence forment une unité tectonique allochtone et se subdivisent en deux unités: la partie Ouest est constituée de monzonites Varisques, l'Est étant constitué par un complexe magmatique Paléogène.

Le granite Varisque est un monzogranite peralumineux biotitique de type S (BUDA, 1985) daté à 280-290 Ma et intrusive dans des schistes Paléozoïques. Ce granite s'est formé sous des pressions de 2 Kbars, 740-500°C près des conditions eutectiques (BUDA 1985, 1993). Dans sa partie sommitale, des petites enclaves (1 m³) pegmatitiques (quartz – feldspaths – biotite – fayalite) sont observables (BUDA 1983). En fin de cristallisation, des diques aplitiques et de granite porphyrique se sont mis en place selon une direction structurale NE-SW (JANTSKY 1957).

Des dykes à monchiquite-spessartite de 0,5 m d'épaisseur (HORVATH et al. 1984) se sont mis en place au Crétacé à 77.6±3 Ma (BALOGH et al. 1983). Ils ne sont pas altérés et n'ont pas altérés l'encaissant.

À l'Est du granite, se trouve un système stratovolcanique andésitique intensément altéré (daté par K-Ar méthode à 28-30 Ma; BAJNOCZI 2003) et souligné par une intrusion dioritique. Des diques andésitiques intrudent le granite dans sa partie Est et induisent de fortes circulations fluides locales. Les séries stratovolcaniques sont intensément altérées en surface alors que des

échantillons non altérés ont été prélevés par sondages. Il s'agit de laves andésitiques à biotite-pyroxéne-amphibole. La signature géochimique de cette andésite est calco alcaline potassique modérément tholéiitique mise en place dans un contexte postcollision (DARIDA-TICHY 1987, BENEDEK et al. 2004).

L'initiation de ce volcanisme est à relier à la collision entre l'Europe et une microplaque Apulienne qui induisit un intense volcanisme le long de la ligne Périadriatique – Balaton (PAL) à 25-40 Ma.

2.1 REGIONAL GEOLOGY

The Velence Mts., are located 50 km southwest from Budapest (Figure 1), to the north from the Velence-lake (Figure 2), east from Székesfehérvár (Longitude: 465 000 E Latitude: 474 000N (EOV)). The aerial extent is 140 km² and, maximum elevation above the sea level is 351m.

In the present setting, the Velence Mts. can be divided into two parts: the western, larger (10 x 4 km) part consists of a granite intrusion of Variscan age (280-300 Ma; BUDA, 1985), whereas the eastern part is built up by an Alpean calc-alkaline andesitic intrusive-volcanic complex of Oligocene age (Nadap Andesite Formation) can be found (Figure 3). Dikes and small stocks related to the volcanic complex also intrude the old granite. The southern part of the granite intrusion has also been intruded by some small lamprophyre dikes of Cretaceous age. The surrounding of the Velence Mts. is covered by young Miocene and Holocene marine-lacustrine, and fluvial sediments (Figure 2).

The host rocks of the magmatic formations is the early Palaeozoic schist (Lovas Slate Formation). Carboniferous and older schist (sedimentary molasse and flysch rocks) of the Velence Mts. and the adjoining Balatonfő area have undergone Carboniferous metamorphism, thrusting and folding. Metamorphism resulted in two phase foliation of the the slate, later their southeast verging folding (DUDKO 1986a). However the granite was not affected by the Variscan metamorphism

Structurally, the Velence Mts. are bordered by the Lovasberény line from north (Figure 3). The Palaeogene Volcanic Unit (PVU) and the granite body are divided by the Nadap-line trending NW-SE which functioned as a normal fault during the Palaeogene volcanic and hydrothermal activity (MOLNÁR 2004). The eastern border of the Mountains is the Vál fault, east from the PVU. To the west the granite gradually subsides below the Neogene sedimentary cover.

In the point of view of regional geotectonic setting, the Velence Mts. is located at the central part of the Pannonian basin. Its structural position is on the border of the Alcapa Megaunit and the Tisza Megaunit and form a part of the Mid-Transdanubain Unit (HORVÁTH et al. 2004; Figure 1). The Periadriatic-Balaton Lineament system (PAL) forms the boundary between the Alcapa and Tisza Megaunit which is a main structural lineament since the Triassic and it has played an important role in the late-Palaeogene–early-Neogene tectonic evolution of the Pannonian basin. The Alcapa Megaunit escaped laterally from the Alpean collision zone along the PAL in the Oligo-Miocene. Along the PAL several allochthonous rock bodies can be found which were sheared during the continental escape (KÁZMÉR & KOVÁCS 1985) and rotation (CSONTOS et al. 1991). One of these allochthonous unit is the Velence Mts. According to the paleomagnetic investigations, the Velence Mts. was the part of the African Plate during the Palaeogene magmatism and joined to the European plate during the late Palaeogene - early Neogene. The Velence Mts. had already been rotated together with the Alcapa Megaunit (77-81° counter clockwise; BALLA 1985) in the Neogene. Other authors suggest that the Velence Mts. can be considered as a part of a tectonic megamelange between the two Megaunits (Tisza and Alcapa) of the Pannonian-basin. It rotated in variable amount during the Neogene and has undergone various subsidence history during the left lateral displacement of the Alcapa Megaunit.

Other small granite plutons of similar age (late Carboniferous – early Permian) are known along the PAL (e.g. Eisenkappel granite in the Alps, drillholes: Sárvár Sá-I, Sá-3, Buzsák Bu-É-1, Dinnyés Di-3, Gá-1a in the Pannonian Basin) and in the Gemeric Mountains (Figure 1). Their age suggest that they were formed in the transitional period between the Variscan and the Alpean orogeny. The listed granite bodies found in drillcores could have been an individual granite intrusion but their displacement resulting from the left-lateral large scale (transpressional to transtensional) faulting during the late Palaeogene – early Neogene cannot be excluded either (KÁZMÉR & KOVÁCS 1985).

The petrochemical character of the andesitic rocks in the eastern part of the Velence Mts. is medium to high-K calc-alkaline, slightly tholeiitic, and they belong to a post-syn collisional andesite-basaltic andesite series (DARIDA-TICHY 1987, BENEDEK et al. 2004). The initiation of the intermediate volcanism can be attributed to the collision of the European and the Apulian microplate of African origin which resulted in intense volcanism along the Periadriatic-Balaton

Lineament system (PAL) for 25-40 Ma. Volcanic and subvolcanic rocks along the PAL can be found in a well defined belt running from Recsk to the Western Alps (Zala Basin, Karawanken, Adamello, Riesenferner, Bergell plutons) and to the south in the Dinarides (Figure 1). An essential difference between the magmatic rocks in the Pannonian basin and the Alpean magmatic rocks is that whereas the volcanic and subvolcanic parts in the Alps have eroded to their root zones due to the intense and rapid compression and uplift, the magmatic series which escaped to the east came into an extensional regime and the erosion was less effective in these zones. Therefore, intrusive rocks which are currently on the surface in the Sava-Vardar zone and along the margin of the Eastern and Southern Alps are tonalites and granodiorites whereas the Paleogene magmatics are represented by andesitic volcanic rocks in the Pannonian-basin. Andesite pebbles in the Neogene molasse in the Alps prove that the upper zones of the series were also present in the Alps but they have been eroded (BENEDEK et al. 2004).

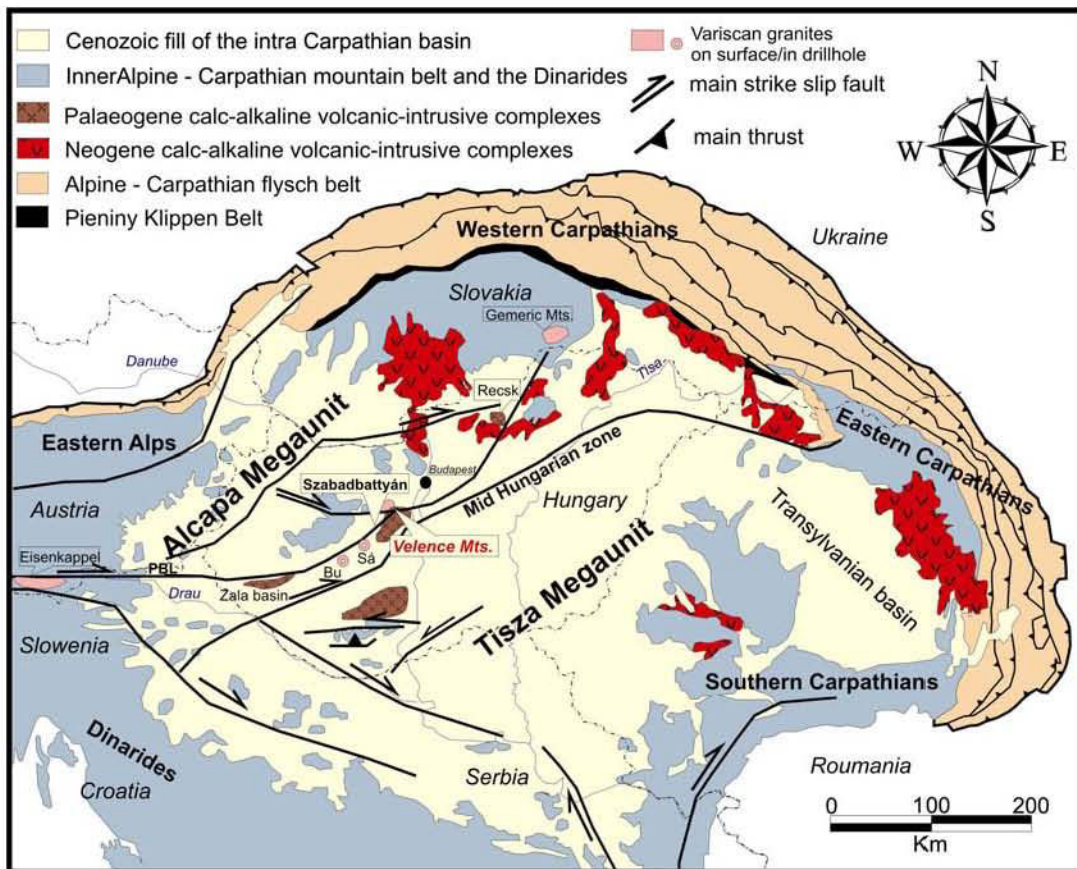


Figure 1. Geological structure of the Alp-Carpathian-Pannonian region. (Modified after CSONTOS et al. 2004)

2.2 MAJOR GEOLOGICAL FORMATIONS OF THE VELENCE MOUNTAINS

2.2.1 Variscan granite (Velence Granite Formation)

The Variscan granite intrusion is a well differentiated, S-type, biotitic, monzogranite which crystallized under near-eutectic conditions (around 600-700°C) from a water saturated melt at about 2 kbars pressure (BUDA 1981, 1985). The mineralogy of the granite is rather simple: quartz, orthoclase, plagioclase and biotite (JANTSKY 1957, BUDA 1985). The accessory minerals are: apatite, zircon, rutile, magnetite, ilmenite, allanite, xenotime, titanite (VENDL 1914, BUDA 1985, BUDA & NAGY 1995). Texture of the main mass of the granite is equigranular, however micro-equigranular textures also occur along the contact with the host slate. The granite of the Velence Mts. does not belong to the classical Variscan orogeny related granites. Geochemically it is peraluminic, S or S/A type, K-subalkaline with alkaline character, therefore it is rather postorogenic or rift related according to UHER & BROSKA (1994).

In conjunction with the crystallization of granite, several aplite and granite porphyry dikes also intruded. The mineralogy of the pinkish, maximum 1 m thick aplite dikes is simple and it consists of quartz and K-feldspar with microgranular texture (VENDL 1914). They fill up few hundred metre long NE-SW trending dilatational fractures. Granite porphyry dikes usually have NE-SW, ENE-WSW strike, mostly parallel with the aplite dikes and their thickness can be up to 25 m. Both the geochemically more basic “Sukoró type” and the more felsic “Pátka type” porphyries contain dihexahedral quartz megacrysts, which are embedded in a pinkish-grey (Sukoró-type) or greenish, yellowish (Pátka type) ground mass (HORVÁTH et al. 2004). They are late differentiates of the residual granite melt which intruded into the opening extensional fractures.

According to HORVÁTH et al. (2004), the granite has two main joint system: a NE-SW and a NW-SE trending one and the N-S and E-W oriented joints are subordinate. HORVÁTH et al. (2004) also showed slight differences in the orientation of the fractures and magmatic dikes of the eastern and the western part of the granite body which can be explained by influences of Neogene tectonism. In conclusions, the body of the granite can be divided into 3 parts (Nadap-Sukoró area, Pákozd area, Székesfehérvár area) which are bordered by N-S trending Neogene faults. In some chapters I differentiated an additional area which is the Nadap area. However it is tectonically

identical with the Nadap-Sukoró area, it is the most affected area of the granite by the Palaeogene magmatic activity.

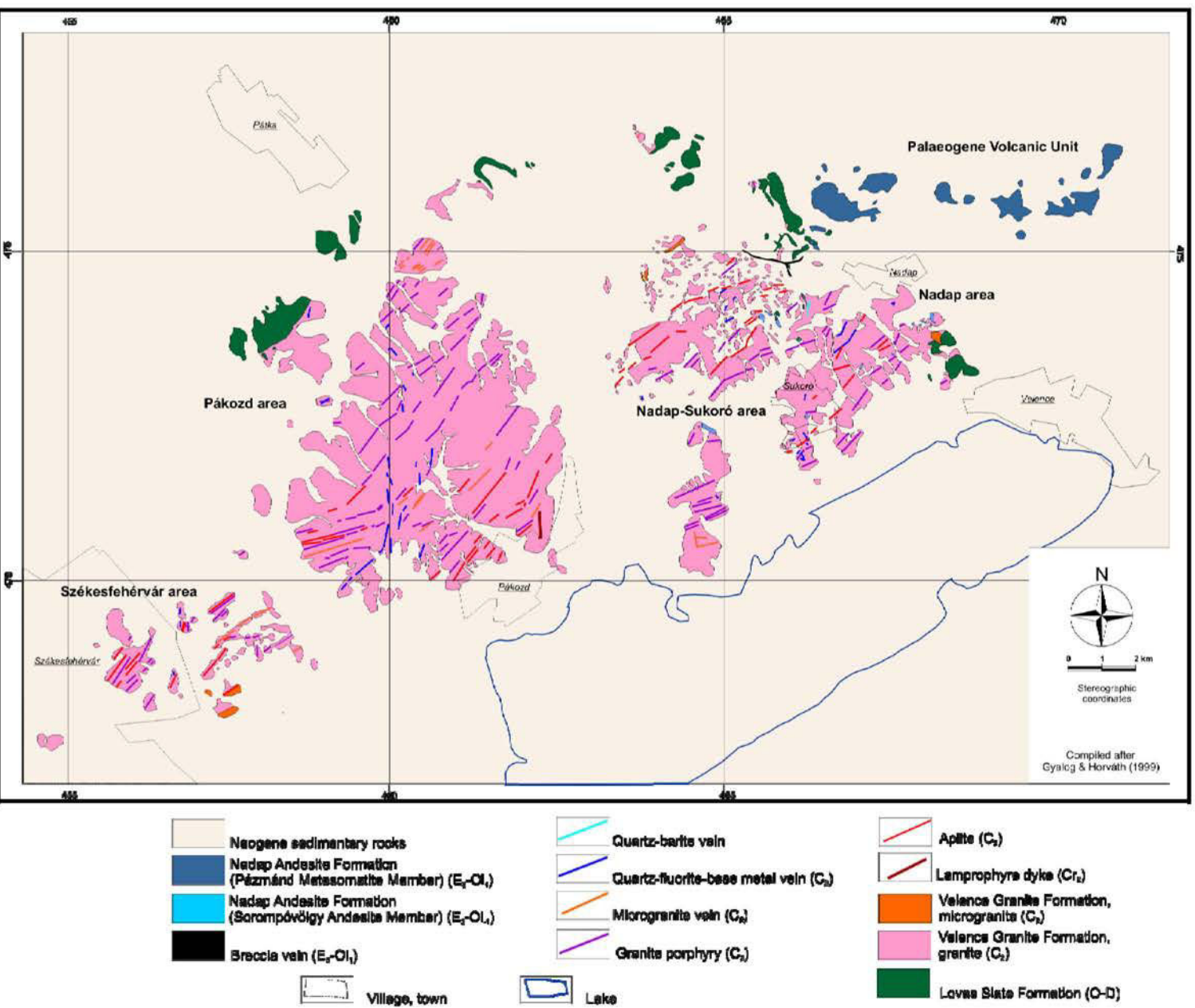


Figure 2. Geological map of the Velence Mts. Modified after HORVÁTH (2004).

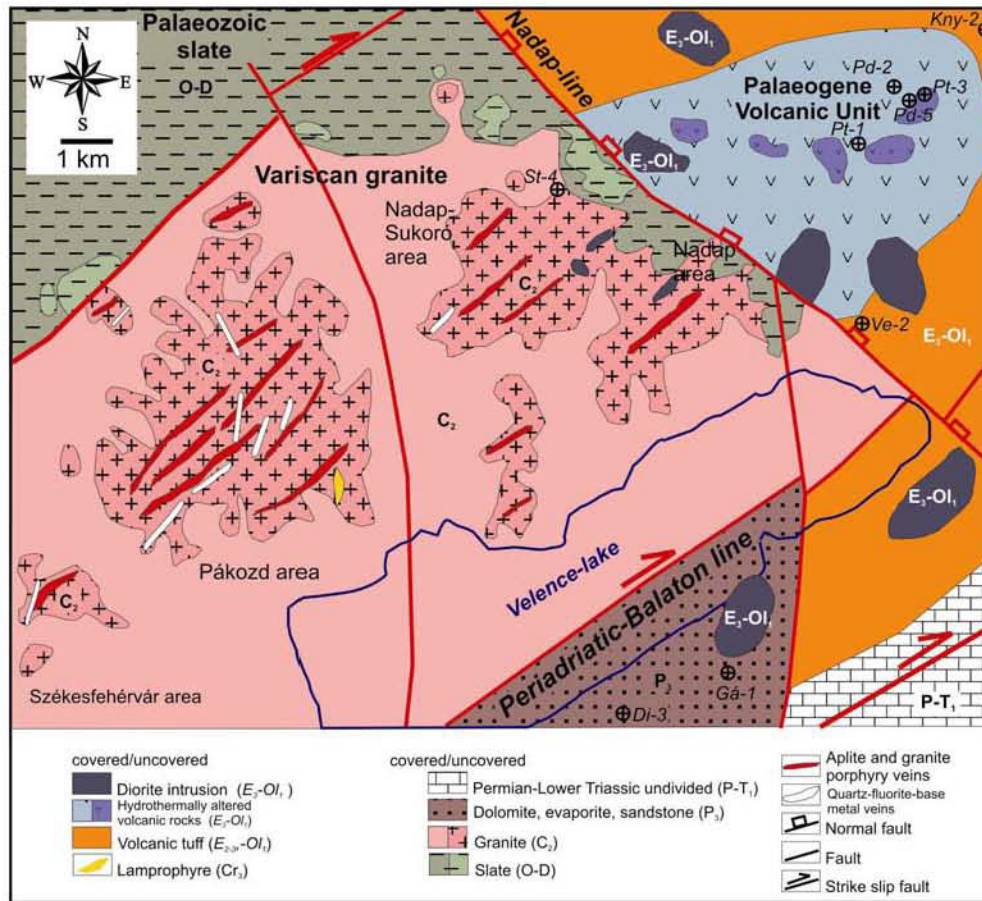


Figure 3. Uncovered geological map of the Velence Mts. Modified after DUDKO (1999)

2.2.2 Early Palaeozoic Slate (Lovas Slate Formation)

The host of the granite is the early Palaeozoic Lovas Schist Formation (Figure 2) which is considered to be a metamorphosed flysch of the Kaledonian(?) -Variscan orogeny (CSÁSZÁR 2005). The contact of the granite and the slate is obviously tectonic at some spots, but the original intrusive contact is also known along the eastern part of the granite body (JANTSKY 1957). Along the original contact, the characteristic thermo-metamorphic alteration minerals are andalusite, tourmaline, muscovite, biotite and quartz. Close to the contact (including the apical eroded zones), basic magmatic enclaves, metapelitic xenoliths and fayalite bearing pegmatitic nests also occur in the granite (BUDA 1993). The metapelitic xenoliths recrystallised and partially melted at the temperature of the granite crystallization (680°C) The basic magmatic enclaves represent a primitive magma while the fayalite bearing pegmatitic nests crystallized at lower temperature (400°C), than the granite.

According to investigations by GOKHALE (1964; 1965) the fracture system of the granite and the slate are basically different, the joint network of the granite has been formed related to the cooling of the intrusion.

2.2.3 Cretaceous igneous rocks (Budakeszi Picrite Formation)

In the late Cretaceous, very few, maximum 1 m thick monchiquite-spessartite lamprophyre dikes intruded the granite body (Figures 2 and 3). K-Ar radiometric age dating on rock forming flogopite crystals of the lamprophyre yielded $77,6 \pm 3$ Ma (BALOGH et al. 1983). Genetical relationships, geochemistry and petrology of these volumetrically insignificant dikes have been widely discussed by DOBOSI & HORVÁTH (1988). Lamprophyre dikes in the southern part of the ALCAPA Megaunit and in the Eastern Alps are also widely known. These dikes emplaced along N-S oriented structures, which are on the compression perpendicular extensional fractures related to the Cretaceous folding and thrusting on the Alacapa megaunit.

2.2.4 Palaeogene igneous rocks (Nadap Andesite Formation)

East from the Nadap-line – between the villages Sukoró and Nadap – remnants of a hydrothermally altered andesitic stratovolcanic series can be found on the surface (Figure 3). During the mineral exploration program of 1970's led by the Hungarian Geological Institute, the hydrothermal centres and the stratovolcanic series were transected by several drillings (Pázmánd Pd-1, Pd-2, Pd-5, Pt-4, Pt-5, Kápolnásnyék Kny-3; Figure 3). The Pázmánd-2 (Pd-2) drillhole was the only one which cut the whole stratovolcanic sequence in at about 620 m thickness. According to the petrological and mineralogical analysis of the fresh drillcores, the stratovolcanic sequence is built up by alternating amphibole and pyroxene andesite, lava, lavabreccia and volcanic agglomerate. Below the volcanic sequence a hydrothermally altered diorite intrusion was found from 620 to 1240 m depth and the drilling did not reach the basement. A number of relatively fresh volcanic rocks were also found in some other shallow drillcores of the area (Kápolnásnyék Kny-2, Velence Ve-2, Kápolnásnyék K-12, K-14, K-15), as well and numerous additional diorite intrusions were found by geophysical methods in the area (DUDKO 1989; HORVÁTH et al. 2004; Figure 3).

West from the Nadap-line, various small glomeroporphyric andesite intrusions and dikes are present in the old granite body (Figure 3). Their compositions are pyroxene andesite, amphibole andesite and biotite-pyroxene andesite with variable intensity of chloritic-argillic hydrothermal alteration (JÓZSA, 1983; DARIDA-TICHY, 1987). The NE-SW orientation of andesite dikes of Palaeogene age in the granite is parallel with the old aplite and granite porphyry dikes. It proposes the possibility of the reactivation of the old structures during the Tertiary magmatic and hydrothermal processes.

2.3 GENERAL GEOLOGY OF THE SZABADBATTYÁN AREA

The Szabadbattyán area is located 30 km apart SW from the Velence Mts. along the PAL (Figure 1). The Szabadbattyán area is a complex thrust block, built up of metamorphosed slate, phyllite, and carbonate nappes (Figure 4). This block can be correlated with the rocks of the Carnic-Alps (CSÁSZÁR 2005). Structurally, the Szabadbattyán Formation (Nötsch strata) tectonically covers the Ordovician Kőszárhegy Aleuolite Formation and the Ordovician Balatonfőkajár Quartzphyllite Formation. The Devonian Polgárdi Limestone Formation covers with tectonical discordance the Balatonfőkajár Quartzphyllite Formation and the Szabadbattyán Formation (FÜLÖP 1990). Intrusive activity is marked by the presence of Carboniferous granite porphyry dikes in the Szabadbattyán Formation, whereas Triassic (BALOGH et al. 1983, BAGDASZARJAN 1989) andesite dikes intrude the Polgárdi Limestone Formation (Figure 4).

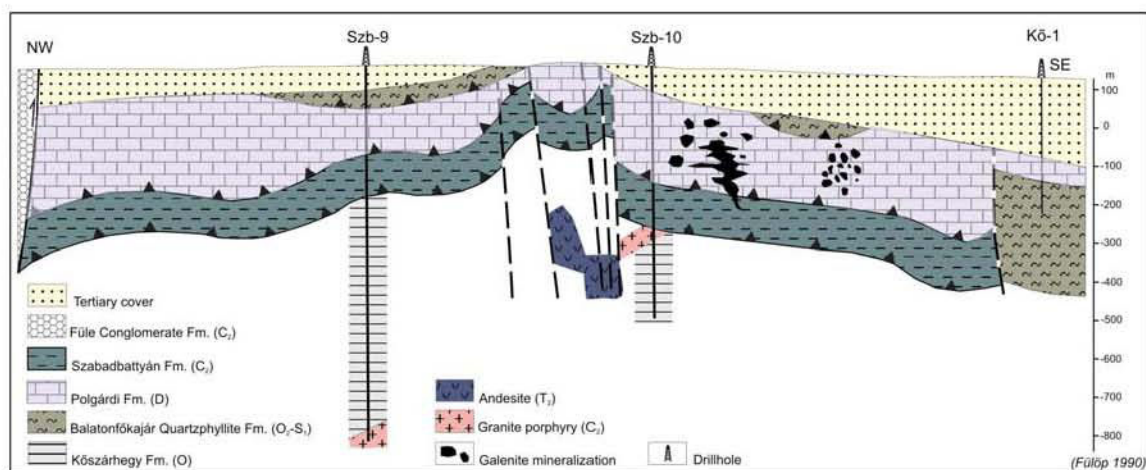


Figure 4. Geological section of the Szabadbattyán area. Modified after FÜLÖP (1990).

2.4 HYDROTHERMAL SYSTEMS IN THE VELENCE MTS.

Mineralization hydrothermale des granites et argiles

Dans la partie sommitale du granite, des petites inclusions pegmatitiques (1 m³) et des cavités myarolitiques avec du Fk, quartz et plagioclases sont présentes. Les températures de formation de ces assemblages ont été calculées par microthermométrie (MOLNAR et al. 1995) et sont de 300-400°C et 500-600°C à 2 kbar.

Dans la zone de Nadap, des veines à Qz molybdène sont connues dans le granite. Les petites veines à Molybdénite contiennent des inclusions de pyrite, galena, sphalerite, chalcopryrite, marcasite et des phases à Ag – Te (JANTSKY 1957, MOLNAR 1997). Les travaux de Molnar (1997, 2004) suggèrent que la minéralisation s'est formée à partir de fluides à CO₂ sous des pressions assez élevées (entre 1-2,4 kbar) and température (280-300°C).

Dans la zone de Székesfehérvár-Pákozd, des veines à quartz-fluorite-sphalerite-galenite-chalcopryrite-calcite (quartz-fluorite-base metal) existent. Les veines minéralisées sont associées à une alteration à silice et argillite du granite. Un long débat a eu lieu en ce qui concerne les relations génétiques sur l'âge des veines. Selon les travaux récents (MOLNAR 1996; 2004) basés sur les inclusions fluides, la formation des veines peut être reliée aux derniers processus hydrothermaux du granite et à un mélange probable d'eau de formation et de fluides magmatiques durant la formation des veines.

Une veine à quartz-barite existe dans la zone de Nadap-Sukoró et a été exploitée dans les années 1940. Cependant les associations minéralisées présentées précédemment y sont absentes et sont plutôt génétiquement associées à des veines métalliques à Qz Fluorite.

Activité ignée Paléocène et processus hydrothermaux

Dans l'intrusion dioritique, des altérations propylitiques (actinolite, albite, epidote, chlorite, magnetite, ilmenite) et métasomatiques potassiques (flogopite, biotite, sericite, pirite) sont connues avec des sulfures cuprifères. Le principal type de minéralisation est de type porphyre cuprifère. L'alteration métasomatique potassique et quelques occurrences de veines quartzieuses à K- feldspath sont accompagnées de stockworks à quartz-pyrite-chalcopryrite-sphalerite superposées par des veines tardives à carbonates zéolites. Une minéralisation à Skarn est

présente à 670 m de profondeur. Les phases minérales de ce skarn sont andradite, epidote, quartz et pyrite. L'altération potassique a lieu à haute température (>350 °C), les fluides hydrothermaux sont complexes et de forte salinité (>40 NaCl equiv. wt%) (MOLNAR (1996) and PROHASZKA (2004)). La séparation de phase des fluides hydrothermaux s'est déroulée dans des conditions intermédiaires entre pressions hydro et lithostatique à 1100 m de profondeur.

Une partie des alterations hydrothermales du strato volcan exposées en surfaces forment des zones hydrothermalisées. Cette altération hydrothermale est de type high-sulphidation (HS) des systèmes épithermaux. Dans la partie centrale des zones hydrothermalisées se sont formées des brèches vacuolaires siliceuses à de faibles pH (pH=1-2). On trouve une alteration à alunite-pyrophyllite-dickite-zunyite, puis illite et illite/montmorillonite vers la zone distale. Des zones vacuolaires siliceuses entourées d'altération à alunite-kaolinite-dickite existent: elles se sont formées à basse température en comparaison avec celles à pyrophyllite-zunyite-topaz. Les fluides hydrothermaux ont migré dans une structure orientée EW (de l'Est vers l'Ouest) car les températures diminuent de 350 à 250°C et le pH augmente.

Minéralisations hydrothermales Paléogènes dans le granite varisque.

À l'Ouest de la ligne Nadap, des diques andésitiques intrudent le granite. De la brechification et une altération hydrothermale existent le long de ces intrusions. Certaines d'entre elles ont une faible chloritisation et certains diques sont fortement argilisés. Fluorite, calcite, quartz, pyrite, epidote, hématite, sphalérite, galena, tétraédrite, et laumontite sont présents dans certaines veines de ces diques.

Au contact entre le granite et les schistes des monts Meleg (partie Est de l'intrusion) se développe des brèches et zones siliceuses à chalcopryrite et concentrations d'Enargite grise. Dans le forage St-4 près de Sukoro se trouvent des veines à quartz-chalcopryrite: le granite y a une altération sericite siliceuse. Les propriétés microthermométriques des inclusions fluides de ces brèches sont fortement similaires à celles existant dans les minéralisations de type Porphyre cuprifère à l'Est de Nadap (MOLNAR 1996). Cette séparation entre fluides à salinité fortement et faiblement élevée se fait à 200-400 bar dans des conditions de pression hydrostatique.

2.4.1 Mineralization of the granite and the shale

In the apical part of the granite, small pegmatitic nests (up to 1 m³ in volume), as well as miarolitic cavities are present. Their mineralogy is dominated by K-feldspar, quartz, plagioclase but occurrence of minor amount of biotite, fayalite, Fe-amphibole, Fe-biotite, ilmenite, molybdenite, apatite, fluorite, molybdenite was also recorded (Jantsky 1957; BUDA 1969, 1985). Pegmatite is enriched in W, Rb, Ce, Y, B, Tl, Be. According to fluid inclusion studies and two feldspar thermometry (MOLNÁR et al. 1995) pegmatite and miarolite filling minerals formed in two temperature range, between 300-400°C and 500-600°C at 2 kbar pressure. The high temperature granite related metasomatic and hydrothermal mineralization can be divided into the following groups:

Tourmaline alteration of the granite and the aplite occurs in nests and cavities which are surrounded by pegmatite-like feldspars at some places.

Quartz-tourmaline veins are present close to the contact of the granite and the slate. These veins also contain some muscovite, garnet as well as ore minerals.

Fluorite alteration of the granite in miarolitic nests is accompanied by albitic alteration and formation of molybdenite and muscovite on the Gécsi Hill.

Molybdenite-quartz stockwork and silicic alteration of the granite, aplite and slate occur in the Nadap area. The molybdenite bearing veinlets also contain grey ore, pyrite, galenite, sphalerite, chalcopyrite, marcasite and an Ag-Te phase (JANTSKY 1957; MOLNÁR 1997). Results of studies in MOLNÁR (1997, 2004; Table 1) suggest that the mineralization was formed from CO₂ rich boiling fluids at a relatively high pressure (between 1-2,4 kbar) and temperature (280-300°C). Salinities for aqueous liquid rich fluid inclusions syngenetically trapped with the CO₂ rich inclusions are between 7,4-13,9 NaCl equiv. wt%, as well as 1,2-5,7 NaCl equiv. wt%.

In the granite (Figure 2 and 3), quartz-fluorite-sphalerite-galenite-chalcopyrite-calcite (quartz-fluorite-base metal) veins occur. The texture of the veins is banded-zoned and brecciated. Cockade texture is also common which also confirms multiple pulses of hydrothermal processes and repeated tectonic activity during the veins' formation. The veins have NE-SW, N-S and NW-SE strike and are up to 7 m thick and 1200 m long. Ore veins are surrounded by silicic and argillic alteration of granite. Both the fluorite and the base metal mineralization were mined during the 50's and 60's at Pátka and Pákozd (Figure 2). On the upper levels of the old mine

workings galena and sphalerite are the major ore minerals with a little amount of antimonite. At the deeper levels, mostly chalcopyrite and pyrite associates to sphalerite (HORVÁTH et al. 2004).

In the Nadap-Sukoró area a quartz-barite vein is located, which was mined during the 1940's. However the above listed mineral assemblage is absent from the vein, its is always discussed and genetically associated in the literature together with the quartz-fluorite-base metal veins.

The age and origin of the granite hosted base-metal and fluorite veins have been debated for a long time. VENDL (1914), JANTSKY (1957) and MIKÓ (1964) connected their formation to the late hydrothermal processes of the granite magmatism. KASZANITZKY (1959) was the first and later KISS (1954), who introduced the possibility of the role of the Palaeogene andesitic magmatism in the formation of these veins. ÓDOR (1985) proposed the possible upper Cretaceous age of the quartz-fluorite veins. This suggestion was based on the comparison of the carbon and oxygen isotope values of calcite in fluorite bearing veins and the carbonate ocellae of the lamprophyre dikes, as well as on the basis of similarities of the REE pattern of fluorite and the lamprophyres. According to HORVÁTH et al. (1989) the role of Triassic magmatic activity in the formation the quartz-fluorite-base metal veins that is not yet known cannot be excluded either.

MOLNÁR, on the basis of fluid inclusion studies (1996, 2004) connected the formation of the veins to the late hydrothermal process of the granite and suggested a theory of the mixing of formational waters of deep basin origin with magmatic fluids during the vein formation. Primary fluid inclusions in the hydrothermal quartz and fluorite from the quartz-fluorite-base metal veins yielded 80-210°C homogenization temperatures. Composition of the fluids was modelled by H₂O-NaCl and by the H₂O-CaCl₂ systems. Salinities were at 6,7-21,1 NaCl equiv. wt% for the H₂O-NaCl system and 10-24,6CaCl₂ equiv. wt% for the Ca-enriched fluids (Table 1).

2.4.2 Hydrothermal processes related to the igneous activity of the Palaeogene age

The hydrothermal mineralization and the alteration of the Palaeogene diorite intrusion and the stratovolcanic sequence were discussed in the last decades by several authors (FÖLDVÁRINÉ 1947; JANTSKY 1957; KOCH 1985; DARIDA-TICHY 1987; MOLNÁR 1996, 2003, 2004; BAJNÓCZI et al. 2002, BAJNÓCZI 2003, PROHÁSZKA, 2004).

In the diorite intrusion, propilitic (actinolite, albite, epidote, chlorite, magnetite, ilmenite) and K-metasomatic (flogopite, biotite, sericite, pirite) alterations together with copper-sulphides

are known. The general features of mineralization correspond to a Cu-porphyry type ore forming system. The K-metasomatic alteration and the sporadic occurrences of the K-feldspar-quartz veins are accompanied by quartz-pyrite-chalcopyrite-sphalerite stockwork mineralization that was superimposed by a late carbonate-zeolite vein system. At 670 m depth (in a few meters thick intercept in the Pd-2 drillhole), skarn mineralization also occur. Characteristic minerals of the skarn are andradite, epidote, quartz and pyrite.

Studies by MOLNÁR (1996) and PROHÁSZKA (2004) indicate that the potassic alteration took place at high temperature (>350 °C), and the composition of the high salinity (>40 NaCl equiv. wt%; Table 1) hydrothermal fluids were rather complex. The hydrothermal fluids have undergone phase separation at relatively low pressure and trapped between lithostatic and hydrostatic conditions at about 1100 m depth. In a later hydrothermal phase, possibly related to the collapse of the magmatic-hydrothermal system, lower temperature (180-200°C) and low salinity (<<20 NaCl equiv. wt.%) epithermal fluids circulated in both of the diorite intrusion and in the stratovolcanic series.







| Type of inclusion | Phase composition | Pegmatite in granite | Quartz-molybdenite stockwork in granite and shale | Quartz-turmaline veinlets in shale | Base metal fluorite veins in granite | Cu-porphyry showings in subvolcanic diorite | Chalcopyrite bearing breccia vein in granite | Enargite bearing breccia granite/shale contact | High-sulphidation type alteration zones in andesite |
|-------------------------------------------------------------------------------------|------------------------------------------------------------------------------|---------------------------------------------------------------------------------|-----------------------------------------------------|----------------------------------------|----------------------------------------------------------------------------------------------------------------|------------------------------------------------------|----------------------------------------------|------------------------------------------------|-----------------------------------------------------|
|  | L+V V<10% | S 90-180°C 6-23 CaCl ₂ | - | - | S-P 80-140°C 10-25 CaCl ₂ S-P 170-210°C 7-21 NaCl Fluorite: P 110-160°C 1-10 NaCl | - | - | - | - |
|  | L+V V=10-30% | S-P 90-250°C 2-20 NaCl S 320-350°C 0-2 NaCl P 320-370°C 3-4 NaCl | S 220-280°C S 280-320°C 1-6 NaCl 8-14 NaCl | S 240-300°C S 330-390°C 0-1 NaCl | - | S 270-370°C 13 NaCl- 24 NaCl+CaCl ₂ | S 260-360°C 1-21 NaCl | S 210-400°C 1-21 NaCl | S-P 310-380°C S 220-290°C 1-13 NaCl |
|  | L+V V=40-60% | S present | - | - | - | - | S-P 400-410°C 3-5 NaCl | S-P 370-450°C 1-8 NaCl | - |
|  | L+V V>80% | S present | - | S 340-380°C | - | S-P 360-500°C | S-P 400-460°C | S-P 310-440°C | S-P 280-290°C |
|  | L+V+H (+Sy+X) V=10-30% | - | - | - | - | S-P 270-520°C 31 NaCl- 79 NaCl+KCl | S-P 410-450°C 36-40 NaCl | S-P 260-450°C 26-40 NaCl | - |
|  | Laq+LCO ₂ (+VCO ₂) LCO ₂ =40- 90% | - | S-P 280-300°C 0-11 NaCl | - | - | - | - | - | - |

Table 1. Types of fluid inclusions according to their phase compositions observed at room temperature and their microthermometric data in various post-magmatic and hydrothermal mineralization of the Velence Mts. (MOLNÁR 2004). Abbreviations: L-aqueous liquid; V-vapor; VCO₂-carbonic vapour; H-halite; Sy-sylvite; X-undetermined daughter mineral; P-Primary inclusion; S-secondary inclusion; NaCl-salinity in NaCl equiv. wt%; NaCl+CaCl₂- salinity in NaCl+CaCl₂ equiv. wt%; CaCl₂-salinity in CaCl₂ equiv. wt%; NaCl+KCl-salinity in NaCl+KCl equiv wt%.

The hydrothermally altered parts of the stratovolcanic series exposed on the surface form individual hydrothermal centres (Figure 2). According to the studies of MOLNÁR (1996; 2003) and BAJNÓCZI (2003), the characteristics of the hydrothermal alteration are comparable with a high-sulphidation (HS) type epithermal system. In the central part of the hydrothermal centers, brecciated vuggy silica bodies have been formed at very low pH conditions (pH=1-2), towards the distal zones, first an alunite-pyrophyllite-dickite-zunyite, then illite and illite/montmorillonite alteration is typical. There are also vuggy silica centers which are surrounded by alunite-kaolinite-dickite alteration: these were formed on a relatively lower temperature in comparison to the pyrophyllite-zunyite-topaz bearing alteration zones. Due to geochemical and structural considerations, the epithermal fluids migrated in an E-W oriented structure from the east to the west, while the temperature decreased from 350°C to 250°C and the pH slightly increased.

Fluid inclusion data indicate that fluids in the epithermal system were in heterogeneous state (boiling) and their salinities were low (1,1-12,4 NaCl equiv. wt%). Temperature of the fluids varied between 220-290°C as well as between 310-380°C (Table 1). The alteration happened at shallow level under hydrostatic conditions at 21-46 bar pressure.

2.4.3 Hydrothermal mineralization of Palaeogene age in the Variscan granite

West of the Nadap-line, andesite dikes and small stocks intruded the Paleozoic granite and slate. Brecciation and hydrothermal alteration along these intrusions and in the dikes and stocks themselves are also present. Most of these small intrusions have weak chloritic alteration only but there are also some dikes with intense argillic alteration. Fluorite, calcite, quartz, pyrite, epidote, hematite, sphalerite, galena, tetradrite, and laumontite appear in small nests and veins of these dikes, as well (MAURITZ 1908a, b; SCHAFARZIK 1908; ERDÉLYI 1939; KOCH 1985). FÖLDVÁRINÉ VOGL (1947) recognised Mo anomalies in the andesite dikes. Mo-anomalies are characteristics to the the whole Palaeogene volcanic unit of the Velence Mts.

Enargite-grey ore and chalcopryrite bearing siliceous breccias and silica rich pods are known along the brecciated contact of the granite and the slate on the Meleg Hill, in the eastern part of the granite intrusion (KUBOVICS 1958, MOLNÁR 1996; Figure 2). JANTSKY (1957) and GASZTONYI & SZABÓ (1978) have also observed occurrences of alunite and pyrophyllite in the brecciated zone of the granite. Trace elements (Mo, Ag, Pb, Cu, Sb, As Te) have also elevated concentrations in this zone. Next to Sukoró in the St-4 drillcore (Figure 3) quartz-chalcopryrite

veins have been identified: the host granite has silicic-sericitic alteration. Studies by MOLNÁR (1996) showed that petrographic and microthermometric properties of fluid inclusions from this breccia-related mineralization carry many similarities with the fluid inclusions found in the Cu-porphyrity type mineralization, east from the Nadap-line (Table 1). The phase separation of high and low salinity fluids happened at 370-460°C, which corresponds to 200-400 bar pressure under hydrostatic conditions.

On the Antónia-hill, in the vicinity of the breccia zone of the Meleg Hill another hydrothermal mineralization containing sphalerite, galenite, grey ore, chalcopyrite, molybdenite and native gold in quartz veinlets surrounded by kaolinite and alunite alteration has been found in the slate (BÖJTÖSNÉ VARRÓK, 1967), HORVÁTH et al. (1987) considers Palaeogene age of this mineralization. The granite below the slate shows chloritic, argillic, silicic and pyritic alteration with geochemical anomalies of Sn, Ag, As, and Bi.

2.5 HYDROTHERMAL MINERALIZATION OF THE SZABADBATTYÁN AREA

Hydrothermal formations of the Szabadbattyán area consist of epigenetic, Pb-(Zn) mineralizations in metamorphosed carbonates (KISS, 2003). The main mineral phase is galena which occurs typically in fractures and along the contacts to the Polgárdi Limestone Formation, as well as in small nests, pods and metasomatic replacements in the silicified limestone (Figure 4). Galena is associated with bournonite, sphalerite, chalcopyrite, tetraedrite and native silver are the dominant mineral phases (MOLNÁR & SZAKÁLL 2003). The epigenetic-metasomatic base metal mineralization has been exploited by the Romans and small scale mining was also conducted during the World War II and following years (KISS, 2003).

The Paleozoic carbonate rocks are intruded by andesitic dikes of Triassic age (DUNKL et al. 2003). Exo-skarn (diopside, predazzite, calcite) and endoskarn (garnet-epidote, clinopyroxen-prehnite and vesuvianite) surround these dikes in narrow zones, however, there is no obvious genetic relationship between the skarn formation and the base metal mineralization.

In analogy with the the Velence Mts., several hypotheses have been formulated about the origin of the epigenetic mineralization at Szabadbattyán. VENDL (1928), KOCH (1943), FÖLDVÁRI (1952) and KISS (1951) suggested relationships to the Variscan granite intrusion of the Velence Mts. KISS (1951) also considered a remobilization effect induced by the Triassic andesite dikes. VENDL (1928) and JANTSKY (1960) suggested an Eocene age for the mineralization. KISS (2003)

completed a whole revision of available geological, mineralogical and geochemical data and suggested that the mineralization at Szabadbattyán is a Mississippi-Valley type epigenetic-hydrothermal Pb-Zn ore deposit.

3. THEORETICAL BACKGROUND AND APPLIED METHODS

APPROCHE THEORIQUE ET METHODES

Il est difficile de reconstituer la chronologie des événements structuraux dans les granites car le principe de superposition ne s'y applique pas. Par ailleurs, les diaclases ne présentent pas d'indices de déplacement. Cela peut être rendu plus compliqué en cas d'altération hydrothermale qui peut effacer tout indice chronologique. Dans les roches riches en quartz, l'outil à utiliser par les géologues sont les plans d'Inclusions Fluides (FIP).

Les plans d'Inclusions Fluides (FIP) sont des microfissures cicatrisées considérées comme étant perpendiculaires à la contrainte mineure locale. Ils sont formés par des alignements d'IF secondaires témoins de circulations hydrothermales qui ont eu lieu. L'analyse de leur géométrie permet d'établir un lien entre contexte structural et écoulements fluides hydrothermaux. Les conditions P-V-T-X existantes au moment de leur cicatrisation peut être déterminée par l'étude de ces IF secondaires.

Les fractures et microfissures sont responsables de l'essentiel de la porosité dans les roches cristallines. L'analyse statistique et géométrique des FIP est indispensable pour quantifier cette porosité à échelle microscopique.

Dans une première partie il est présenté une étude détaillée de terrain. L'analyse a été réalisée le long d'une ligne de base déterminée de façon arbitraire. Différents paramètres ont été mesurés pour enrichir une base de données (type de fracture, longueur, ouverture, orientation, pendage, remplissage, distance interfracturale, ...)

Par la suite, des échantillons orientés ont été collectés pour analyser les réseaux de FIP et microfissures ouvertes. Leur analyse géométrique a été réalisée à la platine Universelle et avec le logiciel AnIma. Enfin, l'étude micro thermométrique des IF secondaires a été réalisée en tenant compte de l'orientation des FIP.

Cela a permis de calculer la porosité / perméabilité de fissures et de déterminer les directions moyennes de contraintes à partir des plans de failles et à l'aide de la méthode Angelier

(1986). La perméabilité a été calculée à partir des longueurs moyennes des fissures et de leur épaisseur. Une analyse fractale de la répartition des veines a été également faite. Cette analyse fractale a permis de déterminer les paramètres de dimension fractale pour les comparer avec d'autres systèmes de veines.

Enfin, les paramètres statistiques ont été comparés à différentes échelles et pour différents paramètres.

3.1 FLUID INCLUSION PLANES

In mechanically isotropic magmatic rocks (granite, andesite) the reconstruction of the tectonic events is often very difficult or even impossible due to absence of layering or other tectonic markers, especially if the rock has undergone multi-phase tectonic evolution, although these rock types, especially the mineralized ones have usually complex fracture systems. The characteristic macroscopic fractures are usually the joints and mineralized veins without any markers of displacement in many cases. Interpretation and correlation of the joint/vein systems is difficult and their connection to faults is often questionable.

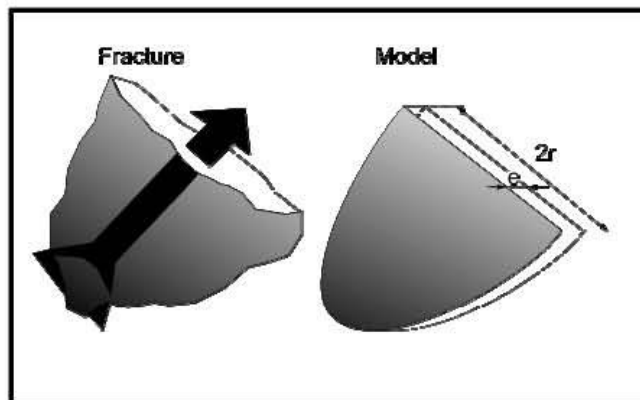


Figure 5. Model of FIP. FIP are Mode I, penny shaped extensional fractures

In magmatic rocks, the hydrothermal fluid circulation is usually related to the fissural porosity of the rock. The fissures form usually both in microscopic and macroscopic scale during the hydrothermal activity as the pore fluid pressure considerably increase the differential pressure and decrease the coherence of the rock. Often, on macroscopic scale the rock shows no sign of former hydrothermal circulation (alteration, veins, etc.), but on microscopic scale the secondary fluid inclusions in the rock forming quartz crystals or pervasive (metasomatic) alteration of

groundmass are clear evidences for the former fluid migration. In these cases, structural analysis of the fluid migration is only possible by means of the healed microfractures, particularly by the FIP.

FIP are healed fossile fluid flow channels (Figure 5). Their formation is rapid considering the geological time (LESPINASSE 1999). These microfractures represent the fluid flow pathways because they form by healing of former microfractures (CATHELINÉAU et al. 1994). Usually, FIP form during brittle tectonism and less commonly they also can be related to ductile deformation. (TUTTLE 1949; PECHER et al. 1985). Microfractures in the majority of the rock forming minerals (feldspars, carbonates) form in connection with the orientation of the twinning or cleavages, therefore the formation of the secondary FIP is not chiefly constrained by the stress field existing during the tectonic process. However, rock forming quartz is isotropic against deformation because crystallographic characters do not influence the development and orientation of microfractures in quartz (LESPINASSE & CATHELINÉAU 1990). Another importance of crystal structure independent microcracks of quartz is that they easily also preserve inclusions of fluids which are present at the time of fracture formation. The strike of microfractures will be parallel with the main tectonic axes of the stress field and thus FIP orientation reflect peculiarities of the stress field during the fluid flow (LESPINASSE & PECHER 1986; LESPINASSE & CATHELINÉAU 1990).

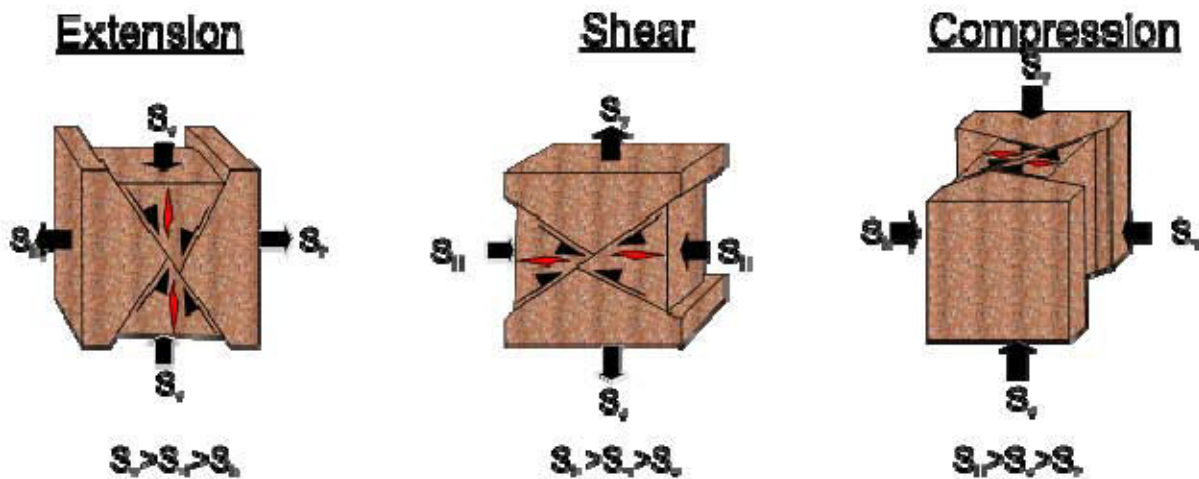


Figure 6. Main types of tectonic regimes in the upper crust and the position of FIP (red fractures) Modified after CSONTOS (1995).

More specifically, FIP are Type I fractures forming perpendicular on the σ_3 axes of the stress field and propagate in the plane which favours the maximal decrease of the total energy of the system (LESPINASSE & PECHER 1986; GUEGEN & PALCIUSKAS 1992; LESPINASSE 2002; LESPINASSE et al. 2005). FIP in the earth crust may generally have three principal orientations according to the actual stress regimes. In a compressional stress field (collisional zones), the main stress axes are horizontal ($S_H > S_h > S_v$) and the smallest is vertical, the FIP will be horizontal (Figure 6). In an extensional ($S_v > S_H > S_h$; e.g. rift zones) or transtensional ($S_H > S_v > S_h$) stress regime, FIP will be necessarily vertical (PETROV et al. 2008). If the age and and/or origin of FIP are known, then the determination of the spatial and temporal evolution of the joint and fault systems is also possible.

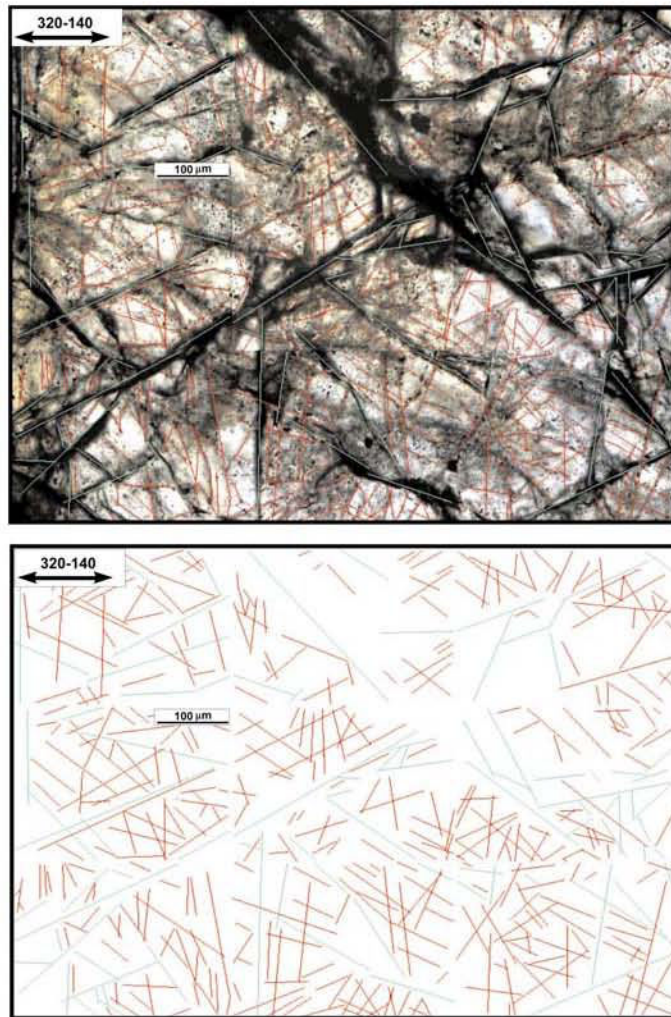


Figure 7. Mapping of FIP by AnIma in oriented thin sections. Measured parameters: FIP and OC dip direction, length, length density, number density

After the formation of the first generation of FIP, the second one will pick up a new orientation with new fluid inclusion assemblages if the orientation of stress field has been changed. In the knowledge of the crosscutting relationships of the FIP the temporal relationships, the porosity and permeability in the different orientations will be determinable ROEDDER (1984).

In addition to the fluid inclusion planes, open microcracks of quartz (OC) are also significant in the evaluation of fracture development and structural evolution in granitoid rocks, because they are part of the current porosity of the rock. OC could form by reopening of older FIP, but can also be related to younger tectonic events as well. Their geometrical analysis is crucial since they may indicate the role of re-opening the healed microcracks that were formed during the hydrothermal activity in the formation of the current micro- and macrofracture system.

Geometrical and statistical analysis of the FIP and OC has been performed in 100-150 μm thick oriented double polished thin sections. Use of relatively thick sections is crucial for the appropriate three dimensional imaging of FIP and OC and it is an additional advantage that these sections are also useful for microthermometric analyses of inclusions hosted by FIP. Image analysis of the selected thin sections has been performed at the University of Nancy by the computer code Anima, developed especially for microfracture analysis. The method of the analysis is the following: quartz crystals in the oriented thin sections have randomly been selected and photographed. Photographs were assembled to cover the surface of selected quartz crystals. The resolutions of the photographs should be adjusted to visibility of FIP and OC on them. In the second step, FIP and open microcracks are marked using the graphic functions of the programme (Figure 7). In function of the orientation of the section and the calibrated magnification of the microscope, the program determines the true orientation and length of the marked FIP and OC. The advantage of the method is the opportunity of completing relatively high number of measurements in a short period of time and the possibility to measure the length of detected fractures. The disadvantage of the method is that the dip angle of FIP in relation to the section's plane is not determinable, and the phase compositions of the individual fluid inclusions in their assemblages are not always visible with the resolution useful used for detection of FIP and OC orientations. To complete the missing geometric and petrographic information (e.g. dip direction and angle of FIP and phase compositions of their fluid inclusions), the image analysis has been supplemented by observations on the same polished sections by means of universal stage. The disadvantage of the latter method is that dip angles less than 40° in relation to the

plane of the section are not measurable and the measurement process is rather slow. The advantage of the method is that FIP and FI assemblages for further microthermometric analyses can be selected, and thus fluid inclusion microthermometry data can be coupled with FIP orientation data, i.e. fluid properties can be connected to stress field data.

Statistical analyses of data collected by methods described above included calculation of number of FIP per unit surface (number density: No/mm^2) and total FIP length per unit surface (length density mm/mm^2). These parameters are in strong correlation with the former apparent effective fissural porosity of the rock (LESPINASSE et al. 2005). It is *apparent porosity* because it is not obvious that all fractures were open and active at the same time of the fluid migration and because re-opening of FIP during superimposing hydrothermal processes are also highly possible. It anyway reflects the *paleoporosity* as the FIP are healed and therefore fluid migration through these channels currently is impossible. It is *effective* since markers of the former fluid flow, the fluid inclusions – small drops of the hydrothermal fluid – are present in the fractures so during the fluid flow these fractures were interconnected with each other and the root of the hydrothermal system.

It is important to note that the porosity and the permeability of the rocks are exclusively influenced by the microcracks. Grain boundaries, cleavages are also important, however fluid inclusions along grain boundaries of the granite were not studied, because intergranular fluid inclusions usually do not preserve their original fluid contents due to ease of fluid migration along grain boundaries (ROEDDER 1984).

3.2 FLUID INCLUSION STUDIES: PRINCIPLES AND METHODS

The first and very important part of the fluid inclusion studies is the fluid inclusion petrography. During the fluid inclusion study two characters of fluid inclusions are observed; their origin and assemblage.

Fluid inclusions can be primary or secondary of origin. Primary inclusions are entrapped during the crystallization of the mineral and therefore the fluid in the inclusions represents the composition of the hydrothermal fluid from which the mineral crystallized. They mostly occur along growth zones or as individual inclusions or clouds. Secondary inclusions are captured along fractures in the mineral, and thus they may form FIP. Their formation could happen any time *after* the crystallization of the mineral. They can form the same fluid from which the mineral

crystallized but can be related to any younger hydrothermal fluid migration event with different composition.

Since the recognition of petrographic characteristics is fundamental during the microthermometric work, single fluid inclusions were never analysed during this work. Microthermometric analyses were always performed on fluid inclusion assemblages (FIA), e.g. on assemblages of fluid inclusions which were in the same FIP. This principle was also used for primary inclusions of vein filling minerals.

Regarding the phase state of the hydrothermal system and the type of the entrapment different possibilities are distinguished:

- If the hydrothermal fluid is homogeneous, the trapping in inclusions is homogeneous. In this case the phase ratios observed on room temperature are equivocal in the inclusions in the same assemblage.
- If the hydrothermal fluid is in heterogeneous phase state (boiling), two possibilities are distinguished:
 - Homogeneous trapping from the heterogeneous system (only liquid or only vapour in individual fluid inclusions)
 - Inhomogeneous trapping from a heterogeneous system (trapping of liquid+vapour±solid phase or trapping of two non-mixing, different type of fluids (e.g. aqueous and carbonic phases))

Petrographically, in a set of fluid inclusions which trapped from a boiling (heterogeneous) fluid the phase ratios (the ratio of the aqueous vapour: V_{aq} and aqueous liquid: L_{aq} phase) observed on room temperature are always highly variable.

During the fluid inclusion microthermometry, eutectic (first melting) temperature (T_e), final melting temperature (T_m) and homogenization temperature (T_h) were determined in the case of the aqueous inclusions. Eutectic temperatures are characteristic values for composition of electrolyte solutions, therefore its determination defines the type of the salt which is present in the fluid (e.g. $-21,2^\circ\text{C}$ is the eutectic temperature of the H_2O - NaCl system, -52°C is the eutectic temperature of the NaCl - CaCl_2 - H_2O system). Final melting temperature of ice is in proportion with the amount of the dissolved salt in the fluid, therefore the T_m defines the salinity of the fluid which is expressed in e.g. NaCl equiv. wt% or CaCl_2 equiv. wt%. Salinities were calculated by

using the equations of BODNAR & VITYK (1994) for NaCl-type fluids and data from OAKES et al. (1990) for NaCl+CaCl₂ and CaCl₂ type fluids.

If the inclusions contains daughter halite phase (H), the salinity is calculated from the melting (dissolution) temperature of the halite by means of the equation of BODNAR & VITYK (1994).

Homogenization temperature defines the *minimum* trapping temperature and pressure of fluid inclusions in the case of homogeneous trapping from a homogeneous fluid. These inclusions could have trapped anywhere along their isochors. Calculation of true trapping conditions can be made by intersecting these isochors with temperature or pressure data gained from independent geological barometers or thermometers (e.g. thermometers bases on isotope fractionation, barometers bases on composition of coexisting minerals etc.).

Minimum of homogenization temperatures defines the true trapping temperature in case of entrapment of inclusions from a heterogeneous (boiling) parent fluid. Minimum values should strictly be considered because of the possibility of inhomogeneous entrapment of coexisting phases (BODNAR 2003). Pressure of boiling was calculated by the equation of ZHANG & FRANTZ (1987).

Carbon dioxide bearing aqueous fluid inclusions may contain three phase at room temperature: a carbonic liquid (L_{car}), a carbonic vapour (V_{car}) and aqueous liquid (L_{aq}) phase. During microthermometric analyses of these inclusions, determination of melting temperature of the carbonic phase is crucial because deviation from the ideal melting temperature (triple point) of the CO₂ system at -56,6°C indicates the presence of other additional volatiles (CH₄, N₂, H₂S) in the inclusion (BURRUSS 1981). Presence of additional volatile components was checked by Raman microspectrometry. The melting temperature of the clathrate phase (T_{mCl}; if it is lower than the ideal 10,1°C T_{mCl} of the pure H₂O-CO₂ system) is in correlation with the salinity of the inclusion (COLLINS 1979). Salinities were calculated from clathrate melting temperatures for inclusions in which carbonic vapour and liquid phases were present at the time of clathrate melting (DIAMOND 2003). The homogenization temperature of the CO₂ liquid and vapour phases is useful for density estimation of the carbonic phase. The calculation for the bulk composition of the carbon dioxide bearing inclusions based on estimation of phase volumes and microthermometric data was carried out according to BAKKER (2003).

Microthermometric studies were carried out using a Chaixmeca MTM90 type apparatus standardised for $\pm 0,1^{\circ}\text{C}$ reproducibility below 0°C and $\pm 1^{\circ}\text{C}$ reproducibility on high temperatures. The Raman microspectrometer is Labram (Horyba–Jobin Yvon) which was equipped with a Edge filter, a holographic grating with 1800 grooves per millimetre, a liquid nitrogen cooled CCD detector. The exciting radiation at 514.5nm is provided by an ionized Argon laser. The laser is focused on the sample using an X80 objective (Olympus) for these analyses.

3.3 METHODS OF ANALYSIS OF HYDROTHERMAL VEIN NETWORKS, JOINTS, FRACTURES

Hydrothermal veins – similar to the FIP – usually form perpendicular to the minimum stress field axis in homogeneous rocks (TOSDAL & RICHARDS 2001). In a deformed rock body rich in fractures, the fluid mobilization is constrained by the pre-existing faults and joints. Formation of hydrothermal vein network fundamentally influences the character of the mineralization therefore the geometrical analysis of hydrothermal vein systems yields important additional information on the understanding of the formation of economically important mineral deposits.

In a well-developed, broad and well-connected fracture system, huge amounts of hydrothermal fluids may be transported. The physical-chemical conditions of the fluid (composition, pressure, temperature) may change in short distances but the fluid/rock interaction has a less important role (because of sealing of veins' walls by the early mineral precipitation in the vein). Rapid physical changes – fluid mixing, phase separation, pH, redox, saturation etc. – within the fracture is the principal factor in mineral deposition. If the system is characterised by few but well connected fractures, the possibility of formation of high grade deposits increase because this kind of system provides focussed fluid flow (COX et al. 2001).

If the mineralizing fluids migrate along cleavages, microfractures or along grain boundaries (e.g. failing any main fluid flow channel), the fluid/rock interaction will play a major role in the formation alteration of host rock and formation of an ore deposit. Depending on the composition of the fluids (e.g. cation ratios, pH, oxygene and sulphur fugacities etc.) and mineralogy of the wall rock, the geochemically sensitive elements will precipitate and disseminated or stockwork type mineralization will form.

For the reason provided above, it is important to investigate not merely the mineralogical and geochemical properties of the alteration zones within a hydrothermal system, but the geometrical properties of the fractures and veins as well.

To be able to compare the macroscopic data of fissures to each other and to the microscopic data of FIP and OC, field analysis has been carried out along selected base lines in rock exposures of the Velence Mts. Setting up base lines in these outcrops was not merely random: they were selected in order to provide representative sections of the rock unit under investigation. Along these horizontal base lines, the following characters of the veins, fractures, faults observable on the field were described (Figure 8):

- distance from the origin of the base line
- dip angle and dip direction of the macroscopic plane (joint, vein fault)
- slickenside orientations of fault planes
- thickness, length, type (joint, fault, magmatic/hydrothermal vein, mineral infilling of the hydrothermal veins)
- alteration of host rock around the fracture
- strike of the base line at the observation point (crosscutting point of planar element of the rock with baseline)

The created database was useful for preparation of different statistical calculations. The stress field analysis has been done by the method of ANGELIER (1986).

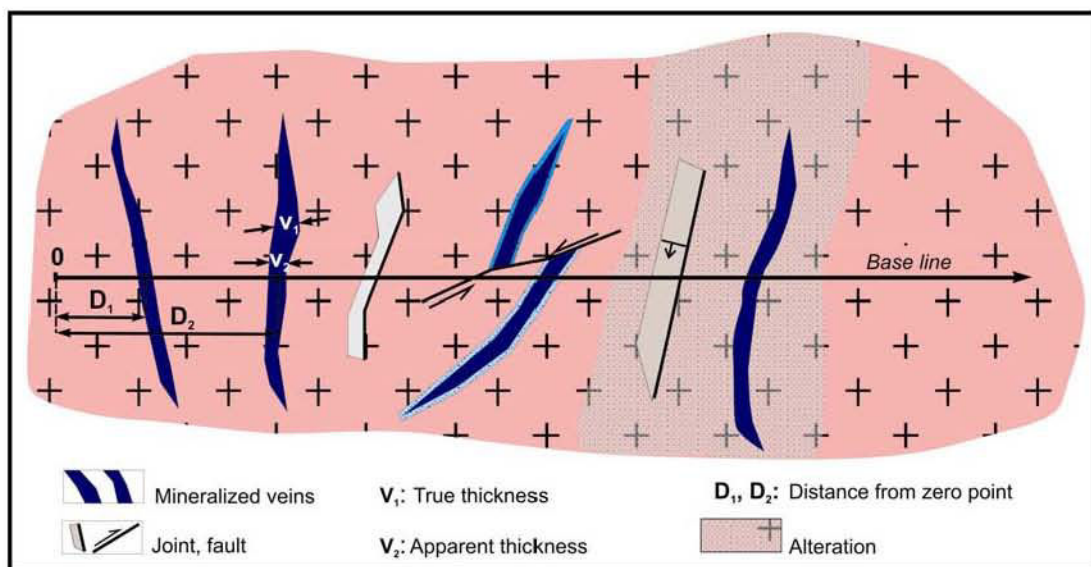


Figure 8. Method of field analysis (theoretical section)

The apparent permeability during the hydrothermal circulation of the rock is possible to be calculated on the basis of the thickness and distance data for the hydrothermal veins, according to the following equation (SNOW 1969):

$$K_m = (g/12\eta) * (A_m^3/S_m),$$

$$S_m = 1/N_m * \sum s_{m,k}$$

where g is the accelerating coefficient (9.81 m/s^2), η is the kinematic viscosity of the hydrothermal fluid ($10^{-6} \text{ m}^2 \cdot \text{s}^{-2}$), A_m is the average thickness of the veins, S_m is the average distance between the veins, N_m the number of the veins, and $s_{m,k}$ is the distance between the $k-1$ and $k+1$ veins.

3.4 FRACTAL ANALYSIS OF HYDROTHERMAL VEINS

Determination of the connectivity of three vein systems and their comparison were done by fractal analysis studies. In the theoretical geometry, any kind of forms can be built up by infinitively fine structure which bear over self-similar characters. In other words, the smallest parts of the form are similar to the whole. The most common and well-known figure incorporating this self-similarity is the Cantor set, which can be constructed from the $[0;1]$ closed interval. In the first iteration we take the middle third of the interval, the left over thirds remain closed. In each following iteration the same procedure is repeated by the middle third. At the end of the iteration n the number of sections is 2^n (TÉL & GRUIZ 2002). Forms built up like this iteration (Koch curve, Sierpinsky triangle) have been called fractals by MANDELDROT (1983).

Self similar sets are rather common in the nature because fractals form during complicated and often arbitrary processes. Examples are for instance river coasts, geometry of a river system, margins of the clouds, the foliage of the trees and the amplitude of earthquakes. Enlarging the smallest parts of these systems, the small portions of the figure resemble on the total, however, they are never the same. Of course, in the nature the number of iterations is finite meanwhile the number of iterations is infinite in case of the mathematical (theoretical) fractals.

In geology, formation of fractures, veins, and faults can be characterised by fractal geometry. By means of the fractal analysis of the vein network, their evolution and connectivity can be investigated. Value of the fractal dimension also carries other important geological information.

GILLESPIE et al. (1999) has constructed synthetical data sets for veins with known vein thickness and distance. The data sets were analysed by different statistical methods and were compared with measured natural data sets. They have constructed the following models:

-in the *periodic model* the veins are evenly distributed and have equal thickness.

-in the *Poisson model* the thickness and distance of the veins is random

-in the *Kolmogorov/power-law model* a line is taken. The line has a break (vein) at a random position, the resulting two fragments are again randomly bisected and the process iterated. The first vein is the thickest and the thickness of the next generation is decreasing by a constant value, *b*. Value of *b* has been taken as 0,3716, based on analysis of natural data sets.

-in the *fractal/power-law model*, both vein thicknesses and distances of veins have power law distributions. The term power-law is used to describe a statistical distribution and the term fractal to describe a geometry.

GILLESPIE et al. (1999) used the following statistical methods to characterise the above listed artificial data sets.

Staircase plot: Cumulative vein thickness is plotted versus distance along the sample line with a vertical line positioned on the centre of each vein. The gradient of a staircase plot is the measure of the extensional strain accommodated by a vein array and the irregularity of the curve is a measure of the heterogeneity of the strain.

Cumulative frequency of vein thickness plot: True vein thicknesses or distances are plotted versus their cumulative frequencies on log-log axes. Straight lines on this plot, as provided by the Kolmogorov and fractal models indicate a power law relationship of the form:

$$N_t \propto t^{-D_m}$$

where, N_t is the cumulative number and $-D_m$ is the slope of the line (fractal dimension).

If $D_m > 1$, than the vein system is dominated by several thin veins, while $D_m < 1$ is dominated by long and thin veins. With analysis of vein arrays at ore deposits ROBERTS et al. (1998) has established the correlation between the value of the fractal dimension and the degree of alteration and type of mineralization.

Cumulative frequency of vein distance plot: Just like in the case of the vein thicknesses, if the slope is straight, vein distributions have fractal clustering, belong the fractal/ power-law or the Kolmogorow/power law otherwise they are random or evenly distributed. The dip of the slope

line is D_s , which is the fractal dimension of the 1D spacing distribution (MANDELBROT 1983). A low value of D_s implies high degree of clustering and the theoretical maximum value of D_s for a line sample is 1.

Variational coefficient: this parameter is used to determine the degree of clustering of points along a line. The coefficient of variation in a line sample, C_v is defined as the ratio of the standard deviation to the mean value of the spaces of veins

$$C_v = \frac{SD(s)}{M(s)}$$

where, $SD(s)$ is the standard deviation and $M(s)$ is the mean of the spaces of veins

Value for C_v in the Periodic model for all thicknesses is 0, whereas $C_v=1$ in the Poisson model. If the veins are clustered $C_v>1$ while if they are anticlustered then $C_v<1$.

As a summary we can conclude that by means of the analysis of the macroscopic parameters of the mineralised veins along a base line, important parameters can be deduced regarding the evolution of the channels of the hydrothermal fluid flow. Just like in the case of the FIP, never the absolute values of the permeability, clustering, fractal behaviour and dimension are important, but the relative values and the deduced tendencies. Fractal dimensions and properties can also be indicative for the type of the mineralization, as it was discussed by ROBERTS et al (1998).

3.5 CLAY MINERAL STUDIES: SAMPLE PREPARATION, METHODOLOGY

The various alteration zones in the granite body of the Velence Mts. have rather different mineralogy, however, their common and most profound feature is the argillic alteration of the granite. Types and varieties of clay minerals are sensitive to the conditions of fluid/rock interaction, therefore their systematic mineralogical characterization is a useful tool to make distinction among different parts of a hydrothermal system or among superimposing hydrothermal events.

For the purpose of clay mineralogical studies, samples have been collected from all characteristic alteration zones of the Velence Granite. After mild hand crushing and sieving, the <0,05mm size fraction was decanted in water columns. After 200 minutes settling time, the upper 5 cm, and after 380 minutes the upper 10 cm of the suspension has been sampled. Using this

method, the $<2 \mu\text{m}$ size clay fraction has remained in the separated liquid only. In some samples, the whole fraction precipitated after a few minutes (10 min) on the bottom of the columns due to coagulation of clay particles. These samples were sampled after 5 minutes settling time.

The separated suspension has been centrifuged (5 minutes) and the high density portion has been precipitated on glass slides in order to achieve oriented settling of clay particles. The oriented samples were analyzed by Siemens D-5000 (crystal monochromator, 41 kV accelerating-voltage, Cr-filter) X-ray diffractometer at the Department of Mineralogy at Eötvös Loránd University. On the same representative samples, Fourier-transformed infrared spectroscopic (IR) measurements have also been carried out at the Department of Organic Chemistry, at the ELTE University. Infrared spectra were recorded at a resolution of 4 cm^{-1} in the $4000\text{-}650 \text{ cm}^{-1}$ spectral range with a Bruker Equinox 55 FTIR spectrometer equipped with a liquid N_2 -cooled MCT detector and a PIKE single-reflection diamond ATR (attenuated total reflection) unit. As in case of attenuated total reflection measurements the penetration depth is inversely proportional to the wavenumber, the spectra were normalized to a constant penetration depth using the $\text{ABS}=1000 \cdot \text{ATR}/\text{wavenumber}$ conversion formula, the resulting absorbance spectra being finally transformed to transmittance units.

Characterization of the illite phase has been done according to SRODON (1984). In the structure of the illite, variable amount smectite layers with variable degree of ordering can be interlayered. If the amount of smectite layers exceeds 50%, the ordering is random, and the illite is classified into the R0 category. In case of 25-50% interlayering, the ordering is statistical and the illite is R1 type, whereas less than 25% interlayering means that the illite is highly ordered and is called R3 or $R \geq 3$ type illite. To determine the amount and quality of smectite layers in the illite fraction we used the methods of SRODON (1984) and EBERL et al. (1987; Scherrer method, Ir (intensity ratio), position of (002) and (003) peaks, infrared spectroscopy (IR)).

Kandite group minerals can be identified by the peaks at 7 \AA (001); $3,5 \text{ \AA}$ (002) and $2,34 \text{ \AA}$ (003) on the XRD pattern. Their distinction from the chlorite is based on the presence of the 14 \AA peak and the disappearance of the peaks after heating up to 500°C . The discrimination of polymorph modifications in the kandite group by XRD analyses is difficult due to the possible presence of quartz and K-feldspar in the separates. Because the formation of the different kandite phases in hydrothermal systems is temperature dependent, it had a great importance their exact determination. Therefore IR-spectroscopic studies were also performed on kandite-mineral

bearing samples. Typical peaks of dickite on the IR spectra are at 3627, 3622, 1117, 1002, 913, 796, 754, 693 cm^{-1} , the nacrite has peaks at 3628, 3620, 1118, 1001, 913, 798, 754, 694 cm^{-1} while the characteristic peaks of kaolinite are at 3694, 3621, 1100, 1032, 1008, 913, 694 cm^{-1} (VAN DER MAREL et al 1976).

Smectite has been identified by the occurrence of peaks corresponding to 14Å lattice distance of (001) on the XRD pattern. This peak moves to 17 Å after ethylene glycole solvation and back to 10Å after 10 hours heating at 250°C of the glycolated sample. The differentiation of trioctahedral and dioctahedral smectites is based on their (060) lattice distance. If it is larger than 1,53 Å, the mineral is trioctahedral, whereas if the (060) peak is between 1,49 and 1,52Å, the smectite is dioctahedral (NEMECZ 1973).

The crystallinity index of dioctahedral smectites was determined by the “v/p” semi-quantitative method of THOREZ (1976). Well crystallized and therefore hydrothermal smectites have v/p ratios close to 1, whereas these ratios are close to 0 in weakly crystallized (detrital) smectites. As the v/p ratio is not independent from the amount of smectite phase in the sample, the v/p ratio is only an estimation for the degree of smectite crystallinity. (THOREZ 1976).

3.6 RADIOACTIVE AND STABLE ISOTOPE STUDIES

K-Ar age determination has been completed at the Nuclear Research Laboratory of the Hungarian Academy of Sciences, in Debrecen. The analytical method is discussed in details by BALOGH (1974, 1975). Age determination has been carried out on rock forming and hydrothermal minerals. In the granite of the Velence Mts., illite was the only useful hydrothermal mineral phase for K-Ar age determination. Illite was present in all alteration zones therefore its age determination was beneficial to determine the temporal relationships of the different alteration zones. Age determination has also been done on rock forming K-feldspars of the granite in order to determine the last (hydro-)thermal event(s) in the granite. K-Ar radiometric age of andesite dikes was measured on whole rock samples and on separated plagioclase and amphibole mineral fractions.

Lead isotope measurements have been done on galena crystals from the base-metal veins of the Velence Granite. Most of these samples were selected from the Mineral Collection of the Department of the Mineralogy, Eötvös Loránd University, Budapest. The galena were dissolved

in 7M nitric acid, and lead was purified using electrodeposition. The analyses were carried out at the Swedish Museum of Natural History, Stockholm, using a Finnigan MAT261 thermal ionization mass-spectrometer (TIMS) and a Micromass IsoProbe ICP-MS instrument. Mass bias corrections were accounted for by using an internal Tl normalization, and NBS 981 were run repeatedly to secure data accuracy. Typically, the precision (2σ error) of Pb runs is $\pm 0.10\%$ or better. Lead isotopes are usually used to outline the source of lead in the ore, to detect remobilization processes and – in some special cases – to determine the model age of the mineralization. In the Velence Mts. the possible source rocks of the quartz-fluorite-base metal mineralization were studied and the results indirectly indicate the age of the mineralization only.

For sulphur isotope analysis, sulphide minerals were prepared by handpicking from bulk ore samples of the quartz-fluorite-base metal veins. Samples were selected from the Mineral Collection of the Eötvös Loránd University. These samples were not identical with the samples of the Pb isotope analysis. The isotope composition of galena and sphalerite was measured at the Department of Geochemistry of the University of Tübingen, by combustion isotopic ratio-monitoring mass spectrometry (C-irmMS) as described by GIESEMANN et al., (1994). The analysis involved a Carlo Erba EA 2500 elemental analyzer connected to a Finnigan MAT Delta Plus XL mass spectrometer via a Finnigan Conflo II split interface. Results are expressed in the conventional δ notation [$\delta^{34}\text{S} = (R_{\text{sa}}/R_{\text{st}} - 1) \cdot 1000$, where R_{sa} and R_{st} are $^{34}\text{S}/^{32}\text{S}$ ratios in the sample and the standard, respectively] as permil (‰) relative to V-CTD. Reproducibilities are better than 0.3 ‰.

4. RESULTS

4.1 DELINEATION AND CHARACTERIZATION OF SUPERIMPOSING HYDROTHERMAL PROCESSES ON THE BASIS OF CLAY MINERALOGY IN THE ARGILLIC ALTERATION ZONES OF THE VELENCE GRANITE

ANALYSE DES PHASES MINERALES ARGILEUSES

Les dikes andésitiques intrusifs ainsi que le granite présentent des alterations argileuses. Leurs relations génétiques ont été pendant longtemps mal connues, de nombreux auteurs reliant ces alterations argilitiques au système hydrothermal post magmatique en les appelant alteration berésitique. Dans ce travail, un échantillonnage systématique des zones altérées a été réalisé en la distinguant les phases minérales argileuses.

L'illite est le principal minéral argileux des zones altérées dans la partie Est du granite, dans et autour des Andésites dans les zones structurales et les brèches hydrothermales. L'altération argilitique est associée aux veines de quartz, à la silicification et à la pyritisation de l'encaissant. Cette illitisation est pénétrative et se substitue aux phases minérales initiales à l'exception du quartz magmatique. L'illite est bien cristallisée de type R3 avec de la smectite interstitielle.

L'altération à illite-dickite est présente en proximité des dikes brechiques hydrothermaux, dans quelques porphyries et plus généralement en proximité des dikes andésitiques. C'est une altération pénétrative avec une illite bien cristallisée. Elle est de couleur rosée à jaune. Les données XRD et Infra Rouges montrent la présence de Dickite qui est un polymorphe de haute température de la kaolinite.

L'altération à Illite-kaolinite-smectite est présente dans le granite mais se localise dans des structures NE-SW et en proximité des dikes à quartz-fluorite-polymétalliques.

Les principales phases minérales des zones altérées sont remplacées par des assemblages verdâtres à biotite- plagioclase-feldspaths potassiques. L'illite est bien cristallisée mais les inter lits de smectites dans la structure cristalline sont plus denses que l'illite ou les assemblages illite-kandite. La kandite est de la kaolinite qui est une de ses modifications de basse température. La phase minérale dioctaédrique est probablement de la montmorillonite.

Dans les systèmes hydrothermaux, les assemblages de minéraux argileux permettent la détermination des températures et Ph (Fig 15).

L'illite est stable autour de 240°C et parfois en dessous de 200°C. La température des circulations hydrothermales était aux environs de 240°C dans et autour des Andésites, des veines de quartz-barite et dans les brèches illitisées.

La Dickite est une modification de haute température du groupe minéral des Kandite et se forme entre 140 et 250°C. Cette valeur de température se surimpose avec le champ de stabilité des illite entre 200-240°C. L'altération des brèches hydrothermales jaunes rosées a lieu à basse température.

La kaolinite est une modification de basse température des kandites et se forme vers 200°C comme les smectites. Concernant les assemblages illite-kaolinite-smectite il y a deux possibilités: elles se forment à 200°C ou alors l'illite se forme en premier à haute température et plus tard, avec le refroidissement des fluides hydrothermaux, les smectites et kaolinites cristallisent. Le second schéma semble plus probable si on considère que l'illite est de type R3 avec de faibles inclusions smectitiques suggérant une plus forte température de formation.

4.1.1 The aim of the clay mineral studies and previous studies

One of the most obvious evidence for fluid-rock interaction is the argillic alteration in hydrothermally altered magmatic rocks. Argillic alteration often affects much larger rock volumes than the mineralized veins. Clay minerals are sensitive to temperature and pH of fluid/rock interaction and K-bearing species such as illite can also be used for radiometric age determination. Therefore mapping of clay mineral alteration zones and mineralogical studies on clay mineral assemblages are useful tools for delineation of aerial extent of hydrothermal systems as well as for determination of the age, temperature and some chemical properties of the hydrothermal processes.

The Variscan granite intrusion of the Velence Mts. has undergone, intense argillic alteration in their various parts. In spite of this easily recognizable feature on the field, previous studies on the hydrothermal formations mostly focused on the mineralogy and geochemistry of the quartz-fluorite base metal veins hosted by the Variscan granite and on the Cu-porphyry-epithermal system hosted by the intrusive-volcanic complex of Palaeogene age. Nevertheless, the products of the fluid-rock interaction, the broad argillic alteration zones have much more

significance from the point of view of the evolution of the fluid flow history than the narrow zones of mineralized veins.

Among the few previous investigators of the clay mineralogy in the Velence Granite, NEMECZ (1963) described three clay mineral phases: the illite, kaolinite and montmorillonite in the alteration zones in the western part of the granite body and found that ratios of these minerals are highly variable at different localities. He concluded that the variation in the clay mineral assemblages is more characteristic for volcanic-hydrothermal systems than for deep-seated granite intrusions, therefore they might rather be related to the Palaeogene volcanic activity known in the eastern part of the Velence Mts.

JANTSKY (1957) suggested that argillic alteration of granite is a typical “beresitic, autometasomatic” type, just like in the granites at Berezovsk, Russia. He recognized that there is a difference in the clay mineral assemblages of the eastern and the western part of the granite, but he explained these differences with the regional differences in the intensity of the fluid flow. He postulated that the argillic alteration is regionally typical in the granite and in spite of mineralogical variation, clay mineral assemblages are syngenetic with the quartz-fluorite-base metal veins.

4.1.2 Argillic alteration in and around the andesite dikes of Palaeogene age and hydrothermal breccias hosted by the granite around the quartz-barite hydrothermal veins

Argillic alteration within the Palaeogene andesite dikes intruding into the granite is definitely of Palaeogene age or younger and argillic alteration zones in the granite centred on these dikes are clear evidences of fluid flow event(s) affecting the granite at the time of the Palaeogene volcanic activity (Figure 14). Since the emplacement of andesite dikes and stocks into the granite has a well defined structural pattern, the same tectonic conditions may be applicable for the argillitization around them.

In the granite and granite porphyry dikes, except for the rock forming quartz, all rock forming minerals and the groundmass altered to white clay mineral mass along the andesite veins of Palaeogene age (Photoplate 1/A). In some andesite stocks, the alteration is similarly pervasive, the porphyryc minerals, the feldspars and the groundmass are all replaced by white clay minerals. The argillic alteration, related to the andesite dikes forms usually a 50-100 m broad alteration

halo around or parallel to the intrusions. The argillic alteration is accompanied by silicic alteration and disseminated pyrite alteration in some structurally controlled, NE-SW trending zones of the altered host rock.

There is a quartz-barite vein located in the Nadap-Sukoró area of the granite body. The characteristic alteration around the vein in the granite contains white clay mineral. Occurrence and the degree of the alteration is the same as in the case of the argillic alteration around the andesite dikes.

Hydrothermal breccia veins occur in the Nadap-Sukuró area of the granite, on the Gécsi Hill. The breccia is matrix supported, the matrix is white clay mineral, the fragments are rock forming quartz crystals and granite clasts up to 2-3 cm. Occurrence of the breccias is sporadically on the Gécsi Hill. Both the matrix of the breccia and the fragments are entirely altered to white clay material, like in the case of andesite dikes. Strike of these breccias is NE-SW and ENE-WSW. While the alteration is complete in the breccia, the alteration in the host rock around the breccia (0,5-1 m) is weak and apart from the dikes the agillitization of granite diminishes. According to the occurrence and the texture this breccia type is considered to hydrothermal breccia.

In the Nadap-Sukoró area of the granite on the margin of the granite and the PVU and close to the andesite dikes (on the Gécsi Hill and the Meleg Hill; Figure 14) hydrothermally altered breccia veins can also be found in the granite and in the slate. Their length thickness and structural control was not possible to determine, as they were found in debries. The argillic alteration is typical both for the breccia matrix and for the breccia fragments the breccia is clast-supported, the breccia fragments are up to 10cm. The breccia fragments are strongly altered granite clasts or mica-schist clasts, which originate from the granite hosting slate (Photoplate 1/C). The matrix is yellow, white or pink, the fragments are angular. The texture of the breccia indicates that this type of breccia is of hydrothermal origin as well.

Similar alteration also occurred in the granite and granite porphyry dike without brecciation, in the Nadap-Sukoró area. The clay was whitish-yellowish, and the whole rock was altered except for the rock forming quartz crystals. The zone of alteration in the granite porphyry is only in a few metre thick but its structural control was not obvious on the basis of the field analysis. The yellowish-whitish clay mineral alteration features the broader vicinity of the andesite dikes and the illite alteration zones.

White clay minerals in the argillic alteration zones of andesite dikes and in the matrix supported hydrothermal breccia veins of the Gécsi Hill are well crystallised: clay mineral particles are 10-15 μm large and long needle-like (Photoplate 1/B.). The settling of the material during sample preparation (sedimentation) was therefore very fast. Because of the very fast sedimentation of clay particles, separation of the quartz from the clay minerals was not always possible. A few sharp and high peaks characterize the XRD patterns with peaks at (001): 9,91-10,32 \AA , (002): 4,97-5,02 \AA , (003): 3,31-3,33 \AA (Figure 9/A). The position of the 10 \AA peak changed neither after ethylene-glycol solvation nor after heating up to 500°C. Since intensity ratio of the (001) and (002) peaks ($I(001)/(002)$) changed between 3,77 and 5,22 versus the 0,7-1 values – which is typical for the sericite – the mineral is illite (THOREZ 1976). On the basis of SRODON'S (1984) classification criteria's – (002) (003) peaks diagram – the clay mineral in these alteration zones is also pure illite. Due to the half height-width peaks at 17 as well as at 26 \AA the interstratified amount of the smectite is below 5% (Figure 13A).

According to the intensity ratios (I_r), the values are the same in the case of two samples. With three other samples the degree of interlayering is 4-5% lower (Figure 13C). The correlation between the two data sets (I_r and half-height width) is high ($R=75\%$). The characteristic peaks of the IR (Figure 12 and 13B) in two samples yielded 4-5% lower, and in an other sample the same value as it was calculated by the half-height width (Table 2 and Figure 13). According to all methods the illites have statistically ordered smectite interstratification, which is below 5% and the clay mineral is therefore *R3 type* illite.

The clay particles in the *yellowish-whitish* alteration zone (granite, granite porphyry and clast supported breccia veins) in the Nadap-Sukoró area are also relatively coarse grained (Photoplate 1D) The XRD patterns are also poor in peaks as well, but next to the peaks of the illite (10 \AA , 5,01 \AA , 3,34 \AA , 2,5 \AA , 2,00 \AA), the characteristic reflections of kandite group minerals also appear at 7,1 \AA (001), 3,56 \AA (002) (Figure 9B). After ethylene-glycol solvation, the position of the peaks did not change, however after heating up the samples to 500°C temperature the 7,1 \AA peak collapsed which is characteristic for kandite minerals.

The ratio of the (001) and (002) peaks of the illite varies between 2,5 and 3,5, thus they are illite and not sericite (THOREZ 1976). Based on the (002)-(003) diagram the smectite interlayering remains below 5% (Figure 13A), interstratification calculated from half height width is $5\pm 1\%$, except for one sample where it was 10%. The I_r values systematically under-

(Figure 13C), meanwhile the IR values overestimate (Figure 13B) the amount of smectite in contrast with the Scherrer-method, but the difference is not higher than 5%. Illite in this assemblage is *R3 type* with ISII ordering.

The IR patterns (Figure 12) confirmed that the kandite group mineral in these samples is dickite, but in one sample the peaks of the nacrite were also present.

4.1.3 Argillic alteration around the quartz-fluorite-base metal veins and regional argillic alteration of granite

The quartz-fluorite-base metal veins are always surrounded by a pervasive greenish-whitish argillic alteration of granite. Occurrence of the greenish-white clay mineral alteration assemblage is also regionally characteristic for the granite (Figure 14) in the granite porphyry and the in the aplite dikes. The degree of alteration varies in the granite. In weakly altered zones, mafic rock forming minerals (amphibole, biotite) are decomposed to clay minerals only. In more intensely altered zones, plagioclase is also altered, and finally the K-feldspar is also totally altered to greenish-white clay mineral mass in the most intensely argillitized zones (Photoplate 1/E.). The most intensive alteration occurred in the aplite dikes and in the groundmass of the granite porphyry dikes. The alteration is generally strongly constrained by 20-30 m broad, NE-SW trending fault zones. At some places, this kind of argillitisation also appears as fracture filling in N-S and NE-SW trending joints and along faults. Silicification of various degrees is also present in these zones. In the most altered, and structurally controlled central zones of the alteration occurrence of cellular textured quartz veins and silicification are common. During argillic alteration free silica forms from the silicates which precipitated in form of narrow silica veinlets and bodies. This type of alteration is absent in the andesite dikes, moreover there is no spatial correlation between the location of the andesite dikes and this type of alteration. Therefore this clay mineral assemblage was certainly produced by a fluid-rock interaction that developed in a hydrothermal system independent from the emplacement of andesitic dikes. These results of recent observations suggest that this kind of argillic alteration is connected to the formation of the quartz-fluorite-base metal veins.

The slow velocity of falling out of clay particles from the suspension indicated that the particle size of this type of clay mineral assemblage is below 2 μm (Photoplate 2/F). Based on the XRD analysis carried out on air-dried oriented samples illite, kandite and smectite forms the

assemblage (Figure 9C). After ethylene-glycol solvation and heating up to 500°C temperature the peaks of the illite did not change (Figure 10A and B). The characteristic peaks of the kandite phase disappeared after heating to 500°C (Figure 10B). The 14 Å peak of the smectite moved to 17 Å after EG solvation (Figure 10A) but after the heating, it moved back to 10 Å (Figure 10B). Since the (060) peak was between 1,19 és 1,52 Å the smectite is dioctahedral.

In all samples the intensity ratio of the 10 Å phase falls between 1,92 Å and 3,5 Å, thus samples contain illite Thorez (1976) and not sericite. On the (001)-(002) diagram they are in the field of the pure illite (Figure 13A). The smectite interstratification calculated from the Ir ratio is equivalent with those estimated from the values on half height width, with 98% of confidence (Figure 13C). The IR method overestimates the smectite incorporation into the illite structure in function of the Scherrer-method, but the difference is lower than 3% (Figure 13B). According to all methods the smectite interlayering in the illite is lower than 25% and the illite is ordered, *R3 type*.

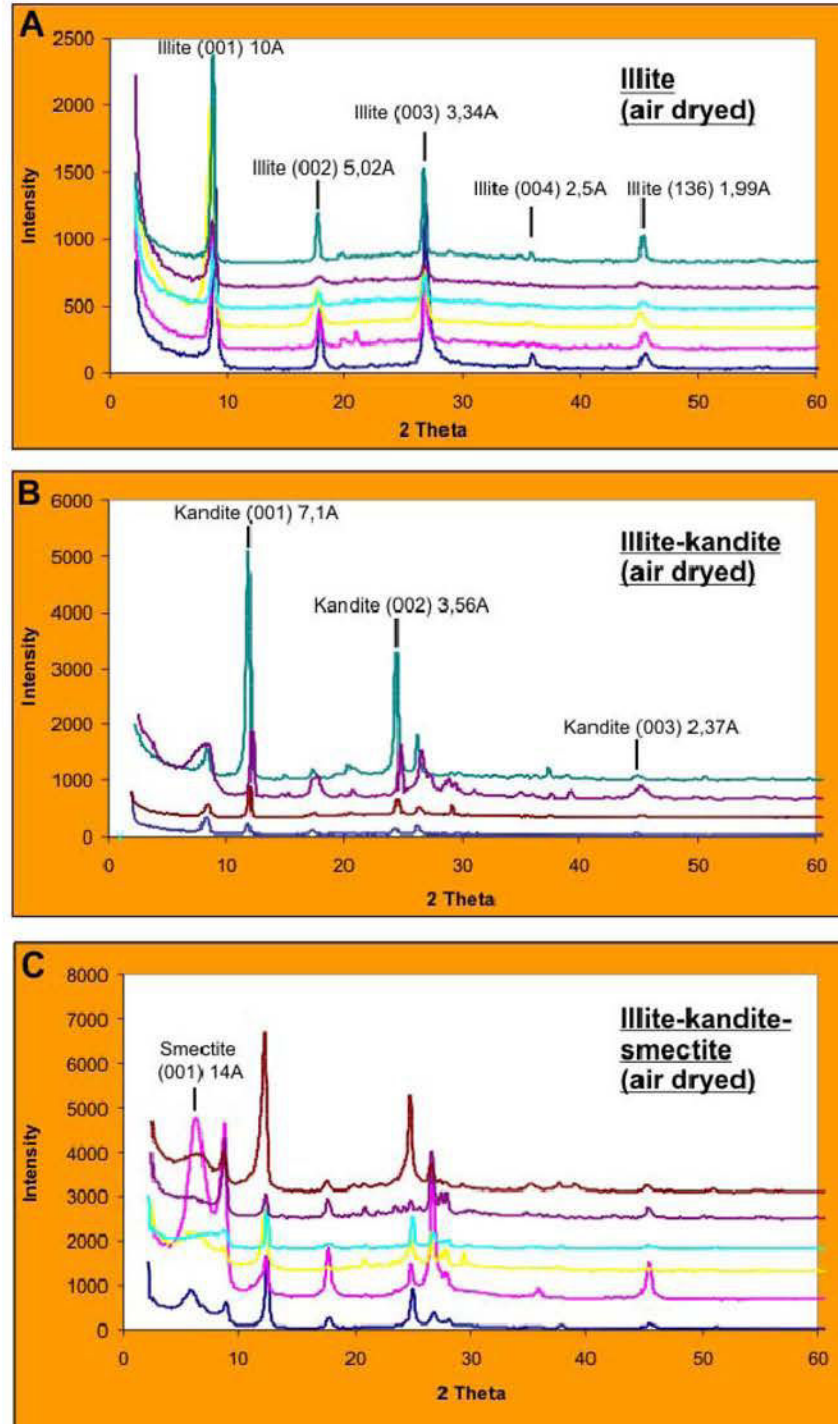


Figure 9. XRD plots of the analysed clay minerals. Sample localities (Appendix 1) from the top to the bottom: *Illite*: Roadcut, hydrothermal breccia (Gécsi Hill), Enyedi quarry, Barite vein (Sukoró), granite inclusion in andesite (Nadap). *Illite-kandite*: Zsellérek pasturale (Sukoró), Meleg-hill – hydrothermal breccia; Meleg-hill - shaft, Lovasberény road– hydrothermal breccia. *Illite-kandite-smectite*: Bentonite vein - Székesfehérvár, Háromszögelési pont-Nadap, Sas-hill – Pákozd, Andesite vein – Sukoró, Kisfalud quarry – Székesfehérvár, Mészeg hill – Sukoró.

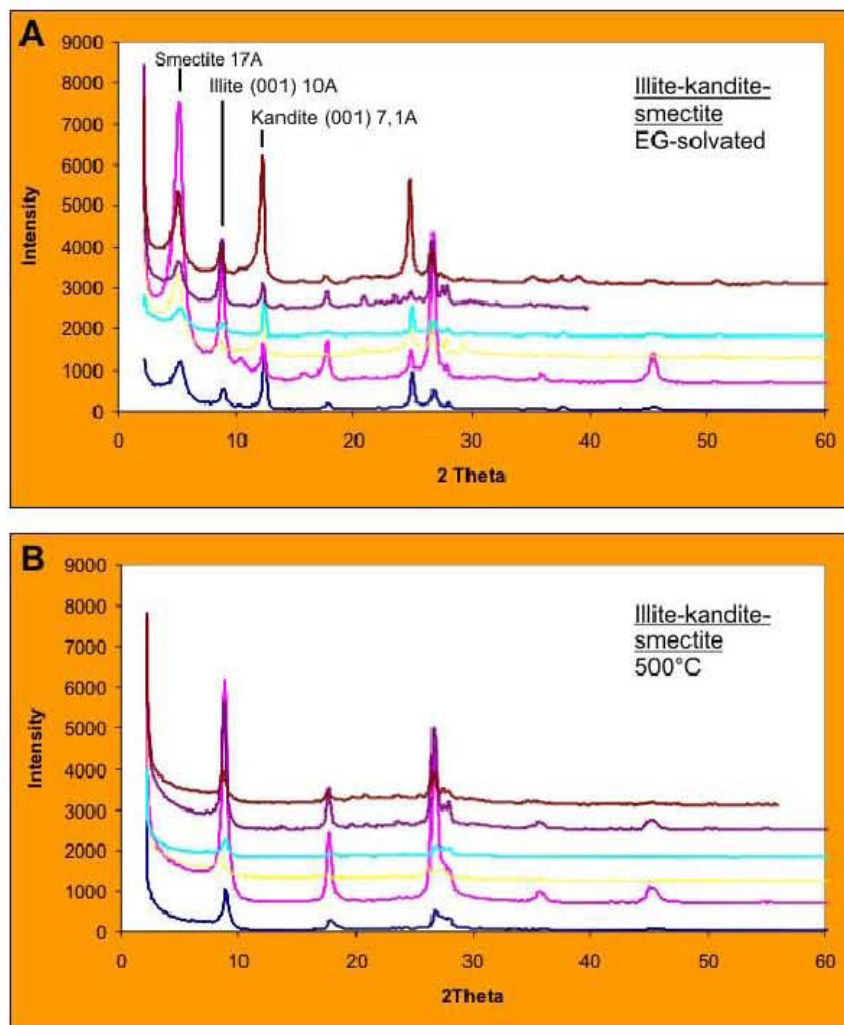


Figure 10. XRD plot of the ethylene-glycol solvated (D) and the heated (500°C) (E) illite-kandite-smectite samples. 001 peak of smectite moves from 14A to 17A after solvation and collapses after heating. 001 peak of candites do not change after solvation but collapse after the heating. Peaks of illite change does not change after solvation or after the heating. Samples are the same as on the Figur 8/C.

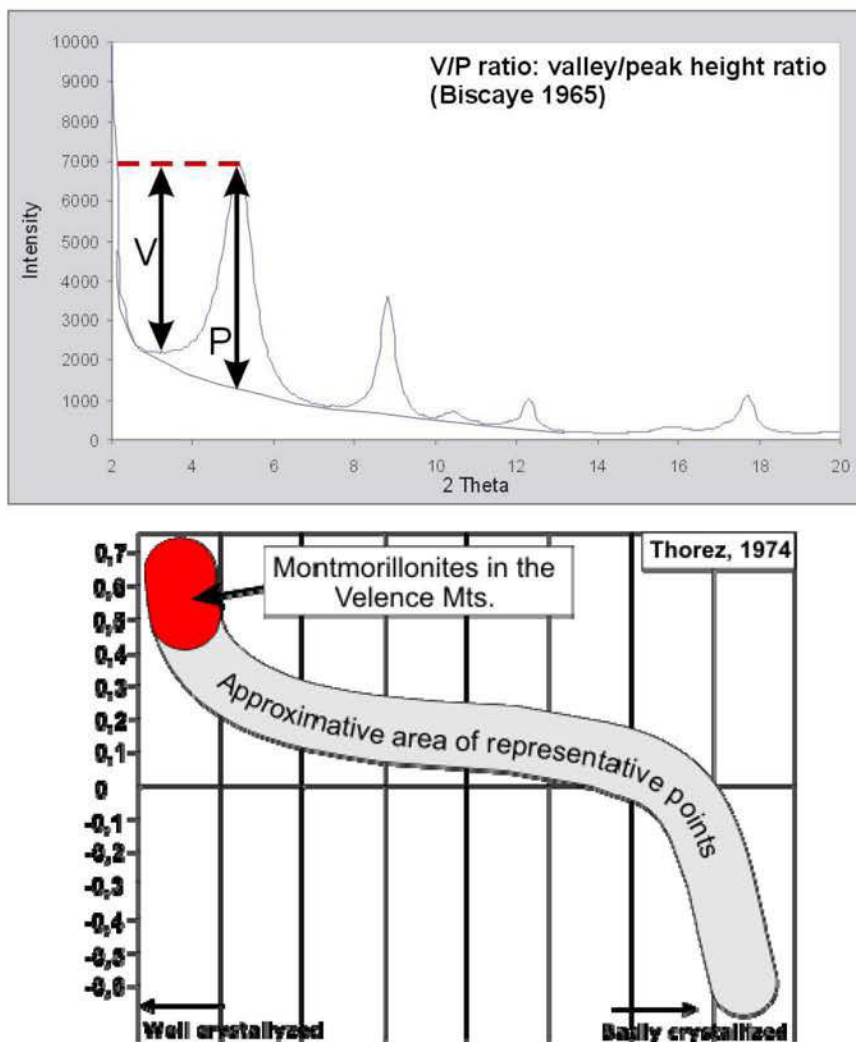


Figure 11. v/p ratio of smectites is a semi-quantitative method for estimation of smectite crystallinity. A) calculation of the v/p ratio. Depth of the valley left from the (001) peak of the smectite has to be divided by the height of the 001 peak. B) In the Velence Mts. the analyzed smectites have high v/p ratio and are therefore well-crystallized.

When comparing the illite with the illite-dickite assemblages, the ratio of swelling smectite interstratification is the highest in these samples. The kandite phase proved to be kaolinite based on the XRD and IR plots (Figure 12). The kaolinite is a slightly less crystallized modification of the kandite group (VAN DER MAREL 1976).

I did not discriminate the smectites in the dioctahedral group, neither is the IR useful for the distinction between beidellite and montmorillonite. Due to the v/p ratio (0,6-0,84) the smectites are A-type, well-crystallized, possibly hydrothermal of origin (Figure 11).

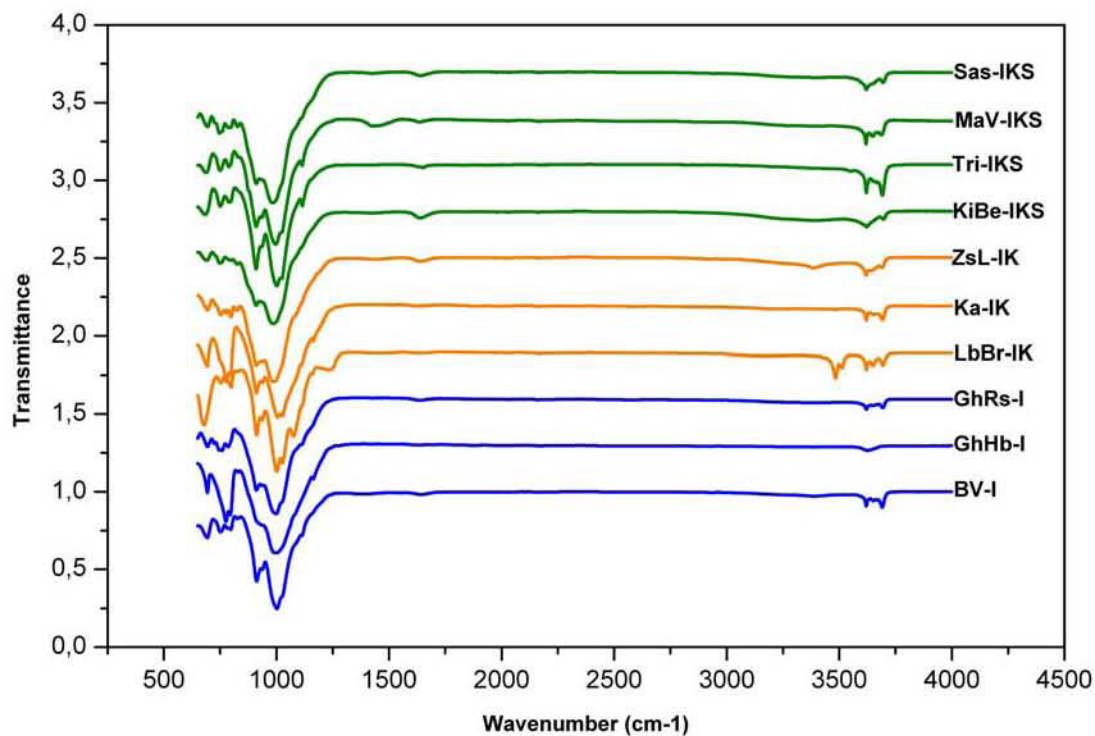


Figure 12. IR plots of the analyzed clay mineral assemblages. Sample names from the top to the bottom: *Illite-kaolinite-smectite* (IKS): Sas-hill (Pákozd), Malom-valley (Pátka), Háromszögelési pont (Sukoró), Bentonite vein (Székesfehérvár). *Illite-kandite*: Zsellérek pasturale (Sukoró), Meleg-hill - hydrothermal breccia, Lovasberény road - hydrothermal breccia. *Illite*: Roadcut – Gécsi hill, hydrothermal breccia – Gécsi Hill, Barite vein (Sukoró)

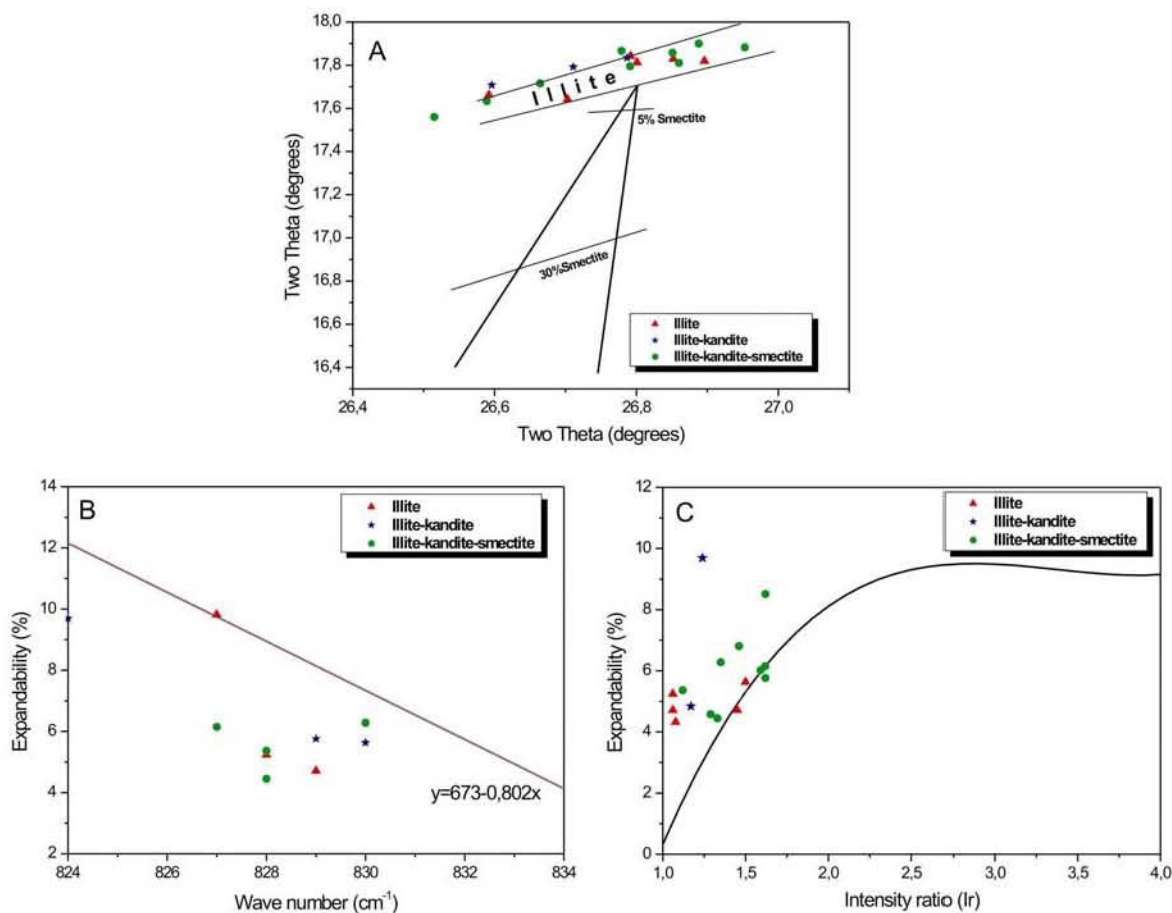


Figure 13. Different methods for estimation of smectite interstratification of illites, after SRODON (1984) and EBERL et al. (1987): A) Plot of 002 vs. 003 reflections of illitic materials. B) Relation between expandability and wave number for the infrared absorption-band that migrates between 826 and 833 cm⁻¹. C) Relation between expandability (calculated by Scherrer method) and intensity ratio (Ir). Colored points indicate the measurements from the Velence Mts.

As a summary, illite occurs only in and around the andesite dikes, in some fault zones and surrounding the quartz-barite vein in the Nadap-Sukoró area (Figure 14)

The illite-dickite alteration is only apparent in the Nadap-Sukoró area, in the broader vicinity of the andesite dikes and in the hydrothermal breccias (Figure 14).

The illite-kaolinite-smectite assemblage is regionally characteristic in the granite, but its occurrence is always structurally controlled by NE-SW or N-S trending fault zones or associated to the quartz-fluorite-base metal veins (Figure 14). *Regional* occurrence indicates that the hydrothermal fluid circulation affected regionally the granite body.

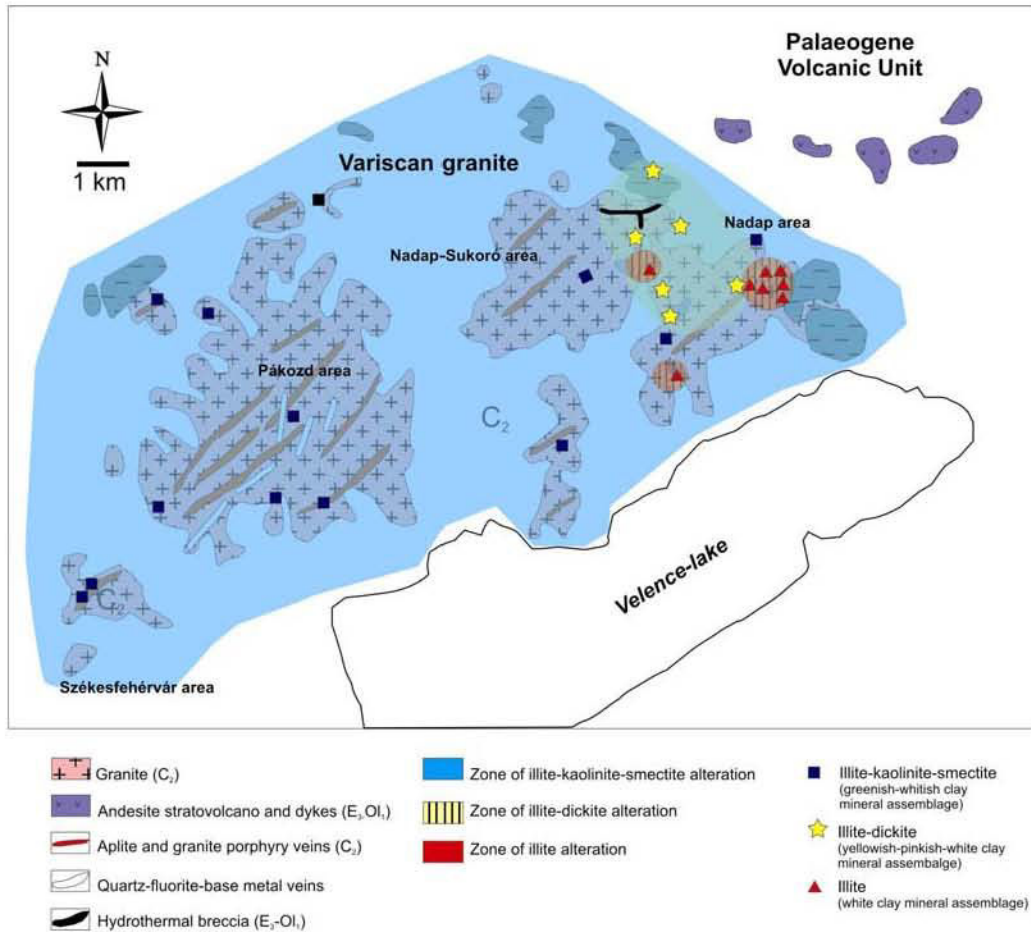


Figure 14. Areal distribution of the clay mineral assemblages in the Velence Mts.

The close spatial relationship of the illite and illite-dickite alteration zones indicates that their formation is related to the same hydrothermal fluid circulation. This fluid flow was, however a *local* fluid flow event, confined on some parts of the Nadap-Sukoró area. Since the illite-kaolinite-smectite assemblage is absent only in the illite alteration zones, the illite alteration postdates the formation of the illite-kaolinite-smectite alteration.

| Mineral assemblage | Locality | Illite | | | | | | | | | | Smectite | | Kandite | | Quartz | |
|--------------------|----------------------------------------|--------|--------|--------|---------------------------------|-----------------------|---------------------------------|-----------------------|-----------------------|-----------------------|----------------------------------------|-----------------------|-----------|---------|--|---------------|--|
| | | (001) | (002) | (003) | 17° peak breadth at half height | Expandable layers (%) | 26° peak breadth at half height | Expandable layers (%) | Intensity ratio (I/r) | Expandable layers (%) | IR absorption band (cm ⁻¹) | Expandable layers (%) | V/P ratio | | | m=minor, n=no | |
| illite | Barite vein | 8,866 | 17,842 | 26,792 | 0,4 | 5,24 | 0,4 | 5,59 | 1,06 | 828 | 8,94 | - | - | m | | | |
| | Granite inclusion in andesite | 8,908 | 17,825 | 26,848 | 0,32 | 4,32 | 0,26 | 3,64 | 1,077 | - | - | - | - | n | | | |
| | Hydrothermal breccia, Gécsi-hill | 8,827 | 17,813 | 26,801 | 0,36 | 4,71 | 0,39 | 5,45 | 1,45 | 829 | 8,14 | - | - | m | | | |
| | Enyedi quarry | 8,681 | 17,82 | 26,896 | 0,43 | 5,63 | 0,49 | 6,85 | 1,5 | - | - | - | - | m | | | |
| | Gécsi Hill quarry | 8,72 | 17,662 | 26,598 | 0,36 | 4,71 | 0,3 | 4,20 | 1,06 | - | - | - | - | m | | | |
| | Roadcut, Gécsi Hill | 8,56 | 17,842 | 26,703 | 0,75 | 9,82 | 0,66 | 9,23 | - | 827 | 9,75 | - | - | n | | | |
| | Meleg Hill shaft | 8,946 | 17,834 | 26,787 | 0,37 | 4,84 | 0,4 | 5,59 | 1,17 | - | - | - | - | m | | | |
| | Hydrothermal breccia, Lovasberény road | 8,38 | 17,294 | 26,288 | 0,44 | 5,76 | 0,43 | 6,01 | - | 829 | 8,14 | - | - | m | | | |
| | Hydrothermal breccia, Meleg Hill | 8,734 | 17,708 | 26,596 | 0,43 | 5,63 | 0,33 | 4,62 | - | 830 | 7,34 | - | - | m | | | |
| | Zselérek pasturale | 8,963 | 17,792 | 26,711 | 0,74 | 9,69 | 0,68 | 9,51 | 1,24 | 824 | 12,15 | - | - | n | | | |
| illite+ kandite | Apilte vein, Székesfehérvár | 8,881 | 17,811 | 26,86 | 0,44 | 5,76 | 0,52 | 7,27 | 1,62 | - | - | - | 0,67 | n | | | |
| | Pákozd, Big quarry | 8,94 | 17,9 | 26,888 | 0,35 | 4,58 | 0,55 | 7,69 | 1,289 | - | - | - | 0,71 | m | | | |
| | Sukorói andesite vein | 8,902 | 17,858 | 26,851 | 0,52 | 6,81 | 0,35 | 4,89 | 1,46 | - | - | - | 0,78 | n | | | |
| | Pákozd Big quarry2 | 8,853 | 17,867 | 26,779 | 0,46 | 6,02 | 0,4 | 5,59 | 1,59 | - | - | - | 0,74 | m | | | |
| | Mészeg hill, Sukoró | 8,806 | 17,795 | 26,791 | 0,65 | 8,51 | 0,5 | 6,99 | 1,62 | - | - | - | 0,71 | m | | | |
| | Sas-hill, Pákozd | 8,749 | 17,716 | 26,664 | 0,41 | 5,37 | 0,38 | 5,31 | 1,12 | 828 | 8,94 | - | 0,6 | m | | | |
| | Háromszögölési pont, Nadap | 8,651 | 17,634 | 26,589 | 0,48 | 6,28 | 0,44 | 6,15 | 1,35 | 830 | 7,34 | - | 0,82 | m | | | |
| | Malom-valley, Pátka | 8,612 | 17,56 | 26,515 | 0,34 | 4,45 | 0,3 | 4,20 | 1,33 | 828 | 8,94 | - | 0,805 | n | | | |
| | Bentonitoe vein | 8,853 | 17,883 | 26,953 | 0,47 | 6,15 | 0,45 | 6,29 | 1,619 | 827 | 9,75 | - | 0,84 | n | | | |
| | Székesfehérvár | | | | | | | | | | | | | | | | |

Table 2. Summary of the XRD analysis of the analyzed samples

4.1.4 Temperature conditions during the formation of the clay mineral assemblages

In hydrothermal systems, hydrothermal clay mineral assemblages are useful for temperature and pH estimation (REYES 1990, PARRY et al. 2002). In the illite-kaolinite-smectite assemblage the presence of three different clay mineral phases are seemingly co-genetic, however they are stable under different temperature and pH conditions. The mineralogical investigations proved that all of them are well-crystallized, and all may have a hydrothermal origin. Smectite forms at low temperature, below 180°C, under neutral pH conditions; kaolinite forms under more acid conditions and this is the typical kandite mineral below 200°C, whereas dickite is more common in acidic zones with temperature above 200°C (REYES 1990). Illite forms at relatively (>200°C) high temperature under both neutral and acid conditions. The stability fields of the three different minerals overlap only in a very narrow temperature range, at around 200°C (Figure 15). Due to the R3 type behavior of the illite phase and the low degree of smectite interstratification, the illite is a high temperature phase suggesting that the clay mineral assemblage reflects a cooling process from temperatures higher than 200°C to temperatures below 200°C.

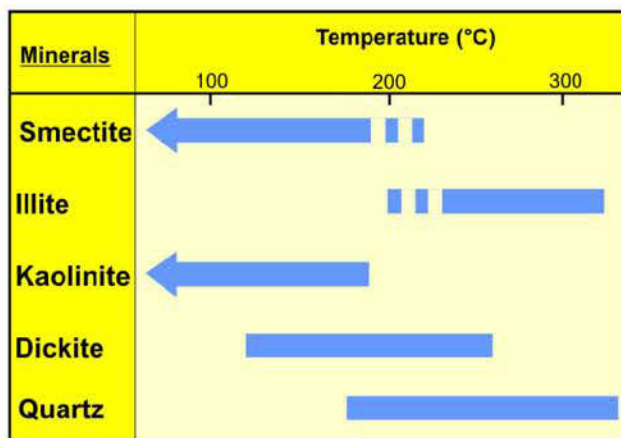


Figure 15. Stability field of hydrothermal minerals, analyzed in the Velence Mts.

The illite of the illite-dickite assemblage is R3 type and has ordered structure, indicating higher than 200°C formation temperature (Figure 15). Dickite is the high temperature modification of kandite minerals, it forms between 140-250°C, the two temperature ranges overlap between 200-250°C. According to the areal distribution of the samples and the mineral

assemblage, this type of alteration is the distal, lower temperature part of the hydrothermal circulation around the andesite dikes.

The illite in and around the andesite dikes is R3 type with very low smectite interstratification. It assumes that illite formed at higher temperatures than 220°C.

To put it concisely the temperature in the illite alteration zones was the highest (>240°C) and the temperature decreased towards to the distal zones which are characterized by the illite-dickite alteration assemblage (200-250°C). In comparison to the high temperature local fluid flow event in the eastern part of the Nadap Sukoró area, the temperature of the regional hydrothermal circulation was lower (<200°C).

4.2 AGE, ORIGIN AND TEMPERATURE OF HYDROTHERMAL FLUID FLOW EVENTS IN THE VELENCE MTS.

AGE, ORIGINE ET TEMPERATURE DES ECOULEMENTS FLUIDS DANS LES MONTS VELENCE

K-Ar analyses

Un age K-Ar a été déterminé pour les phases potassiques du granite, les plagioclases et des amphiboles provenant des andésites ainsi que pour les illites hydrothermales des différents assemblages argileux. Ceci pour établir les relations temporelles entre les différents types d'altérations et leurs interférences avec les événements magmatiques.

Des âges K-Ar radiométriques ont été déterminés pour 2 feldpaths potassiques. L'un d'entre eux provenant d'un granite très peu altéré a un age de 220,9±6,7 Ma alors que l'autre, issu des monts Gécsi Hill, (Nadap area) est daté à 89,26±2,77Ma. Le K-feldspath magmatique ne peut pas toujours être utilisé pour des datations de l'intrusion car sa température de fermeture est basse (160°C) et le temps de refroidissement est long. De ce fait, en considérant un gradient géothermique moyen de (33°C/km), on peut déterminer que à 6 km de profondeur la température d'emplacement du granite est supérieure à celle de fermeture des K-feldpaths. Donc, cette méthode de datation donne l'âge à partir duquel la température a été inférieure à 160°C et donc durant les derniers instants de l'évolution structurale du massif.

Pour les dykes andésitiques, les ages K-Ar sont de 29,1±1,1 Ma. C'est probablement l'âge réel de l'emplacement car les minéraux initiaux se refroidissent rapidement en dessous de leur température de fermeture et la cristallisation des petites intrusions andésitiques s'est faite rapidement dans un magma froid. Trois âges ont été déterminés à partir des amphiboles et

plagioclases. Les âges K-Ar sont respectivement de $34,0 \pm 1,2$ Ma, $30,8 \pm 1,1$ Ma et $27,1 \pm 0,8$ Ma. L'âge de l'amphibole est un maximum alors que celui de l'encaissant est une estimation minimale. L'âge probable des dikes est de 30 Ma.

Les âges des assemblages illite-kaolinite-smectite varient entre 209-232 Ma. Les plus fortes teneurs en K (%) et $^{40}\text{Ar}_{\text{rad}}(\%)$ ont été déterminées à partir de l'échantillon 6616 daté à $221,2 \pm 6,7$ Ma. L'âge de cette altération argilitique est de 227-213 Ma. Deux échantillons (6614, 6618) ont des faibles teneurs en K et $^{40}\text{Ar}_{\text{rad}}(\%)$ dans la zone de Nadap-Sukoró ce qui suggère un enrichissement en Ar et une perte de K durant les événements hydrothermaux.

L'échantillon 6613 provenant des dikes andésitiques est daté à $38,0 \pm 1,2$ Ma, ce qui suggère que l'effet du rechauffement Paléogène a eu un effet sur la composition sur les assemblages mineralogiques hydrothermaux dans le granite de la zone de Nadap-Sukoró.

Dans cette zone l'âge des associations illite-dickite varie entre 125 et 55 Ma (Table 3C, Figure 16A.) sur une très faible distance. Ces âges sont reproductibles (respectivement $62,7 \pm 2$ Ma et $64,5 \pm 1,5$ Ma pour les échantillons 6622 et 6819) mais, en raison de leur faible teneur en K et Ar, ils sont considérés comme des mélanges.

Les illites forment 2 groupes en fonction de leur âge (8-40 Ma et 29-32 Ma (Table 2D, Figure 13 A). Les échantillons Vand et Vten sont datés à $30 \pm 0,7$ Ma et $31,8 \pm 1,1$ Ma. Ces âges sont comparables à ceux des andésites. Les teneurs en K et Ar sont supérieures mais les pertes ou gains en Ar ne sont pas déterminées. La teneur en Ar pour les illites les plus vieilles sont faibles. Le gain en K ou Ar provient d'un hydrothermalisme plus récent suggérant que les âges plus anciens (38-40 Ma) sont représentatives d'un seul événement hydrothermal.

En comparant la distribution des assemblages argileux et les variations des âges K-Ar dans les monts Velence, il est clair qu'il y a une relation directe entre les âges radiométriques et les occurrences argileuses. Comme l'assemblage à illite-kaolinite-smectite a un âge triasique, on peut en déduire que les circulations fluides triasiques affectent le granite régionalement. Dans la zone de Nadap, là où beaucoup de dykes andésitiques sont localisés, les âges K-Ar sont équivalents aux âges mesurés dans les PVU et les assemblages d'illite pur ont des âges Paléogènes. Le magmatisme andésitique génère localement des circulations fluides locales et des altérations dans le granite.

Quoiqu'il en soit, il y a une zone de transition entre les altérations à illite et illite-kaolinite-smectite ou le principal minéral argileux est illite-dickite avec des âges différents. Ces âges témoignent d'un mélange et ne témoignent pas d'un seul événement hydrothermal.

4.2.1 K-Ar analyses

K-Ar age determination procedure has been carried out on the illite mineral fraction of the different clay mineral assemblages to compare the age relationships of the different hydrothermal fluid circulation events. However, to highlight the relationship between the hydrothermal circulation events and magmatic activity, the age determination procedure has also been applied for the rock forming mineral phases (amphibole, plagioclase, whole rock) of some fresh andesite dikes and on the rock forming K-feldspar of the granite as well. To get a wholesome picture of the succession of the Carboniferous, Triassic, Cretaceous (?), Palaeogene magmatic and hydrothermal events data from earlier studies (BUDA 1985; BALOGH et al. 1983 and BAJNÓCZI 2004) were also used. (Table 3).

4.2.1.1 K-Ar ages for rock forming minerals

BALOGH et al. (1983) published 137-291 Ma ages on rock forming biotite from the granite (Table 3A and 16B). The remarkable spread of data is in connection with the different degree of chlorite alteration of biotite, but there was no correlation found between the location of the samples and the degree of alteration. The minimum age of the granite is 280-290 Ma (BUDA 1985) based on the oldest biotite ages and on an unpublished U/Pb age data measured on a zircon crystals (BUDA, pers. comm.).

The K-Ar radiometric age for two rock forming fresh K-feldspars of the granite was determined during the current studies. One of the K-feldspars from a very slightly altered granite yielded $220,9 \pm 6,7$ Ma age, whereas the other one on the Gécsi Hill, (Nadap area) provided $89,26 \pm 2,77$ Ma. (Table 3A and Figure 16B).

Magmatic K-feldspar in abyssal intrusive rocks is not entirely suitable for K-Ar age determination of the intrusion (FAURE 1977; RICHARDS & NOBLE 1998) because its closure temperature is low (160°C; HARRISON et al. 1979) and long time can elapse – due to the low

cooling rate – between the emplacement of the intrusion and the cooling of the K-feldspar below its trapping temperature. On the other hand, assuming an average geothermal gradient ($33^{\circ}\text{C}/\text{km}$), at 6 km depth, the emplacement depth of the Velence Granite the temperature is higher than the closure temperature for the K-feldspar. Therefore K-Ar data for K-feldspar provide that age when the host granite was cooled below 160°C at the last time during the elongated structural evolution.

In the Nadap-Sukoró area of the granite block, we measured radiometric ages on whole rock samples from two small fresh andesite dikes (BAN – whole rock, M12, M24, M10 – amphibole, plagioclase, whole rock).

The andesite dike (BAN), located north from the village Sukoró (Figure 2) (close to the quartz-barite vein) has aphanitic texture, therefore the separation of plagioclase or amphibole was impossible. The whole rock age is $29,1 \pm 1,1$ Ma. (Table 3.B, Figure 16B). This age is most probably equal to the true age of the emplacement because the rock forming minerals cooled rapidly below their closure temperature, as the crystallization of the small, up to the few metre wide andesite dikes was rapid when they intruded into the cold granite host. Thus the complete cooling was most likely rapid, and the whole rock radiometric age is equal with the true age of the dike.

The other andesite dike is located on the margin of the PVU and the Nadap area of the granite (Figure 17). Prior to the analysis the rock forming mineral phases were petrographically checked and no alteration was detected. Separated amphibole and plagioclase provided $34,0 \pm 1,2$ Ma and $30,8 \pm 1,1$, respectively (M12, M24, M10 samples (Table 3B)). The whole rock sample has $27,1 \pm 0,8$ Ma, K-Ar age (Figure 16B). Amphibole has the highest closure temperature $400\text{--}350^{\circ}\text{C}$ (DAMON 1968) or 540°C STEIGER (1966) therefore generally the best estimation of an intrusion's age is provided by that data. The closure temperature of the plagioclase is lower (200°C ; HARRISON et al. 1979) and it is the lowest for the glass. The measured data and the closure temperatures would suggest that the cooling of the dike lasted 7 million years, still it is apparently not likely since the cooling of the small andesite dikes at volcanic/subvolcanic level in a cold host rock is certainly more rapid. What is more plausible is that the thermal effect of the andesite liberated Ar from the K-feldspar and biotite from the host granite, successively the Ar entered selectively into the crystal structure of the amphibole and plagioclase yielding excess Ar in it and lead to older K-Ar age than the true age of the dike. The age of the amphibole can be

considered as maximum age of the andesite and the age of the whole rock as minimum age, respectively.

Table 3. K-Ar ages of rock forming minerals of the Velence Granite and the lamprophyre.

| Laboratory Number | Own number | Locality | Rock type and type of hydrothermal alteration | Selected mineral fraction | K-content (%) | ⁴⁰ Ar rad/g(cm3/g) | ⁴⁰ Ar rad (%) | K/Ar age (million year) | Reference |
|-------------------------------|------------|-------------------------|-----------------------------------------------|---------------------------|---------------|-------------------------------|--------------------------|-------------------------|--------------------|
| Biotite in granite | | | | | | | | | |
| 743 | | Dinnyés-3 777,7m | granodiorite | biotite | 5,91 | 94 | 6,737x10-5 | 272±11 | Balogh et al 1983 |
| | | Sukoró Kf | monzogranite | biotite | | | | 291±11 | Balogh et al 1984 |
| | | Sukoró Kf | monzogranite | biotite | 4,65 | 77 | 5,242x10-5 | 271±11 | Balogh et al 1985 |
| | | Nadap | monzogranite | biotite | | | | 196±9 | Balogh et al 1986 |
| | | Pákozd | monzogranite | biotite | | | | 137±6 | Balogh et al 1987 |
| | | Ságvár | monzogranite | biotite | | | | 259±10 | Balogh et al 1988 |
| | | Székesfehérvár 4 sz. f. | monzogranite | biotite | | | | 280±11 | Balogh et al 1989 |
| | | Székesfehérvár aplite | mikrogranite-pegmatite | biotite | | | | 246±10 | Balogh et al 1990 |
| | | Székesfehérvár aplite | mikrogranite-pegmatite | biotite | | | | 192±8 | Balogh et al 1991 |
| | | Székesfehérvár aplite | mikrogranite-pegmatite | biotite | | | | 165±7 | Balogh et al 1992 |
| Orthoclase in granite | | | | | | | | | |
| 6610 | M1 | Nadap, Gécsi-hill | granite pegmatite argillic alteration | orthoclase | 8,878 | 3,1587x10-5 | 78,90 | 89,26±2,77 | this study |
| 6620 | M11 | Sukoró, Rigó-hill | granite, no alteration | orthoclase | 9,747 | 8,9088x10-5 | 89,60 | 220,9±6,72 | this study |
| Biotite in lamprophyre | | | | | | | | | |
| 742 | | Sukoró-1 drillhole | Lamprophyre, beforosite | biotite | 6,92 | 80 | 2,132x10-5 | 77,6±3 | Balogh et al. 1983 |

| Laboratory Number | Own number | Locality | Rock type and type of hydrothermal alteration | Selected mineral fraction | K-content (%) | ⁴⁰ Ar rad/g(cm3/g) | ⁴⁰ Ar rad (%) | K/Ar age (million year) | Reference |
|--------------------------------------------------------------------|---------------|----------------------------------------------------|-----------------------------------------------|---------------------------|---------------|-------------------------------|--------------------------|-------------------------|---------------------|
| Andesite in the granite and in the Palaeogene Volcanic Unit | | | | | | | | | |
| 805 | - | Sukoró, protected quarry | andesite | teljes kőzet | 1,52 | 1,732x10 ⁻⁶ | 81 | 29,1±1,2 | Horváth et al. 1987 |
| 6820 | BAN | Sukoró, Meleg hill, barite vein | andesite, no alteration | whole rock | 2,26 | 2,579x10 ⁻⁶ | 46,60 | 29,1±1,1 | this study |
| 4773 | MPV-2 | Sukoró-Nadap pasturale andesite vein, western part | andesite | amphibole | 0,56 | 6,835x10 ⁻⁷ | 24,3 | 31,2±2,0 | Bajnóczy (2003) |
| 4775 | MPV-1 (Ve-40) | Sukoró, protected quarry | andesite | amphibole | 0,34 | 4,781x10 ⁻⁷ | 48,8 | 36,2±1,6 | Bajnóczy (2003) |
| 4774 | MPV-3 | Sukoró-Nadap pasturale andesite vein, eastern part | andesite | amphibole | 0,53 | 8,460x10 ⁻⁷ | 49 | 40,3±1,7 | Bajnóczy (2003) |
| 6621 | M12 | Nadap, Lovasberény street | andesite, no alteration | amphibole | 0,462 | 6,135x10 ⁻⁷ | 48,70 | 33,99±1,24 | this study |
| 6624 | M24 | Nadap, Lovasberény street | andesite, no alteration | plagioclase | 0,4 | 4,827x10 ⁻⁷ | 51,80 | 30,78±1,09 | this study |
| 6619 | M10 | Nadap, Lovasberény street | andesite, no alteration | whole rock | 1,915 | 2037x10 ⁻⁶ | 79,30 | 27,1±0,84 | this study |
| 1601 | | Sukoró-Nadap közti legelő | andesite | biotit | 5,86 | 72 | 7,34x10 ⁻⁶ | 31,9±1,2 | Horváth et al. 1987 |
| 1601 | | Sukoró-Nadap közti legelő | andesite | amfibol | 0,46 | 39 | 6,798x10 ⁻⁷ | 37,8±1,4 | Horváth et al. 1987 |
| 968 | | Pázmánd, Pd-2 drillhole | diorite, argillic alteration | amphibole, biotite | 1,17 | 1,429x10 ⁻⁶ | 42,00 | 31,2±1,4 | Horváth et al. 1987 |

Table 3B K-Ar ages of andesites of the PVU and andesite stocks in the granite. Sample localities are indicated in the Appendix 1

| Laboratory Number | Own number | Locality | Rock type and type of hydrothermal alteration | Selected mineral fraction | K-content (%) | ⁴⁰ Ar rad/g(cm3/g) | ⁴⁰ Ar rad (%) | K/Ar age (million year) | Reference |
|-------------------------------------------------------------|------------|----------------------------------------------------------|------------------------------------------------------------------|-----------------------------|---------------|-------------------------------|--------------------------|-------------------------|------------|
| Illite-kaolinite-smectite in the granite | | | | | | | | | |
| 6613 | M4 | Sukoró, protected quarry | granite, argillic alteration | illite, kaolinite, smectite | 4,108 | 6,131x10 ⁻⁶ | 66,40 | 37,97±1,23 | this study |
| 6818 | MA1 | Pátka, Malom-völgy | granite, argillic alteration | illite, kaolinite, smectite | 2,83 | 1,337x10 ⁻⁵ | 66,60 | 117,6±3,8 | this study |
| 6614 | M5 | Sukoró, polymetallic veins | granite, argillic alteration, quartz-polymetallic veining | illite, kaolinite, smectite | 3,853 | 2,0953x10 ⁻⁵ | 77,30 | 134,7±4,21 | this study |
| 6615 | M6 | Pákozd, "Pegmatite quarry" | granite, argillic alteration | illite, kaolinite, smectite | 4,214 | 3,6442x10 ⁻⁵ | 89,30 | 209,8±3,68 | this study |
| 6611 | M2 | Székesfehérvár, Kisfalud quarry, next to the aplite vein | granite, argillic alteration | illite, kaolinite, smectite | 3,185 | 2,8262x10 ⁻⁵ | 75,00 | 214,6±6,74 | this study |
| 6616 | M7 | Pákozd, Big quarry | granite, argillic alteration | illite, kaolinite, smectite | 5,01 | 4,5827x10 ⁻⁵ | 90,20 | 221,2±6,7 | this study |
| 6354 | Vszi | Székesfehérvár, Kisfalud quarry | granite, argillic alteration | illite, kaolinite, smectite | 3,26 | 3,038x10 ⁻⁵ | 97,30 | 232,3±5,1 | this study |
| Illite-dickite in granite breccia and in the granite | | | | | | | | | |
| 6622 | M13 | Nadap, Lovasberény street | hydrothermal breccia at the contact of the granite and the slate | illite,dickite | 4,731 | 1,0384x10 ⁻⁵ | 74,30 | 55,42±1,74 | this study |
| 6819 | LBB2 | Nadap, Lovasberény street | hydrothermal breccia at the contact of the granite and the slate | illite,dickite | 4,14 | 1,042x10 ⁻⁵ | 33,80 | 63,6±2,9 | this study |
| 6816 | ZSL2 | Sukoró, Zsellérek pasturale | granite porphyry, argillic alteration | illite,dickite | 5,28 | 1,309x10 ⁻⁵ | 64,7 | 62,7±2,0 | this study |
| 6356 | VZSL | Sukoró, Zsellérek pasturale | granite porphyry, argillic alteration | illite,dickite | 6,35 | 1,6456x10 ⁻⁶ | 90,00 | 64,5±1,5 | this study |
| 6617 | M8 | Sukoró Meleg-hill shaft | granite, argillic alteration | illite,dickite | 3,527 | 1,0473x10 ⁻⁵ | 73,80 | 76,64±2,42 | this study |
| 6618 | M9 | Sukoró, south from the barite vein | granite porphyry, argillic alteration | illite,dickite | 3,282 | 1,654x10 ⁻⁵ | 82,30 | 125,2±3,86 | this study |

Table 3C K-Ar ages of the illite-dickite and the illite-kaolinite-smectite assemblages. Sample localities are indicated in the Appendix 1

| Laboratory Number | Own number | Locality | Rock type and type of hydrothermal alteration | Selected mineral fraction | K-content (%) | $^{40}\text{Ar rad/g(cm}^3\text{/g)}$ | $^{40}\text{Ar rad (%)}$ | K/Ar age (million year) | Reference |
|---------------------------------------------------------|--------------|--------------------------------------|------------------------------------------------------|---------------------------|---------------|---------------------------------------|--------------------------|-------------------------|-----------------|
| Illite in the granite breccia and in the granite | | | | | | | | | |
| 4878 | MPV-6 (Ve-3) | Nadap, Gécsei-hill, protected quarry | andesite, argillic alteration | illite | 6,95 | $8,123 \times 10^{-6}$ | 62,90 | 29,8±1,2 | Bajnóczy (2003) |
| 6353 | Vand | Nadap, Gécsei-hill "Big quarry" | andesite, argillic alteration | illite | 7,43 | $8,499 \times 10^{-5}$ | 81,40 | 30±0,7 | this study |
| 6354 | Vand | Nadap, Gécsei-hill "Big quarry" | andesite, argillic alteration | illite | 7,23 | $8,499 \times 10^{-6}$ | 81,40 | 30±0,7 | this study |
| 6612 | M3 | Sukoró, Meleg-hill barite vein | granite, argillic alteration | illite | 5,925 | $7,124 \times 10^{-6}$ | 77,00 | 30,64±0,95 | this study |
| 5392 | Ve-4 | Nadap, Big quarry | granite, argillic alteration | illite | 7,48 | $9,587 \times 10^{-6}$ | 80,60 | 32,7±1,3 | Bajnóczy (2003) |
| 6355 | Vten | Sukoró, Enyedi-quarry | granite, argillic alteration | illite | 6,62 | $8,233 \times 10^{-6}$ | 87,10 | 33±0,8 | this study |
| 6355 | Vten | Sukoró, Enyedi-quarry | granite, argillic alteration | illite | 6,37; 6,2 | $8,247 \times 10^{-6}$ | 52,20 | 31,8±1,1 | this study |
| 6623 | M15 | Nadap, Gécsei-hegy roadside | granite, argillic alteration | illite | 6,221 | $9,308 \times 10^{-6}$ | 56,40 | 38,09±1,31 | this study |
| 6352 | Verd | Nadap, Gécsei-hill | hydrothermal breccia in granite, argillic alteration | illite | 6,1 | $9,391 \times 10^{-6}$ | 80,50 | 40,5±1 | this study |
| 6352 | Verd | Nadap, Gécsei-hill | hydrothermal breccia in granite, argillic alteration | illite | 5,91 | $9,076 \times 10^{-6}$ | 75,2 | 37,9±1,2 | unpubl. |

Table 3D K-Ar ages of the illite. Sample localities are indicated in the Appendix 1

4.2.1.2 K-Ar ages measured on hydrothermal minerals

The K-Ar ages that were determined from the illite of the illite-kaolinite-smectite assemblage vary between 209-232 Ma (Table 2C and Figure 16A). Due to the high K (%) and $^{40}\text{Ar}_{\text{rad}}(\%)$ content and the K-Ar ratios of the samples, potassium and argon gain or loss of the illite does not seem to be possible, however no mass balance calculation has been done on the mineral mixture. The highest values (K (%) and $^{40}\text{Ar}_{\text{rad}}(\%)$) are in the sample 6616 (Table 3C), and the K-Ar age is $221,2 \pm 6,7$ Ma. Therefore the age of this type of argillic alteration is 227-213 Ma (Upper Triassic). Two samples (6614, 6618; Table 3C) have lower K (%) and $^{40}\text{Ar}_{\text{rad}}(\%)$ values in the Nadap-Sukoró area of the granite, indicating Ar gain or K loss during younger hydrothermal events. One sample (6613) from the vicinity of an andesite dike yielded $38,0 \pm 1,2$ Ma, suggesting that the Palaeogene heat effect caused intense geochemical overprint on the hydrothermal mineral assemblages in the Nadap-Sukoró area of the granite (Figure 16A).

In the Nadap-Sukoró area of the granite intrusion the age of the illite-dickite assemblage varies between 125 and 55 Ma on a very broad interval (Table 3C and Figure 16A.). These ages are reproducible (see samples 6622 and 6819: $62,7 \pm 2$ Ma and $64,5 \pm 1,5$ Ma, respectively), but due to their low K and Ar content they are regarded as mixed ages.

In these zones the temperature was probably not high enough (at around 200-220°C – based on the clay mineral assemblage), or the fluid migration was not pervasive enough to overprint the K-Ar “clock” of the Variscan rock forming or Triassic hydrothermal minerals. The ages might be mixed Variscan-Triassic-Palaeogene ages.

In the Nadap-Sukoró area of the granite body, illite is the dominant clay mineral in the argillic alteration zones related to the Palaeogene magmatic activity. Their ages can be divided into two groups 38-40 Ma and 29-32 Ma (Table 2D, Figure 16 A). Three samples (Vand, Vten, Verd; Table 3D) were measured both at the Nuclear Research Lab of the Hungarian Academy of Sciences, Debrecen, Hungary and at the Lab of the Okoyama University, Japan. Concerning one of the samples the (Vand) ages were equal, while with the Vten and Verd significant differences were found (1 and 2 million years, respectively).

The K and Ar content of the samples (Vand and Vten) are high therefore Ar loss or gain is not assumed. The Ar content of samples 6623 and 6352 is low. K gain or Ar loss may be the

result of a younger hydrothermal overprint, therefore I cannot assume that the old ages (38-40 Ma) represent an individual hydrothermal event.

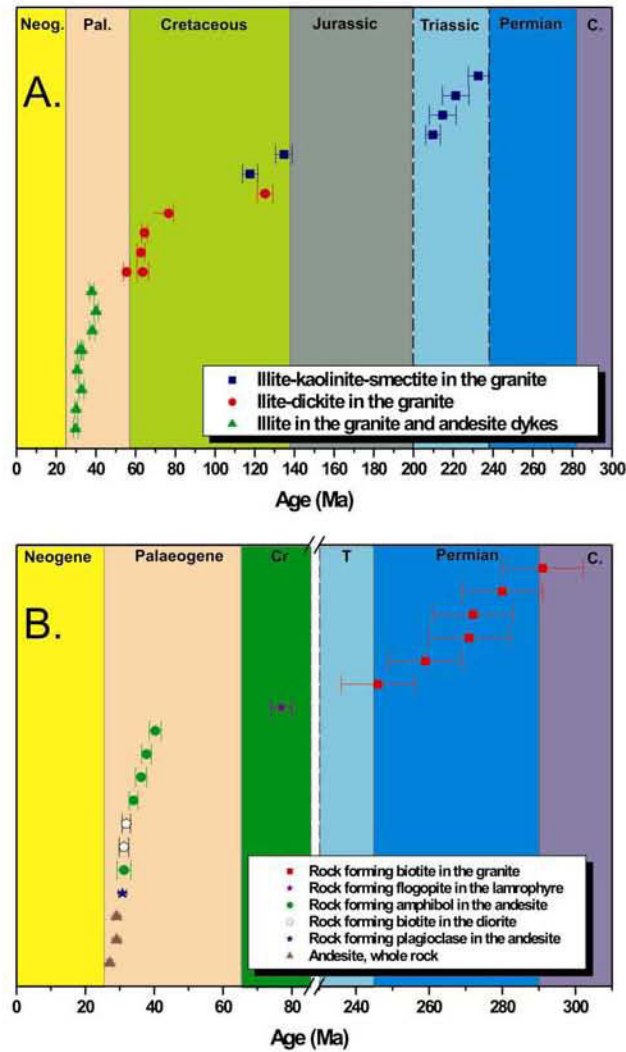


Figure 16. Results of K-Ar radiometric age determinations on: A) illite crystals of the different clay mineral assemblages and B) on separated rock forming minerals/whole rock samples

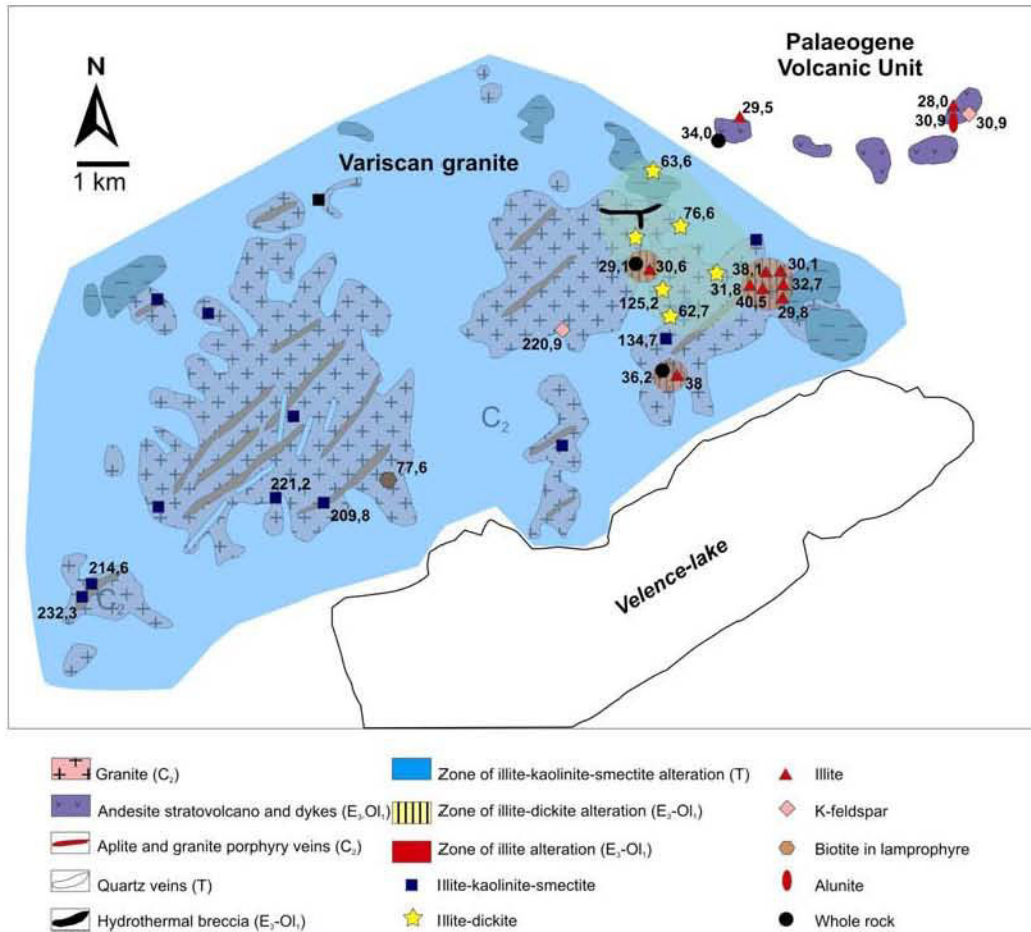


Figure 17. Comparison of the areal distribution of the clay mineral assemblages and the measured K-Ar ages on the illite fractions of the same clay mineral assemblage

4.2.1.3 Interpretation of K-Ar radiometric age data from the aspect of the extent of superimposing hydrothermal events that affected the granite intrusion

Comparing the areal distribution of the clay mineral assemblages and the variability of the K-Ar ages in the Velence Mts. it is obvious that there is a direct link between the radiometric ages and the occurrence of the clay minerals (Figure 17). The K-Ar ages of the regionally occurring illite-kaolinite-smectite assemblage do not show any correlation with the distance from the andesite dikes (with the distance of the Nadap area, where most of the andesite dikes were found). As the illite-kaolinite-smectite assemblage has Triassic age, it can be concluded that the Triassic fluid circulation event affected the granite regionally.

In the Nadap area, where most of the andesite dikes are located, the K-Ar ages equal with the radiometric ages measured in the Palaeogene Volcanic Unit, and measurements on the pure illite assemblage confirmed Palaeogene ages in every case. Therefore it is obvious that the Palaeogene andesitic magmatism generated local fluid circulation and hydrothermal alteration in the granite.

However there is a transition zone between the illite and illite-kaolinite-smectite alteration zones where the characteristic clay minerals are illite-dickite and the ages distributed on a broad interval. These ages are regarded as mixing ages and do not represent an individual hydrothermal event.

4.2.2 Pb isotope studies: age and genetical relationships of the quartz-fluorite-base metal veins and their geotectonical connections

Etude des isotopes du Pb

Cette étude a pour objectif de déterminer l'âge des galènes et de comparer les données isotopiques ($^{206}\text{Pb}/^{204}\text{Pb}$, $^{207}\text{Pb}/^{204}\text{Pb}$, $^{208}\text{Pb}/^{204}\text{Pb}$) pour les minéralisations des monts Velence et de la zone Szabadbattyán avec d'autres occurrences le long de la ligne PAL. Les rapports isotopiques du Pb dans les monts Velence et de la zone Szabadbattyán se correspondent parfaitement bien que plus élevés dans la zone Szabadbattyán. Les valeurs de μ ($\mu=9.8-10.3$) selon les modèles de STACEY & KRAMERS (1975) sont supérieures à celles de la croûte ($\mu=9.74$ STACEY & KRAMERS 1975). Les modèles d'âge Stacey&Kramers sont supérieurs à l'âge du granite et donc peu utilisables pour obtenir l'âge des minéralisations à quartz-fluorite. En accord avec les modèles de ZARTMAN & DOE (1981), les rapports obtenus suggèrent une dominante crustale dans cette zone.

Les rapports isotopiques des veines à quartz-fluorite-base metal sont identiques à ceux des galènes de type Mississippi-Valley présentes le long de PAL dans les Alpes du Sud (Figure 18 A, B). Les deux gisements étudiés dans les monts Velence et la zone Szabadbattyán sont également Triasiques .

The aim of the Pb isotope studies has two objects: to determine the model age of the galena and to compare the isotope data ($^{206}\text{Pb}/^{204}\text{Pb}$, $^{207}\text{Pb}/^{204}\text{Pb}$, $^{208}\text{Pb}/^{204}\text{Pb}$) for mineralization

in the Velence Mts. and the Szabadbattyán area with other deposits in Eastern and Southern Alps along the PAL .

The lead isotope ratios, and the calculated μ values and model ages are based on the dynamic model of CUMMINGS AND RICHARDS (1975) and the two-stage model of STACEY & KRAMERS (1975) are given in Table 4. The obtained μ values ($\mu=9.8-10.3$) following the STACEY & KRAMERS (1975) model are higher than the crustal average value ($\mu=9.74$ STACEY & KRAMERS 1975). The $^{206}\text{Pb}/^{204}\text{Pb}$ and $^{207}\text{Pb}/^{204}\text{Pb}$ data give quite consistent model ages at around 300 Ma when the C-R model is applied. The S-K model ages vary considerably (286-412 Ma). The former are comparable with the K-Ar ages (275-280 Ma) measured on fresh biotite (BUDA 1985) and 285 Ma U/Pb zircon age (BUDA, unpublished data) for the granite intrusion of the Velence Mts. In the Szabadbattyán block, the acquired data on galena are similar ($^{206}\text{Pb}/^{204}\text{Pb}= 18.29-18.35$, $^{207}\text{Pb}/^{204}\text{Pb}=15.67-15.74$ and $^{208}\text{Pb}/^{204}\text{Pb}=38.55-38.78$), and only marginally different from the data on the galena from Velence Mts. Also lead model ages show a similar pattern as those observed from Velence Mts. data, with S-K model ages typically being 100-200 Ma older.

Apparently, the galena data of two areas form a relatively tight cluster and a tendency to form a linear array with the Szabadbattyán data that are slightly higher in ^{207}Pb and ^{208}Pb . According to the plumbotectonic model of ZARTMAN & DOE (1981) the observed isotope ratios suggest a dominant upper crustal source for ore lead in both areas.

| Sample number | Analyzed mineral | Area | $^{206}\text{Pb}/^{204}\text{Pb}$ | $^{207}\text{Pb}/^{204}\text{Pb}$ | $^{208}\text{Pb}/^{204}\text{Pb}$ | μ value | S-K model age (Ma) | C-R model age (Ma) |
|---------------|------------------|-------------------|-----------------------------------|-----------------------------------|-----------------------------------|-------------|--------------------|--------------------|
| 0ES0301 | galena | Velence Mountains | 18.298 | 15.679 | 38.687 | 10.08 | 412 | 310 |
| 0ES0306 | galena | Velence Mountains | 18.276 | 15.663 | 38.608 | 9.96 | 399 | 310 |
| 0ES03030 | galena | Velence Mountains | 18.306 | 15.682 | 38.429 | 9.99 | 289 | 300 |
| 0ES1339 | galena | Velence Mountains | 18.288 | 15.646 | 38.481 | 9.91 | 390 | 300 |
| 0ES1041 | galena | Velence Mountains | 18.363 | 15.690 | 38.699 | | | |
| 0ES1069 | galena | Velence Mountains | 18.316 | 15.660 | 38.488 | | | |
| 0ES0991 | galena | Velence Mountains | 18.313 | 15.664 | 38.443 | | | |
| 336 | fluorite | Velence Mountains | 18.511 | 15.697 | 38.647 | | | |
| 0ES0399 | galena | Szabadbattyán | 18.286 | 15.667 | 38.662 | 10.01 | 390 | 310 |
| 0ES1064 | galena | Szabadbattyán | 18.339 | 15.710 | 38.694 | 10.16 | 436 | 290 |
| 0ES1094 | galena | Szabadbattyán | 18.346 | 15.736 | 38.781 | 10.28 | 477 | 290 |
| 0ES0300 | galena | Szabadbattyán | 18.293 | 15.679 | 38.688 | 10.08 | 408 | 310 |

accuracy: $\pm 0.10\%$

Table 4. Pb isotope data from the quartz-fluorite-base metal veins. Sample localities are indicated in the Appendix 1

Lead isotope ratios in the quartz-fluorite-base metal veins in the Velence Mts. and Szabadbattyán essentially overlap with data for galena from Mississippi-Valley type mineralizations along the PAL in the Southern Alps (Figure 18 A and B). We compared our data with source rocks of the Alpean variety of Mississippi-Valley type Pb-Zn mineralization in the Southern Alps (KÖPPEL 1983, KÖPPEL et al. 1988).

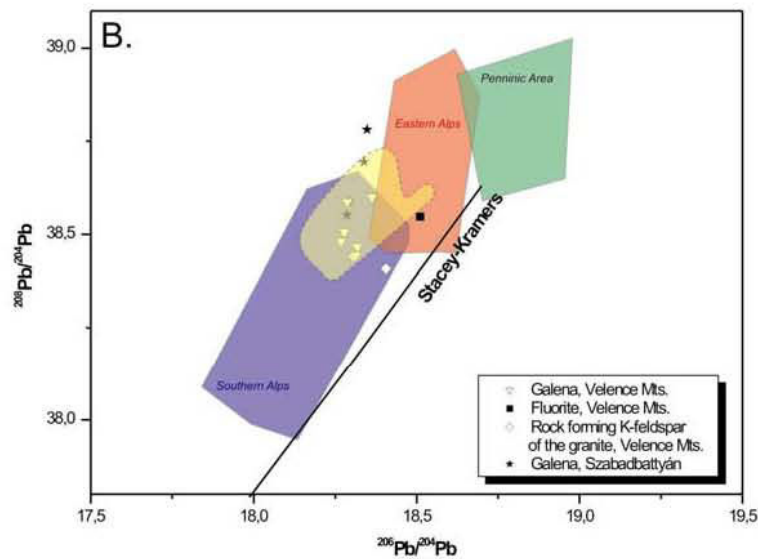
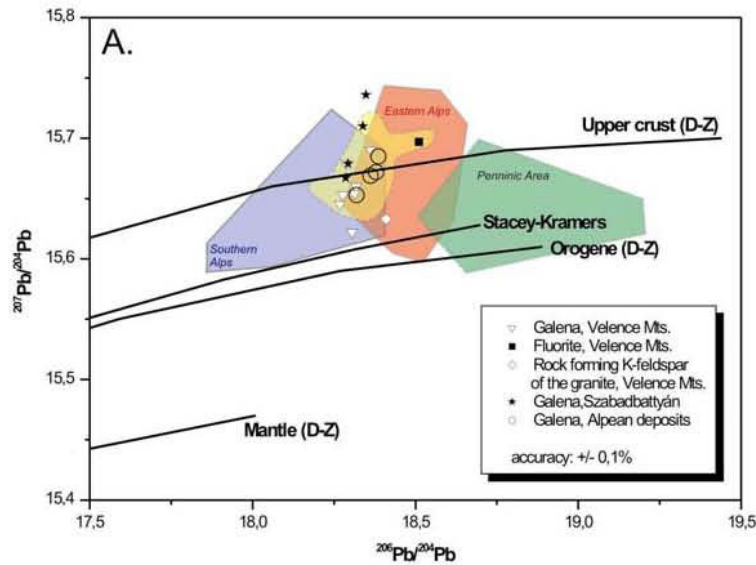


Figure 18. Pb isotope plots of the analyzed galena (black dots). Colored boxes indicate Pb isotope data from different parts of the Alps. The yellow shape indicates Pb isotope data from the Alpean type Mississippi valley type Pb-Zn deposits from the vicinity of the PAL. Sample localities are indicated in the Appendix 1

Except for two data values from the Szabadbattyán region, all data equal with the isotope ratios source rocks of the Pb-Zn mineralizations along the PAL (Bleiberg-Krauth, Mezica, Salafossa, Raibl, Gorno, Auronzo, Lafatsch; Figure 18). Since the stratiform-stratabound Mississippi Valley-type Pb-Zn mineralization in the Eastern and Southern Alps are of Triassic age, the two analyzed deposits in the Velence Mts. and the Szabadbattyán area are also Triassic, based on the very similar Pb isotope patterns of the ore minerals and the source rocks.

4.2.3 Sulphur isotope analysis: temperature estimation for the formation of the quartz-fluorite-base metal veins

Etude des isotopes du S

Les isotopes du soufre permettent de mieux connaître l'origine des fluides hydrothermaux et peuvent être utilisés pour comparer différentes minéralisations entre elles. Le $\delta^{34}\text{S}$ permet de calculer la température des processus hydrothermaux pour des phases minérales qui coexistent et résultent de ces fluides hydrothermaux. Les isotopes du soufre ont été étudiés dans des assemblages de galena-sphalérite pour connaître les relations entre les minéralisations Pb-Zn Alpines et celles des veines à quartz-fluorite-base métal. L'utilisation des coefficients de fraction sphalérite-galena de LI & LIU (2006) permet de déterminer une température de 250 – 270°C qui sont légèrement inférieures à celles déduites des équations de CZAMANSKE & RYE (1974). On peut en déduire que les précipitations de sulfures ont lieu vers 250°C dans les veines à quartz-fluorite. Les isotopes du soufre ont des valeurs similaires légèrement supérieures aux 0– -10 $\delta^{34}\text{S}$ $\delta^{34}\text{S}$ des MVT Alpines ou à Bleiberg et Mezica le long de PAL. Cela confirme que ces gisements ont une même origine.

Syngenetic galena and sphalerite was collected from the quartz-fluorite-base metal veins from the Pákozd area to carry out sulphur isotope measurements.

Sulphur isotope data are used for two purposes in this study: the values themselves may represent the source region of the hydrothermal fluids and are applicable for the comparison of different mineralizations. On the other hand, in coexisting mineral phases precipitating from the hydrothermal fluid $\delta^{34}\text{S}$ values can be used for calculation of the temperature of hydrothermal processes. The most common mineral pair used for sulphur isotope thermometry is the galena-sphalerite (FAURE 1977).

Galena shows values in the range -1.5 to 0.2 $\delta^{34}\text{S}\%$, whereas sphalerite data distributed between 2.3 and 2.7 $\delta^{34}\text{S}\%$ (Table 5). Four of our samples form two co-genetic galena-sphalerite pairs: Ve-17 and Ve-19 ($\Delta^{34}\text{S}=2.7$), as well as Ve-18 and Ve-21 ($\Delta^{34}\text{S}=2.9$). As the isotopic differences between sphalerite and galena appear to be quite consistent, the calculation of an equilibrium temperature of their formation is justified. By using the most recent fractionation sphalerite-galena equation of LI & LIU (2006), the values indicate temperatures of 250 and 270°C , respectively, whereas slightly lower temperatures in the range 235 - 250°C are obtained using e.g. the equation of CZAMANSKE & RYE (1974). Thus it can be concluded that the sulphide precipitation occurred at around 250°C in the quartz-base-metal-fluorite veins of the Velence Mts.

| Sample No. | Mineral | Locality of sample | $\delta^{34}\text{S}$ (‰) |
|------------|------------|------------------------------------|---------------------------|
| Ve-17 | sphalerite | Pálka | 2.3 |
| Ve-19 | galena | Pálka | -0.4 |
| Ve-18 | sphalerite | Pálka, Kőrösis-begy, "acélcs-árok" | 2.7 |
| Ve-21 | galena | Pálka, Kőrösis-begy, "árok-102" | 0.2 |
| Ve-20 | galena | Pálka, Székely-árok, "Tuzsok árok" | -1.5 |

Table 5. S isotope data of some minerals from the quartz-fluorite-base metal veins. Sample localities are indicated in the Appendix 1

Sulphur isotope composition of galena and sphalerite from the Velence Mts. are -0.4 – 2.7 $\delta^{34}\text{S}$. These values are similar or slightly higher than the 0 – -10 $\delta^{34}\text{S}$ values of the Alpean MVT ore at Bleiberg and Mezica along the PAL. This is in accordance with the similar origin for the deposits that have been compared.

4.3 FLUID INCLUSION STUDIES

La compilation de données antérieures concernant les formations hydrothermales dans les monts Velence en liaison avec les écoulements fluides Varisques et Alpains fait apparaître que trois assemblages d'IF peuvent être connectés. Dans les quartz magmatiques du granite et dans les veines hydrothermales, les assemblages d'IF suivants ont été mis en évidence:

Type I FIA identifié par Molnar (1997) dans les veines de quartz-molybdénite comme inclusion primaire. Ces inclusions apparaissent dans la zone de Nadap comme IF secondaires dans le quartz magmatique. Les inclusions de type I ont une phase aqueuse (L_{aq}) et deux phases carboniques (L_{car}: carbonique liquide et V_{car} vapeur carbonique). Le rapport (L_{aq}/L_{car}+V_{car}) de ces phases de type I varie de 0.4 à 0.95.

Leurs caractéristiques pétrographiques suggèrent un piégeage inhomogène à partir d'un fluide hétérogène. Les inclusions de type I/b ont une phase vapeur de 30% ce qui suggère un piégeage homogène à partir d'un parent homogène. Les Th sont de l'ordre de 220-320°C. La température de l'Eutectique à -21°C témoigne d'un système NaCl-H₂O avec une salinité de 0,5-7,7 NaCl equiv. wt%. Cet assemblage représente une plus jeune phase du système fluide qui a piégé les inclusions de type I/a.

Les inclusions de *Type II and III* FIA se trouvent partout dans les plans d'IF dans les quartz magmatiques excepté en proximité des veines andésitiques du secteur de Nadap. Elles apparaissent également comme IF primaires dans les fluorite et les quartz des veines à quartz-fluorite-base metal. Comme les assemblages à illite-kaolinite-smectite sont syngénétiques des veines à quartz-fluorite-base metal qui ont été datés du Trias, les IF concernées le sont également. Le ratio phase Liq/Vapeur est de 0,3 dans les veines hydrothermales et les plans d'IF de la zone de Nadap-Sukoró. Ce ratio est systématiquement inférieur à 0,1% dans le bloc Székesfehérvár-Pákozd. Des ratios équivalents dans des assemblages identiques indiquent des piégeages homogènes à partir de fluides homogènes. Les Th de la zone de Nadap-Sukoró varient entre 160-240°C et 70-180°C dans la zone de Székesfehérvár-Pákozd. Les IF de Type II et III se différencient par leur salinité. Les IF du Type II ont des faibles salinités 1,3-12,4 NaCl equiv wt% et ces fluides peuvent être modélisés par un système électrolytique binaire NaCl-H₂O alors que le Type III correspond à un système ternaire CaCl₂-NaCl-H₂O déduit de la faible température de son eutectique -50°C.

La salinité des IF de Type III est supérieure entre 16-22 NaCl+CaCl₂ equiv wt%. La Th dans un système fluide homogène nécessite un minimum de P et T pour nécessiter des conditions

P,T de piégeage du fluide. Le piégeage peut avoir lieu partout le long de l'isochore. Cependant, on peut déterminer une pression de piégeage de l'ordre de 700-1000 bar en calculant l'intersection des isochores avec les isothermes (250°C) déduits des données isotopiques des sulfures présents dans les veines de quartz-fluorite-base métal. Cette pression est inférieure aux conditions de piégeage du granite mais supérieure aux conditions P,T du système volcanique. La répartition bimodale des sTh des blocs Nadap-Sukoró et Székesfehérvár-Pákozd suggère un important déplacement horizontal de ces blocs l'un par rapport à l'autre post Triasique.

Des IF de Type IV sont présentes dans la zone Nadap et le Qz magmatique des zones illitisées autour des dikes andésitiques. Les phases vapeur sont de 30 à 100% suggérant un piégeage inhomogène à partir d'un fluide initial hétérogène (ébullition). On peut subdiviser en trois ce groupe selon la salinité. Le sous groupe de Type IV/a. se caractérise par des faibles salinités (0,5-11 NaCl equiv. wt%), avec une composition NaCl-H₂O .

La composition des IF de Type IV/b. peut être modélisée par un système ternaire CaCl₂-NaCl-H₂O à partir de la salinité de l'eutectique sachant qu'elle est de 17-25 CaCl₂+NaCl equiv. wt%. Les propriétés microthermométriques des IF de Type IV a et b sont identiques des zones hydrothermalisées des unités volcaniques paléogènes. La pression minimum est de 17-22 bars ce qui correspond à un enfouissement de 220 à 280 sous la surface hydrostatique. Ces fluides ont migré dans le granite au Paléogène.

Dans les inclusions de Type IV/c , de la halite apparaît et les ratios de phase vapeur suggèrent de l'ébullition. Les Th minimales sont 230°C pour une salinité de 20-30 NaCl equiv wt%. Ces données sur les IF confirment des déplacements horizontaux dans le granite au Paléogène.

Earlier studies by MOLNÁR et al. (1995) and MOLNÁR (1996; 1997; 2004) distinguished three major types of fluid inclusion assemblages in various mineralization of the granite intrusion of the Velence Mts. They were related to the Alpine and the Variscan fluid flow processes. Samples of the current studies were collected systematically in the Velence Mountains: in the vicinity of the hydrothermal veins, in the fresh granite and in the granite porphyry. In the rock forming quartz crystals of the granite and in the hydrothermal veins, the following fluid inclusion assemblages have been discriminated:

4.3.1 Type I FIA: Carbonic-aqueous fluid inclusion assemblages trapped from an inhomogeneous fluid (Photoplate 1/A.)

Type I FIA has been identified in FIP of rock forming quartz from granite and granite porphyry in the eastern part of the Nadap area, in the Gécsi Hill quarry. Phase compositions of this kind of fluid inclusions consist of one aqueous (L_{aq}) and two carbonic phases (L_{car}: carbonic liquid and V_{car}: carbonic vapour). The L_{aq}/L_{car}+V_{car} phase ratio ranged from 0.4 to 0.95. The varying phase ratio in the same FIA is characteristic for inhomogeneous trapping from a heterogeneous parent fluid (effect of necking down has been excluded by petrography). The melting of the L_{car} phase took place between -56,6 – -57,6°C in these inclusions. The lower melting temperatures than the triple point of the CO₂-system may indicate the presence of small amount of other volatiles (N₂, CH₄, H₂S). However, the Raman spectroscopic studies did not confirm this assumption, or at least the amount of volatiles remained under the detection limit of the equipment. Melting of the clathrate phase took place in the presence of liquid and gas carbonic phase between 7,5 – 9,4°C. The measured clathrate melting temperatures suggest that salinities of the aqueous phase is 1,4-4,8 NaCl equiv. wt% in these inclusions. Homogenization of the L_{car} and V_{car} was between 24,4 – 30°C into L_{car}. The total homogenization was not possible to achieve before decrepitation upon heating. Assuming pure CO₂ without any other volatile component and approximately 2 NaCl equiv. wt% salinities, the composition of the immiscible end members in the heterogeneous parent fluids of Type I/a. FIA are $X_{H_2O}=0,8012$ $X_{CO_2}=0,1886$ $X_{NaCl}=0,0100$ and $X_{H_2O}=0,2986$ $X_{CO_2}=0,6976$, $X_{NaCl}=0,03756$, respectively.

Type I/B fluid inclusions appeared in FIP of the rock forming quartz crystals of the granite porphyry, in the same outcrop where Type I/a inclusions were identified. Petrographically, the ratio of the V_{aq} was at around 30%, therefore their entrapment was homogenous. The homogenization temperature was between 220-340°C (Figure 19). The eutectic temperatures at -21°C reveals NaCl-H₂O system, the salinity was low 0,5-7,7 NaCl equiv. wt%. These electrolyte solutions are carbon dioxide free or pure in carbondioxide, since no chlatrate melting was observed. MOLNÁR (1997) identified fluid inclusions with the same homogenization temperatures and ice melting temperatures as primary inclusions in the quartz-molybdenite veins at the same locality. Although he observed chlatrate melting in some inclusions, these inclusions can be regarded microthermetrically carbon-dioxide poor. It was explained by the degassing of non-mixing carbon-dioxide bearing fluid system, related to cooling and decreasing pressure (MOLNÁR

1997). This assemblage represents a younger phase of the fluid system from which Type I/a. inclusions trapped.

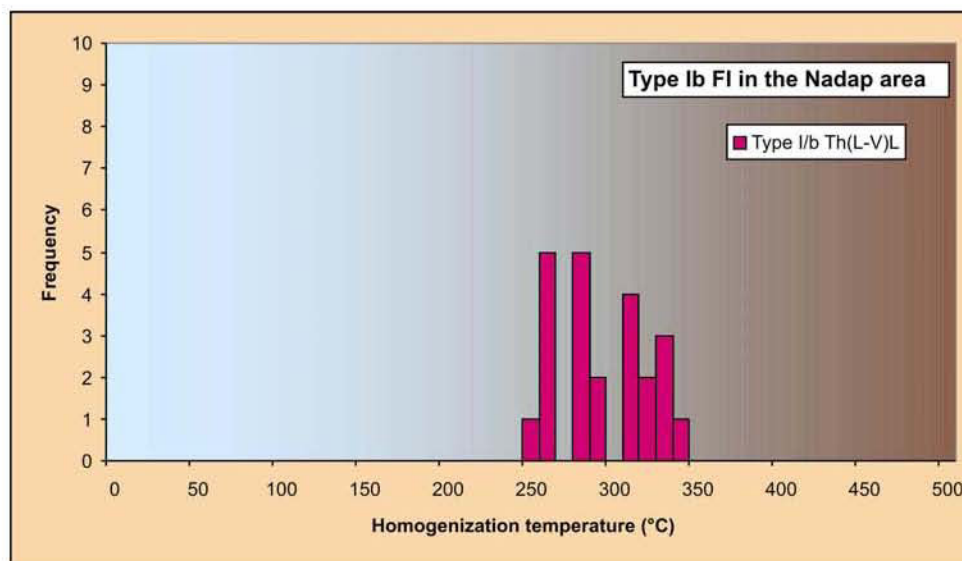


Figure 19. Homogenization temperature distribution of the Type I/b. FIA.

4.3.2 Type II and Type III FIA: Aqueous fluid inclusion assemblages trapped from homogeneous parent fluid

Type II FIA (Photoplate 1/B and 1/C) occur everywhere in the FIP of the rock forming quartz of the granite, except for the close vicinity of the andesite veins in the Nadap area of the granite. They also occur as primary fluid inclusions in fluorite crystals of the quartz-fluorite-base metal veins. Volume ratio of the vapour to liquid phase is around 0.3 in the hydrothermal veins and in FIP in the Nadap-Sukoró area. In the Székesfehérvár-Pákozd block this ratio is systematically below 0.1. The phase ratio is the same in trails of co-genetic (fracture related and primary) fluid inclusions indicating homogeneous trapping from a homogeneous parent fluid. Homogenization temperatures varied between 70-180°C (modus: 140°C) in the Székesfehérvár and Pákozd areas and around 160-240°C (modus: 220°C) in the Nadap-Sukoró area, respectively (Figure 20). Eutectic temperatures varied between -21– -29°C which is close to the eutectic temperature of the pure NaCl-H₂O system. Deviation from the ideal -21°C eutectic temperature of the H₂O-NaCl indicates little amount of additional cations (Ca²⁺, Mg²⁺...) in the fluid or

metastable eutectic temperature. Final melting temperatures were between $-0,2$ – $-8,6^{\circ}\text{C}$ corresponding to 0,3-12,4 NaCl equiv. wt%.

Type III FIA is also common in the rock forming quartz of the granite and granite porphyry, as well as primary inclusions in the quartz crystals of the quartz-fluorite-base metal veins. It is petrographically identical with Type II FIA (Vaq – 10% in the Székesfehérvár – Pákozd area and Vaq – 30% in the Nadap-Sukoró area) but their behaviour during freezing was different. Eutectic temperatures are between -49 and -56°C and final ice melting temperatures are between -12 and -23°C . The fluid composition can be modelled by the NaCl-CaCl₂-H₂O ternary system and the salinity is 16-22 NaCl+CaCl₂ equiv. wt%. In the Székesfehérvár – Pákozd area, their homogenization temperatures varied between 80 - 180°C (modus: 140°C), and in the Nadap-Sukoró area between 180 - 260°C (modus: 220°C ; Figure 21).

4.3.3 Type IV FIA: Aqueous fluid inclusion assemblages, trapped from inhomogeneous fluid

Occurrences of *Type IV FIA* (Photoplate 2D-H) are restricted to the Nadap area. On that location they occur in FIP of the the rock forming quartz of the granite with illite alteration. They were also detected in FIP of rock forming quartz from an andesite dike, and as secondary fluid inclusions in the quartz crystals of the early Palaeozoic slate. They were also identified as primary inclusions in NE-SW trending quartz veins in the Gécsi Hill pegmatite, in the Gécsi Hill quarry (Nadap area) and in the barite crystals of the quartz-barite vein in the Nadap-Sukoró area (Figure 1).

Type IV FIA is generally characterized by variable phase compositions from vapour rich to liquid rich reflecting inhomogeneous entrapment from a heterogeneous (boiling) aqueous fluid system. The minimum volume of vapour in the liquid rich inclusions is about 30%, whereas the vapour rich end-member inclusions apparently do not contain liquid phase (due to optical problems with observations of thin liquid films along the walls of these inclusions). In Type IV/a. and IV/b. FIA liquid-rich aqueous fluid inclusions are associated with the vapour phase rich fluid inclusions while in Type IV/c. FIA halite bearing liquid rich inclusions are associated with the vapour phase rich inclusions.

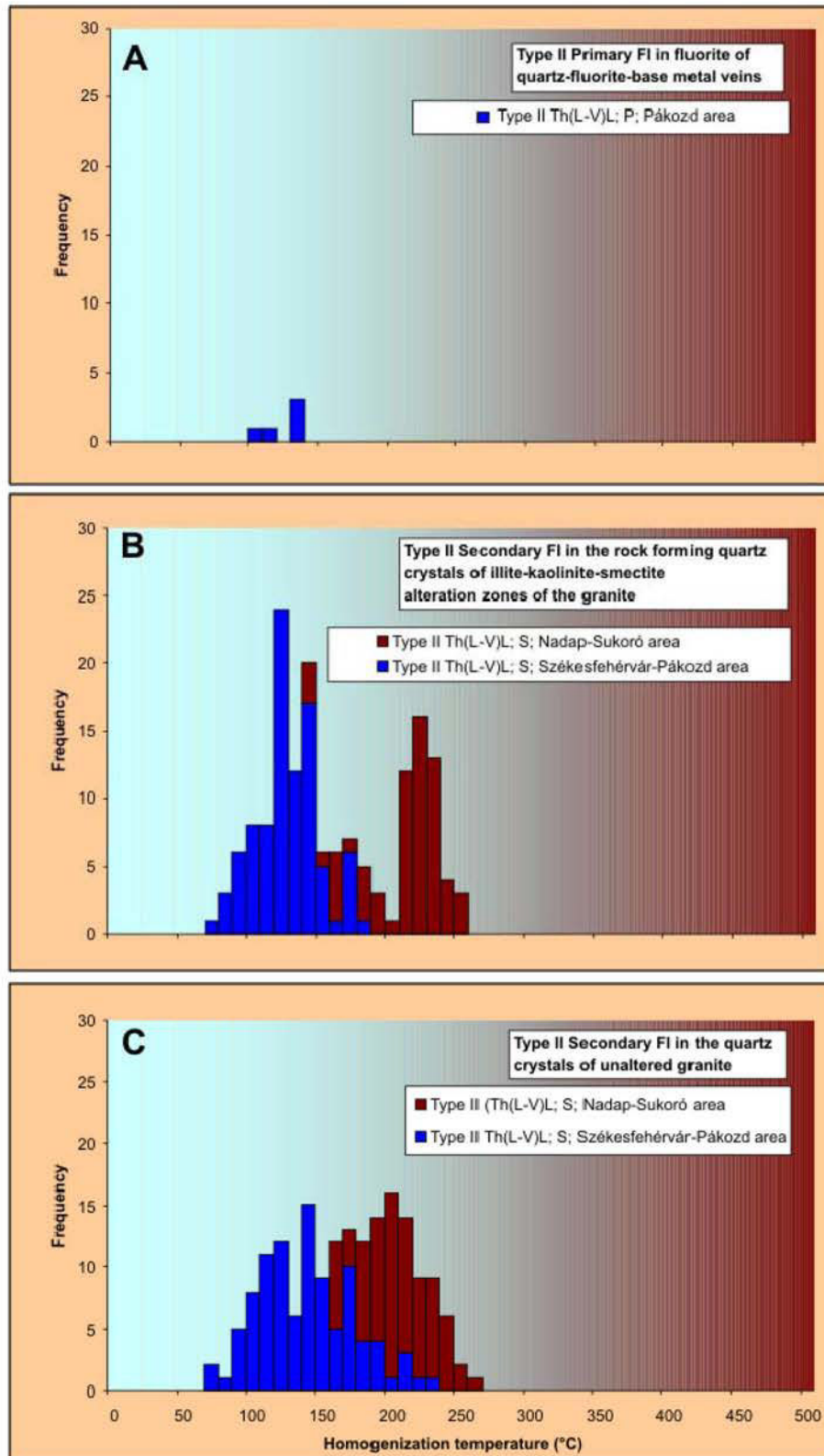


Figure 20. Frequency distribution diagrams for homogenization temperatures of Type II fluid inclusions from the Velence Mts. Abbreviations: L – liquid, V – vapor, Th(L-V)L – homogenization to liquid by vapor phase disappearance; S – secondary fluid inclusion

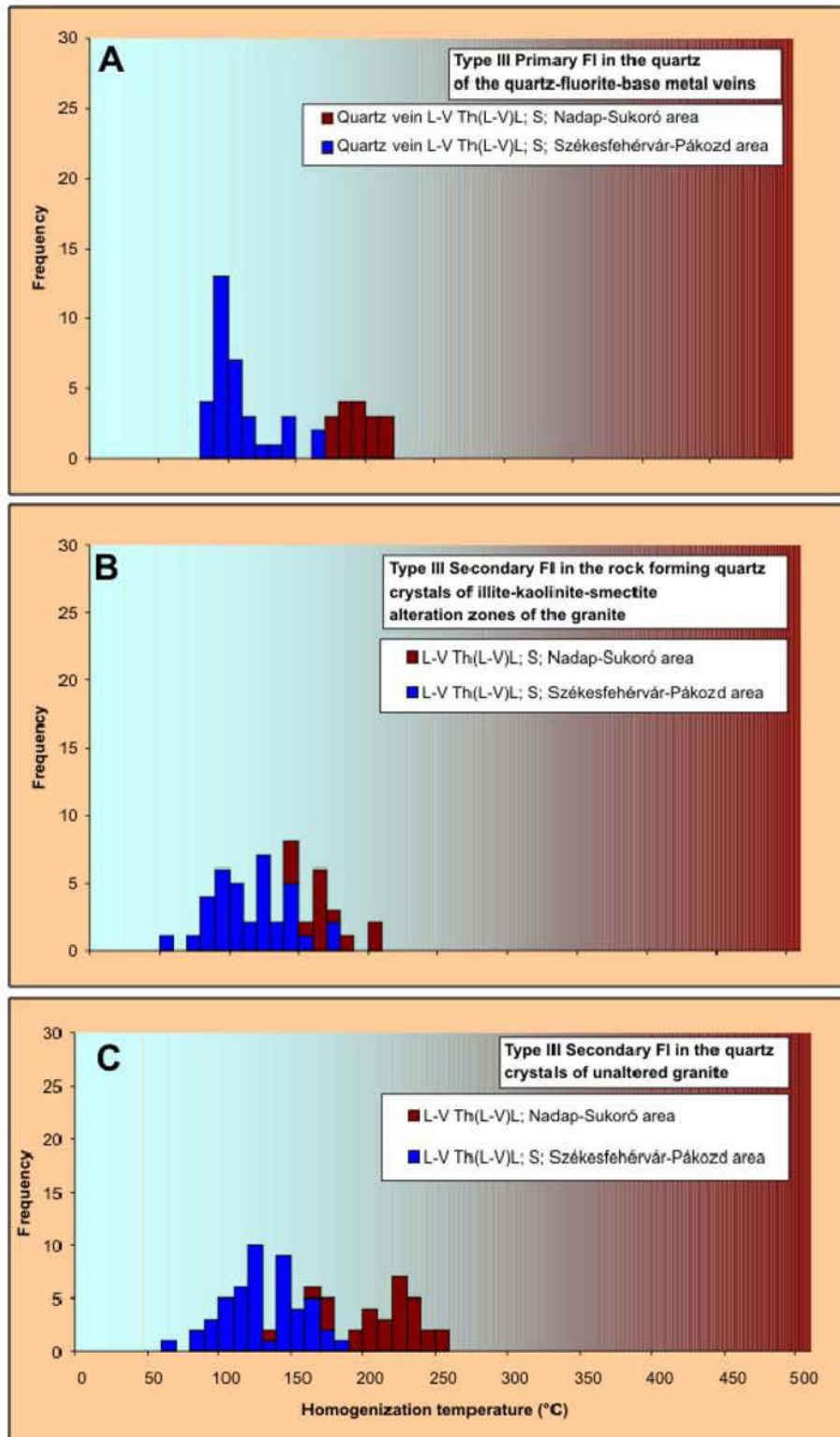


Figure 21. Frequency distribution diagrams for homogenization temperatures of fluid inclusions from the Velence Mts. Abbreviations: L – liquid, V – vapor, Th(L-V)L – homogenization to liquid by vapor phase disappearance; S – secondary fluid inclusion

The distinction between Type IV/a and Type IV/b FIA is based on the microthermometric data. In *Type IV/a* FIA eutectic melting temperatures are around -21°C , which assume a NaCl dominated aqueous solution. The final melting of the ice took place between $-0,7^{\circ}\text{C}$ and $-7,4^{\circ}\text{C}$ which corresponds to 1,2-11 NaCl equiv. wt%. Minima of homogenization temperatures vary depending on the locations. In the quartz crystals of the slate the minimum of the homogenization temperatures was 330°C and the same temperatures were measured in the inclusions of the pegmatite on the Gécsi Hill as well. In the quartz veins, crosscutting the same pegmatite the minima of the homogenization temperatures was 390°C . 220°C minimum homogenization temperature was measured in the primary and secondary fluid inclusions of the barite crystals of the quartz-barite veins and in the quartz-fluorite-barite-zeolite paragenesis (Figure 22 A and C). Homogenization took place both in liquid and in vapour phase depending on the degree of filling.

Type IV/b FIA was found in secondary fluid inclusions in the rock forming quartz of an andesite dike. The FIA is characterized by low eutectic temperatures at -49 – -55°C indicating NaCl-CaCl₂-H₂O composition. A final ice melting took place between -14 and -29°C corresponding to 17-25 NaCl+CaCl₂ equiv. wt%. Homogenization into liquid phase was observed between 210 - 290°C (Figure 22B). The homogenization temperatures correspond to 14-22 bar pressure under hydrostatic conditions.

Type IV/c FIA is present in the rock forming quartz of granite with illite alteration. Melting of the halite took place between 80°C and 200°C , and homogenization of vapour phase into liquid phase occurred between 230 - 270°C (Figure 22A). The calculated salinities are between 27,7-32 NaCl equiv. wt%. In a gas rich inclusion from the same assemblage homogenization into the vapour phase occurred at 232°C .

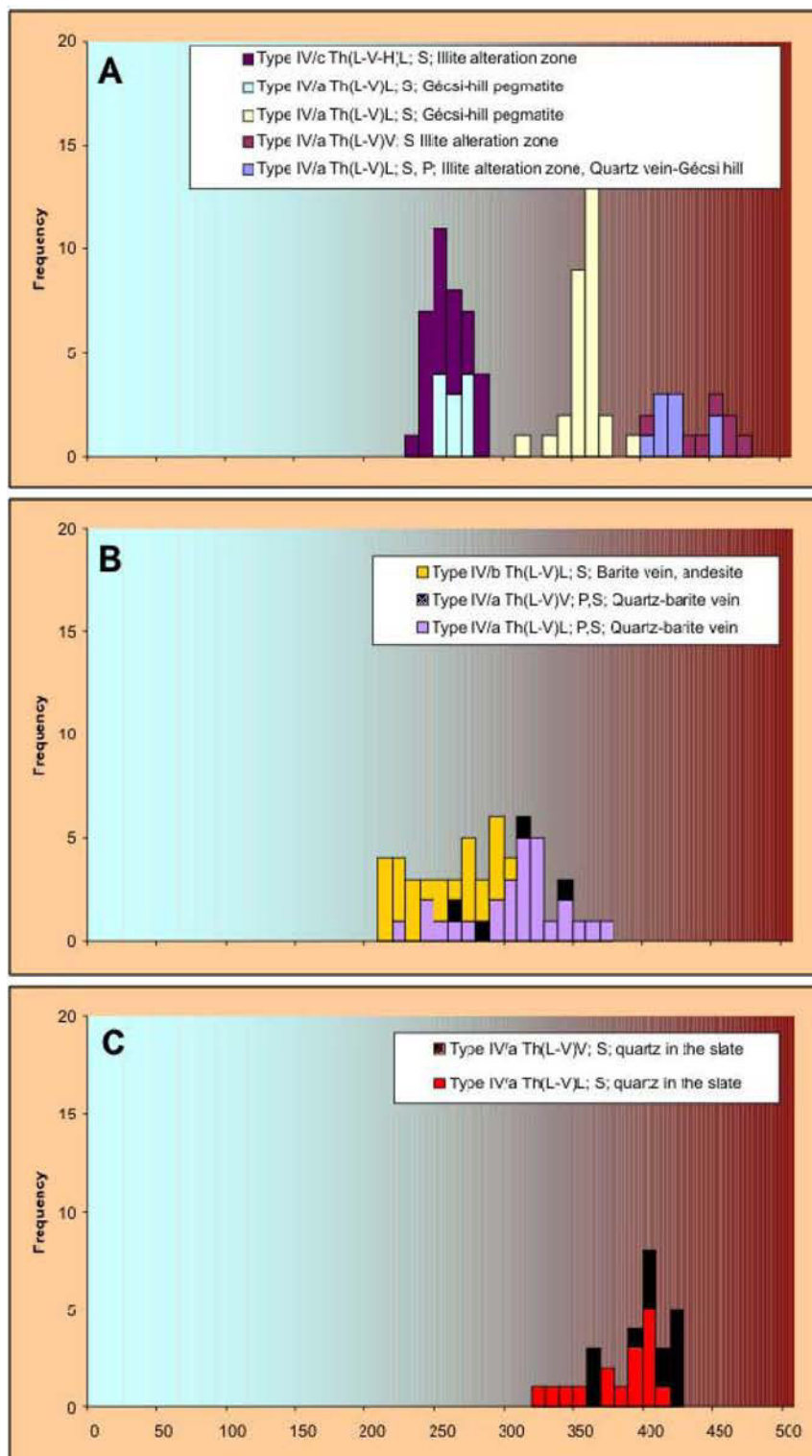


Figure 22. Frequency distribution diagrams for homogenization temperatures of fluid inclusions from the Nadap area of the Velence Mts. Abbreviations: L – liquid, V – vapor, Th(L-V)L – homogenization to liquid by vapor phase disappearance, Th(L-V)V – homogenization to vapor by liquid phase disappearance; S – secondary fluid inclusion; P – primary fluid inclusion

4.3.4 Interpretation of the fluid inclusion analysis

Petrographically three different fluid inclusion types have been distinguished in the Velence granite (Table 6, Photoplate 1). Type I FIA trapped from an inhomogeneous carbonic-aqueous fluid system. They were found but locally in the Nadap area in one locality. MOLNÁR (1997, 2004) found fluid inclusion assemblages with similar petrography and microthermometric properties for primary inclusions in the hydrothermal quartz crystals of quartz-molybdenite stockwork mineralization also locating in the Nadap area. Trapping pressure was estimated to be 1,6-2,1 kbar and the trapping temperature 390-400°C for these inclusions. Since the calculated trapping conditions are close to the crystallization conditions of pegmatites and the granite (BUDA 1993; MOLNÁR et al. 1995) formation of the quartz-molybdenite veins, and the CO₂ rich fluid system are connected to the postmagmatic-hydrothermal system of the cooling Variscan granite. Petrographic and microthermometric properties of Type I FIA are identical with these results.

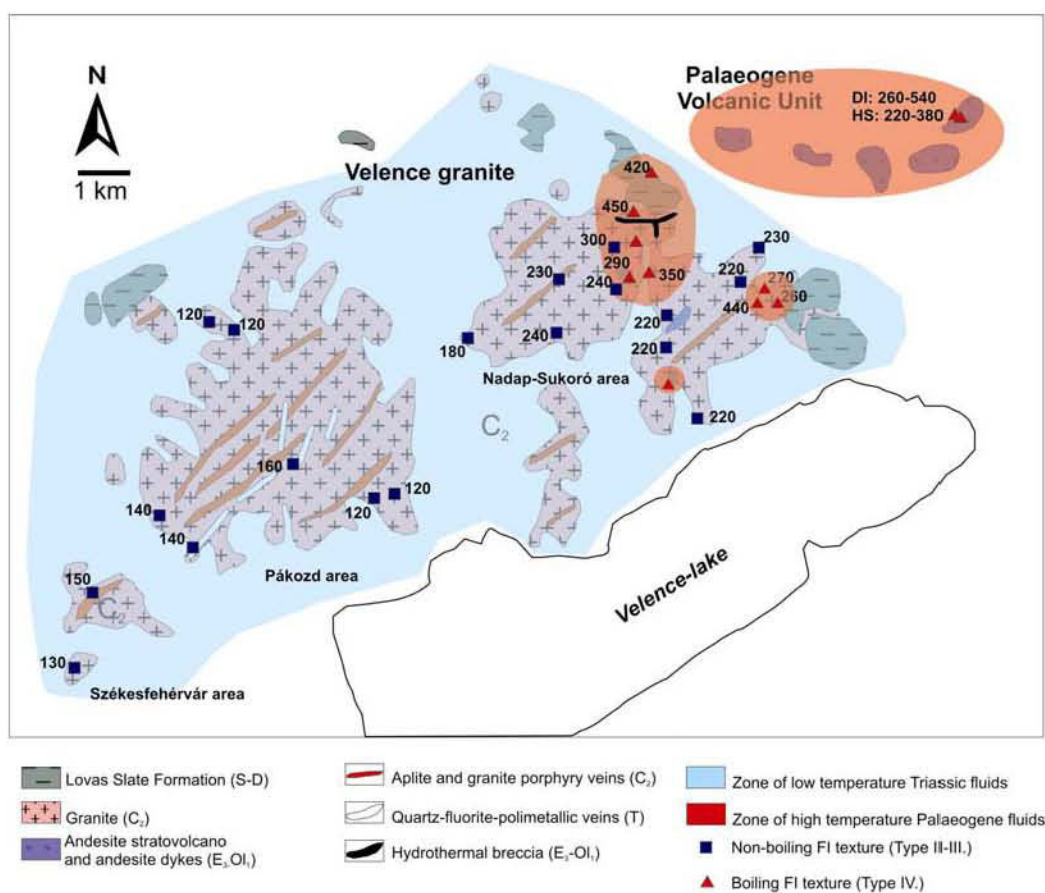


Figure 8.

Figure 23. Distribution of the modus of the homogenization temperatures in the Velence Mts.

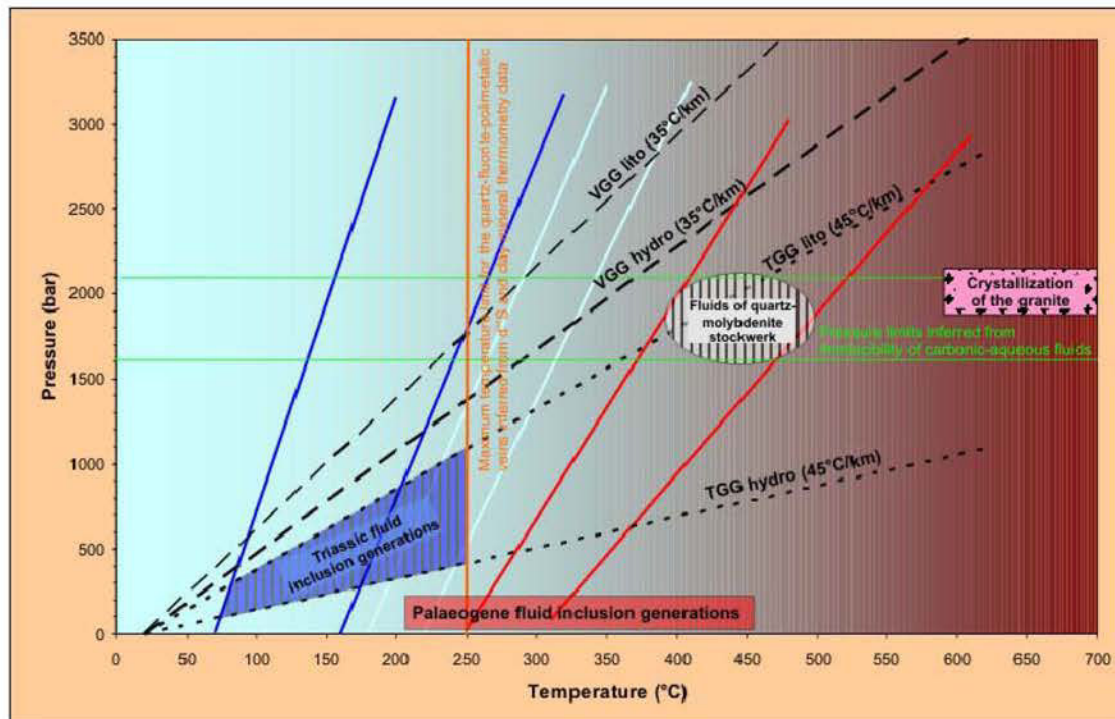
Type II (NaCl-H₂O) and III FIA (CaCl₂-NaCl-H₂O) was trapped homogeneously from a homogeneous parent fluid, therefore it is impossible to calculate the pressure and temperature for their entrapment using only fluid inclusion data. They have the same homogenization temperature distribution in the two blocks of the granite, and the only difference was found in their salinity. They are regionally present in the granite but they were found also as primary inclusions in the quartz-fluorite-base metal veins, therefore these types of fluids were responsible their formation and they can be connected to the same fluid circulation event. Since the quartz-fluorite-base metal veins date back to Triassic on the basis of the K-Ar data of the co-genetic illite-kaolinite-smectite assemblage, Type II and III FIA can be connected to the Triassic fluid circulation event.

The homogenization temperature distributions and their mean in all outcrops are similar (Figure 20 and 21). However, a 80°C difference was found in the mean of homogenization temperatures between the Székesfehérvár-Pákozd and Nadap-Sukoró areas (Figure 23). If we assume that these inclusions relate to the cooling of the granite which crystallized at 2 kbars pressure, the isochore of the low homogenization temperature inclusions should cross the 2 kbar isobar at 150-220°C. This low temperature at 6-8 km, according to the 2 kbar pressure, assumes a very low geothermal gradient (~20°C/km). However, the average geothermal gradient in the Variscan orogen belt was at around 35°C/km (SCHUSTER et al. 1995). In the case of a cooling granite body we would have expected even higher temperature than the normal geothermal gradient, consequently the observed inclusions cannot be related to the postmagmatic-hydrothermal system of the granite.

Migration of quartz-fluorite-base metal vein forming hydrothermal fluids started at approximately 250°C according to the sulphur isotope results. This is an estimate also which is supported by the formation temperatures of the clay mineral assemblage (220-250°C). Intersecting the isochors of the higher homogenization temperature group (180-220°C) with the 250°C isotherm causes pressures between 450-1000 bar that corresponds to 1700-3700 metre depth under lithostatic conditions (calculating by 2600 kg/m³ rock density; Figure 24). This pressure is lower than the pressure at the time of the formation of the granite, but higher than the pressure (30-100 bar) of the Palaeogene hydrothermal system (Figure 24).

For the outlined ore-forming fluid, the geothermal gradient should have been 70-75°C/km, if no magmatic heat source and lithostatic conditions for the 1700-3700 m depth are

assumed. This is an exceedingly high value (the Triassic thinning resulted in maximum $45^{\circ}\text{C}/\text{km}$, SCHUSTER et al. 1999). Consequently, a magmatic heat effect cannot be excluded, but except for the granite no other magmatic body have been detected in drillholes or by geophysical surveys in the Velence Mts. (Bouger-anomaly maps, residual anomaly maps; PINTÉR 1983). However, it cannot be excluded, either that there is a hidden magmatic body below the granite knowing that there are only shallow drillholes exist. It is therefore possible that geophysics might not have been sensitive enough to differentiate between various types of magmatic rocks.



- Representative isochors for Type IB FIA
Th(L-V)/L=180-220°C
- Representative isochors for Type I/II FIA in the Székesfehérvár-Pákozd area
Th(L-V)/L=70-180°C
- Representative isochors for Type I/II FIA in the Nádap-Sutócső area
Th(L-V)/L=180-220°C
- - - VGG hydro: Variscan geothermal gradient for hydrostatic pressure (Schuster et al. 1995)
VGG lito: Variscan geothermal gradient for lithostatic pressure (2800 kg/m³)
- · · TGG hydro: Triassic geothermal gradient for hydrostatic pressure (Schuster et al. 1999.)
TGG lito: Triassic geothermal gradient for lithostatic pressure (2800 kg/m³)

Figure 24. Temperature-pressure conditions of fluid inclusion entrapment in the Variscan, Triassic and Alpine hydrothermal systems of the Velence Mts. Isochors were calculated on the basis of data from ZHANG & FRANTZ (1987).

Fluid inclusion analysis on galena, fluorite and calcite crystals of stratabound Pb-Zn mineralizations along the PAL (Mezica, Bleiberg) indicate very similar petrographic and microthermometric properties (ZEEH et al. 1998). ZEEH et al. (1998) reported that the temperature of the hydrothermal fluids ranged between 122 and >200°C. In their study, the salinity of the fluids was 8-12 NaCl equiv. wt% in dolomite, 15-19 NaCl equiv. wt% in fluorite. The salinity of the second hydrothermal phase was higher as in fluorite, but the temperature was lower (150-175°C). Similarities in microthermometric data between the Alpine deposits and the Velence Mts. are obvious. Mixing of primary low salinity magmatic fluids and high salinity formational fluids in the Velence Mts. was first suggested by MOLNÁR (1996), who considered the primary fluids to have originated from the granite. Maintaining the concept of a mixing model including two types of fluids, we postulate a Triassic magmatic origin for the low salinity fluid component.

The Type IV FIA trapped heterogeneous from an inhomogeneous system. The calculated pressure of the entrapment from the minimum of the homogenization temperatures (220-230°C) is 17-22 bar which corresponds to 220-280 m depth below the paleo-water table under hydrostatic conditions. The density of the liquid was taken to 0,8 g/cm³. The calculated pressures and the corresponding paleodepths indicate shallow level hydrothermal circulation. MOLNÁR (1996; 2004) found FIA with similar petrographic and microthermometric properties in the hydrothermal minerals in the Palaeogene hydrothermal centres of the stratovolcanic series and in the hydrothermal minerals of the diorite intrusion. The Type IV FIA occur only in the Nadap-Sukoró area with perfect overlap with the pure illite clay mineral assemblage occurrences (Figure 17 and 22). This two arguments evidently confirm that the hydrothermal fluids from which the Type IV FIA trapped are Palaeogene of age.

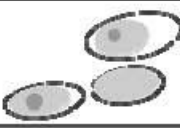






| Inclusion type | Phase ratio | Petrography | Salinity (equiv. wt%) | Homogenization temperature | Age | Characteristic mineral phases in the alteration zones |
|----------------|-----------------------------------------------------------------------------------------------|-------------------------------------------------------------------------------------|---------------------------------|----------------------------------------------------------------|-----------|-------------------------------------------------------|
| IA. | $L_{CO_2}+V_{CO_2}$ =40-95%, L_{aq} =10-40% |  | 1,4-4,8 NaCl | $Th(L_{CO_2}-V_{CO_2})L_{aq}$ =24,4-30°C Th_{H_2O} >300°C | C_1 | quartz-molybdenite stockwork |
| IB. | L_{aq} - 70% V_{aq} - 30% |  | 0,5-7,7NaCl | 220-340°C | C_1 | quartz-molybdenite stockwork |
| II. | Sz-Pá area, Na-Su area. L_{aq} - 93% L_{CO_2} - 70% V_{aq} - 10% V_{CO_2} - 30% |  | 0,3-12,4 NaCl | Sz-Pá area: 70-190°C Na-Su area:160-240°C | T | illite-kaolinite-smectite |
| III. | Sz-Pá area, Na-Su area. L_{aq} - 93% L_{CO_2} - 70% V_{aq} - 10% V_{CO_2} - 30% |  | 16-22 NaCl+CaCl ₂ | Sz-Pá area: 80-190°C Na-Su area:160-260°C | T | illite-kaolinite-smectite |
| IVa. | L_{aq} -70-9% V_{aq} -30-69% |  | 0,5-11 NaCl | 220-470°C | E_3-O_1 | illite |
| IVb. | L_{aq} -70-9% V_{aq} -30-69% |  | 17-25 NaCl+CaCl ₂ | 210-290°C | E_3-O_1 | illite |
| IVc. | L_{aq} -60-9% V_{aq} -30-69% H-9-10% |  | 20-31,9 NaCl | 230-270°C | E_3-O_1 | illite |

Table 6. Petrographic, microthermometric properties of FIA-s, identified in the rock forming quartz crystals of the Velence Mts. granite. Abbreviations: LCO₂ – carbonic liquid; VCO₂ – carbonic vapor; Laq – aqueous liquid; Vaq –aqueous vapor; H – halite; Sz-Pá area – Székesfehérvár-Pákozd area; Na-Su – Nadap-Sukoró area.

4.3.5 Proving vertical movements in the granite by means of fluid inclusion studies

As we have observed, both Type II and Type III have a bimodal homogenization temperature distribution at around 140°C and 220°C. In the Nadap-Sukoró area the higher, whereas in the Székesfehérvár-Pákozd area the lower homogenization temperatures are characteristic. No significant difference was detected in their salinity and FIP orientation, consequently they can be connected to the same hydrothermal fluid circulation event.

But what is the reason of the different homogenization temperatures between the two areas? The deviation in the homogenization temperatures could result from the vertical tectonic

movements of the different blocks of the granite. To determine the magnitude of the movement is nonetheless very difficult because the exact trapping conditions are unknown: Type II and Type III inclusions trapped anywhere along their isochors. The maximum trapping conditions are around 240-260°C and at around 700-1000 bar. As the isochores are very steep, a small change in the pressure estimation means very high pressure differences.

During the procedure of pressure estimation 3 different possible scenarios can be established: The first possibility is that all FI were trapped at the same pressure (at the same depth), but under different temperature conditions and the hydrothermal system cooled to the west. We consider this scenario to be unlikely because the homogenization temperature distribution diagrams do not show any continuous tendency from east to the west. The modulus of the Th distributions is equal between the samples of the two blocks. Another possibility is that they all trapped at the same temperature, for example at 240°C and they started to cool down along their isochores. In this case the low homogenization temperature inclusions should have trapped at 3,5 kbar which means higher pressure than the formation of the granite. The third scenario seems to be the most likely of all: The FI in the two blocks were trapped at different pressure and different pressure conditions, thus at different levels of the same hydrothermal system and their juxtaposition happened during younger tectonic events. The Nadap-Sukoró block was the the hotter and deeper during the Triassic fluid migration. Assuming 250°C trapping temperature for the FI in the Nadap-Sukoró area with 210°C homogenization temperature they have trapped at 760 bar. For the estimation of the pressure estimation of the lower homogenization temperature group I used the intersection of the lithostatic geothermal gradient line and the isochore corresponding to 150°C homogenization temperature. This possible temperature and pressure conditions are at 180°C and 600 bar. Difference between the two pressures (760 bar and 600 bar) is 160 bar which corresponds to 615 m difference under lithostatic conditions. However it has to be noted that little changes in the parameters (e.g. in the homogenization temperatures) led to significant differences in the estimation. In summary we can conclude that there was a significant vertical movement between the Nadap-Sukoró area and the Székesfehérvár-Pákozd area after the termination of the hydrothermal activity during the Triassic. Yet, this observation is not surprising, since Velence type granite blocks (Buzsák, Sárvár; Figure 1) – that are located southwest from the Mts. – are buried deep below the Neogene sedimentary cover.

In an epithermal system salinities of FIA can be highly variable, as due to the shallow level phase separation the fluid segregates on a high and low density part. While the high density fluids remain in the deeper part of the hydrothermal system (e.g. at the level of the subvolcanic intrusion), the low density fluids ascend to the volcanic levels (HEDENQUIST et al. 1994).

In the Velence Mts. the Type IV/a, b. FIA represent the low density part of the hydrothermal fluids and the Type IV/c., the deeper levels of the system. In the easternmost part of the Nadap area, in the Palaeogene illitic alteration zones the Cu-porphyry related high salinity fluid inclusions (Type IV/c. FIA) can be found together with the HS-type, low salinity FIA-s (Type IV/a, b.) in the granite on the surface. The HS-type epithermal mineralization related FIA-s formed at a shallow depth of 100-200 m, meanwhile the Cu-porphyry related FI-s trapped much deeper, at around 900 m below the paleo-water table. Because the surface of the granite is now on the same level with the HS-type epithermal alteration centers of the PVU, an approximately 500 m syn-hydrothermal vertical movement can be postulated between the granite and the PVU. The zone of the movement was the Nadap-line, the granite block can be regarded as the footwall and the PVU as the hanging wall block. This also proves uplift of the Nadap-Sukoró block

In its current position the Nadap-Sukoró area of the granite is the most uplifted and the Székesfehérvér-Pákozd together with the Palaeogene Volcanic units are in a relatively depressed position.

4.4 ANALYSIS OF THE STRUCTURAL ELEMENTS OF THE GRANITE AND THE ANDESITE DIKES

ANALYSE STRUCTURALE: PRINCIPAUX RÉSULTATS

Le granite a été divisé en quatre blocs en plus de l'analyse structurale de l'unité volcanique Paléogène. Cette division a été réalisée afin de comparer entre eux des blocs relativement homogènes en ce qui concerne leurs données structurales afin de mieux déterminer leurs rotations relatives. La nature lithologique a été également prise en compte.

Les aplites et dikes porphyriques sont orientées NE-SW et sont tous subverticaux. Les diaclases sont soit NE-SW soit NW-SE avec des pendages NE ou SW.

Les microfissures ouvertes sont subparallèles aux systèmes de diaclases macroscopiques.

Dans la zone de Sukoro les diaclases sont NE-SW mais une nouvelle orientation apparait: ENE-WSW.

Dans le bloc Nadap, en plus des NE-SW apparait également une orientation NNE-SSW. Les plans d'IF sont orientés selon NE-SW et NW-SE mais la densité de plans d'IF NE-SW est plus forte. De nouvelles orientations EW et NS apparaissent dans la zone de Nadap-Sukoro et Nadap mais leurs densités sont moindres que les autres directions.

Les diaclases des dikes de granites porphyrique sont orientées différemment de celles des granites. L'orientation principale est NS avec des pendages E ou W ; elles forment sur certains affleurements des systèmes conjugués de Mohr.

Cette orientation est caractéristique pour beaucoup de zones bien que le système NE-SW soit plus important dans la zone de Nadap. Les microfissures ouvertes dans les dikes porphyriques sont parallèles avec les joints macroscopiques mais à l'échelle microscopique les orientations NW-SE, EW et NE-SW sont bien exprimées. Les plans d'IF ont également les mêmes orientations avec une orientation NS bien exprimée.

Les veines minéralisées soulignées par une alteration à illite-kaolinite-smectite dans la zone de Székesfehérvár sont orientées NS alors que celles de la zone de ákozsd et Sukoró sont surtout NE-SW. Les veines a Qz Pyrite ainsi que les dikes béchiques hydrothermaux de la zone a illite de Nadap sont plutôt orientées ENE-WSW.

Les diaclases des dikes andésitiques intrusifs dans le granite sont NS et NW-SE avec un pendage de 60 à 80°.

Les centres hydrothermal de l'unité volcanique Paléogène (PVU) sont alignés selon EW et forment une ligne de chenalisation des fluides minéralisateurs.

Dans la zone de Székesfehérvár, Pákozsd , ils sont moyennement pentés, ont des stries verticales et des mouvements en failles normales. Leurs orientations sont NE-SW et NW-SE, certaines sont jeunes et les plus anciennes avec des minéralisations a quartz-fluorite-polymétalliques. Dans la zone altérée à illite de Nadap, des failles dextres orientées NE-SW ont été observées comme étant une réactivation de failles normales plus anciennes. Ces failles dextres jouent un rôle important dans la chenalisation des fluides minéralisateurs.

Dans le PVU un réseau de failles dextres orientées NW-SE à été observe et pas ailleurs.

To determine the relative horizontal displacement and rotation between the blocks we analyzed the macroscopic and microscopic tectonic features in every block separately (Figure 26). In this chapter, I made a comparison of the different tectonic elements (magmatic dikes,

joints, mineralised veins, OC, and FIP measured by AnIma) between the different areas and the elements among each other. Detailed maps with sample localities and rose diagrams can be found in Appendix (2-5).

4.4.1 The Székesfehérvár area

(Appendix 2)

The granite porphyry and the aplite dikes have constant NE-SW strike and their dip is vertical-subvertical (70-90°). Joints of the granite have NE-SW strike with NW and SE dip direction and NW-SE strike with NE and SW dip direction. The dip angle is steep (60-90°). Open microcracks in the rock forming quartz of the granite are parallel with the joints. The strike of the subvertical mineralised veins (filled by quartz±fluorite±base metal minerals), illite-kaolinite-smectite clay mineral assemblage, limonite) is N-S (Figure 26).

Joints in the granite porphyry dikes form an apparent conjugated fracture system (Figure 25) dipping to the east and to the west and with northern strike.

Several faults have also been analysed in the block both in the granite and in the granite porphyry. All faults proved to be normal fault with vertical slickensides and high dip angles (75-90°), dipping to NW and SE as well as to NE and SW (Figure 29). At some places the faults were conjugated. The relative temporal sequence of the faults was determinable at two places only. In an outcrop, the joints which are parallel with a main fault were filled by illite-kaolinite-smectite clay mineral assemblage. On the wall of some quartz (quartz-fluorite-base metal) veins which is syngenetic with the illite-kaolinite-smectite alteration, normal faults were measured. Necessarily, if the veins and the formation of the clay mineral assemblage were syngenetic, the faults on the wall of the quartz vein have to be younger than the Triassic. The parallelism of the fault systems with the mineralised veins indicates that the old structural lines have been reactivated during younger tectonic events.

OC in the rock forming quartz of granite porphy are partly parallel with the joints, however a NW-SE direction also appears on the rose diagrams (Figure 26; Appendix 2B).

The orientation of the FIP are parallel with the joints (NE-SW and NW-SE) in the granite. In the granite porphyry an additional N-S striking FIP generation appears, as well.

4.4.2 Pákozds area

(Appendix 3)

The Pákozds area is very similar to the Székesfehérvár area. The strike of the granite porphyry and aplite dike is NE-SW. The joints of the granite are characterised by steep dip angles ($60\text{-}80^\circ$) and with NW and NE strike, dipping to the NE, SW, and to SE, NW, respectively. Orientation of the joints in the granite porphyry is similarly different from the joint system of the granite, N-S striking, dipping to the E and W, dip angles are at about 60° . Geometrically, the joint system corresponds to a well developed conjugated Mohr fault system. Quartz (quartz-fluorite-base metal) veins in the granite are parallel with the aplite and granite porphyry dikes and with the NE-SW trending group of joints (Figure 26). In the studied area only a few vertical/subvertical faults with displacement markers have been found, but those were similar to the NE-SW and NW-SE trending faults, found in the Székesfehérvár area (Figure 29). The faults were often filled by illite-kaolinite-smectite (Triassic) clay mineral assemblage and the same type of alteration was also present in the granite around the faults.

Only one Cretaceous lamprophyre dike was found in the studied area: it has N-S strike. No sign of hydrothermal alteration was found around the dike.

The OC-s in the rock forming quartz of granite are parallel with the joints (Figure 26).

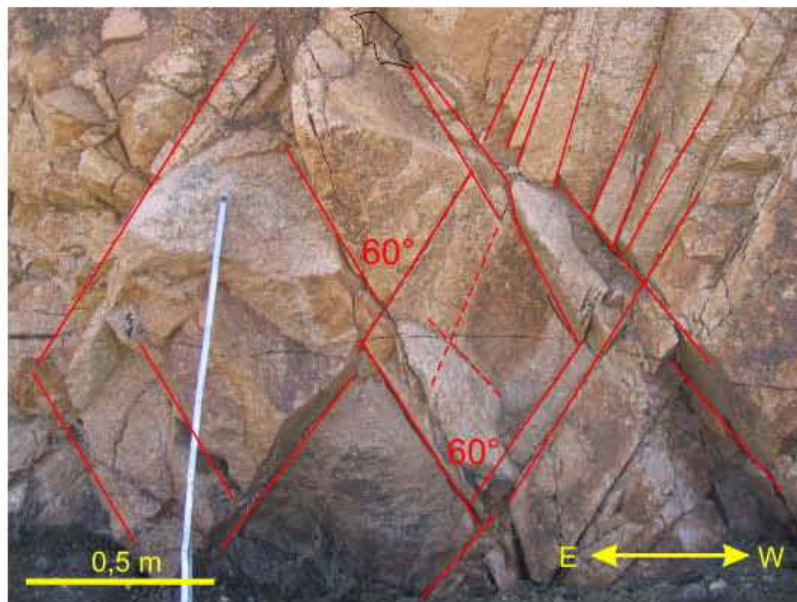


Figure 25. Joints of the granite porphyry in the Székesfehérvár area. The angle of the joints is 60° and forms a conjugate Mohr fracture system

Orientation of the FIP in the rock forming quartz of the granite have unimodal distribution with NE-SW strike in the majority of the outcrops. The NW-SE orientation is absent or subordinated. The strike of the FIP is absolutely parallel with the strike of the quartz veins (NE-SW and subordinately NNE-SSW; Figure 26).

4.4.3 The Nadap-Sukoró area

(Appendix 4)

The orientation of the granite related magmatic dikes (aplite and granite porphyry) is steadily NE-SW and their dip angle is vertical. The NE-SW orientation of the joints is less characteristic, the ENE-WSW orientation is more typical. The NE-SW orientation is absent in some outcrops but it is present in others. Dip angle of joints is subvertical (60-80°) dip directions are NNW-SSE. Joints of the granite porphyries have NNE-SSW strike with 60° dip angle, slightly turned counterclockwise in comparison to the Székesfehérvár and Pákozd areas.

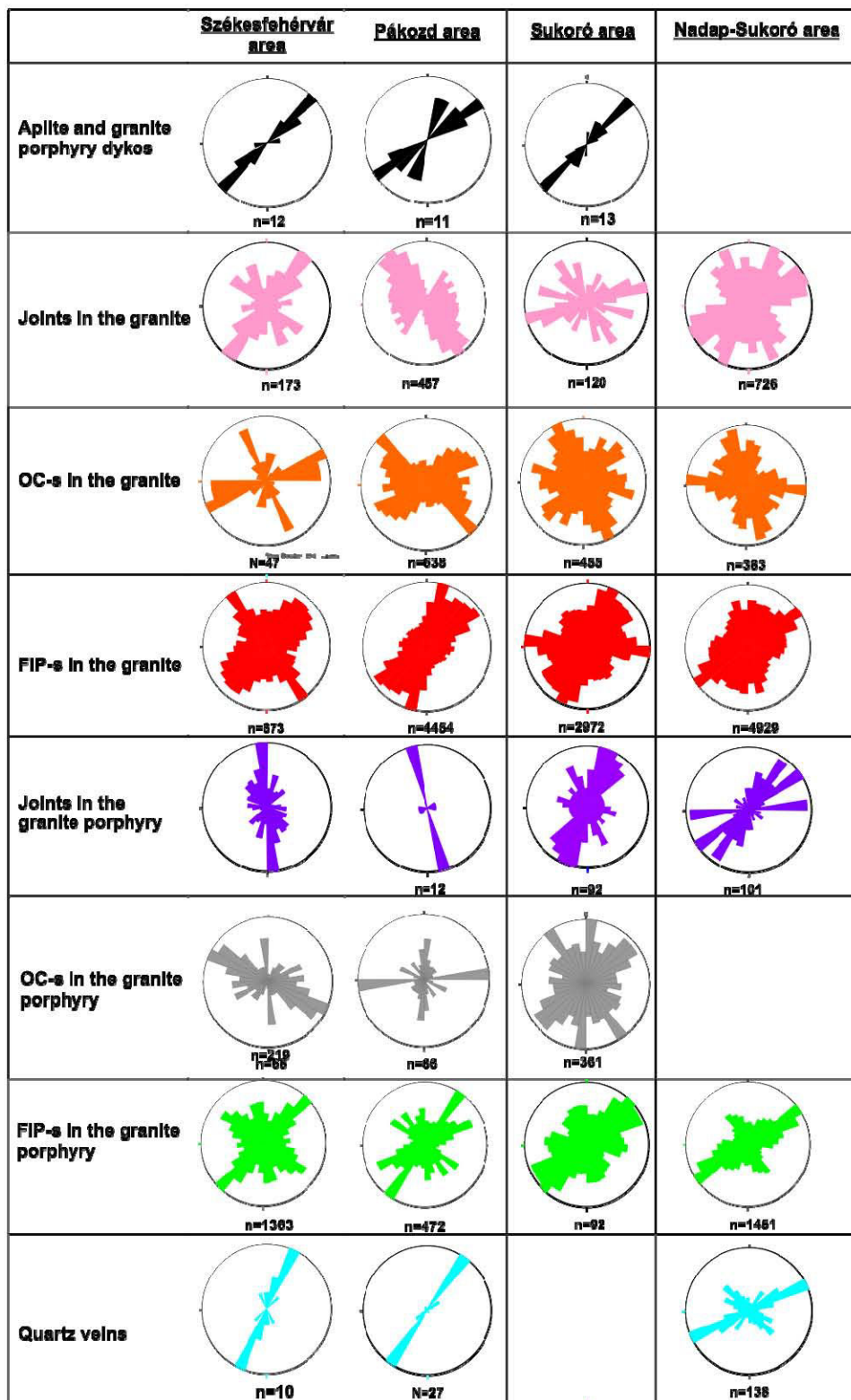


Figure 26. Structural elements in the different blocks of of the granite

OC are parallel with the joints in the granite as well as in the granite porphyry. FIP both in the granite and in the granite porphyry have NE-SW, NW-SE and E-W major orientations (Figure 26).

4.4.4 The Nadap area

(Appendix 5)

The orientation of granite porphyry and aplite dikes could not be measured on the field due to the paucity of occurrences of these features in outcrops, but data from the geological map of the Velence Mts. in 1:25 000 scale (DUDKO 1999) confirm that they are parallel with the dikes in the other three areas.

The NE-SW and the NW-SW strike with 60-80° dip angle is characteristic for the joints just like in the other areas of the Velence Mts dipping to the NW, SE and to the NE, SW, respectively. However, a NNE-SSW striking population is also present with approximately 80° dip angle, dipping to the WNW and ESE. Quartz veins are of Palaeogene age due to the primary Type IV FIA in the growth zones of the crystals. The strike of the quartz veins, in the illite alteration zones is NE-SW and NW-SE, as well as ENE-WSW, their dip is subvertical-vertical (Figure 26).

OC in the rock forming quartz of the granite is parallel with the joints, but the NE-SW orientation is statistically subordinate. In the granite porphyry two joint directions predominate, the NE-SW and the E-W, contrarily to the Pákozd and Székesfehérvár blocks. The orientation of the FIP has four maximums, the NE-SW and NW-SE are prevailing but there are numerous FIP with N-S and the E-W strikes. In the granite porphyry only two orientations are characteristic, the NE-SW and the NW-SE (Figure 26).

The joints of the andesite dikes have N-S and NW-SE strike with 60-80° dip angle, dipping to the W. The N-S striking joints belong to a N-S fault zone (Figure 29). Vertical hydrothermal breccia veins with illite alteration have NE-SW strike. Breccia dike fragments with illite-dickite alteration were found at the contact of the slate and the granite, but the orientation of the contact was not measurable. However, based on the 1:25 000 scale geological map of DUDKO (1999), the strike of the contact is E-W.

In the Nadap area several vertical NE-SW dextral fault zones were measured, which were partly parallel with the illite alteration zones (Figure 26 and 28). The fault crosscuts the Palaeogene quartz veins in the illitic altered granite porphyry. Superimposing slickensides indicate that the dextral displacement rejuvenated the older normal NE-SW trending fault zones.

In the Gécsi Hill quarry (Figure 27) several crosscutting relationships were identified supporting understanding the temporal and spatial relationship of the different magmatic and hydrothermal processes. On the western wall of the quarry the contact of an andesite dike and an illite alteration zone is well exposed. The granite has illite alteration, however, the andesite is characterized by nontronitic alteration and the contact between the granite and andesite, as well as between the alteration assemblages is sharp. Therefore, the illite alteration did not affect the andesite dike. However, in the central part of the quarry, an andesite stock *with* illite alteration also occurs. The nontronitic andesite has though undergone a younger hydrothermal alteration during the Palaeogene as the quartz-fluorite-barite-zeolite paragenesis was found in this dike with primary Type IV/a. FIA.

4.4.5 Palaeogene Volcanic Unit

Hydrothermal centres of the PVU lie on an E-W trending tectonic line (BAJNÓCZI 2003). In the stratovolcanic series the NE-SW and the NW-SE trending fault zone, which was characteristic for the granite, is absolutely absent, only a NW-SE striking joint set was identified. With parallel strike with the joints and flat dip, dextral faults were identified.

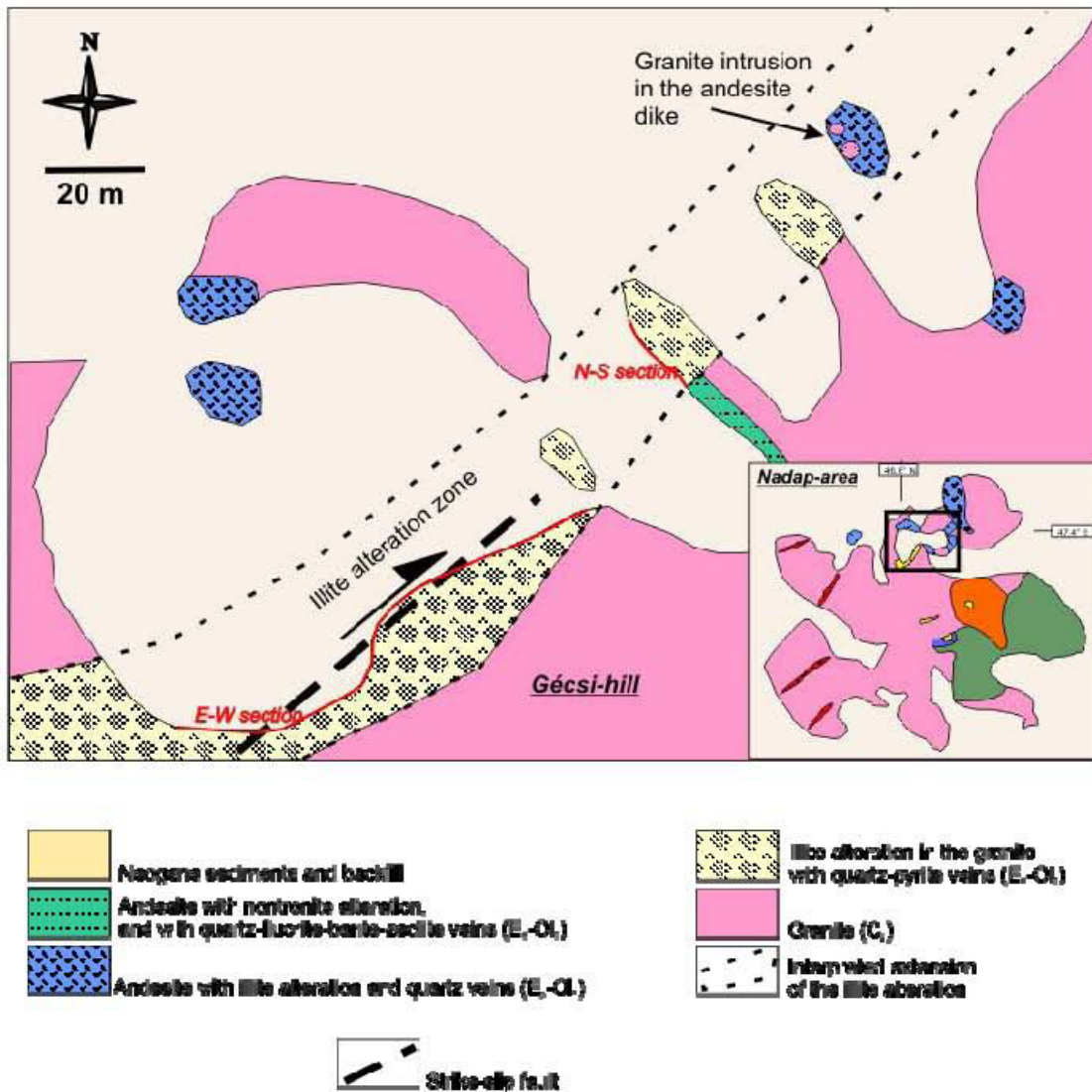


Figure 27. Geological map of the Gécsi Hill quarry, Nadap area, Velence Mts.

4.4.6 Relationships between FIP orientations, fluid inclusion petrography and microthermometry

FIP orientations were also analyzed in function of the FI type, by universal stage.

Type *I* has NE-SW orientation, which is parallel with the strike of the quartz-molybdenite veins (Figure 28A). This is not surprising, because Type *I* has entrapped parent fluids of this type of mineralization. The number of Type *I* FI is very low and is confined only on the Nadap area. The quartz-molybdenite veins and the parent fluids from which Type *I* FIA entrapped are of

Variscan age. According to the strike of the FIP and the quartz-molybdenite veins for the Variscan age NE-SW extension can be revealed.

Type II and Type III FIA-s dip to the NW and SE, the dip angle is high (80-90°) (Figure 28B) in the Székesfehérvár-Pákozd area. The NW-SE orientations are rare or absolutely absent in some samples. In the Nadap-Sukoró area and in the samples far away from the illite-kaolinite-smectite alteration zones, throughout the entire mountain chain, the NE-SW and the NW-SE orientations are in balance, but the NE-SW strike seems to be slightly more important. Locally N-S orientations may occur, but the number of FIP with this orientation is very low. FIP in quartz of the granite porphyry dikes often have N-S and E-W strike in all areas. Dip angles are almost subvertical both in the granite and in the granite porphyry. Type II and III FIP are always parallel with the strike of the quartz-fluorite-base metal veins and with the structural zones in which the illite-kaolinite-smectite alteration developed. The predominantly NE-SW strike of the Triassic Type II and III FIA bearing FIP confirms principally NW-SE extension during their formation. Formation of FIP with NW-SE strike cannot be explained with the same stress field. A possible explanation for this phenomenon is the stress field permutation.

Parallelism of the FIP and the syngenetic quartz-fluorite-base metal veins indicate that the structural control of the fluid flow channels can also be followed on microscopic scale.

Type IV Palaeogene FIP have NE-SW, NW-SE and E-W strike with almost vertical dip angles in the Nadap-Sukoró area, close to the Nadap-line and in the vicinity of the andesite dikes in the granite. The above listed orientations in the Palaeogene alteration zones, in the Nadap area are in balance (Figure 28B) and are parallel with the older Triassic FIP directions. The three different, almost perpendicular Palaeogene directions in these samples would presume very fast changes in the stress field orientation in a relatively short time (8 Ma years, 36-28 Ma) or reactivation of the older healed fractures.

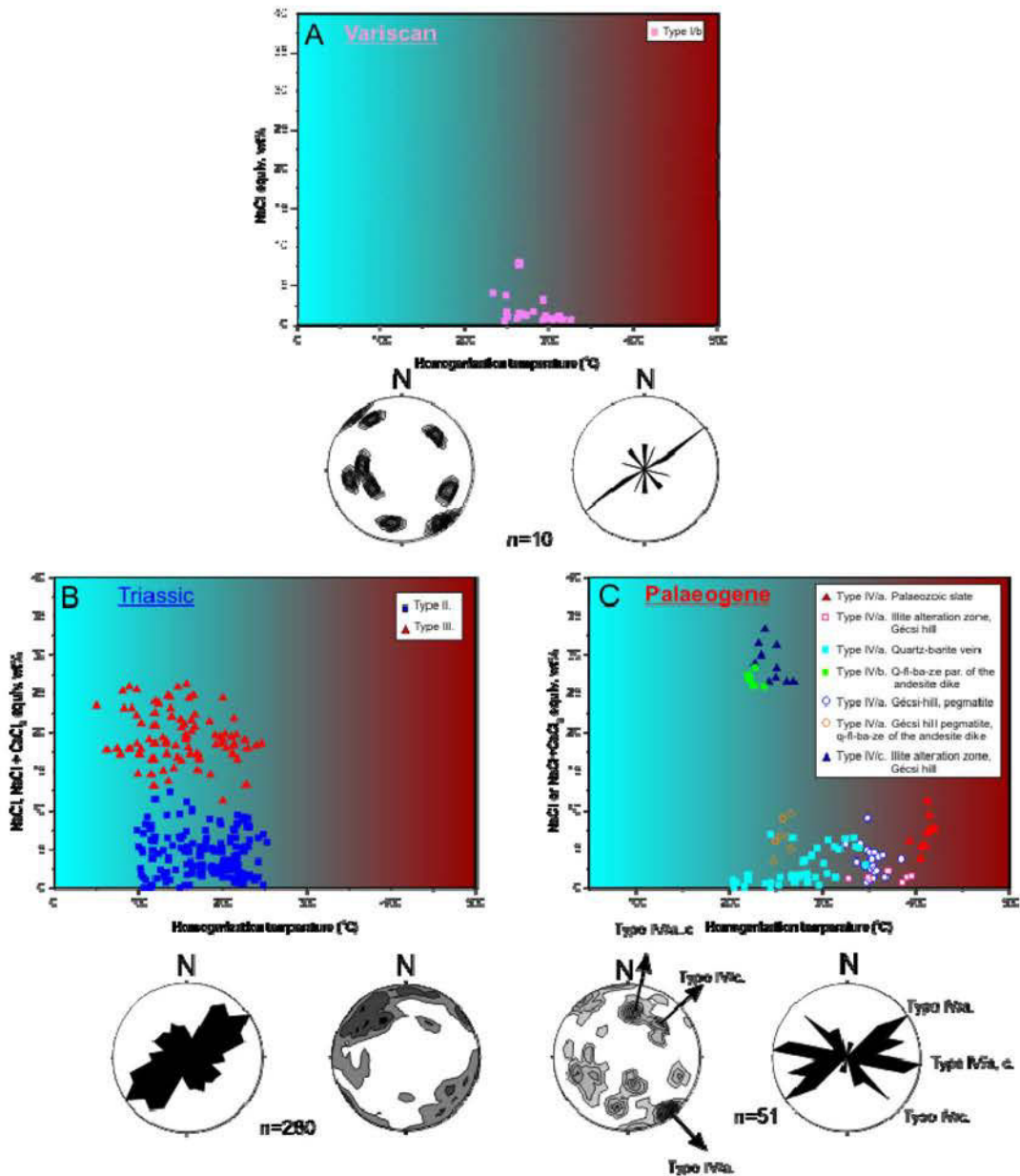


Figure 28. Salinity-homogenization temperature diagram of the FIA and related FIP measured by universal stage

Considering the structural data the following general statements can be established :

1. The strike of the aplite and granite porphyry dikes is constant in all blocks of the granite, indicating a NW-SE extension during the cooling of the granite (G1 phase; Figure 26).

2. According to the observed geometric intersection relationships of the quartz-fluorite-base metal veins and the fault systems – especially in the Székesfehérvár-Pákozd areas – and the FIP with Triassic Type II and III FIA-s, the Triassic can be characterised by two extensional direction: principally with a NW-SE oriented extension and with another that is perpendicular. It is the G2 phase (Figure 29). Perpendicular stress fields in the same time interval can be explained only by stress field permutation TWISS & MOORES (2007). It is important to note that the principal stress field during the Triassic was parallel with the Carboniferous.
3. By the time of the Cretaceous the orientation of the stress field changed to E-W extension (G3 phase; Figure 29)
4. During the Palaeogene, basically the old faults and fracture systems were reactivated, but the type of the stress field changed. NE-SW trending fractures were reactivated principally in the Nadap area in a transtensional stress field (ENE-WSW compression and NNW-SSW extension), related to the dextral PAL fault system (G4 phase). Possibly the NE-SW trending normal faults reactivated at the same time in the Székesfehérvár and Pákozd area.
5. The G5 phase (NE-SW extension; Figure 29) was established basically by the fluid inclusion studies. The Nadap fault acted as a normal fault during the Palaeogene hydrothermal processes, as it was discussed in Chapter 4.3. The FIP of the Palaeogene Type IV assemblage indicates NE-SW, N-S and NW-SE extensional direction, which partly matches the macroscopically analyzed stress field orientations (G4-G5 phase).
6. The N-S and NW-SE strike slip faults in the andesite dikes (G6 phase; Figure 29) and in the PVU (G7 phase; Figure 29) represent the post-Palaeogene tectonic events. The G6 phase indicates NNW-SSE compression and perpendicular extension. Faults of the G7 phase formed in a NE-SW compressional system.

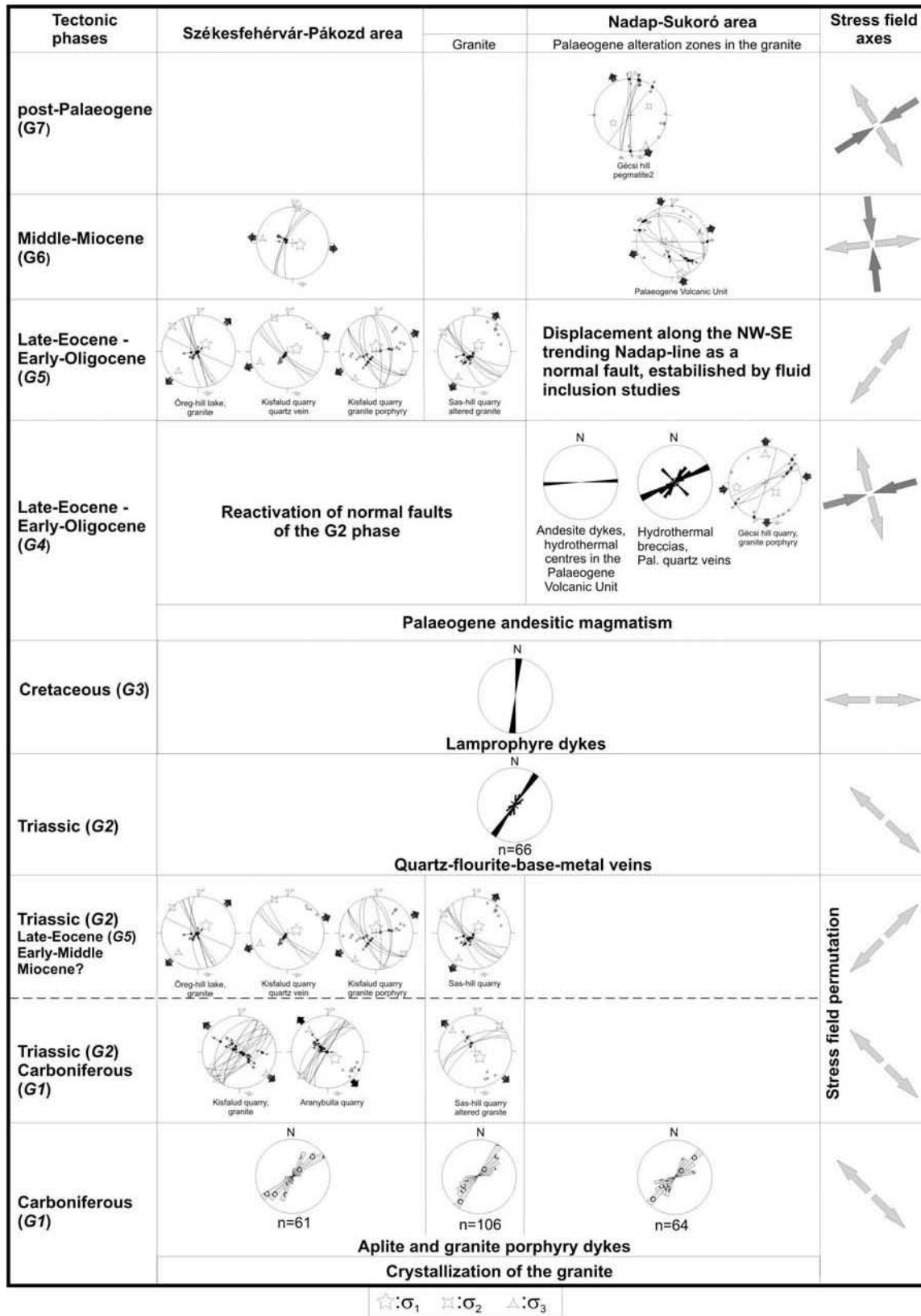


Figure 29. Summary of the analyzed tectonic phases. Stress field analysis has been done by the computer code of ANGELIER (1986)

4.5 STATISTICAL ANALYSIS OF PALAEOGENE HYDROTHERMAL VEIN ARRAYS: FRACTAL ANALYSIS AND PERMEABILITY CALCULATION

4.5.1 Fractal analysis

Fractal analysis has been carried out in three selected outcrops in the Nadap area. Two sections are located in the Gécsi Hill quarry next to Nadap: the N-S and the E-W sections (Figure 27; Appendix 1). The two sections belong to the same NE-SW trending illite alteration zone. The host rock of the quartz-pyrite veins is illitic granite porphyry (Figure 26). The veins are confined on the illitic most altered parts of the granite porphyry. Type IV primary FIA has been found in the veins quartz suggesting that these veins are of Palaeogene age.

The third locality is spatially not far away from Gécsi Hill roadcut. This exposure is characterized by weaker illitic alteration.

The staircase plot constructed from the distance of the veins along the base line and their thickness – (Figure 30A) is irregular, the veins are clustered, reflecting the heterogeneous strain which they represent in all sections. It is remarkable that the quartz veins cluster on a relatively short distance in the intensively altered alteration zones (the E-W and N-S sections of the Gécsi Hill quarry versus the less altered granite (Gécsi Hill roadcut). The cumulative thickness of the Gécsi Hill quarry veins is definitively higher than in the Gécsi Hill, roadcut section. Distribution of vein thicknesses is much smoother in the Roadcut than in the other two discussed outcrops.

On the basis of the vein thickness versus cumulative thickness diagram it is obvious that the veins of the Roadcut quarry are much thinner than the veins in the Gécsi Hill quarry. Veins thicknesses and the thickness distribution in the two sections of the Gécsi Hill quarry are equivalent. This is not surprising, as they belong to the same alteration zone (Figure 30B). In case of each plot there are parts on which linear correlation with high correlation coefficient exist. This indicates that the vein thickness distributions have fractal properties in a certain thickness range (1 mm - 20 mm). Veins beyond and below a certain thickness threshold value are under sampled. This is a natural feature since thin veins are not measurable or visible. Characteristic anomalies from the ideal straight line in this range were also analyzed on other areas (GILLESPIE et al. 2001). Fractal dimension values (D_m) are close to each other (Roadcut:0,7937 Gécsi Hill quarry N-S: 0,7937, E-W: 0,8233, respectively) in the sections and confirm clustered vein arrays. The values are in the 0,7-1,1 range, which is characteristic for vein systems hosted by not layered rocks (GILLESPIE et al. 1999). However the lowest D_m value occurs in the Roadcut section. It is

in contradiction with other studied areas where high **Dm** values were analyzed for less clustered/developed vein systems while low values for well-clustered systems (ROBERTS et al. 1998).

Linear correlation with sufficient correlation coefficient among data points on the vein distance-cumulative frequency diagrams is not possible (Figure 30C). The plot can be best approximated by log-normal distribution which is characteristic for the Kolmogorov random bisection model. This behavior is typical for non-stratabound vein arrays (GILLESPIE et al. 1999, BENKÓ et al. 2008).

The coefficient of variation (**C_v**; Figure 30D) in the Roadcut section yielded 1 or values lower than 1, which means that they are anticlustered. It suggests that the veins in this outcrop are not connected to a definitive structural zone, but the hydrothermal fluids migrated in the open space of the equally fractured granite. The uniform weak alteration of this outcrop supports this interpretation. In the Gécsi Hill Quarry the **C_v** values exceed the threshold value 1, indicating that they are clustered on a narrow zone. Field analysis has shown – that the alteration and formation of this alteration is structurally controlled (Figure 27), therefore a high degree of clustering in this zone is not surprising.

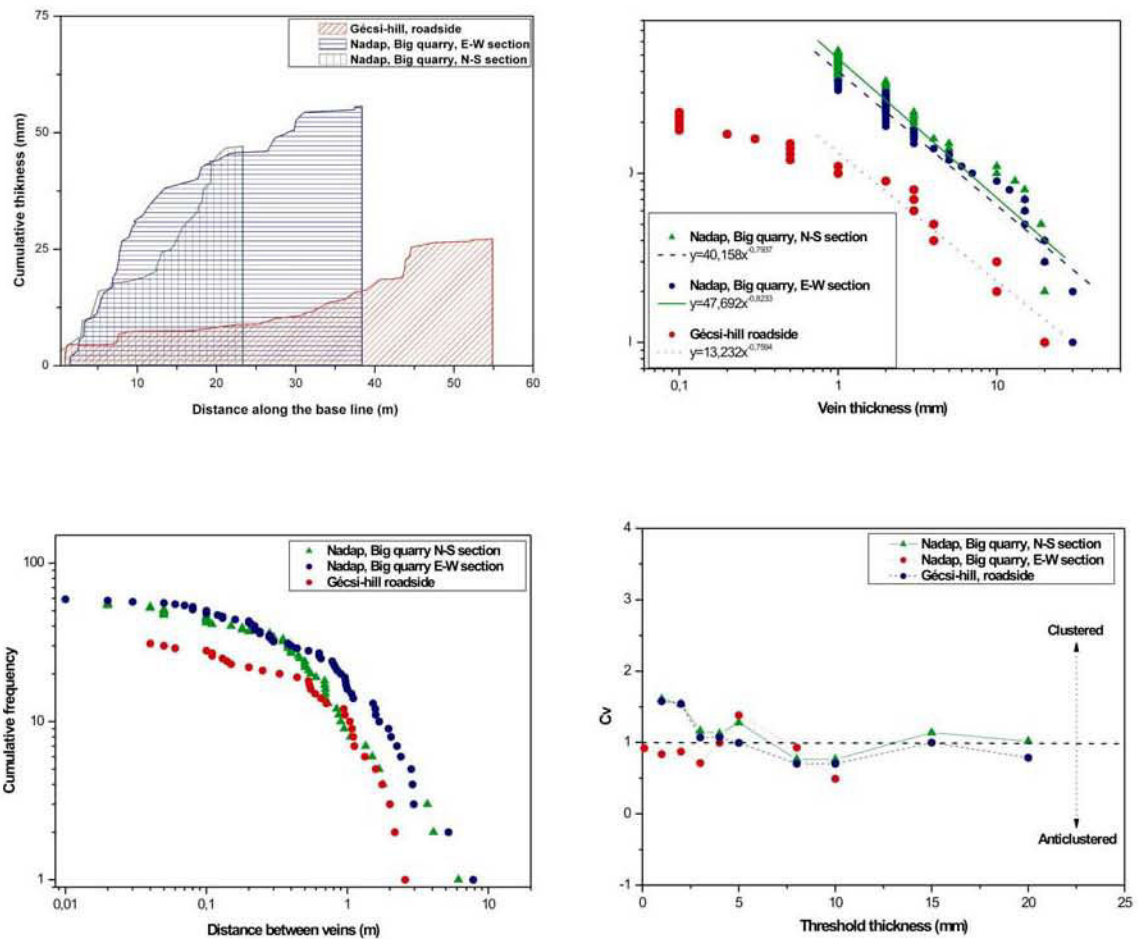


Figure 30. Results of fractal analysis measurements

4.5.2 Permeabilities calculated from the geometrical data of the veins

Calculation of permeability from vein thicknesses and distances have been carried out from the same three localities (Gécsi Hill Roadcut, Gécsi Hill quarry N-S and E-W sections; Figure 27). In each sections illite alteration of Palaeogene age was detected but the degree of alteration was different. Concerning the Gécsi Hill quarry sections, illite alteration is equally pervasive in both sections, and in the Roadcut section it is weaker. In perfect accordance with the degree of alteration the highest values were calculated for the Gécsi Hill quarry outcrops and a lower value for the roadcut section (Table 7.).

| | Gécsi Hill Roadcut | Gécsi Hill quarry E-W section | Gécsi Hill quarry N-S section |
|-------------------------------|---------------------------|--------------------------------------|--------------------------------------|
| No. | 31 | 59 | 57 |
| Am (m) | 0,002 | 0,004 | 0,005 |
| S_{m,k} (m) | 44,53 | 107 | 75,87 |
| S_m (m) | 1,33 | 1,81 | 1,33 |
| K_m (mDarcy) | 0,007 | 0,04 | 0,08 |

Table 7. Permeability of the rock at the time of the hydrothermal fluid flow calculated from the thickness, number and distance of the hydrothermal veins

4.6 FIP STATISTICAL PARAMETERS: AVERAGE LENGTH, LENGTH DENSITY, NUMBER DENSITY

The density (cumulative length/area – called “length density”, number/area – called “number density”) and the average length of the FIP have been investigated as a function of the distance from the alteration zones rock type (granite, granite porphyry) and in function of their orientation (Figure 31 and Table 7).

The rock forming quartz grains in the weakly or almost unaltered granite always contain fractures with Type II and Type III FIA-s, which verifies that these two FIA are related to a Triassic fluid mobilization process. Although density of their FIP is very low in some samples (localities: 4, 5, 9, 12, 13, 6-8 mm/mm²; Table 7), they are always present in the rock forming quartz. It reflects that the parent fluids of Type II and Type III FI regionally migrated in the granite intrusion. Type II and III FIA also occur in the segregation quartz crystals of the granite hosting slate (locality 57; 3,7 mm/mm²; Table 7) suggesting that this kind of hydrothermal fluid flows affected the surrounding rocks as well. In the granite and in the granite porphyry, we detected a small variation. The unaltered granite porphyry usually (localities: 18-28) contains less (15-45 1/mm²) and shorter (average length: 0,21 mm) FIP than the unaltered granite (localities: 1-17; 19-69 1/mm² and 0,22 mm), resulting in lower FIP density (granite porphyry average: 5 mm/mm², granite average: 7 mm/mm²; Figure 32, Table 7.).

FIP number density increase rapidly in the illite-kaolinite-smectite alteration zones of the granite (localities: 29-38; granite average: 39 1/mm², altered granite average: 72 1/mm²) meanwhile the surface density decreases (from 8,5 to 5,5 mm/mm²) and in the close vicinity of the quartz-fluorite-base metal veins. FIP density in the altered granite porphyry (localities: 39-44; ~5 mm/mm²) is again lower in comparison to the altered granite (5-10 mm/mm²; Figure 32).

The FIP length density and average length is the highest in the illitic alteration zones (localities: 45-52; 25-40 mm/mm² Table 7), but not significantly higher than in the illite-kaolinite-smectite alteration zones (15-25 mm/mm²; Figure 32). In these zones Type II and Type III FIA containing FIP are absent, and the FIP contain merely Type IV FIA. The highest FIP length density was measured in a unique sample: a granite inclusion in an andesite dike (37 mm/mm², sample 59). High values were measured in the segregation quartz close to the Palaeogene alteration zones as well (19 mm/mm², sample 58), clearly showing, that Type IV (Palaeogene) fluids also affected the granite hosting slate in some zones.

I also studied the average lengths in the two conjugated NW-SE and NE-SW FIP orientations (with Type II and III FIA), with the purpose to compare the fracture evolution in the two different areas. In general, in the unaltered or slightly altered granite the FIP are longer (average: 0,23 mm) in the NE-SW orientation, whereas there are shorter (average: 0,19 mm) FIP in NW-SE direction. In the alteration zones the tendency changed, the NW-SE trending fractures were longer (0,32 mm) and the FIP –s parallel with the main alteration zones (NE-SW) became shorter (0,25 mm).

The conclusion is that FIP length density increases towards the alteration zones, indicating that the microscopic scale fracture system (FIP) played an important role in the channeling of the mineralizing fluids. Average length decreased towards the illite-kaolinite-smectite alteration zones, but the decrease was compensated by the increasing number of the FIP. However towards to the illite alteration zones the decrease of the average length was not observed.

Another important feature is the difference between the FIP length density in the granite and in the granite porphyry.

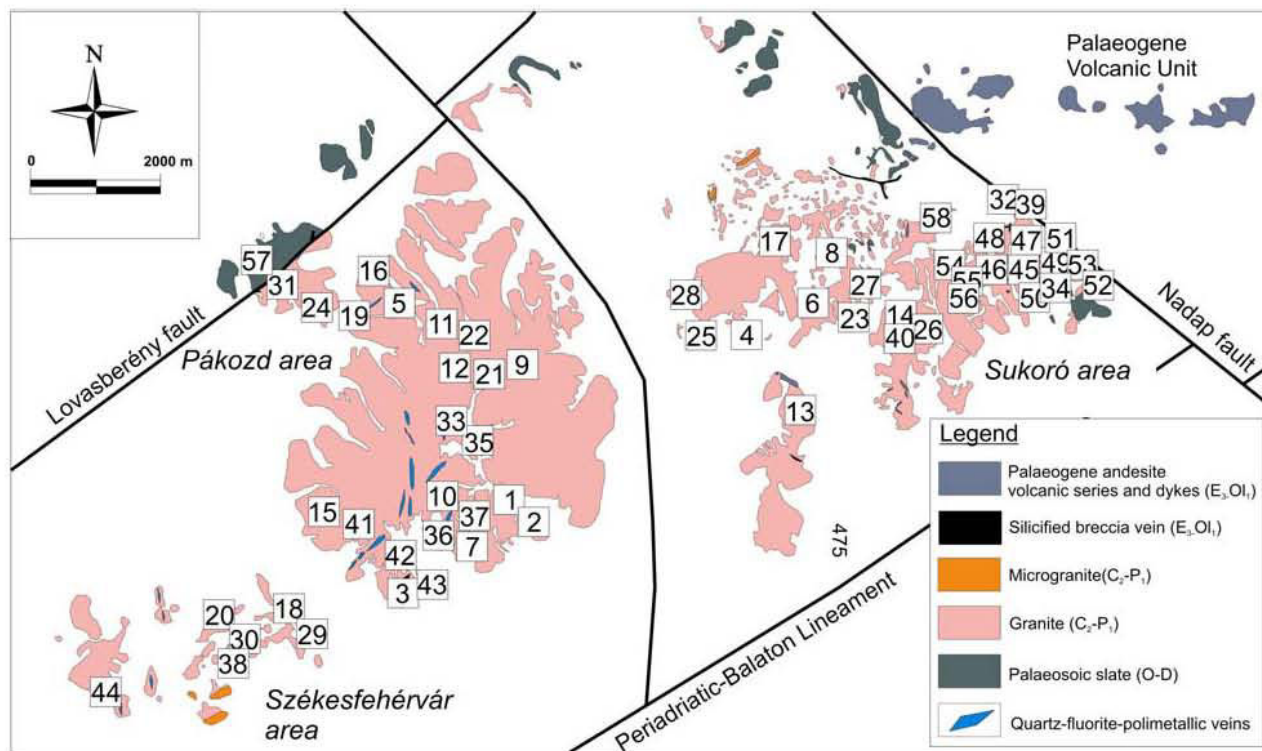


Figure 31. Sample localities of FIP measurements

| Unaltered granite | | | | | | | | | | | | | | | | | |
|-----------------------------------------|------|------|------|------|------|------|------|------|------|------|------|------|------|------|------|------|------|
| Locality | 1 | 2 | 3 | 4 | 5 | 6 | 7 | 8 | 9 | 10 | 11 | 12 | 13 | 14 | 15 | 16 | 17 |
| Average length (mm) | 0,16 | 0,19 | 0,19 | 0,22 | 0,12 | 0,16 | 0,20 | 0,17 | 0,31 | 0,29 | 0,31 | 0,19 | 0,31 | 0,24 | 0,28 | 0,27 | 0,21 |
| Summa length/Area (mm/mm ²) | 10,7 | 9,9 | 10,1 | 7,0 | 4,6 | 7,5 | 10,2 | 9,1 | 6,0 | 10,4 | 9,5 | 6,6 | 6,4 | 9,6 | 9,9 | 8,4 | 8,3 |
| Number/Area (No/mm ²) | 69,1 | 57,3 | 52,9 | 31,2 | 38,8 | 46,6 | 22,5 | 54,2 | 19,0 | 35,8 | 30,7 | 34,6 | 20,7 | 40,4 | 35,8 | 31,5 | 39,8 |

| Unaltered granite porphyry | | | | | | | | | | | |
|-----------------------------------------|------|------|------|------|------|------|------|------|------|------|------|
| Locality | 18 | 19 | 20 | 21 | 22 | 23 | 24 | 25 | 26 | 27 | 28 |
| Average length (mm) | 0,19 | 0,12 | 0,11 | 0,22 | 0,27 | 0,24 | 0,28 | 0,18 | 0,18 | 0,28 | 0,20 |
| Summa length/Area (mm/mm ²) | 4,4 | 3,9 | 5,0 | 4,9 | 4,4 | 3,6 | 7,7 | 1,9 | 5,4 | 8,6 | 6,9 |
| Number/Area (No/mm ²) | 23,9 | 32,5 | 45,8 | 22,2 | 16,1 | 15,2 | 27,8 | 10,4 | 21,0 | 30,5 | 34,2 |

| Granite with (Triassic) illite-kaolinite-smectite alteration | | | | | | | | | | |
|--------------------------------------------------------------|------|------|------|------|------|------|------|-------|------|------|
| Locality | 29 | 30 | 31 | 32 | 33 | 34 | 35 | 36 | 37 | 38 |
| Average length (mm) | 0,19 | 0,32 | 0,27 | 0,17 | 0,20 | 0,26 | 0,27 | 0,21 | 0,24 | 0,10 |
| Summa length/Area (mm/mm ²) | 13,9 | 9,7 | 17,2 | 15,2 | 18,5 | 12,7 | 20,8 | 25,1 | 10,0 | 7,5 |
| Number/Area (No/mm ²) | 73,8 | 37,7 | 63,6 | 89,0 | 93,4 | 48,1 | 76,3 | 122,2 | 41,4 | 73,7 |

| Granite porphyry with (Triassic) illite-kaolinite-smectite alteration | | | | | | |
|-----------------------------------------------------------------------|------|------|------|------|------|------|
| Locality | 39 | 40 | 41 | 42 | 43 | 44 |
| Average length (mm) | 0,18 | 0,21 | 0,26 | 0,31 | 0,17 | 0,30 |
| Summa length/Area (mm/mm ²) | 9,4 | 7,8 | 13,3 | 11,3 | 7,5 | 13,1 |
| Number/Area (No/mm ²) | 53,6 | 37,4 | 50,6 | 35,9 | 43,5 | 44,1 |

| Granite with (Palaeogene) illite alteration | | | | | | | | |
|---------------------------------------------|------|------|------|------|------|------|-------|------|
| Locality | 45 | 46 | 47 | 48 | 49 | 50 | 51 | 52 |
| Average length (mm) | 0,41 | 0,33 | 0,31 | 0,32 | 0,32 | 0,35 | 0,32 | 0,24 |
| Summa length/Area (mm/mm ²) | 23,0 | 11,9 | 16,9 | 17,0 | 15,4 | 31,4 | 31,1 | 19,4 |
| Number/Area (No/mm ²) | 55,9 | 36,2 | 53,8 | 51,1 | 48,7 | 89,4 | 104,2 | 80,0 |

| | Granite porphyry with illite alteration | | Transitional zone with weak illite alteration (Pal) | | | Un-altered schist | Altered schist (Pal) | Granite inclusion in andesite (Pal) |
|-----------------------------------------|-----------------------------------------|------|-----------------------------------------------------|------|------|-------------------|----------------------|-------------------------------------|
| Locality | 53 | 54 | 54 | 55 | 56 | 57 | 58 | 59 |
| Average length (mm) | 0,22 | 0,28 | 0,32 | 0,31 | 0,38 | 0,25 | 0,25 | 0,46 |
| Summa length/Area (mm/mm ²) | 11,2 | 24,7 | 10,0 | 11,9 | 13,5 | 3,7 | 18,8 | 36,9 |
| Number/Area (No/mm ²) | 51,9 | 86,0 | 31,3 | 38,6 | 35,5 | 14,9 | 75,4 | 79,7 |

Table 8. FIP parameters of the analyzed samples assorted by alteration type of the granite

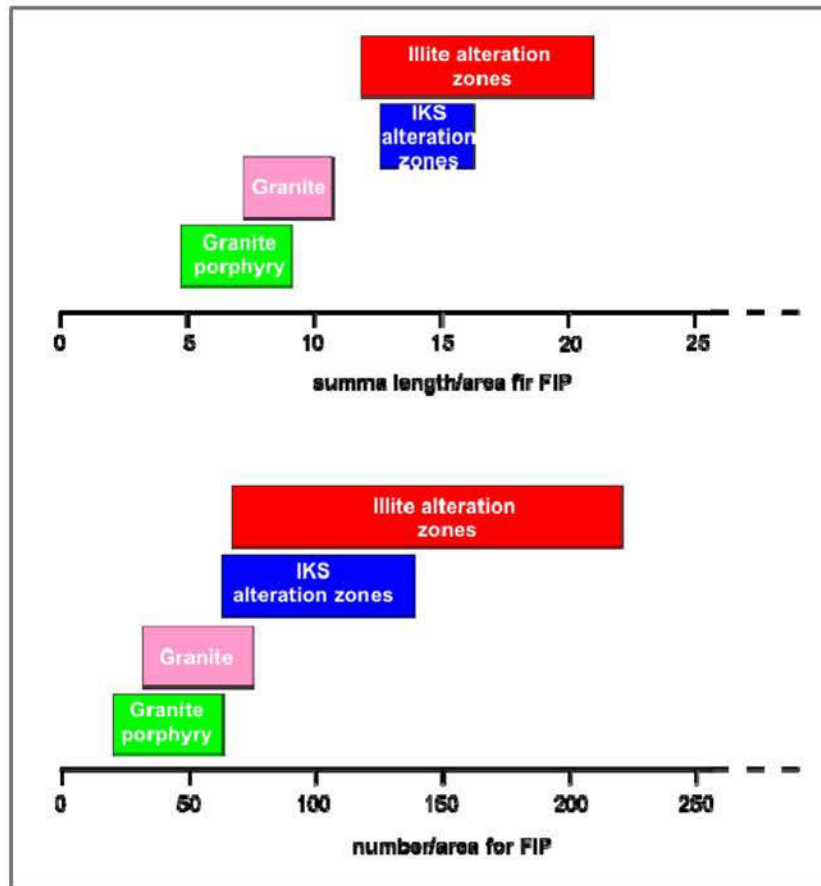


Figure 32. FIP statistical properties in the different alteration types of the granite and in the granite porphyry. Abbreviation: IKS – Illite-kaolinite-smectite

4.6.1 Iso-Fracture density map of the Nadap area and comparison of statistical parameters

By means of systematical sample collection and mapping of FIP I have constructed the iso-fracture density map the Gécsi Hill in the Nadap area (Figure 33). The tectonically most affected zone is the E-W section of the Gécsi Hill quarry and the highest fracture densities were measured in this zone. The fluid flow was controlled by a NE-SW striking dextral fault zone. An other characteristic feature of the Palaeogene fluid flow is that the occurrence of the illite alteration and the fluid inclusions with boiling texture are confined on the 150-200 m vicinity of the andesite dike of the Gécsi Hill quarry. Therefore the intrusion of the andesite dike resulted in only a very narrow zone the reopening of the older FIP and the illite alteration.

The analyzed quartz vein system in the three sections (Gécsi Hill Roadcut, Gécsi Hill quarry N-W section and Gécsi Hill quarry E-W sections) can be divided into two groups. The veins in the two sections of the Gécsi Hill quarry bear with very similar properties (D_m (fractal dimension), k (permeability), FIP-density, C_v (variational coefficient)), while the Roadcut on the top of the Gécsi hill has characteristically different values (Table 9). The vein network in the Roadcut section is badly developed, veins are narrow, the veins are not clustered and the permeability is the lowest in this zone. The fluids migrated in an existing fracture system, a main (backbone) channel of fluid migration did not form. According to these phenomena it could have been assumed that this vein network belongs in those group of veins/alteration types where the fluid migration affects big volumes of rock body, but the alteration and mineralisation is weak. However in this section it is not true as the cumulative thickness of the veins is low, therefore I regard this section to the distal alteration zone of the Palaeogene alteration zones. An additional argument for the weak penetration capacity of Palaeogene fluids is the very low number of Palaeogene FIA-s: the fluids migrated in the open space, in the joints – but no new fractures have formed.

Quartz veins in the Gécsi Hill quarry are well clustered and their formation can be connected to a well defined fault system and stress field. Well-defined backbones have formed which channelled the bulk of the fluids and focused the fluid migration on very narrow zone. The fracture (FIP) density is very high, and the granite has intense illite alteration, therefore the calculated permeabilities from the FIP of the rock forming quartz are really just apparent. Vein networks of the Gécsi Hill quarry belong to that first group of vein networks where the mineralization is confined on a very narrow alteration zone.

| | Gécsi Hill quarry N-S section | Gécsi Hill quarry E-W section | Gécsi-hill roadcut |
|---------------------------------------------------------------------|----------------------------------------------|----------------------------------------------|-------------------------------|
| k (permeability, calculated from quartz vein thickness) | 0.08 | 0.04 | 0.007 |
| FIP length density (mm/mm³) | 34 | 31 | 10 |
| D_m (fractal dimension of vein thicknesses) | 0.783 | 0.823 | 0.7894 |
| C_v (variational coefficient) | >1 | >1 | <1 |

Table 9. Comparison of statistical parameters of three sections on the Gécsi Hill

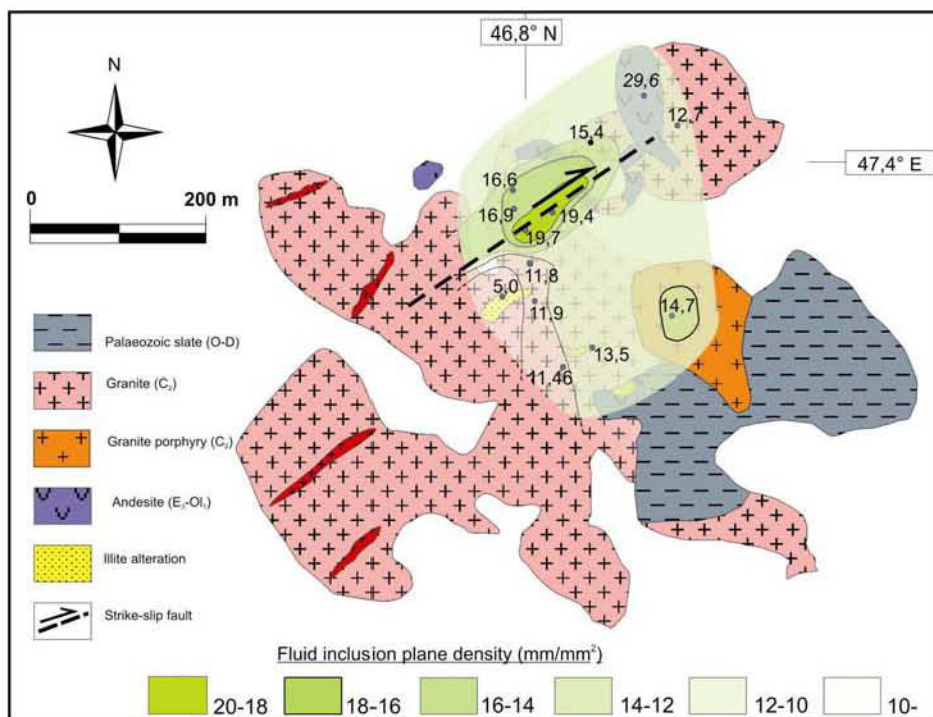


Figure 33. FIP density map in the Nadap area. The most “permerable” zone is parallel with a NE-SW trending fault zone which was the principal zone of Palaeogene fluid migration

5. DISCUSSION

5.1 VARISCAN TECTONISM AND ITS CONSEQUENCES ON THE FORMATION OF THE INITIAL FRACTURE SYSTEM OF THE GRANITE

TECTONIQUE VARISQUE ET SES CONSEQUENCES SUR LA FORMATION DU RESEAU DE FRACTURES DU GRANITE

Le granite des monts Velence s'est mis en place il y a 289 – 290 Ma au cours d'un épisode extensif NW-SE. Les évidences de terrain en sont les porphyres et diques aplitiques NE-SW, les veines à quartz molybdénite NE-SW et les plans d'IF de type I de même direction.

Selon la théorie de Griffith, les roches auraient initialement des fractures d'orientations aléatoires. Cependant, les travaux de ZAPPERI et al. (1999) montrent qu'elles ne peuvent pas être aléatoires tant que le magma ne se met pas dans un champ de contraintes homogène. Les systèmes de failles et diaclases conjuguées orientées NE-SW sont à relier à une extension NW-SE. Ce sont les systèmes de failles et diaclases initiales qui ont été reouverts et réinitialisés durant les événements tectoniques postérieurs.

The early-Palaeozoic slate – the host of the granite – metamorphosed during the Variscan orogeny. The Velence granite intruded for 280-290 Ma – in the final stage of the Variscan orogeny – into the metamorphosed slate. By the time of the emplacement of the granite, the orientation of the stress field was NW-SE extensional according to the strike of the NE-SW trending aplite, granite porphyry dikes and to the orientation of Type I FIP and the quartz-molybdenite veins (G1 phase). This orientation of the extension was parallel to the orientation of the stress field during the peak of the Variscan metamorphism (DUDKO 1988). Therefore the stress field did not change considerably during the late Variscan epoch.

It is an essential question what kind of fracture system was active during granite emplacement and during the cooling phase?

According to GRIFFITH's theory (1920) all rocks have an initial, penny shaped micro-joint system with random fracture length and orientation. According to laboratory experiments (TWISS & MOORES 2007), much more energy is required to break an intact rock, than calculated from the bound energies in the crystals. This assumption, however, is not necessarily plausible on the basis

of the studies of ZAPPERI et al. (1999). Stress field regimes in the Earth's crust are never homogeneous but can be characterized by the three principal regime types: extensional, compressional or transtensional/transpressional (PETROV et al 2008).

In case of the Velence Mts., the granite did not settle in a homogeneous stress field during the late Carboniferous, which is obvious on the basis of the NE-SW strike of the granite porphyry and aplite dikes. Therefore, the orientation of the GRIFFITH's joints cannot be random, but oriented to the stress field during the Variscan age (NW-SE horizontal extension).

Assuming a NW-SE extension during the formation of the initial fracture system – after the cooling of the granite below the ductile-brittle transition temperature – formation of faults dipping to the NE and SW with approximately 60° dip angle and formation of extensional, subvertical Type I joints with NE-SW strike are expected in a Mohr fracture system (G1 tectonic phase). These types of joints and faults were regionally found in the granite, therefore their formation can be derived from the stress field which was present at the time of the cooling of the granite.

5.2 REGIONAL TRIASSIC FLUID FLOW IN THE GRANITE: GENETIC MODEL AND STRUCTURAL CONTROL

ÉCOULEMENTS FLUIDES REGIONAUX TRIASIQUES DANS LE GRANITE: MODELE GENETIQUE ET CONTROLE STRUCTURAL.

En accord avec les âges K-Ar mesurés sur les assemblages à illite-kaolinite-smectite qui sont syngénétiques avec les veines à quartz-fluorite, l'âge des veines minéralisées est Triasique supérieur.

L'alteration hydrothermale triasique est temporairement reliée au magmatisme Carbonifère contrairement aux dykes lamprophyriques ou au volcanisme Paléogène de la partie Est des monts Velence. On peut suggérer que ces événements magmatiques sont à l'origine des flux de chaleur des fluides minéralisés. Cependant le magmatisme Triasique est inconnu dans les monts Velence, ce qui suggère que le magmatisme peut être source de chaleur pour former les veines de quartz-fluorite. L'activité magmatique Triasique est connue le long de la ligne PAL et dans la région des Carpathes Alpines. Dans la zone de Szababattyán les dikes andésitiques sont Triasiques, les tuffs volcaniques sont présents dans la région d'Alcázar mais des basaltes

océaniques sont également connus le long de la ligne PAL. Un modèle de type Mississippi-type pour les minéralisations a Pb-Zn dans les Alpes peut être proposé pour les veines a quartz-fluorite dans les monts Velence.

D'intenses circulations fluides ont été initiées dans la croûte supérieure durant les premiers stades d'ouverture de la branche océanique Vardar de la Neo-Thetis et/ou un diapirisme mantellique mis en place au milieu ou à la fin du Trias. Les fluides descendants étaient réchauffés par le fort gradient géothermique ainsi que l'activité magmatique et s'enrichissaient en Chlore ou autres éléments en traversant les sédiments clastiques et les niveaux évaporitiques. Ces fluides chauds et agressifs dissolvaient le Pb et le Zinc des sédiments et probablement des roches cristallines du substratum. Dans la partie ascendante des cellules de convection, les fluides refroidissaient et se mélangeaient avec des fluides météoriques. La capacité de transporter des ions diminuait et les Pb-Zn se déposaient. La théorie de remobilisation proposée par ARRIBAS et al (1994) et BREVART et al. (1982) de vieux granites (Paléo-Protérozoïque) liés à des minéralisations Pb-Zn doit également être prise en considération. L'unité ALCAPA, incluant la zone étudiée, était originellement localisée entre le Sud et l'Est des Alpes. Dans cette région, la géologie est analogue à celle de la région étudiée en Hongrie. Des gisements de type Mississippi Vallée y sont bien connus et d'âge Triasique. Cependant, on peut considérer que les minéralisations Pb-Zn des monts Velence ne peuvent pas être considérées comme un type Mississippi-Valley classique Alpin. Durant le Trias, le champ de contraintes régional était une extension NW-SE et en raison d'une permutation des réseaux de plans d'IF conjugués se sont formés avec une direction majeure NE-SW et secondaire NW-SE. La formation des failles NW-SE pentées NW et SE résulte de ce processus. Cette permutation du champ de contrainte est à relier à une montée de granite Alpin.

5.2.1 Radiometric age constraints

Considering the 210-230 Ma K-Ar ages measured on the illite-kaolinite-smectite assemblage of the hydrothermal (ore-related) alteration zones, these data almost overlap within error, and a lower Triassic (Ladinian-Norian) ca. 220 Ma old ore-forming age is established. The 220.9 Ma age of the orthoclase from the western part of the granite body adds support to a regional upheating of the granite body above 160°C in Triassic times. Evidently, the Triassic

hydrothermal alteration was neither temporarily related to the Carboniferous magmatism (host granite), nor to the Palaeogene magmatic activity in the eastern part of the Velence Mts. Therefore, we can rule out any hypothesis assuming either of these magmatic events to have acted as the heat source of the mineralizing fluids.

Triassic magmatic activity in the Velence Mts. is unknown, however age of andesite dikes in the Szababattyán block (BALOGH et al. 1983, BAGDASZARJAN 1989, DUNKL 1991) are equivalent with ages obtained on illites in the Velence Mts. On whole rock samples of the Szababattyán andesite vein BAGDASZARJAN (1989) measured 210 ± 4 Ma, whereas BALOGH et al. (1983) measured 213 ± 13 Ma. DUNKL (1991) analyzed titanite minerals with fission track method and it yielded to a result 214 ± 49 Ma years, which corresponds to the K-Ar radiometric ages. It is not implied that there is a direct link between the magmatism-in the Szababattyán block and the hydrothermal alteration in the Velence Granite, but it confirms lower Triassic magmatism along the Hungarian part of the PAL. Middle-to upper Triassic magmatism is regionally known along the PAL, Darnó-line and in the Southern Alps. The ladinian (243-227 Ma) tuffaceous Buchenstein Formation (RICHTHOFEN 1860) in the Transdanubian Unit can be correlated with the Livinallongo Formation in the Southern Alps (HAAS 2004). PAMIC (1984) reported Ladinian 216-250 Ma (U/Pb, Rb/Sr and K-Ar data) magmatic activity in the Karawanken, which may be related to the rift phase of the Dinaric part of the Tethys ocean. CASTELLARIN et al. (1988) documented Ladinian bimodal magmatites from the Southern Alps, however, based on geochemical data they emphasized the orogenic origin of the magmas. This magmatic activity indicates that the heat flow has elevated in the Tethys realm. (KISS et al. 2008; PALINKAS et al. 2008)

It is not the aim of this study to discuss whether the Ladinian magmatic rocks in both the Alpine region and along the PAL have a rift or an orogenic origin. Still, as a general theory (cf. HAAS 2004), we prefer the rift origin and we connect the Ladinian hydrothermal circulation in the Velence Mts. and the Szababattyán region to contemporaneous to rift events in the Tethys ocean.

The new K-Ar radiometric ages doubtlessly exclude Variscan (JANTSKY 1957, MOLNÁR 2006), Cretaceous (HORVÁTH et al. 1984) or Palaeogene (KISS 1954) magmatic relationship of the discussed base metal and fluorite veins.

5.2.2 Model for the Triassic fluid mobilization processes in the Velence Mts.

According to the models of KRAHN et al. (1996); ARRIBAS et al. (1994); KUHLEMANN et al. (2001); KÖPPEL (1983); KÖPPEL et al. (1988) for the Mississippi valley type deposits in the Alps, the following model was established on the formation of the Pb-Zn mineralization in the Velence Mts and in the Szabadbattyán area:

Due to the early stage opening of the Vardar-oceanic branch of the Neo-Tethys or/and mantle diapir (NEUGEBAUER et al. 1983), which took place during middle to late Triassic, intense fluid flow started in the attenuated upper crust. This crust was at the time of the opening made up of early Palaeozoic schists, limestones, late Palaeozoic limestones, sandstone granites and metamorphic crystalline rocks as well as early Triassic clastic sedimentary and evaporitic rocks.

The descending waters got heated up due to the high geothermal gradient (45°C/km; SCHUSTER et al. 1999) and ongoing magmatic activity, and when migrating through clastic sedimentary and evaporitic layers, chlorine and other elements were gained. The hot and aggressive fluids dissolved Pb and Zn from the sedimentary rocks and probably also from the rocks of the crystalline basement. In the ascending part of the convection cell, the formational fluids cooled down when mixed with other (magmatic±meteoric) fluids. As a result the ion transportation capacity decreased and Pb-Zn deposits formed.

KÖPPEL et al. (1988), based on lead isotopic analysis, proved the importance of early Palaeozoic high-grade metamorphic crystalline basement rocks (gneiss, amphibolite, mica-schist) as source rock of the Alpean-type Mississippi-Valley type deposits. High-grade metamorphic rocks are not known in the studied area but pebbles of such rocks were documented (FÜLÖP 1990) in a late Variscan molass formation, close to the investigated deposits (Carboniferous conglomerate). It is therefore possible that the metals in the investigated deposits of Hungary were derived from a range of rocks, including spatially associated magmatic rocks (the host rock granite in the Velence Mts. and potentially existing andesite dikes at Szabadbattyán), the underlying sedimentary rocks as well as the deeply situated metamorphic basement.

According to the perfect overlap of the Pb isotope data between the galenas of the Eastern Alpean Mississippi valley type deposits and their source rocks with the isotope values of the Velence Mts. and the Szabadbattyán area, their common origin can be assumed.

The remobilization theory that was suggested by ARRIBAS et al (1994) and BREVART et al. (1982) of old (early Palaeozoic-Proterozoic) granite related Pb-Zn deposits should also be taken into consideration. The upheating of the bedrock and associated fluid flow was a large-scale regional feature during the Triassic and it could have affected all granite bodies along the PAL (FERRARA & INNOCENTI 1974). Following this, metals linked to any hypothetical pre-Triassic deposits may have remobilized. In the Velence Mts; secondary fluid inclusion planes of ore forming fluids are regionally present in the granite, supporting a regional process. The K-Ar ages for hydrothermal clay minerals surrounding the quartz-fluorite-base metal veins and magmatic K-feldspar in a fresh part of the granite reinforces the idea of a regional fluid flow process of Triassic age.

In the Velence Mts., direct Triassic magmatic relationship cannot be confirmed, but in the Szababattyán block it is quite probable, as it was suggested by KISS (2003) based on the Triassic age of the andesite dikes and sills. Sulphur isotope composition of galena and sphalerite from the Velence Mts. are similar or slightly higher than the $\delta^{34}\text{S}$ values of the Bleiberg and Mezica mineralizations (KUHLEMANN et al. 2001), the latter clustering close to 0– -10 ‰ $\delta^{34}\text{S}$. This is in accordance with a similar origin for the deposits being compared. –Sulphur isotope composition of stratabound Pb-Zn mineralizations in the Alps are generally low (KUHLEMANN et al. 2001) below ca. -10, which is interpreted as the result of bacterial activity. However, the $\delta^{34}\text{S}$ values, close to 0 ‰ in the Velence Mts., in Mezica and in the entire Drau Range suggest a magmatic origin of the fluids. In the Velence Mts., a plausible mechanism is either remobilization or leaching of sulphur from the host granite, or a direct input of sulphur from unexposed andesite dikes.

5.2.3 Geotectonical considerations

The ALCAPA Megaunit, comprising the studied areas, was originally located between the Southern and Eastern Alps. The close genetic relationship of Palaeozoic and Mesozoic sedimentary sequences and fauna provinces between the Eastern-Southern Alps and the ALCAPA Megaunit has been widely discussed by several authors (DULAI 1990, VÖRÖS 1993, GÉCZY 1984, HAAS et al. 1995, EBNER et al. 1998). Due to the convergence and intense north-south compression between the European and Africa Plates, the ALCAPA Unit escaped from the

Alpine collision zone (KÁZMÉR & KOVÁCS 1985), which was accompanied by counterclockwise rotation (BALLA 1985, CSONTOS et al. 1991, CSONTOS 1995, MÁRTON & FODOR 2003). The total apparent dextral displacement along the dextral PAL is 350-550 km (TARI 1996). In a palinsaptic reconstruction, located back the Velence Mts. by approximately 400 km to southwest, results in a position before the continental escape along the PAL near the eastern Karawanken Mts., close to Eisenkappel and Mesica (Figure 34). In the latter region, the geology broadly resembles that of the studied areas in Hungary (Figure 34). The PAL (which is here a broad zone) consists of biotitic granites with syngenetic granite porphyry dikes and Cretaceous lamprophyre dikes, Palaeogene subvolcanic intrusions (here called tonalites). South from the granite intrusion, Precambrian metamorphic rocks are present in the Alps. As pointed out earlier, such rocks are not exposed in the Hungarian study areas, but the presence of metamorphic gravels – which cannot resist any long distance transport – in the Carboniferous conglomerate at Szabadbattyán demonstrates that their parent rocks must exist at depth. Also the so called Karawanken tonalite pluton (30-28 Ma; PAMIC et al. 2002a), located south from the metamorphic rocks, has an equivalent rock in the Velence Mts. (BENEDEK 2004), namely the diorite intrusion (PVU) the age of which is 30-28 Ma (unpublished data).

North from the granite belt, successively Ordovician-Silur slate, upper Permian sandstone, Bellerophon Limestone and the lower Triassic Werfen beds are known. The middle Triassic reef limestones (Wetterstein Limestone; Ladinian) hosts the Pb-Zn mineralization, the upper Triassic is represented by the main Dolomite in the Mezica region. The Triassic carbonate sequence resembles more on the coeval carbonate sequences of the northeastern part of the ALCAPA Unit, however Jurassic and Cretaceous sequences perfectly corresponds to the facies of the Transdanubian Mts. (CSÁSZÁR 1994, CSÁSZÁR et al. 2001).

The Pb-Zn mineralizations at Mezica occur in Ladinian Wetterstein limestone mostly as stratiform and stratabound bodies. However, mineralization often occurs as matrix of tectonic breccia, fissure filling, karst filling or fault-related epigenetic ore (BRIGO et al. 1977). It proves, that diagenesis and carbonate host rock are not terms of the mineralization, but they can occur in very different forms and in different type of rocks.

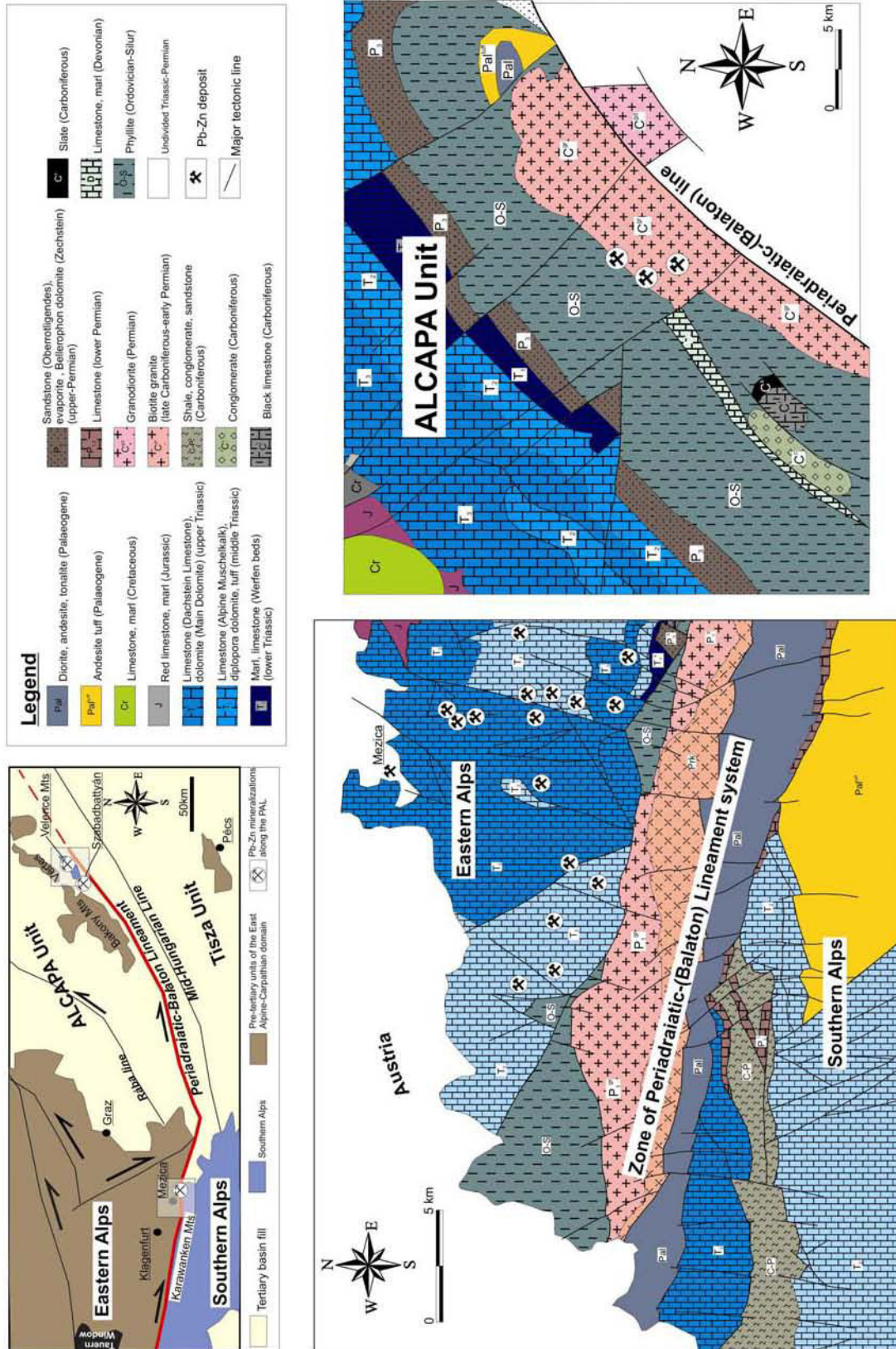


Figure 34. Geological maps of the broader vicinity of the Velence Mts. and the Karawanken at Mezica. Both are located along the PAL

However, the Velence Mts. and the Szababattyán Pb-Zn mineralizations cannot be considered as classical Alpean type Mississippi valley type deposits –considering the nature of the host rock – but their mineralogy (galena, sphalerite, fluorite, calcite, quartz), isotope composition (lead and sulphur), tectonic setting transporting fluids (similar fluid inclusion characteristics, WOLTER 1985; ZEEH et al 1998) are thought to be clear evidences for similar origin.

5.2.4 Structural control of the Triassic fluid flow: uplift of the granite and its effect on the fracture evolution on the granite

During the late Permian-Triassic the general stress field in the Tethys region was extensional due the opening of the Tethys-ocean. It led in the Tethys region to subsidence and transgression. However, the subsidence was not uniform in the whole region, it was slower in some regions and faster in others, and some places even uplifts were likely.

The granite crystallized at a pressure of 2 kbars, which corresponds to a 6 to 8 km depth under lithostatic conditions. For the Triassic fluid circulation 450-1000 bar was calculated from the fluid inclusion and sulphur isotope data in the granite. This pressure corresponds to approximately a 1,7 to 3,7 km paleodepth. The difference between the Variscan and Triassic paleodepths indicates that the granite should rise during the Permian and Triassic at least 2-3 kms. The uplift of the granite might have continued during the late Triassic fluid flow.

During an uplift three factors determine the stress field and the opening of the new fractures in a rock body. The first one is evidently the regional stress field, the second one is the Poisson effect and the third one is the thermal contraction. When uplift happens, an elastic rock body should expand vertically as the vertical load decrease. But rocks are not free to change their horizontal dimensions, therefore the horizontal components of stress must decrease sufficiently to offset exactly the Poisson contraction. Starting from an ideal homogeneous stress field where $\sigma_1=\sigma_2=\sigma_3$, uplift and erosion will result in a decrease in all components of the compressive stress, but the horizontal stress would decrease less than the vertical. Necessarily the horizontal stresses would end up as the maximum compressive stresses. During the uplift the temperature decreases, which results in thermal contraction of the ascending rock body. Because the rocks cannot change their horizontal dimension, the horizontal compressive stress decreases by an amount that exactly offsets the thermal contraction. This decrease added to the decrease

associated to the Poisson effect can be sufficient to make the horizontal principal stress become the minimum principal stress (TWISS & MOORES 2007). To release the tension caused by the contraction, extensional fractures will form in terms of the orientation of the regional stress tensors and the pore fluid pressure. This Type I extensional vertical fractures will be perpendicular on the minimum stress tensors of the stress field. If the rock is fluid saturated, those microfractures will seal in the form of FIP. With the fast release of the tension of the rock in this direction due to the brittle deformation, the new minimum stress tensor will be perpendicular on the former one. In addition the new set of tensional fractures will form perpendicular on the first network. This process is the stress field permutation.

In the Velence Mountains the main minimum stress tensor could have been NW-SE by the time of the Triassic (analogously with the Variscan stress field), and with stress field permutation a perpendicular, conjugate FIP network has developed with mainly NE-SW and subordinately NW-SE strike as well as with a very high dip angle (G2 phase). Formation of the NW-SE trending faults and joints dipping to the NW and SE might also be associated with this process.

The Triassic Type II and Type III FIA-s were seemingly simultaneously in the same rock, due to their homogenization temperature distributions in the granite and their parallel FIP. However, contemporaneous migration of two fluids with such a different ion content and concentration is impossible. According to our model – based on the model of KUHLEMANN et al. (2001) – the Triassic fluid migration was a regional and long existing fluid migration event. The high salinity, metal rich fluids originate from the distant hinterlands and transport the metal, while the low salinity fluids are connate meteoric or more probably seawater. During a slow uplift (?), the local stress field in the granite changed in several steps – due to the stress field permutation – resulting in formation of a perpendicular FIP set. The long term deformation triggered multi-phase fluid migration in the granite, resulting in dilution of the high salinity fluids or fluid mixing of two parent fluids. Another important argument for multi-phase evolution of the hydrothermal system is the rhythmic and zebra ore texture of the mineralized veins.

5.3 EVOLUTION OF THE FRACTURE SYSTEM OF THE GRANITE RELATED TO THE PALAEOGENE MAGMATIC-HYDROTHERMAL PROCESSES

EVOLUTION DES SYSTEMES DE FRACTURES DU GRANITE EN LIAISON AVEC LES PROCESSUS MAGMATIQUES ET HYDROTHERMAUX PALEOGENES

Des inclusions fluides triasiques existaient dans la zone de Nadap. L'activité magmatique paleogene a eue pour effet de faire disparaître les IF de type II'III; le type II-III a une Th de 180 a 250°C. La mise en place d'andésites et donc l'initiation d'écoulements fluides de températures élevées a accru la pression des IF de type II et III le long de leur isochore. Comme ces isochores sont redressées, une faible variation de température augmente fortement la pression et les IF ont décrépité. Quand ces petites IF triasiques de type II et III ont été chauffées a plus de 400°C, la différence de pression a atteint 1,5 Kb provoquant leur décrépitation. Ces décrépitations ont réouvert les plans d'IF qui ont a nouveau servi d'canaux pour des fluides plus tardifs Paléogènes (type IV/a FIA). Par ailleurs, le champ de contrainte Paléogène a également contribué a ces réouvertures. La formation de fractures et fissures est différente selon que l'on est en presence de "réouverture thermique" ou d'un champ de contraintes; il faut regarder les données statistiques. Dans le premier cas, la formation de réseaux de microfissures Triasiques dépendait seulement de la pression fluide et du champ de contrainte. Il en résulte la formation d'un réseau dense de microfissures de petite taille. Par contre, dans les zones peu affectées du granite, les plans d'IF sont longs et peu denses. La géométrie des microfissures Paléogène a été contrôlée par celle des fissures Triasiques et les variations statistiques observées sont à relier à leur réouverture thermique et propagation. Ce processus est l'inverse de celui proposé précédemment. La réouverture et le nouveau remplissage de ces dernières relié a leur interconnectivité favorise la presence de microfissures plus petites et plus denses.

5.3.1 Reopening of FIP in the illitic Palaeogene alteration zones and thermal propagation of the fracture network

During the Palaeogene three main structural orientations (stress fields) have been identified on the basis of the field and fluid inclusion studies. The NE-SW trending dextral faults are may connected to the PAL (G4 phase). The E-W trending line, formed by the hydrothermal

centres of the PVU is may also connected to the same stress field. The third one is the Nadap-line which was a normal fault during the palaeogene, based on the fluid inclusion studies (G5 phase). However fracture formation related to this tectonic phases might also have played an important role in the hydrothermal fluid circulation during the Palaeogene, according to my studies the fracture reopening and refilling played a more important role in the channeling of the fluids.

Both the regional FIP studies in the granite, and the microthermometric studies have shown that a Triassic regional fluid flow process occurred in the Velence Granite. In the Nadap area, in the illitic alteration zones of Palaeogene age the Triassic FIA-s are absent and only Type IV FIA occurs. Because of the regional presence of the Triassic fluid inclusions I assume that the Triassic fluid inclusions were also present in the Nadap area. The thermal effect of the Palaeogene magmatic activity caused the disappearance of Type II-III assemblages according to the following process: Type II-III inclusions have homogenization temperatures between 180-250°C, but their trapping took place somewhere along their isochors (Figure 35). The settlement of the Palaeogene andesite dikes and the beginning of the high temperature fluid flow led to rapid increase of the pressure in Type II and Type III inclusions along their isochors. Because of the very steep slope of this FIA, a minor temperature increase leads to building up high pressures within the inclusion. The differential pressure between the pressure in the inclusion and pressure in the geological environment will be so high that these inclusions will decrepitate. The emplacement of andesite dikes and the hydrothermal circulation evolved at around 30 – 300 bar pressure. Temperature conditions of the Palaeogene hydrothermal system varied above 240°C. Due to the minima of the homogenization temperatures in some localities the temperature could have been up to 400°C. Large inclusions (30 µm) are not able to resist higher pressure difference than 1 kbar, whereas smaller inclusions (5 µm) will decrepitate only above 3 kbar difference (ROEDDER 1984). When the characteristically (10-20µm) small size Triassic Type II-III inclusions with low homogenization temperature (180-240°C) were heated up to 400°C, the differential pressure should rise up to 3 kbar or higher (Figure 35), which is much higher than the pressure which they could resist (1-1,5 kbar), therefore they necessarily decrepitated. Decrepitation of all fluid inclusions led to the weakening of these fractures and finally to the reopening of the Triassic sealed fractures (FIP). The reopened fractures functioned as channels for the new Palaeogene (Type IV FIA) fluid migration.

We refer to the formation of the Palaeogene fractures as '*thermal reopening*', where the thermal effect of the intruding magmatic body and the hydrothermal fluid flow had higher importance in the formation of the fractures than the stress field. Yet, the effect of the stress field cannot be excluded on the basis of the stress field analysis. Both the G4 and G5 tectonic phases were appropriately oriented to form fractures with NE-SW or NW-SE orientations. However, they might have also contributed to the reopening, our assumption is that similar stress field towards the former one is not enough to reopen and refill all the old FIP.

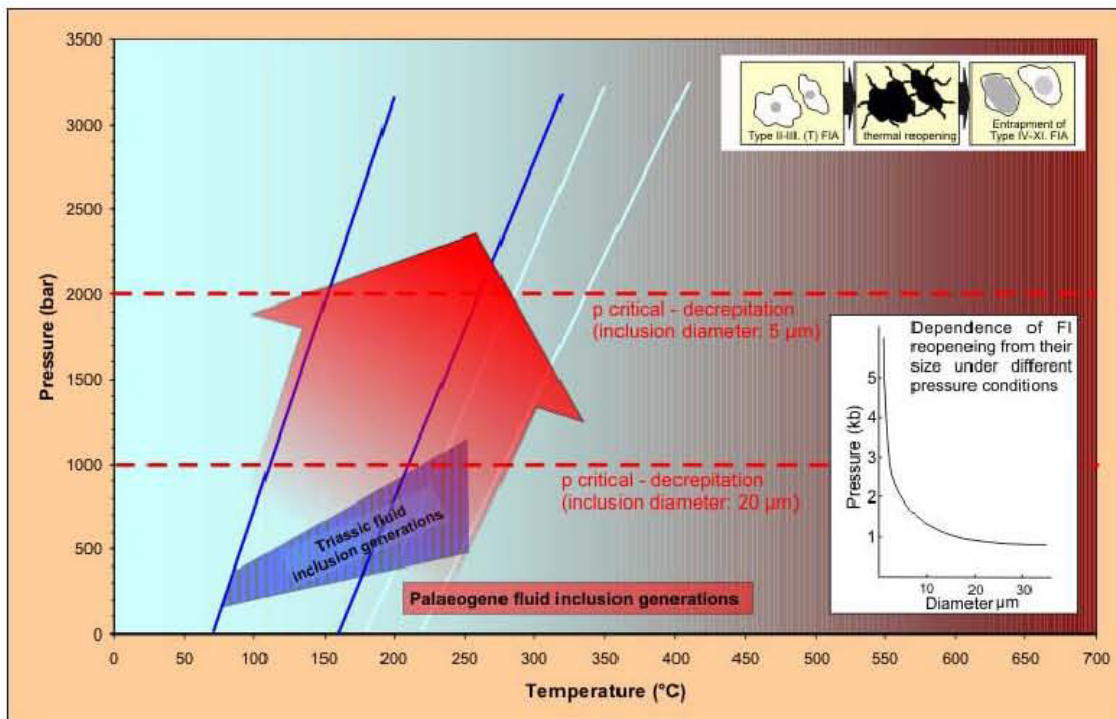


Figure 35. Changes of p-T conditions in the Type II and III fluid inclusions, on the effect of the Palaeogene upheating. p-T conditions will increase in the inclusions along their isochors. Above a certain critical pressure, inclusions will decrepitate as the structure of the quartz withstands maximum 2 kbar pressure. The decrepitated fluid inclusions will reopen and the FIP which will be sealed again by the Palaeogene fluids

5.3.2 Fracture formation and evolution: thermal reopening versus mechanical fracture formation

Several papers have been published recently, discussing the opening and reopening of open fracture systems and the statistical parameters related to them, such as fracture density, fracture length, orientation (HOXHA et al. 2005). Based on experimental tests two different

behaviours have been described: according to the first one, under a certain stress level, the properly oriented fractures will propagate in proportion with their length, meanwhile the number of fractures (fracture density) does not change (NEMAT-NASSER, 1985, 1988; KACHANOV 1982; HORII & NEMAT-NASSER, 1983). On the basis of the other theory, and examinations of natural rock samples, the number of fractures on a certain surface increases, meanwhile the average length of fractures stagnates (HOXHA & HOMAND 2000, HOMAND et al. 2000). Most recent investigations (HOXHA et al. 2005) confirmed both fracture propagation and formation of new fractures as well, however, according to the authors the nucleation of new cracks has higher importance in the formation of fracture network. Yet all of these observations were done on natural rocks with unknown tectonic history and focused mostly on the open fracture systems and the role of the temperature change in fracture reopening was not considered.

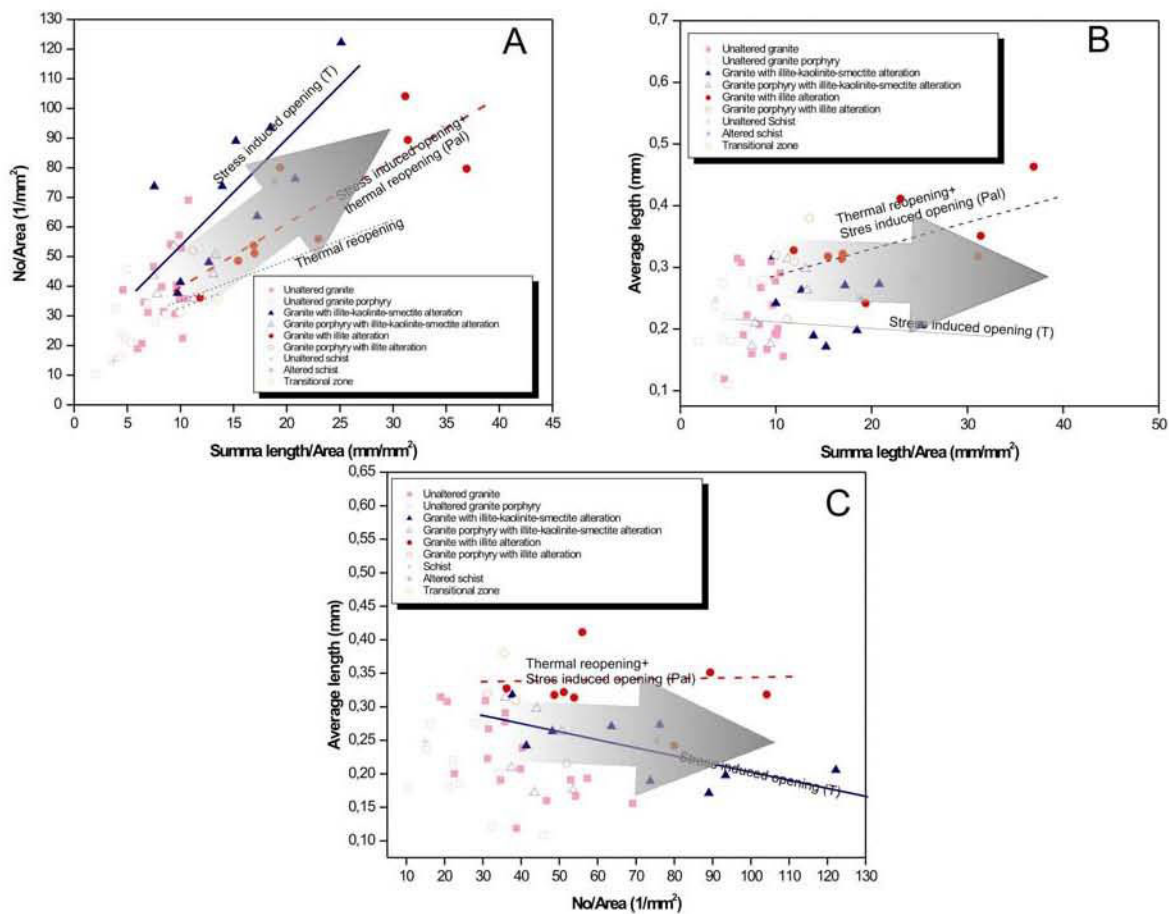


Figure 36. Comparison of the different statistical parameters of the FIP

To put the development and propagation of the fracture systems under scrutiny, it is interesting to compare the FIP properties (average length, length density, number density) in the two different, illitic Palaeogene (Nadap-Sukoró area and Pákozd-Székesfehérvár area), and in the Triassic, illite-kaolinite-smectite alteration zones (regionally present in the granite). We compared the FIP properties of both alteration types.

The length density (mm/mm^2) has the highest values in the alteration zones, independent from the age of the alteration (Table 7), therefore the only question we have is how to explain the following: there is an increasing number of cracks, or formation of low number but long fractures, or even both. To answer this question we analyzed the number density and the average length distributions in terms of the length density and compared the changes in the number of cracks in terms of the average FIP length.

On the length density-number density diagram (Figure 36A) two significantly different trends can be discerned. In the Triassic, illite-kaolinite-smectite alteration zones, the increase in the number of FIP is much more noticeable in comparison to the Palaeogene zones, which suggests that in these zones a higher number, but relatively short FIP were formed. Nevertheless, in the Palaeogene zones the increase of FIP density is more moderate, the increase in the length density moderate, which demonstrates the dominance of the increase in average lengths.

Looking at the relation between the length density and the average length (Figure 34B) we can obtain the following results: meanwhile the average length decrease in function of the length density towards to the Triassic alteration zones, the two parameters increase simultaneously in the Palaeogene alteration zones. From these correlations we can deduce that deformation in the Triassic alteration zones led to the formation of numerous but short fractures (Figure 36B). One question still remains: what is responsible for the higher length density in the Palaeogene alteration zones: is it the propagation of the FIP solely or the formation of new fractures, too? According to Figure 36C, in function of the number density average length does not change in the Palaeogene zones. It reflects that the theoretical length rise is compensated by the formation of new and short fractures

The explanation for this phenomenon can be that E-W trending new FIP were formed with small length in the vicinity of the thermally propagated conjugate fracture system in the G4 tectonic phase. In the E-W direction, the fracture propagation was impossible because no pre-existing fractures existed, therefore they formed “mechanically”, clearly by the combined effect

of the pore fluid pressure and the current stress field. In conclusion, the complex effect of thermal and mechanical fracture formation is manifested in the Palaeogene alteration zones.

But how would the thermal affect influence the propagation of preexisting fractures and the statistical parameters if no new fractures were formed and only the thermal effect would lead to the fracture propagation? Three samples could give the answer, which are close to the Palaeogene alteration zones (100 m), in the illite-dickite alteration zones. At these locations the Palaeogene FIA-s are absent, but the homogenization temperatures of the Triassic Type II-III assemblages are not typical. Phase ratios are exactly 30% and the homogenization temperatures scatter in a very narrow range, between 220-240°C. It can be explained by the partial stretching and reequilibration of the Triassic FIA-s on the thermal effect of the Palaeogene magmatic activity.

Reequilibration of FI means little change in their volume. It depends on several factors (inclusion size, host mineral, shape of inclusion, fluid composition). In case of the quartz, reequilibration is principally dependent on the size of the inclusion. According to BODNAR (2003) to reequilibrate an inclusion in quartz with 20µm diameter at least 800 bar and to reequilibrate a 5 µm inclusion 2 kbar pressure is required.

Illite and dickite form together between 200-250°C, therefore the granite in these zones was heated up to this temperature at shallow level (14-300 bar pressure). In inclusions having homogenization temperature below 200°C (e.g. 180°C) heating up to 250°C the differential pressure will be above 1,3 kbar. This pressure is enough to reequilibrate inclusions having diameter above 5 µm. In comparison to the illite alteration zones the temperature was not high enough to reopen and refill the FIP.

During the reequilibration the fluid inclusions and the fractures stretched and modest fracture propagation might have taken place. All of the diagrams (Figure 36) suggest that meanwhile the number of fractures of these moderately propagated fractures remains standard or slightly decrease, the average length definitely increases in the high temperature (Palaeogene) alteration zones. Our assumption is that in the case of pure thermal propagation the number of fractures would decrease in terms of the rise of the average length through connection of individual short fractures: As the short fractures connect to each other, the length density and the average length increase, meanwhile the number density decreases.

In conclusion, two models of fracture formation and propagation can be distinguished: In the first case, formation of the Triassic microfracture system was only influenced by the pore fluid pressure and the acting stress field. Deformation of the rock resulted in formation of a relatively short, but high number of extensional fractures. In contrast – in the less affected parts of the granite – the FIP are slightly longer and the number of FIP is lower. An increasing number of fractures was shown by HOXHA et al. (2005) on the basis of experimental studies in two magnitude of fractures as well.

In the second case, the geometry of the Palaeogene fracture network was determined by the preexisting older Triassic FIP, and the change of the statistical parameters of the FIP were influenced by the thermal reopening and propagation. This process is the reverse of the stress field induced fracture formation discussed above. Fracture reopening and refilling on a thermal shock leads to the interconnection of pre-existing FIP resulting lower number but higher average length for the FIP. However, the exempt of the granite of the Velence Mts. has also shown that there is a possibility for formation of new fractures in function of the actual stress field in these rejuvenated, intensively fractured zones. Because the formation of this Palaeogene fracture system is only controlled by the fluid pressure, temperature and the stress field, the FIP statistical properties will be the same as in the case of the Triassic fracture system (high number and short FIP).

5.4 POST-PALAEOGENE STRUCTURAL EVENTS

The post-Palaeogene tectonic events (G6, G7) which were established in the andesite dikes and in the Palaeogene Volcanic Unit can be excellently correlated with the regional tectonic events discussed by MÁRTON & FODOR (2003). The tectonic phase and the related faults were regionally identified on the ALCAPA block and were connected to the Late Middle Miocene transpressional event of the Carpathian basin.

The identification of the timing of the G7 phase is difficult, but MÁRTON & FODOR (2003) published a similar tensional phase during the late Miocene on the basis of their measurements on the ALCAPA Unit.

5.5 STATISTICAL ANALYSIS OF THE FRACTURE SYSTEMS AT DIFFERENT SCALES: PRACTICAL APPLICABILITY

As it has been shown in this work the used methods are especially useful on the field of economic geology and regional geology. During the mineral exploration a common question is the extension and structural control of the mineralizing hydrothermal fluid circulation. To answer this question is often difficult lacking sufficient amount of outcrops or useful samples. This work has shown, that if the general characters of the hydrothermal system are known (e.g. fluid inclusion properties, clay mineral assemblage), the analysis of the healed microfracture systems yield an appropriate tool for delineation of fluid flow zones in crystalline rocks. The complex application of mineralogical, geochemical, fluid inclusion and structural data answered several open questions related to the evolution of the superimposing hydrothermal systems in the Velence Mts.

In HS-type epithermal mineralization often disseminated gold mineralization occurs. Since the PVU east from the Nadap-line is represented by HS-type hydrothermal centers on the surface, a relevant question could be the extension and physical-geochemical parameters of the Palaeogene fluid flow in the granite. This work has shown that the physical and chemical characters of the Palaeogene alterations are similar to the hydrothermal centers of the PVU, the alteration is local and did not effect important volumes of the granite. On the contrary, the Triassic fluid flow was a regional fluid flow event, therefore exploration for further vein type Pb-Zn deposits is perspective. The applied new methods during the investigation of the hydrothermal systems have confirmed that fluid flow events can be proven even at those places where it was earlier impossible with the old approaches. With the fail of the conventional vein type mineral deposits, similar non-visible mineral deposits appreciate more and more attention during modern mineral exploration.

Other fields of the application of the statistical analysis of the microfracture systems consider the deposition and safe storage of medium and high nuclear waste. One of the most favorable rock environment for these deposits are granites. However, even though the estimation or the calculation of the active porosity and permeability is relatively easy, the effect of fracture reopening on thermal or tectonical effect and the related increase in the porosity and permeability is unknown and is usually disregarded. This work has shown that fracture reopening on thermal

or tectonical effects may considerably increase the permeability of the rocks and therefore the analysis of healed fracture systems is crucial during the planning of a nuclear waste deposit.

The slow fail of the classical porous hydrocarbon deposits draws the attention of the geologists on the non-conventional deposits (e.g. hydrocarbon reservoirs in crystalline rocks). Exploitation from the above described low-permeable rocks is highly dependent on the effective porosity of the host rock. With the analysis of the microfracture system (OC) we obtain important information about the tectonic control of the active fissures. On the other hand fissural porosity can be increased by artificial rupture. Fracture formation (fracture density, orientation) during this process will be highly influenced by the healed microfractures, if they are present in the granite or gneiss.

6. SUMMARY

- ✚ In the Velence Mts., eight tectonic events can be distinguished. These events are related to the late Variscan and to the Alpine orogenic processes. The initial fracture system formed during the Variscan and Triassic magmatic and tectonic events. The formation and propagation of the younger fracture systems during the young Alpine tectonic phases were essentially determined by those older features.
- ✚ Variscan fluid flow has solely been identified in the eastern part (Nadap area) of the granite intrusion. It took place in a NW-SE oriented extensional stress field, which also determined the orientation of granite porphyry and aplite dikes.
- ✚ The Triassic fluid flow took place in a permutating stress field which is usually characteristic of ascending rock bodies. Regionally, the extensional stress field was NW-SE oriented, parallel with the Variscan one.
- ✚ In the Triassic fluid flow zones the characteristic clay mineral alteration assemblage is illite kaolinite-smectite clay mineral assemblage, which surrounds the quartz-fluorite-base metal veins. The first mineral phase was illite, which formed at 250°C, whereas the illite and smectite formed during the cooling of the hydrothermal system below 200°C.
- ✚ It has been documented that the quartz-fluorite-base metal veins formed during the Triassic fluid flow events in relation to the advanced stage of rifting in the Neotethyan system. Direct evidences are based on the K-Ar radiometric age dating. Indirect evidences are from the results of the regional fluid inclusion studies, mineralogical characteristics of argillic alteration zones and from the lead and sulphur isotope analysis.
- ✚ Formation of the quartz-fluorite-base metal veins terminated at 250°C and at 700-1000 bar pressure. Vein formation was a multi-phase process, increasing salinity of the ore forming fluids was attended by decreasing temperature.
- ✚ Bimodal distribution of the homogenization temperatures of the Triassic fluid inclusion assemblages confirms post-Triassic tectonic displacement between the two blocks of the granite.
- ✚ The fluid inclusion properties, lead and sulphure isotope values, K-Ar radiometric age of the quartz-fluorite-base metal veins of the Velence Granite are similar to the Alpine-type

epigenetic stratiform-stratabound Pb-Zn ore deposits located on the border of the Southern and Eastern Alps.

- ✚ According to the similarities of the deposits and geology in the Velence Mts; the Szabadbattyán area and the Karawanken, the original position of the Velence Mts and the Szabadbattyán area before the Palaeogene was in the close vicinity of Eisenkappel and Mesica.
- ✚ The Palaeogene magmatic-hydrothermal process also affected the eastern part (Nadap-Sukoró area) of the granite body. The Palaeogene fluid flow was confined to the zones of Palaeogene andesite dikes and stocks and some NE-SW trending structural zone, therefore it was a local fluid flow event.
- ✚ According to the new K-Ar radiometric age data the magmatic activity and fluid flow happened between 32-28 Ma (early-Oligocene).
- ✚ In the Palaeogene alteration zones, illite and illite-dickite are the characteristic clay mineral phases. The well crystallized illite with low smectite interstratifications indicates that for the Palaeogene fluids the minimum temperature was 250°C. The illite-dickite alteration indicates lower, 200-250°C temperature during the fluid mobilization.
- ✚ Three different Palaeogene fluid inclusion assemblages were distinguished in the rock forming quartz crystals of the granite which are analogous with the fluid inclusion assemblages described earlier, from the hydrothermal veins and from the Palaeogene Volcanic Unit.
- ✚ Palaeogene fluid inclusion assemblages appear only in the illite alteration zones in the fluid inclusion planes hosted by the rock forming quartz of the granite. Fluid inclusion assemblages record boiling parent fluids, thus salinities vary on a broad range. According to the homogenization temperatures, the minimum temperature of these fluids was between 240-250°C, in accordance with clay mineral thermometer. Locally, high temperature (up to 400-450°C) hydrothermal spots were also detected in the vicinity of the andesitic bodies. The fluid inclusion properties indicate shallow volcanic and subvolcanic levels.
- ✚ The quartz-barite vein close to Sukoró, which was earlier believed to be Variscan, was proven to be Palaeogene according to the new K-Ar radiometric age data and the fluid inclusion studies.

- ✚ Appearance of volcanic and subvolcanic level related Palaeogene fluid inclusion assemblages at the same level in the granite indicates syn-magmatic and syn-hydrothermal tectonic activity east from the granite body. The Sukoró area of the granite lifted up during the Palaeogene while the Palaeogene Volcanic Unit – on the eastern side of the Nadap line – subsided.
- ✚ Upheating of the Nadap area during the Palaeogene led to partial equilibration or total reopening and refilling of the Variscan and Triassic fluid inclusion assemblages.
- ✚ It has been confirmed that FIP orientation analysis has essential importance during the investigation of the tectonic analysis of the granite: Variscan NE-SW trending FIP evidently confirm the NW-SE extensional stress field in which they formed. FIP orientation analysis was essential in the recognition of the uplift of the granite during the Triassic fluid flow. The orientation of the Palaeogene FIP confirmed that the initial fracture system of the granite basically influence the formation of the younger fractures. Dating and understanding the evolution of the macroscopic fracture and fault systems was possible only by means of the FIP analysis.
- ✚ FIP were parallel with the syngenetic mineralized veins, OC are parallel with the open macrofractures in the same outcrop. Its theoretical importance is that the fracture systems are self similar at different scales. Its practical importance during exploration is that if we lack large outcrops even a small piece of rock might be enough to analyse the tectonic evolution of the crystalline rock.
- ✚ The number of fluid inclusion planes towards the main Triassic fluid flow channels increase in comparison to with the unaltered granite, whereas the average length decrease. As a result of these two phenomena the length density though increases in the Triassic alteration zones. Therefore the stress field influenced fracture evolution leads to increasing number of fractures.
- ✚ Due to the magmatic and hydrothermal heat shock in the transitional zones, where the Triassic fluid inclusions reequilibrated, FIP connected to each other. This process led to the decrease in the number of FIP and the increase of the summa length of FIP. Eventually, a more intensely connected and better developed fracture system formed with high length density. In the illitic Palaeogene alteration zones the heat shock led to the reopening of the elder Triassic fractures and their refilling by Palaeogene FI. However

refilling and reopening process was accompanied by formation of new fractures as well. The average length and the number densities increased, but due to the formation of the new and short fractures the rise in the average length was not characteristic. As a consequence thermal reopening leads to a well-connected fracture system, providing excellent fluid channels for the hydrothermal fluids.

- ✚ The high fracture density areas indicate the main fluid flow channels during the period of the Palaeogene fluid mobilization. The most permeable zones and the main structural zones – mapped on the field – overlap with each other. From a practical point of view it can be very important when the mapping conditions on the field are insufficient and only some small rock chips are at hand.

7. ACKNOWLEDGEMENT

I have worked with a great number of people whose contribution in assorted ways to the research and the making of this thesis deserved special mention. It is a pleasure to convey my gratitude to them all in my humble acknowledgment.

In the first place I would like to express my gratitude to *Dr. Molnár Ferenc* for his exceptional supervision, advice, and guidance. He also encouraged me to work on this special topic and helped me to be able to conduct part of my research in France.

I gratefully acknowledge *Marc Lespinasse* for guiding me throughout my studies in France and helping me with his expertise and providing the facilities and equipment for the measurements. His crucial contribution with his professional advice to elaborate the findings and results made him a backbone of this research and so to this thesis.

Many thanks go in particular to *Emese Gáspár, Katalin Benkó, Zsófia Wácsek, András Prohászka, Tamás Pocsai, Krisztián Szentpéteri, János Borsodi, and Zsolt Hefner* for their contribution with the field work.

I gratefully thank *Bernadett Bajnóczi* for providing me with samples and sulphur isotope measurement data.

I am much indebted to *Kjell Billström* and the *Synthesys* Program for the lead isotope measurements.

Special thanks to *Zoltán Pécskay* for the K-Ar analysis.

It is a pleasure to acknowledge *Dr. Elemér Vass* for the infrared spectroscopy analysis.

It is a pleasure to pay tribute also to my colleagues at UHP1 and the Department of Mineralogy at the Faculty of Sciences of ELTE.

I owe *Rita Gyukics* for inspiring me in the last phase of my thesis work. Words fail to express how much she contributed with her cheerfulness and with being a special person.

And last but not least *my parents and my sister* deserve special mention for their inseparable support in my work and for standing by all the time.

This work was supported by the HNSF (OTKA) T 035095 grant to Ferenc Molnár; by the Balaton Project of the French-Hungarian Science and Technology Agreement supervised by Marc Lespinasse and F. Molnár and by the grant of the Synthesys program (SE TAF-3772).

8. REFERENCES

- ANGELIER J. (1986): Tectonic analysis of fault slip data sets. - *J. Geophys. Res.* 8. (B7), 5835-5848.
- ARRIBAS A. JR. AND TOSDAL R. M. (1994): Isotope composition of Pb in the ore deposits of the Betic Cordillera, Spain: Origin and relationship to other European deposits – *Economic Geology* Vol. 89. 1074-1093.
- BAGDASZARJAN G. P. (1989): Velencei-hegységi minták radioaktív koradatai – *Manuscript*, Geological Institute of Hungary.
- BAJNÓCZI B. (2003): Palaeogene hydrothermal processes in the Velence Mountains, Hungary. – *PhD Thesis. Department of Mineralogy, ELTE University, Budapest*, 116.
- BAJNÓCZI B., MOLNÁR F., MAEDA K., NAGY G., VENNEMANN T. (2002): Mineralogy and genesis of primary alunites from epithermal systems of Hungary – *Acta Geologica Hungarica*, Vol. 45/1., 101-118.
- BAKKER R. J. (2003): Package FLUIDS 1. Computer programs for analysis of fluid inclusion data and for modelling bulk fluid properties. *Chemical Geology*, vol. 194, 3-23.
- BALLA Z. (1985): The Carpathian loop and the Pannonian basin: a kinematic analysis. - *Geophys Trans.*, Vol. 30(4). 313-353.
- BALOGH, K. (1974): A kálium-argon földtani kormeghatározási módszer alkalmazási lehetőségei és korlátai. - *ATOMKI Közlemények*, 16/4. 373-387.
- BALOGH, K. (1975): Radiometrikus földtani kormeghatározási módszerek. - *Fizikai Szemle*, 25/11. 1-5.
- BALOGH, K., ÁRVA-SÓS, E. & BUDA, GY. (1983): Chronology of granitoid and metamorphic rocks of Transdanubia (Hungary). - *Annales Inst. Geol. Geofiz.*, 61, *Contribution of the 12 Congress of CBGA*, Bucuresti, *Metamorf. Magmat. Isot. Geol.* 359-364.
- BENEDEK K., PÉCSKAY Z., SZABÓ CS., JÓSVAI J., NÉMETH T. (2004): Palaeogene Igneous Rocks in the Zala Basin (Western Hungary): Link to the Palaeogene Magmatic Activity Along the Periadriatic Lineament. – *Geologica Carpathica*, Vol. 55, 1., 1-8.
- BENKÓ ZS. (2003): Hidrotermális áramlási rendszerek szerkezeti kontrollja a Velencei-hegység keleti részében repedésrendszerek, érhálózatok és fluidzárvány-síkok vizsgálata alapján. – *Manuscript Master theses (in Hungarian)*
- BENKÓ ZS., MOLNÁR F., LESPINASSE M. (2008): Fluidzárványsíkok és repedésrendszerek vizsgálatának alkalmazása granitoid kőzetek repedezettségének fejlődéstörténeti rekonstrukciójában I.: módszertani alapvetés és alkalmazás a Velencei-hegység fluidummobilizációs folyamataira. – *Földtani Közlöny* Vol. 138/2., 445-468.
- BOIRON, M.-C., CATHELINÉAU, M., BANKS, D.A., FOURCADE, S., AND VALLANCE J., (2002). Mixing of metamorphic and surficial fluids during the uplift of the Hercynian upper crust: consequences for gold deposition. - *Chemical Geology*, 194(1-3): 119-141.
- BODNAR R. J., VITYK M. O. (1994): Interpretation of microthermometric data for H₂O-NaCl fluid inclusions. *In: De Vivo. B., Frezzotti M. L. (Eds.): Fluid inclusions in minerals: Method*

and applications. *Short course of the working group (IMA) „Inclusions in Minerals”*, 117-130.

- BODNAR R. J. (2003): Introduction to aqueous-Electrolyte fluid inclusions. – In: *Fluid Inclusions, Analysis and Interpretation, Mineralogical Association of Canada Short Course Vol. 32*. 81-99.
- BÖJTÖSNÉ VARRÓK, K. (1967): A palaköpeny hidrotermális ércesedése a Velencei-hegység K-i részén. – *MÁFI Évi Jelentése az 1965. évről*, 499-505.
- BRACE W. F. (1984): Permeability of crystalline rocks: new in situ measurements. – *Journal of Geophysical Research Vol 89*. 4327-4330.
- BRIGO L., KOSTELKA L., OMENETTO P., SCHNEIDER H. J., SCHROLL E., SCHULZ O., ŠTRUCL I. (1977): Comparative reflections on four Alpine Pb-Zn deposits. In: Klemm DD, Schneider HJ (eds) *Time- and strata- bound ore deposits*. Springer, Berlin Heidelberg New York, pp 273–293
- BREVART O., DUPRÉ B. AND ALLÉGRE J. (1982): Metallogenic Provinces and the remobilization process studied by lead isotopes: Lead-Zinc Ore deposits from the Southern Massif Central, France – *Economic Geology* 77. 564-575.
- BUDA, GY. (1969): Genesis of granitoid rocks of the Mecsek and Velence Mountains on the basis of the investigation of the feldspars. - *Acta Geologica Academiae Scientiarum Hungaricae*, Vol. 13. 131-155.
- BUDA, GY. (1981): Genesis of the Hungarian granitoid rocks. - *Acta Geologica Academiae Scientiarum Hungaricae*, Vol. 24/2-4. 309-318.
- BUDA GY. (1985): Origin of collision-type Variscian granitoids in Hungary, West Carpathian and Central Bohemian Pluton.- *Unpublished Ph. D. Thesis, 95 p. (in Hungarian)*
- BUDA Gy. (1993): Enclaves and fayalite bearing pegmatitic „nests” in the upper part of the granite intrusion of the Velence Mts., Hungary. – *Geologica Carpathica*, 44, 3, 143-153.
- BUDA, GY. & NAGY, G. (1995): Some REE-bearing accessory minerals in two types of Variscan granitoids, Hungary. - *Geologica Carpathica*, Vol. 46/2. 67-78.
- BURRUSS, R.C (1981): Analysis of phase equilibria in C-O-H-S fluid inclusions. In: L.S. Hollister and M.L. Crawford (eds), *Fluid inclusions: application to petrology. Mineralogical Association of Canada Short Course Series v. 6*, 39-74.
- CASTELLARIN A., LUCCHINI F., ROSSI, P. L., SELLI L. SIMBOLI G. (1998): The Middle Triassic magmatic-tectonic arc development in the Southern Alps. – *Tectonophysics*, Vol. 146., 79-89.
- CATHELINÉAU M., LESPINASSE M., BOIRON M. C. (1994): Fluid Inclusion Planes: A geochemical and structural tool for the reconstruction of paleofluid migration. – In: *De Vivo B. Frezotti M.L. (Eds) Fluid inclusion in minerals: methods and applications. Short course of the working group of the IMA*. 271-283.
- COLLINS, P.L.F. (1979): Gas-hydrates in CO₂ bearing fluid inclusions and the use of freezing data for estimation of salinity. – *Economic Geology* Vol. 74. 1435-1444.

- COX S. F., KNACKSTEDT M. A., BRAUN J. (2001): Principles of structural control on permeability and fluid flow in hydrothermal systems. – *Reviews in Economic Geology* Vol. 14. 1-22.
- CUMMING G. L., RICHARDS, J. R. (1975): Ore lead isotope ratios in a continuously changing Earth. – *Erath and Planetary Science Letters* Vol. 28, 155-171.
- CSÁSZÁR G. (1994): Some notes concerning the correlation of the Jurassic and Lower Cretaceous Successions of the northern Karavanke and the Transdanubian Central Range. – *Jubiläumsschrift 20 Jahre Zusammenarbeit Österreich-Ungarn* Teil 2 403-408.
- CSÁSZÁR G., FÖZY I., VÖRÖS A. (2001): Preliminary results on Jurassic and Lower Cretaceous formations in the Karavanke Mountains and Lienz Dolomites Austria. – *Acta Geologica Hungarica*, Vol. 44/4. 439-462.
- CSÁSZÁR G. (2005): Regional Geology of Hungary and its surroundings I. Palaeozoic-Palaeogene. – *ELTE Eötvös Kiadó, Budapest*
- CSONTOS L. (1995): Tertiary tectonic evolution of the Intra-Carpathian area: a review. – *Acta Vulcanologica* 7, 1-13.
- CSONTOS L. (1995): Szerkezetföldtan. – *Egyetemi Jegyzet*. Eötvös Kiadó, Budapest
- CSONTOS L., NAGYMAROSY A., HORVÁTH F., KOVÁC M. (1992): Tertiary evolution of the Intra-Carpathian area: a model. – *Tectonophysics*, Vol. 199: 73-91.
- CSONTOS L., VÖRÖS A. (2004): Mesozoic plate tectonic reconstruction of the Carpathian region. – *Palaeogeography, Palaeoclimatology, Palaeoecology* Vol. 210. 1-56.
- CZAMANSKE, G.K., RYE, R.O. (1974): Experimentally determined sulfur isotope fractionations between sphalerite and galena in the temperature range 600C to 275C. - *Economic Geology*. Vol. 69, 17-25
- DARIDA-TICHY, M. (1987): Paleogene andesite volcanism and associated rock alteration (Velence Mountains, Hungary). - *Geologický Zborník-Geologica Carpathica*, Vol. 38/1. 19-34.
- DIAMOND L.W. (2003): Introduction to Gas – bearing Aqueous Fluid Inclusions *In: Fluid Inclusions, Analysis and Interpretation, Mineralogical Association of Canada Short Course* Vol. 32. 101-159.
- DOBOSI, G. & HORVÁTH, I. (1988): High- and low-pressure cognate clinopyroxenes from alkali lamprophyres of the Velence and Buda Mountains, Hungary. - *Neues Jahrbuch für Mineralogie, Abhandlungen*, Vol. 158/3. 241-256.
- DUDKO A. (1986a): A balatonfő-Velencei-hegység variszkuszi szerkezetalakulása. – *A Magyar Állami Földtani Intézet Jelentése 1984-évről*. 26-36.
- DUDKO A. (1988): A Balatonfő-Velencei terület szerkezetalakulása. – *Földtani Közlöny* 118, 3, 207-218.
- DUDKO, A. (1999): Geological map of pre-sarmatian surface of the Balatonfő-Velence area. *MÁFI, Budapest*.
- DUDKO, A., DARIDÁNÉ TICHY, M., MAJKUTH, T. & STOMFAI R. (1989): A kelet-velencei paleovulkán szerkezete. - *Általános Földtani Szemle*, Vol. 24. 135-148.

- DULAI, A., (1990): The Lower Sinemurian (Jurassic) brachiopod fauna of the Lókót Hill (Bakony Mts., Hungary). Preliminary results – *Ann. Hist.-Nat. Mus. Natl. Hung.* Vol. 82, 25– 37.
- DUNKL I. (1991): A fission track módszer használata a geokronológiai kérdések megoldásában. - Kandidátusi értekezés. *Manuscript*, Hungarian Academy of Sciences
- DUNKL I., HORVÁTH I., JÓZSA S. (2003): A Polgárdi Szár-hegy andezittelérei és szkarnos képződményei. 55-83. – *In: A Polgárdi-Szár hegy ásványai* Miskolc, 2003.
- EBERL D. D., SRODON J., LEE M., NADEAU P.H., NORTHROP R. H. (1987): Sericite from the Silverton Caldera, Colorado: Correlation among structure, composition, origin and particle thickness. – *American Mineralogist*, Vol. 72. 914-934.
- EBNER F., KOVÁCS S., SCÖNLAUB H. (1998): Stratigraphic and facial correlation of the Szendrő-Uppony Palaeozoic (NE Hungary) with the Carnic Alps-South Karawanken Mts. and Graz Palaeozoic (Southern Alps and Central Eastern Alps), some paleogeographic implications. – *Acta Geologica Hungarica*, Vol. 41/4. 355-388.
- ERDÉLYI, J. (1939): Der Baryt und Hämatit von Nadap. - *Földtani Közlöny*, Vol. 69/10-12., 290-296.
- ESSARAJ S., MOIRON M-C., CATHELINEAU M., FOURCADE S. (2001): Multistage deformation of Au-quartz veins (Laurieras, French Massif Central): evidence for late gold introduction from microstructural, isotopic, and fluid inclusion studies. – *Tectonophysics* Vol. 336 79-99.
- FAURE G. (1977): Principles of Isotope Geology. – John Wiley & Sons, New York
- FERRARA G. INNOCENTI F. (1974): Radiometric age evidences of a Triassic Thermal Event in the Southern Alps – *International Journal of Earth Sciences*. Vol. 63. 572-581.
- FÖLDVÁRI A. (1952): A Szabadbattyáni ólomérc és kövületes karbonátelőfordulás. (In Hungarian) – *MTA Műszaki Tud Oszt. Közl.* Vol. 5/1-2. 25-53
- FÖLDVÁRINÉ VOGL, M. (1947): Színképanalitikai molibdén-meghatározások a Velencei-hegység közeteiben. - *MÁFI Évi Jelentése, B. Beszámoló a vitáulésekről*, Vol. 9/1-6. 21-38.
- FÜLÖP J. (1990): Geology of Hungary, Paleozoic. – *Magyar Állami Földtani Intézet*. 131-186.
- GASZTONYI É., SZABÓ M. (1978): Jelentés a Velencei-hegység K-i részén 1975-76 évben végzett földtani térképezésről. – *Manuscript*. Országos Földtani és Geofizikai Adattár, Budapest.
- GAUTHIER B. D. M., FRANSEN R.C.W.M., DREI S. (2000): Fracture networks on Rotliegend gas reservoirs of the Dutch offshore: implications for reservoir behaviour. – *Netherlands Journal of Geosciences* Vol. 79. 45-57.
- GÉCZY, B. (1984): Provincialism of Jurassic ammonites: examples from Hungarian faunas. - *Acta Geologica Hungarica* Vol. 27 (3– 4), 379–389.
- GILLESPIE P., JOHNSTON J. D., LORIGA M. A., MCCAFFREY K. J. W., WATTHEYSON J. (1999): Influences of layering on vein systematics inline samples. - *In: McCaffrey K. J. W., Lonergan L., Wilkinson J.: Fractures, fluid flow and mineralization, Geological Society Special Publication*, London, Vol.155. 35-56.

- GIESEMANN, A., JÄGER, H.-J., NORMANN, A. L., KROUSE, H. R. & BRAND, W. A. (1994): On-line sulfur-isotope determination using an elemental analyzer coupled to a mass spectrometer. - *Analytical Chemistry*, Vol. 66/18, 2816-2819.
- GILLESPIE P.A., Walsh J. J., Watterson J., Bonson C. G., Manzocchi T., (2001): Scaling relationships of joint and vein arrays from The Burren, Co. Clare, Ireland. - *Journal of Structural Geology* 23., 183-201.
- GOHKAHLE N. W. (1964): Közetszerkezeti vizsgálatok a Velencei-hegységi gránitban és kvarcfillitekben. - *Földtani Közlöny* Vol. 94. (2). 177-183.
- GOKHALE N. W. (1965): A Velencei-hegység gránit és metamorf kőzeteinek áványtani, kőzettani és közetszerkezeti vizsgálata. Kandidátusi értekezés. - *Manuscript*. A Magyar Tudományos Akadémia Adattára, Budapest.
- GRIFFITH, A. A. (1920): The phenomena of rupture and flow in solids. - *Phil. Trans. Royal Soc. London Ser.A*, Vol. 221, 163-197.
- GUEGUEN, Y. AND PALCIAUSKAS, V. (1992): Introduction à la Physique des Roches. - *Hermann, Paris*, 299.
- HAAS J. (2004): Geology of Hungary, Triassic – ELTE Eötvös Kiadó, Budapest
- HAAS J., KOVÁCS S., KRYSZTYN L., LEIN R. (1995): Significance of Late-Permian Triassic zones in terrane reconstructions in the Alpine-North Pannonian domain. - *Tectonophysics* Vol. 242. 19-40.
- HARRISON, T.M., ARMSTRONG, R.L., NAESER, C.W., AND HARAKAL, J.E., (1979): Geochronology and thermal history of the Coast Plutonic Complex, near Prince Rupert, British Columbia – *Canadian Journal of Earth Sciences*, Vol. 16., 400–410.
- HEDENQUIST, J. W. & LOWENSTERN, J. B. (1994): The role of magmas in the formation of hydrothermal ore deposits. - *Nature*, 370, pp. 519-527.
- HOORI, H., NEMAT-NASSER, S., (1983): Overall moduli of solids with microcracks: load-induced anisotropy - *Journal of the Mechanics and Physics of Solids* 31 (2), 155–171.
- HORVÁTH, I., ÓDOR L. (1984): Alkaline ultrabasic rocks and associated silicocarbonatites in the NE part of the Transdanubian Mts., Hungary. - *Mineralia Slovacia*, Vol. 16., 115-119.
- HORVÁTH, I., ÓDOR, L., DARIDÁNÉ TICHY, M., DUDKO, A. & Ó KOVÁCS, L. (1987): A Velencei hegység-Balatonfő környékének ércprognózisa. I. Ércprognózis. II. Vegyes ásványprognózis. III. Kutatási javaslatok. *Kézirat, MGSZ Adattár*, Budapest.
- HORVÁTH I., DARIDÁNÉ-TICHY M., DUDKO A., GYALOG L., ÓDOR L. (2004): Geology of the Velence Hills and the Balatonfő. - *Explanatory Book of the Geological Map of the Velence Hills.*, Geological Institute of Hungary.
- HOMAND, F., HOXHA, D., BELEM, T., PONS, M.N. (2000): Geometric analysis of damaged microcracking in granites. - *Mechanics of Materials* Vol. 32, 361–376.
- HOXHA, D., HOMAND, F. (2000): Microstructural approach in damage modeling. - *Mechanics of Materials* Vol. 32, 377– 387.
- HOXHA D., LESPINASSE M., SAUSSE J., HOMAND F. (2005): A microstructural study of natural and experimentally induced cracks in a granodiorite. - *Tectonophysics*, Vol. 395, 1-2, 99-112.

- JANTSKY B. (1957): Geology of the Velence Mts. *Geologica Hungarica. Series Geologica* 10, 166. (in Hungarian and in French).
- JANTSKY B. (1960): Szabadbattyáni metasomatikus ércesedés újabb vizsgálata (manuscript in Hungarian) – *MGSZ Adattár*, Budapest
- JÓZSA, S. (1983): Velencei-hegységi felszíni andezit kizettani-geokémiai vizsgálata. – *Master theses (in Hungarian)*, ELTE Kizettani és Geokémiai Tanszék, Budapest, 107 p.
- KACHANOV M. (1982): Microcrack model of rock inelasticity: Part II. Propagation of microcracks. – *Mechanics of Materials* 1, 29–41.
- KASZANITZKY, F. (1959): A pátkai kőrákáshegyi érckutatás jelenlegi állása. - *Földtani Közlöny*, Vol. 89/2. 133-142.
- KÁZMÉR, M., KOVÁCS, S. (1985): Permian-Paleogene paleogeography along the eastern part of the Insubric-Periadriatic Lineament system: evidence for continental escape of the Bakony-Drauzug Unit. - *Acta Geologica Hungarica.*, 28/1-2. 617-648.
- KISS G., MOLNAR F., PALINKÁŠ L. A. (2008): Volcanic facies and hydrothermal processes in Triassic pillow basalts from the Darnó Unit, NE Hungary. – *Geologica Croatica*, in press.
- KISS J. (1951): A szabadbattyáni Szár-hegy földtani és ércgenetikai adatai. – *Földtani Közlöny* Vol. 81, 264-274.
- KISS, J. (1954): A Velencei-hegység É-i peremének hidrotermális ércesedése. - *MÁFI Évi Jelentése az 1953. évről*. 111-127.
- KISS J. (2003): Geology and ore mineralization of the Szár Hill, Polgárdi, Hungary – *Topographica Mineralogica Hungariae* Vol. 8. 29-54.
- KOCH S. (1943): A fejeér-megyei Szár hegy ólomérc előfordulása. – *Acta Mineralogica Petrographica*, Szeged 1. 1-40
- KOCH, S. (1985): Magyarország ásványai. 2., átdolgozott kiadás (Szerk.: Mezősi, J.), Akadémiai Kiadó, Budapest, 562. p.
- KÖPPEL V. (1983): Summary of Lead Isotope Data from Ore Deposits of the Eastern and Southern Alps: Some Metallogenic and Geotectonic Implications. – *Mineral Deposits of the Alpine Epoch in Europe*. Springer Verlag, Berlin-Heidelberg 1983.
- KÖPPEL V., SCHROLL E. (1988): Pb-isotope evidence for the origin of lead in stratabound Pb-Zn deposits in Triassic carbonates of the Eastern and Southern Alps. – *Mineralium Deposita* Vol. 23. 96-103.
- KRAHN L., BAUMANN A. (1996): Lead isotope systematics of epigenetic lead-zinc mineralization in the western part of the Rheinisches Schiefergebirge, Germany – *Mineral Deposita* Vol. 31, 225-237.
- KUBOVICS, I. (1958): A sukorói Meleghegy hidrotermális ércesedése. – *Földtani Közlöny*, Vol. 88, 299-314.
- KUHLEMANN J., VENNEMANN T., HERLEC U., ZEEH S., BECHSTÄDT T. (2001): Variations of sulfur isotopes, trace element compositions, and cathodoluminescence of Mississippi Valley type Pb-Zn ores from the Drau-Range, Eastern Alps (Slovenia-Austria): Implications for ore deposition on a regional versus micro scale. – *Economic Geology* Vol. 96. 1931-1941.

- LESPINASSE M., PECHER A. (1986): Microfracturing and regional stress field: a study of preferred orientations of fluid inclusion planes in granite from the Massif Central, France. – *Structural Geology* Vol. 8. (2) 169-180.
- LESPINASSE M., CATHELINÉAU M. (1990). Fluid percolation in a fault zone: a study of fluid inclusion planes in the St. Sylvertre granite, northwest Massiff Central,, France. – *Tectonophysics*, Vol. 184 pp. 173-187.
- LESPINASSE M. (1999): Are fluid inclusion planes useful in structural geology? – *Journal of Structural Geology* Vol. 21., 1237-1243.
- LESPINASSE M. (2002): Fluid Inclusion Planes and their application in economic geology, structural geology and environmental studies. – *ELTE TTK Departement of Minearalogy, short course*
- LESPINASSE M., DÉSIDÉES L., FRATCZAK P., PETROV V. (2005): Microfissural mapping of natural cracks in rocks: Implications for fluid transfers quantification in the crust. – *Chemical Geology* Vol. 223. 170-178.
- LI Y., LIU J. (2006) Calculation of sulfur isotope fractionation in sulfides. - *Geochimica et Cosmochimica Acta* Vol.70. 1789 - 1795.
- MANDELBROT B.B. (1983): The fractal geometry of nature. – Freeman, New York.
- MAURITZ, B. (1908a): Új zeolith lelethely. - *Földtani Közlöny*, Vol. 38. 190.
- MÁRTON E., FODOR L. (2003): Tertiary paleomagnetic results and structural analysis from the Transdanubian Range (Hungary): Rotational disintegration of the Alcapa unit. - *Tectonophysics*, Vol. 363 (2003) 201– 224.
- MIKÓ, L. (1964): A velencei-hegységi kutatás újabb földtani eredményei. - *Földtani Közlöny*, Vol. 94/1. 66-74.
- MOLNÁR F. (1996): Fluid inclusion characteristics of Variscan and Alpine metallogeny of the Velence Mts., W-Hungary. – *Plate Tectonic Aspects of the Alpine Metallogeny int he Carpatho-Balkan Region Proceedings of the Annual Meeting-Sofia, 1996 UNESCO-IGCP Project No. 356* Vol. 2., 29-44.
- MOLNÁR F. (1997): New data about the origin of molybdenite in the Velence Mts: mineralogical and fluid inclusion studies of the mineralization in the Retezi adit. - *Földtani Közlöny*, Vol. 127/1-2, 1-17. (in Hungarian).
- MOLNÁR F. (2004): Characteristic of Variscan and Palaeogene Fluid Mobilization and Ore Forming Processes int he Velence Mts., Hungary: A Comparative Fluid Inclusion Study. - *Acta Mineralogica-Petrographica, Szeged* 45/1. 55-63.
- MOLNÁR F., TÖRÖK K., JONES P. (1995): Crystallization conditions of pegmatites from the Velence Mts., Western Hungary, on the basis of thermobarometric studies. – *Acta Geologica Hungarica*, Vol. 38/1. 57-80.
- MOLNÁR F., SZAKÁLL S. (2003): Primary and secondary minerals of the Szabadbattyán ore deposit (W-Hungary). – *Minerals of the Szár Hill, Polgárdi, Hungary*, 45-175.
- NEMAT-NASSER S. (1988): A microcrack model of dilatancy in brittle materials. – *Journal of Applied Mechanics* 55, 24-35.

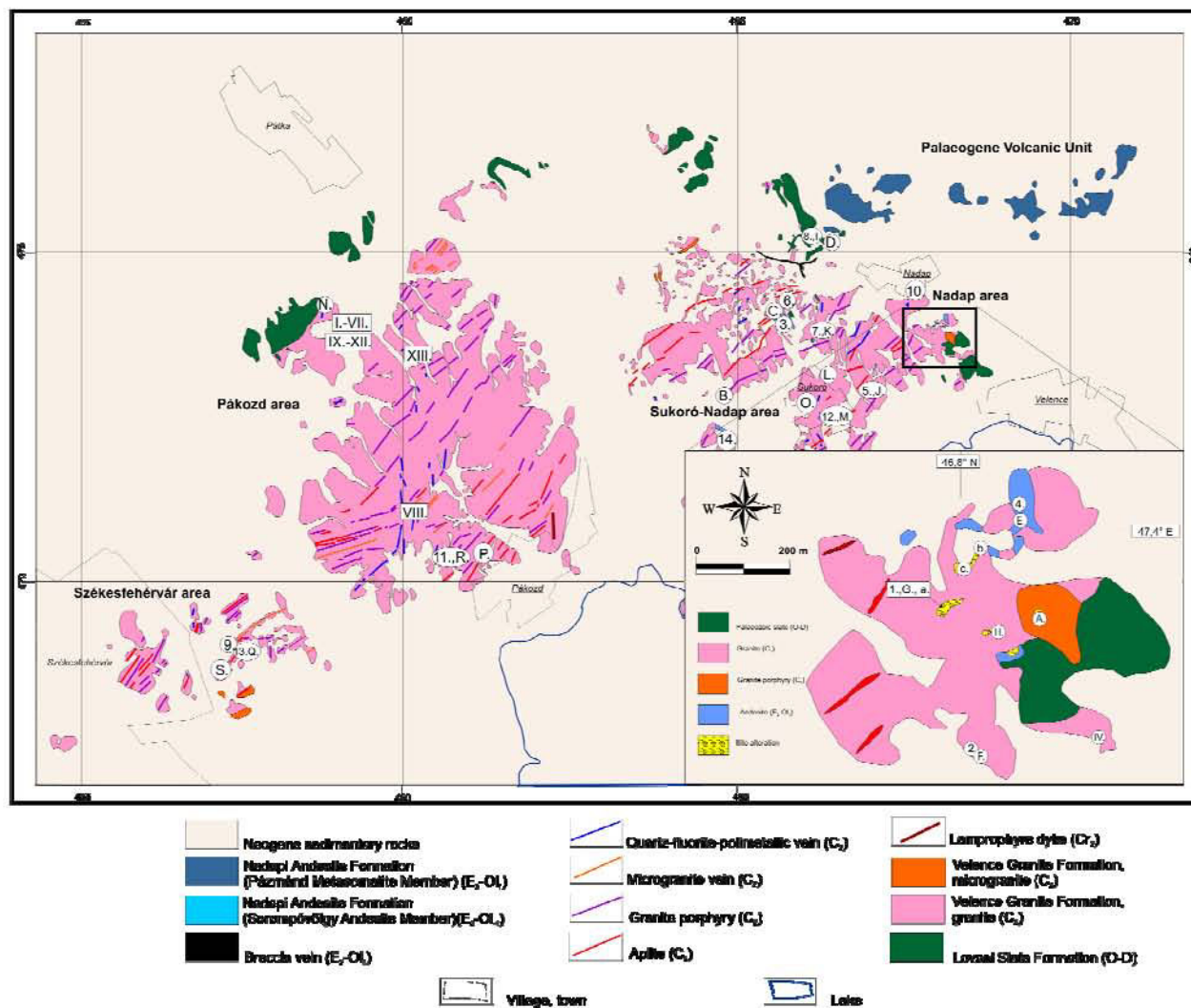
- NEMECZ E. (1963): Agyagásványok. – *Akadémiai Kiadó*, Budapest 1973.
- NEUGEBAUER H.-J., WOJDIT W.-D., WALLENER H. (1983): Uplift, volcanism and tectonics: evidence for mantle diapirs at the Rheinisch massif. In: Fuchs, K., Gehlen, K.V., Málzer, H., Murawski, H., Semmel, A. (eds.) Plateau uplift. Springer Berlin-Heidelberg-New York. 381-403
- NEX P.A.M., KINNAIRD J. A., OLIVER G. J.H. (2001): Petrology, geochemistry and uranium mineralisation of post-collisional magmatism around Goanikontes, Southern Central Zone, Damaran Orogen, Namibia.- *African Earth Sciences* Vol. 33. 481-502.
- OAKES C. S., BODNAR R. J. SIMONSON J. (1990): The system NaCl-CaCl₂-H₂O: I. The ice liquidus at 1 atm total pressure. – *Geochimica et Cosmochimica Acta* Vol. 54. 603-610.
- ÓDOR, L. (1985): A Velencei-hegységi kutatások néhány ércföldtani eredménye. - In: Gatter, I. (szerk.): *Ásványtan-geokémiai szemelvények* (A Magyarhoni Földtani Társulat 1984. november 8-9. közötti szegedi továbbképző tanfolyamának anyaga), MFT Ifjúsági Bizottsága és Ásványtan-Geokémiai Szakosztálya, Budapest, pp. 171-187.
- PALINKAS A. L., BERMANEC V., BOROJEVIC SOSTARIC S., KOLARJURKOVSEK, T., STRIMIC PALINKAS, S., MOLNAR F., & KNEWALD G. (2008): Volcanic facies analysis of a subaqueous basalt lava-flow complex at Hruškovec, NW Croatia - evidence of advanced rifting in the Tethyan domain. – *Journal of Volcanology and Geothermal Research*, in press.
- PAMIC J. J. (1984): Triassic magmatism of the Dinarides in Yugoslavia. – *Tectonophysics*, Vol. 109. 273-307.
- PAMIC J., BALEN D., and HERAK M., (2002a): Origin and geodynamic evolution of late palaeogene magmatic associations along the Periadriatic-Sava-Vardar magmatic belt. – *Geodynamica Acta* Vol 15. No 4. 209-231.
- PARRY W. T., JASUMBACK M. (2002): Clay Mineralogy of Phyllic and Intermediate Argillic Alteration at Bingham, Utah. – *Economic Geology* Vol. 97. 221-239.
- PECHER A., LESPINASSE M., LEROY J. (1985): Relations between fluid inclusion trails and regional stress field: a tool for fluid chronology - An example of an intragranitic uranium ore deposit (northwest Massif Central, France). – *Lithos*, Vol. 18. 229-237.
- PETROV V. A., LESPINASSE M., HAMMER J. (2008): Tectonodynamics of Fluid-Conducting Structural Elements and Migration of Radionuclides in Massifs of Crystalline Rocks. – *Geology of Ore Deposits*. Vol. 50. (2) 89-111.
- PINTÉR A. (1983): Gravitációs és földmágneses anomáliák értelmezése bonyolult tektonikájú területen (Velencei-hegység). – *Geofizikai Közlemények* Vol. 29. (4) 265-296.
- POROS Zs., MOLNÁR F., KOROKNAI B., LESPINASSE M., MAROS GY. BENKÓ ZS (2008): Application of studies on fluid inclusion planes and fracture systems in the reconstruction of fluid flow systems in granitoid rocks III: Results of studies in drillcores from the radioactive waste depository site at Bábaapáti (Üveghuta) - *Földtani Közlemények* 138/2, 445–468.

- PROHÁSZKA A. (2004): A Pázmánd Pd-2 fúrásban (Velencei-hegység) harántolt diorit intrúzió repedésrendszereinek szerepe a hidrotermális fluidummobilizációban. – *Master theses* (In Hungarian). 1-72.
- REYES A. G. (1990): Petrology of Philippine geothermal systems and the application of alteration mineralogy to their assesment. – *Journal of Volcanology and Geothermal Research* , 43, 279-309.
- RICHARDS, J.P. AND NOBLE, S.R. (1998): Application of radiogenic isotope systems to the timing and origin of hydrothermal processes - *Reviews in Economic Geology*. Vol. 9-10., 199-233.
- RICHTHOFEN (1860): Geognostische Beschreibung der Umgegend von Predazzo, Sant Cassian, und der Seisser Alpe in Süd Tyrol. – *Pertes, Gotha* 327.
- ROBERTS S., SANDERSON D.J., AND GUMIEL P. (1998): Fractal analysis of Sn-W mineralization from Central Iberia: Insights into the role of fracture connectivity in the formation of an ore deposit. – *Economic Geology* Vol. 93. 360-365
- ROEDDER E. (1984): Fluid Inclusions. – *Reviews in Mineralogy*, 12, 71.
- SCHAFARZIK, F. (1908): Ásványtani közlemények. 1. Molybdänit Nadapról (Fejér vármegye). 2. Fluorit Nadapról. - *Földtani Közlöny*, Vol. 38/6., 590-592.
- SCHUSTER R., SCHARBERT S., ABART R. (1995): Permo-Triassic crustal extension during opening of the Neotethyan ocean in the Austroalpine-South Alpine realm. – *Tübinger Geowissenschaftliche Arbeiten, Series A*, Vol. 52. 5 - 6. Abstracts of the 4th Workshop on Alpine Geological Studies, Tübingen 21-24 Sept. 1999
- SNOW D. T. (1969): Anisotropic permeability of fractured media. – *Water Resour. Res.* 5(6) 1273-1289.
- SRODON J. (1984): X-ray powder diffraction identification of illitic materials. – *Clays and Clay Minerals* Vol. 32.(5). 337-349.
- STACEY J. S., KRAMERS J. D. (1975): Approximation of terrestrial lead isotope evolution by a two-stage model. – *Earth and Planetary Science Letters*, Vol. 26. 207-221.
- SZABÓ B., BENKÓ ZS., MOLNÁR F., LESPINASSE M. (2008): Fluidzárványsíkok és repedésrendszerek vizsgálatának alkalmazása granitoid kőzetek repedezettségének fejlődéstörténeti rekonstrukciójában II.: A Mórágyi Gránit repedésrendszerei. – *Földtani Közlöny* 138/2, 445–468.
- TARI G. (1996): Neoalpine tectonics of the Danube Basin (NW Pannonian Basin, Hungary). – In: Ziegler P. A. and Horváth F. (eds): *Peri-Tethys Memoir 2: Structure and prospects of Alpine basins and forelands*. – Mem. Mus. Nat. Hist. Nat. 170 439-454.
- TÉL T., GRUIZ M. (2002): Kaotikus dinamika. Bevezetés a kaotikus dinamika világába a klasszikus mechanika jelenségein keresztül. – *Nemzeti Tankönyvkiadó Rt.*, Budapest 43-67.
- THOREZ J. (1976): Practical identification of clay minerals. – *Handbook for Teachers and students in clay mineralogy Editions G. Lelotte Dison*. 87.
- TOSDAL R. M., RICHARDS J. P. (2001): Magmatic and Structural Controls on the Development of Porphyry Cu±Mo±Au Deposits. – *Reviews in Economic Geology* Vol. 14. 157-181.

- TUTTLE O. F. (1949): Structural petrology of planes of liquid inclusions. – *The Journal of Geology* Vol. 57. (4). 331-356.
- TWISS R. J., MOORES E. M. (2007): Structural Geology. – *W. H. Freeman and Company, New York*.
- UHER, P., BROSKA, I. (1994): The Velence Mts granitic rocks: geochemistry, mineralogy and comparison to Variscan Western Carpathian granitoids. *Acta Geologica Hungarica*, 37/1-2, pp. 45-66.
- VALLANCE J., CATHELINEAU M., MARIGNAC C., BOIRON M-C., FOURCADE S., MARTINEAU F., FABRE C. (2001): Microfracturing and fluid mixing in granites: W-(Sn)ore deposition at Vaulry (NW French Massif Central). – *Tectonophysics* Vol. 336. 43-61.
- VAN DER MAREL H. W., BEUTELSPACHER H.(1976): Atlas of Infrared Spectroscopy of Clay Minerals and their Admixtures. – *Elsevier Scientific Publishing Company, New York*. 1-356.
- VENDL, A. (1914): A Velencei-hegység geológiai és petrográfiai viszonyai. - *Földtani Intézet Évkönyve*, Vol. 22/1. 1-170.
- VENDL A. (1928): A Somlyó és Szárhegy geológiája s egykori hévforrásai. - *Hidrológiai Közlöny* Vol. 4-6. 37-44.
- VÖRÖS, A. (1993): Jurassic microplate movements and brachiopod migrations in the western part of the Tethys. - *Palaeogeogr., Palaeoclimatol., Palaeoecol.* Vol. 100, 125– 145.
- WOLTER R., SCHNEIDER H.-J. (1985): Solerelikte in Erz und Nebengesteinen der Blei-Zink-Lagerstätte Bleiberg-Kreuth. - *Arch. F. Lagerst. Forsch. Geol. B.-A.* Vol. 6. 201-208
- ZAPPERI, S., PURUSATTAM, R., EUGENE STANLEY, H., VESPIGNANI, A. (1999): Analysis of damage clusters in fracture processes. - *Physica. A* 270, 57–62.
- ZARTMAN R. E., DOE B. R. (1981): Plumbotectonics-The Model. – *Tectonophysics*, Vol. 75, 135-162.
- ZEEH, S., KUHLEMANN, J., AND BECHSTÄDT, T., (1998): The classical Pb-Zn deposits of the eastern Alps (Austria/Slovenia) revisited: MVT deposits resulting from gravity driven fluid flow in the Alpine realm. – *Geologija*, 41, 257–273.
- ZHANG, Y.G. AND FRANTZ, J.D. (1987): Determination of the homogenization temperatures and supercritical fluids in the system NaCl-KCl-CaCl₂-H₂O using synthetic fluid inclusions.- *Chemical Geology*, Vol. 64., 335-350.

APPENDIX

Appendix 1. Sample localities



Appendix 1. Sample localities

Localities of the clay mineral samples

Smectite samples

1. Roadcut, hydrothermal breccia (Gécal-hill)
2. Eryedi quarry (Sukoró)
3. Berite vein (Sukoró)
4. Granite inclusion in andesite (Nadap)

Smectite-chlorite samples

5. Zsallirak pasturale (Sukoró)
6. Meleg Hill, hydrothermal breccia (Sukoró)
7. Meleg Hill shaft (Sukoró)
8. Lovasberény road - hydrothermal breccia (Nadap)

Smectite-karinite-amacrite samples

9. Berite vein (Székesszékhérvér)
10. Héromszögalmi pont (Nadap)
11. Sas Hill (Pákozd)
12. Andesite vein (Sukoró)
13. Kistalud quarry (Székesszékhérvér)
14. Mészeg Hill (Sukoró)

Localities of Pb and S isotope studies

Pb isotope samples

- I. BE0001 Pátka-Szűzvár
- II. BE0008 Pátka
- III. BE 303730 Pátka LE/O Shaft
- IV. BE51339 Részai quarry
- V. BE51041 Pátka
- VI. BE51059 Pátka
- VII. BE50691 Pátka
- VIII. S35 Pákozd, fluorite vein

S isotope samples

- IX. Va-17 Pátka
- X. Va-18 Pátka
- XI. Va-19 Pátka "Kőrisás hill, incline-shaft"
- XII. Va-20 Pátka "Kőrisás hill shaft-106"
- XIII. Va-21 Pátka "Szűzvár malom, fluorite mine"

Localities of fluid inclusion studies are indicated on the Appendix (2/a-2/e) printed by italic paragraphs

Localities of samples of K-Ar analysis

K-feldspar

- A. 6610 Nadap, Gécal Hill, pegmatite
- B. 6620 Sukoró, Rigó Hill

Andesite clites

- C. 6620 Sukoró, Meleg Hill berite vein (whole rock)
- D. 6621, 6619, 6624 Nadap, Lovasberény street
whole rock, plagioclase, amphibole

Smectite samples

- E. 6353, 6354 Nadap, Gécal Hill quarry, andesite
- F. 6355 Sukoró, Eryedi-quarry, granite
- G. 6623 Nadap, Gécal Hill, roadcut, granite
- H. 6352 Nadap, Gécal Hill, hydrothermal breccia

Smectite-chlorite samples

- I. 6622, 6618 Nadap, Lovasberény street, hydrothermal breccia
- J. 6618, 6358 Sukoró Zsallirak-pasturale
- K. 6617 Sukoró, Meleg Hill shaft
- L. Sukoró, south from the berite vein

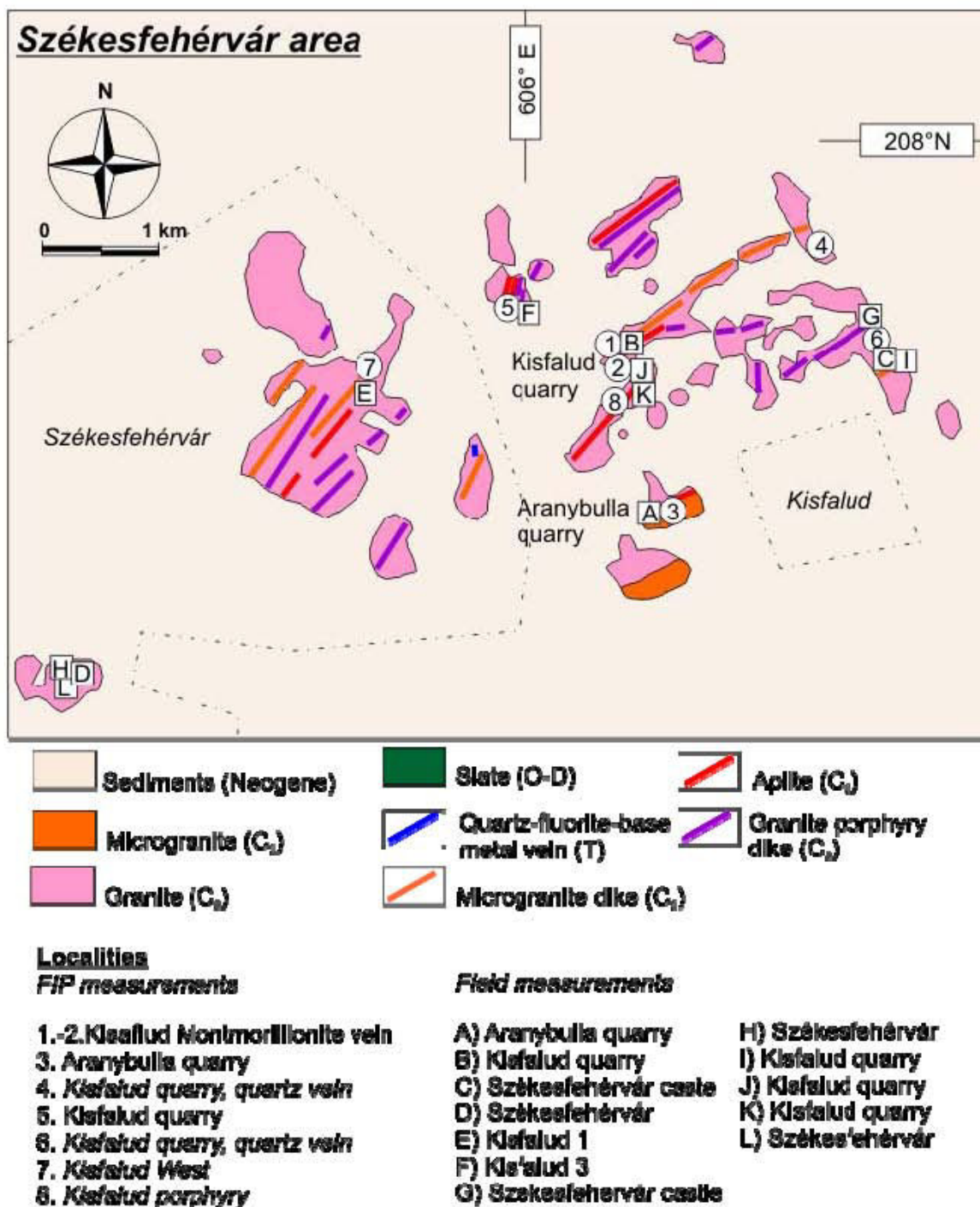
Smectite-berillite-amacrite samples

- M. 6613 Sukoró, protected quarry
- N. 6618 Pátka Malom-valley
- O. 6614 Sukoró, quartz-fluorite-base metal veins
- P. 6616 Pákozd, pegmatite quarry
- Q. 6611 Székesszékhérvér Kistalud quarry, next to the apite vein
- R. 6618 Pákozd, Big quarry
- S. 6354 Székesszékhérvér, Kistalud quarry

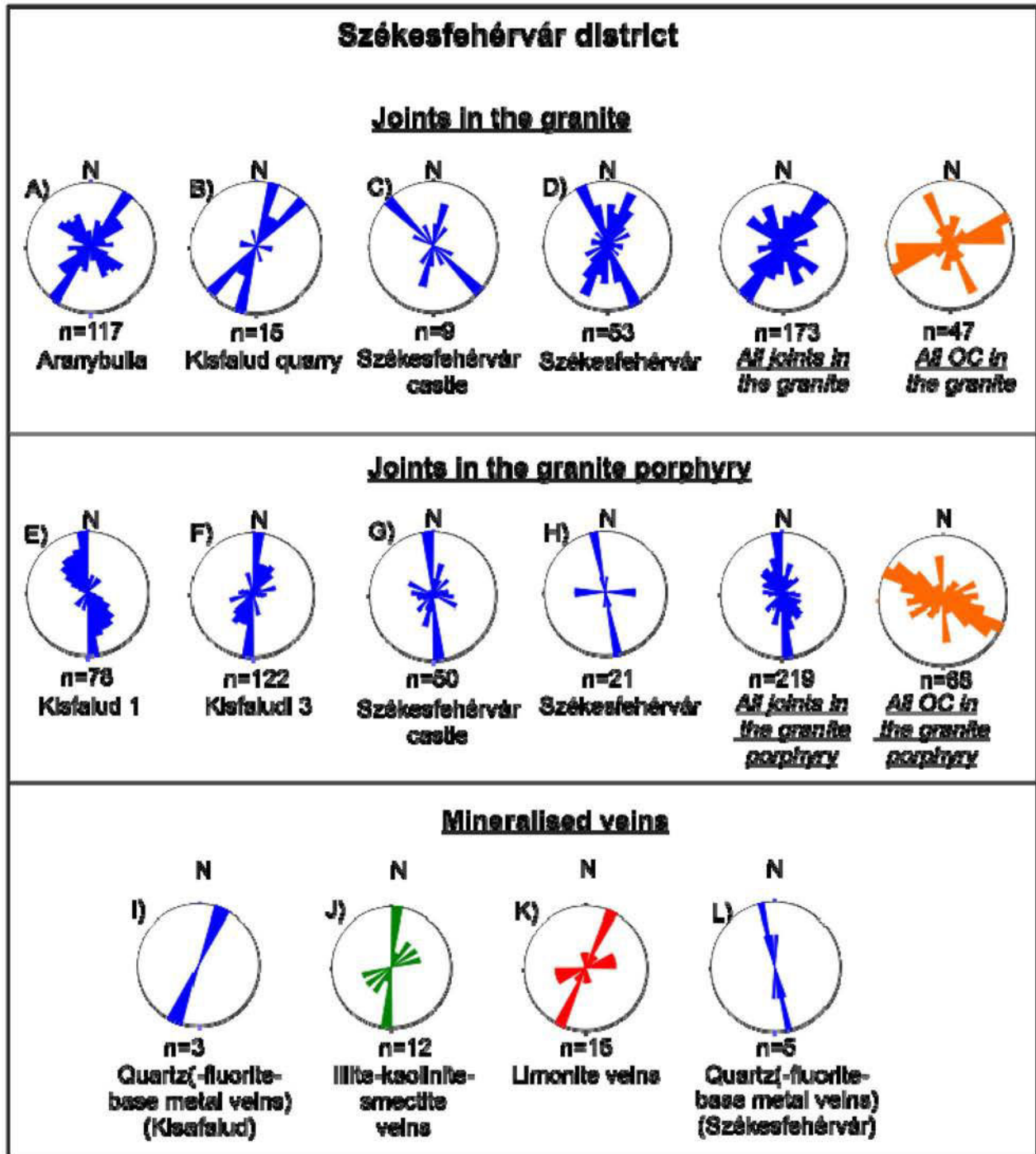
Sections of the fractal analysis studies

- a. Gécal Hill, roadcut
- b. Gécal Hill quarry, N-S section
- c. Gécal Hill quarry, E-W section

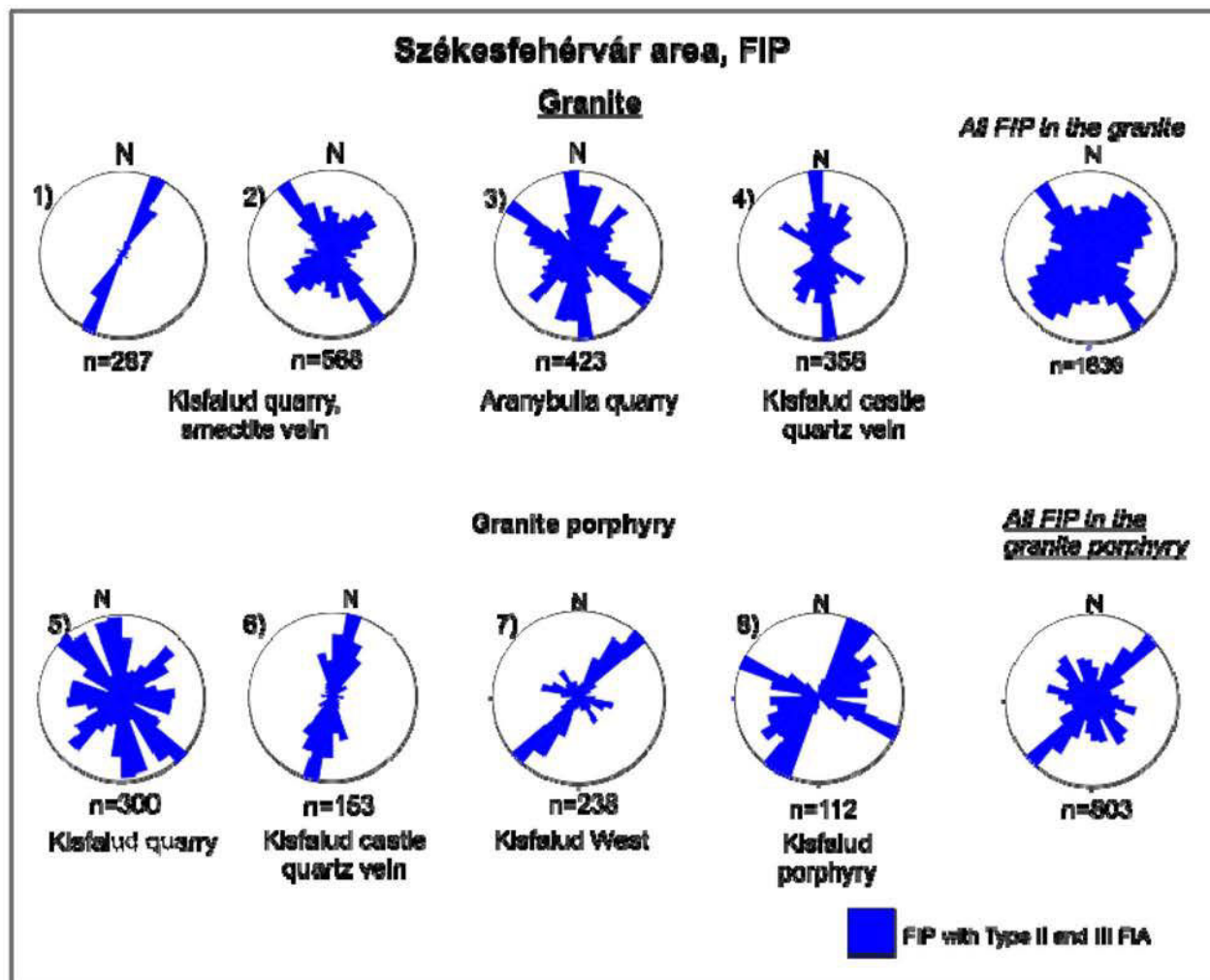
Appendix 2/A.



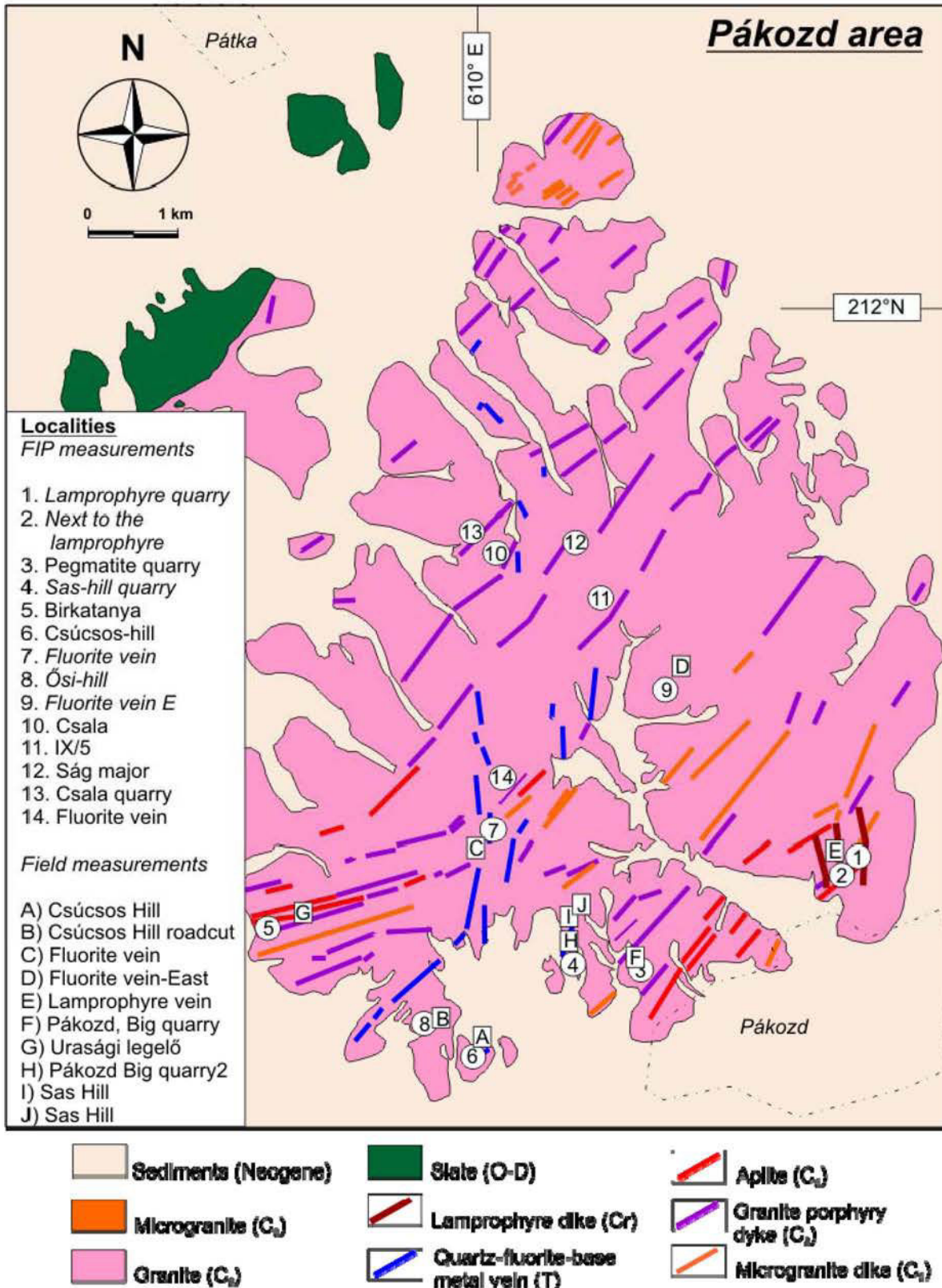
Appendix 2/B.



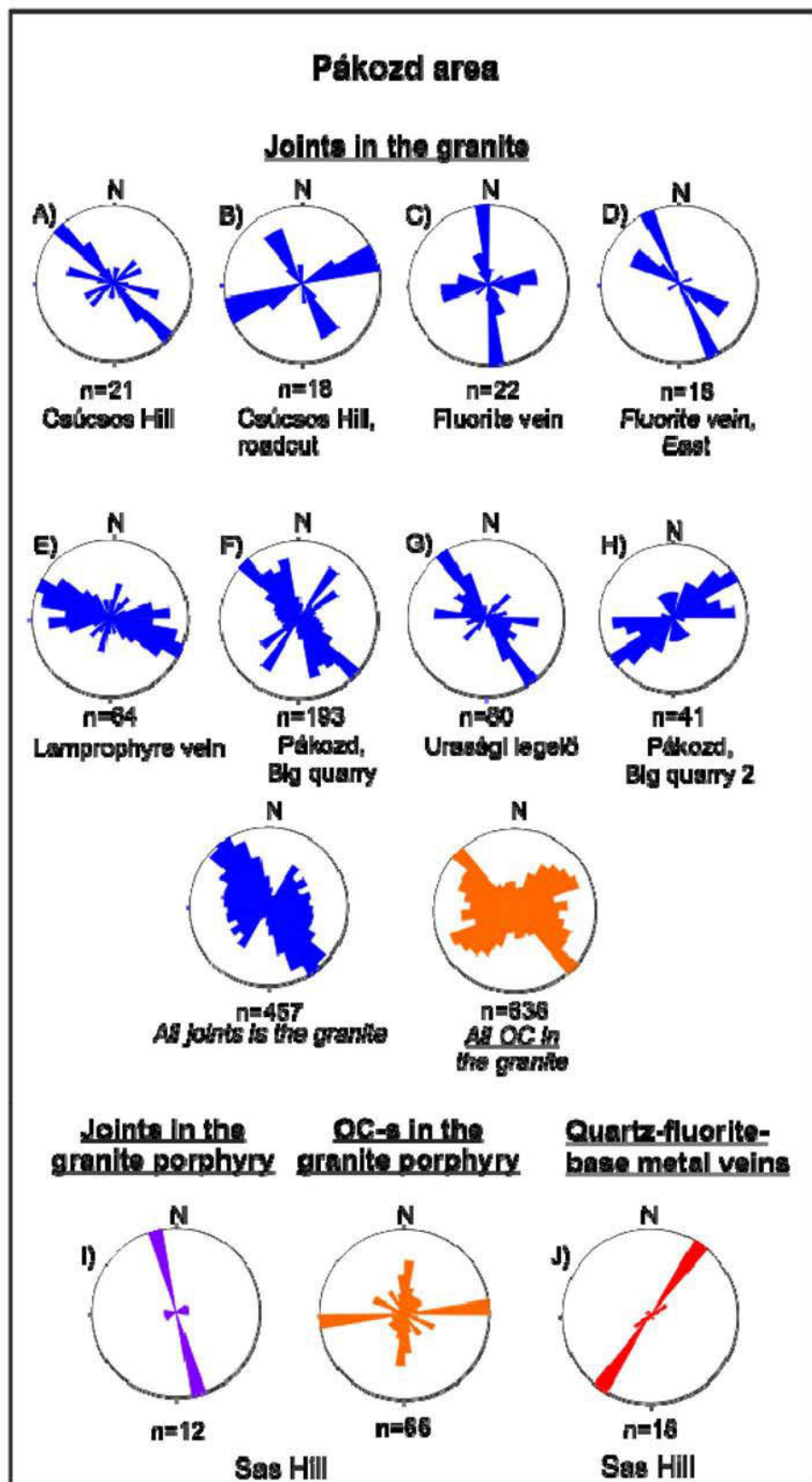
Appendix 2/C.



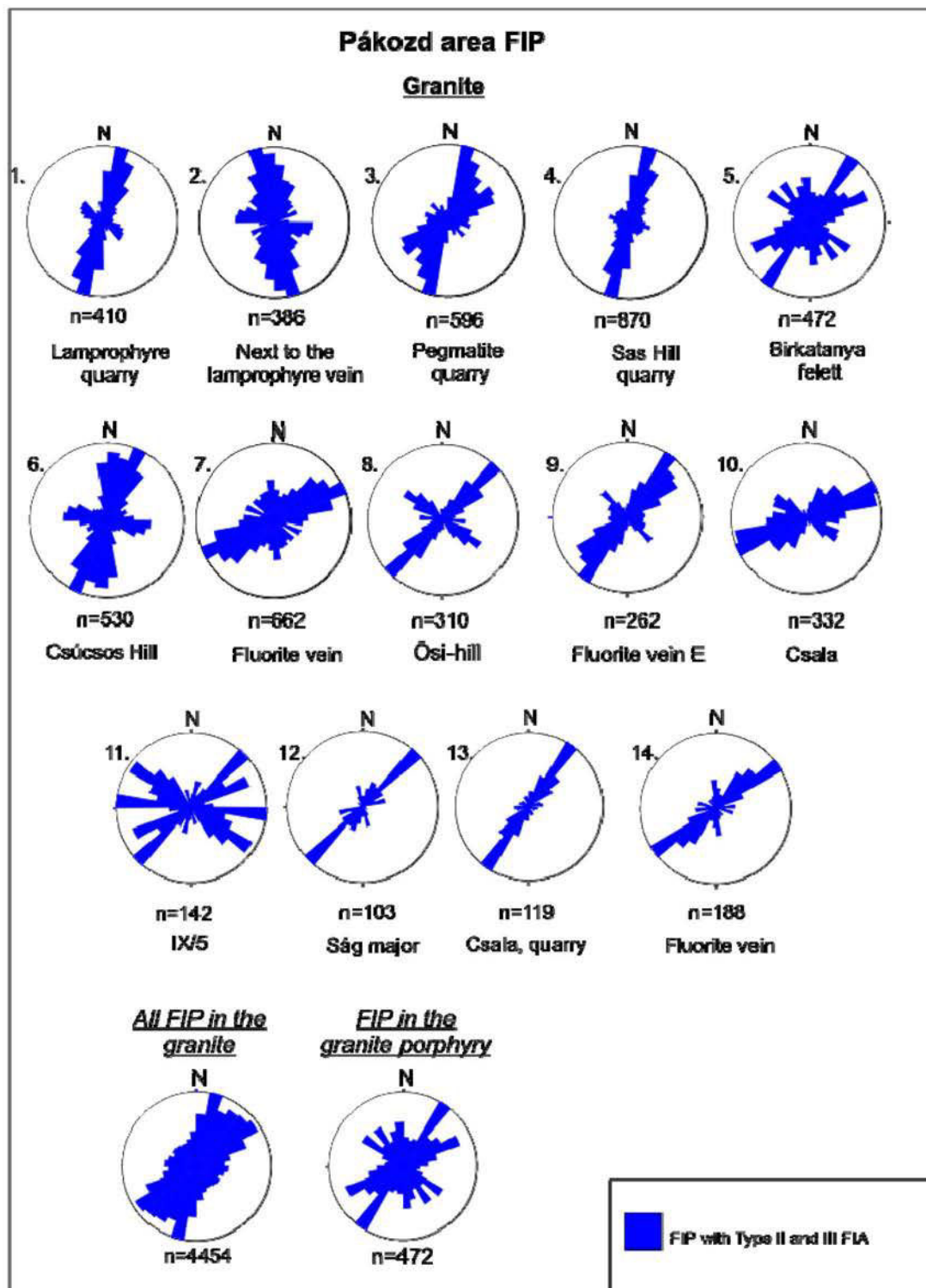
Appendix 3/A.



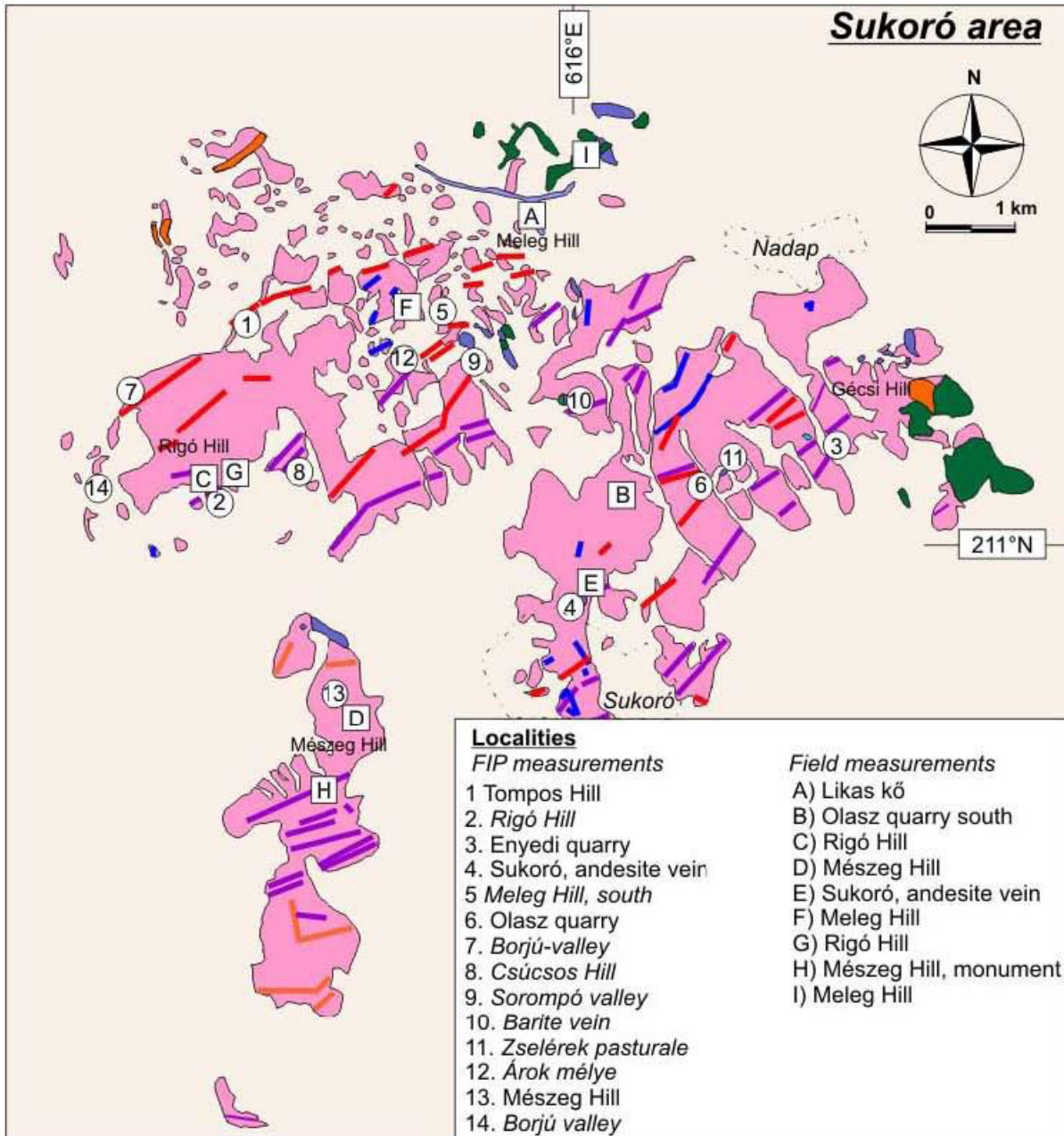
Appendix 3/B.



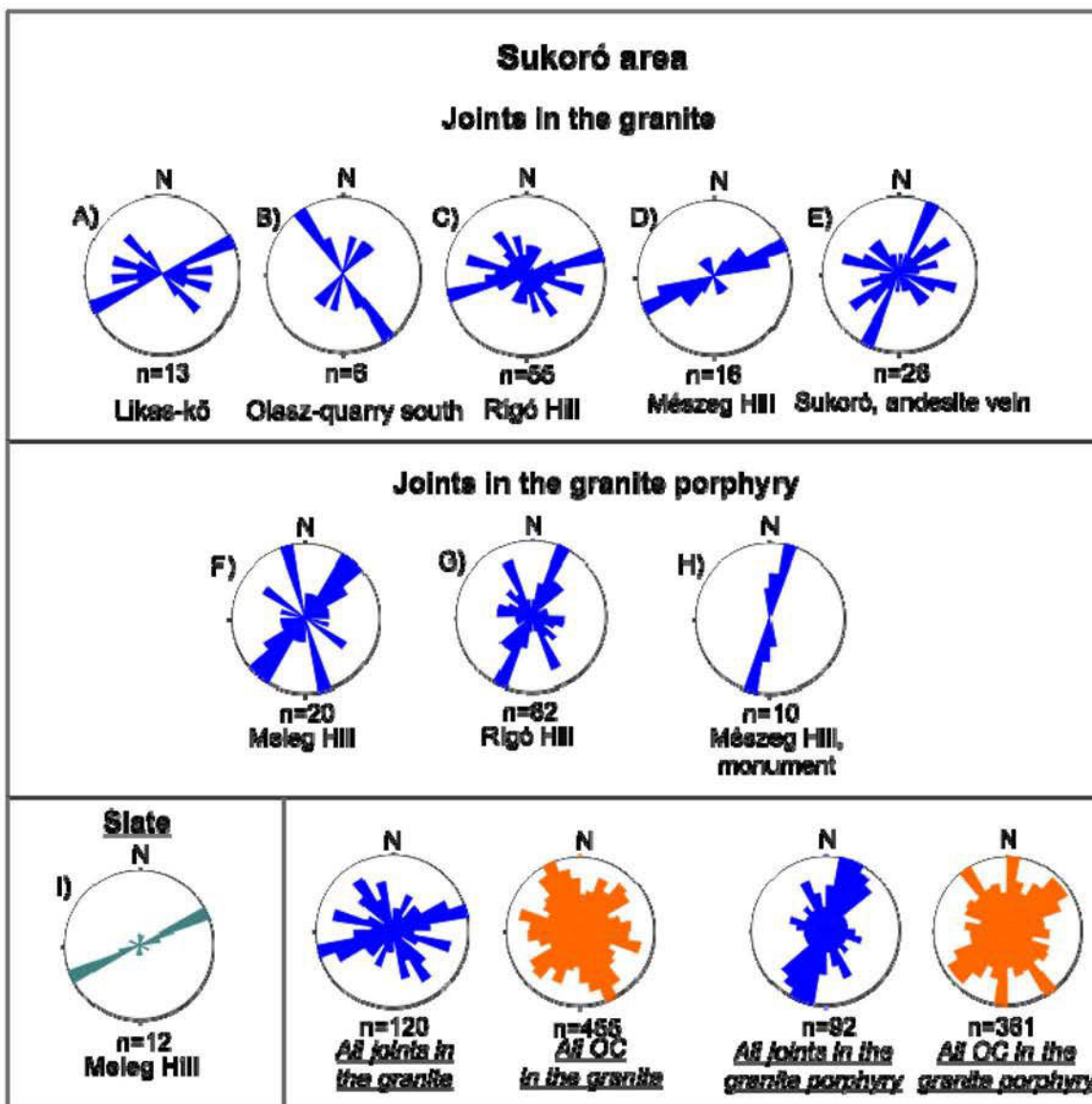
Appendix 3/C.



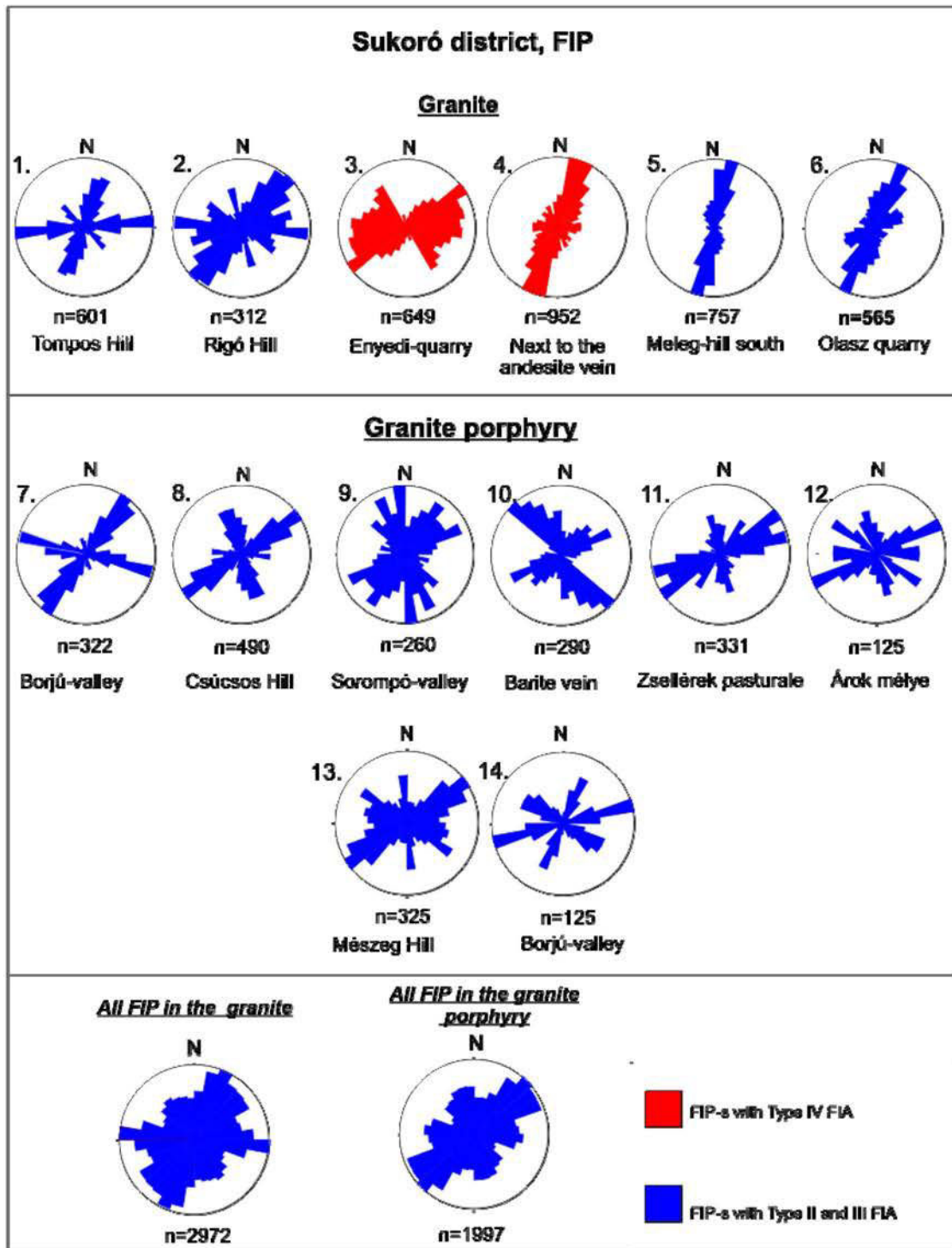
Appendix 4/A.



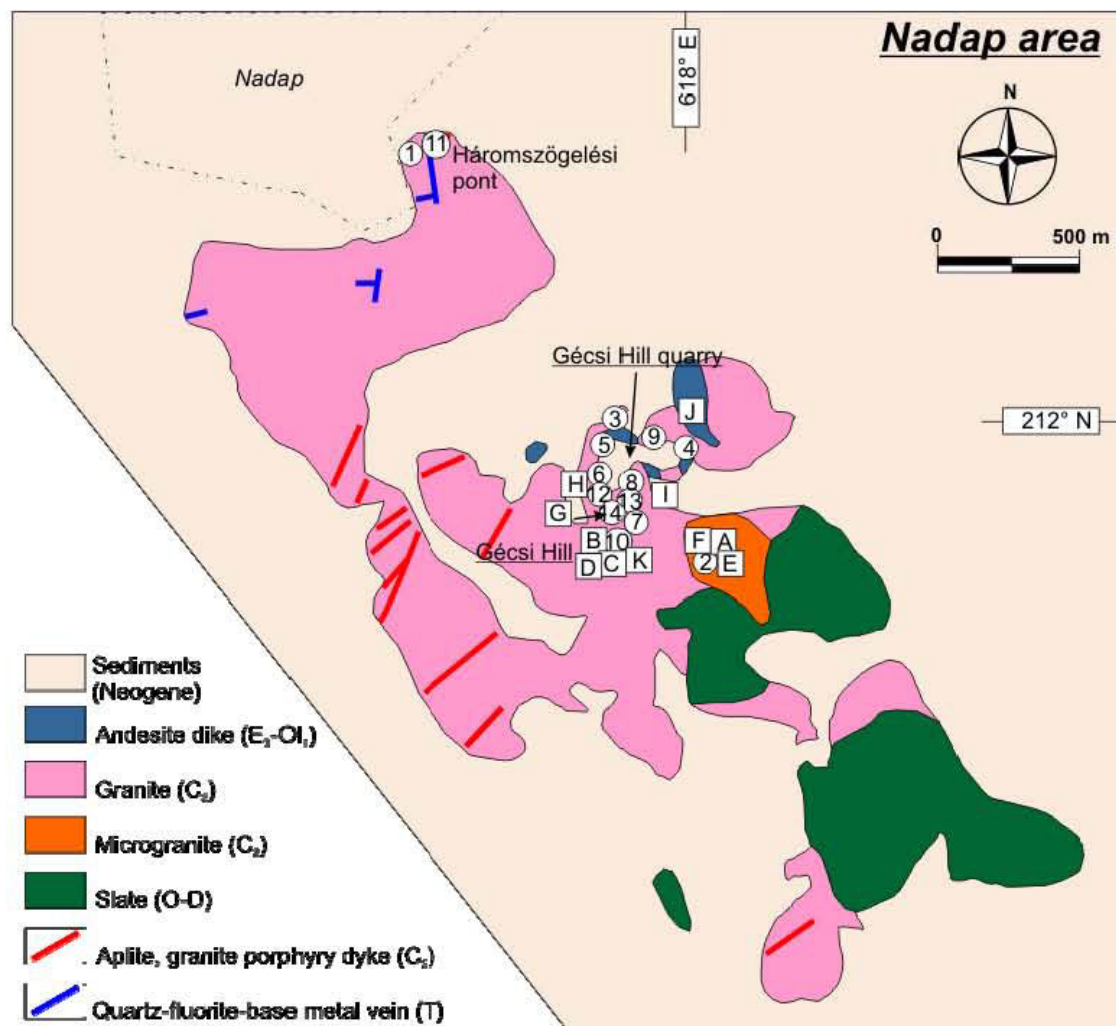
Appendix 4/B.



Appendix 4/C.



Appendix 5/A.

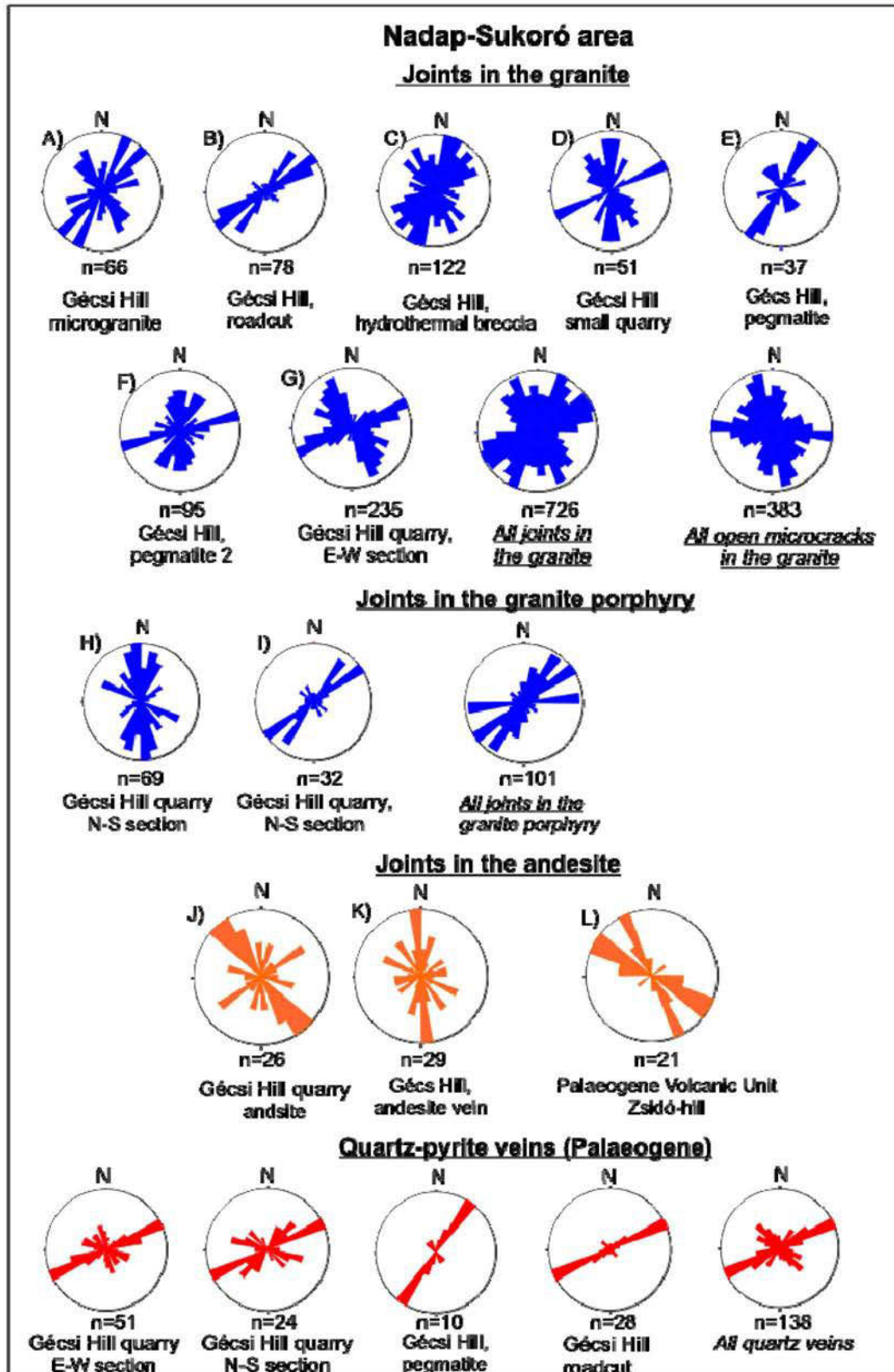
**Localities***FIP measurements*

1. Nadap, Háromszögelési pont
2. Gécsi Hill pegmatite
3. Gécsi Hill quarry entrance
4. Gécsi Hill quarry, end of illite zone
5. Gécsi Hill quarry, entrance
6. Gécsi Hill quarry, N-S section
7. Gécsi-Hill, granite with hematite alteration
8. Gécsi Hill quarry southern wall
9. Gécsi Hill quarry, valley
10. Gécsi Hill, roadcut
11. Nadap, háromszögelési pont
12. Gécsi Hill quarry, 1
13. Gécsi Hill quarry, 2
14. Gécsi Hill quarry, 5
15. Nadap, háromszögelési pont

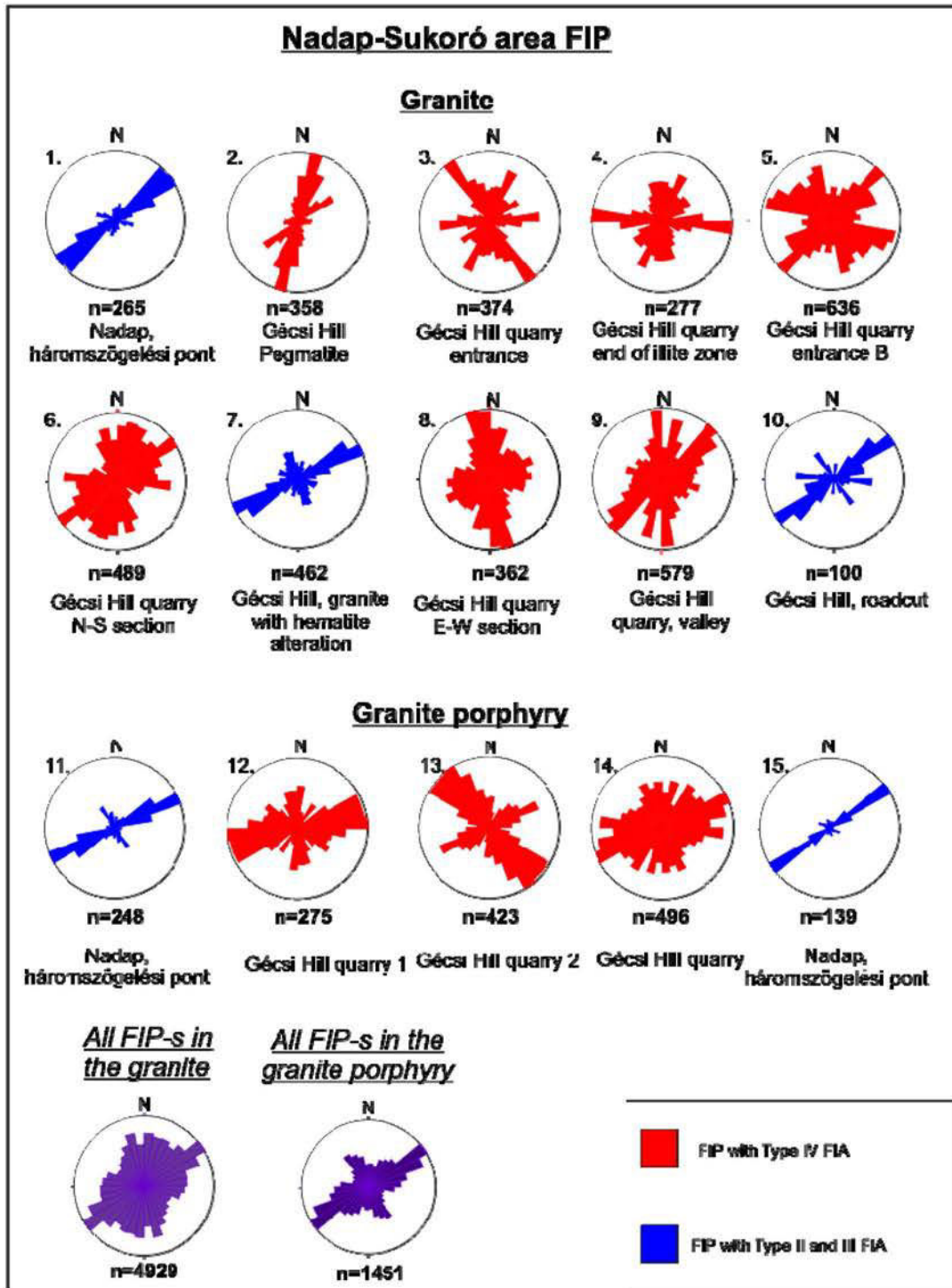
Field measurements

- A) Gécsi-hill, microgranite
- B) Gécsi-hill, roadcut
- C) Gécsi-hill, hydrothermal breccia
- D) Gécsi-hill, small quarry
- E) Gécsi-hill, pegmatite
- F) Gécsi-hill pegmatite2
- G) Gécsi Hill quarry, E-W section
- H) Gécsi Hill quarry, N-S section
- I) Gécsi Hill quarry, Eastern wall
- J) Gécsi Hill quarry, andesite
- K) Gécsi Hill andesite vein

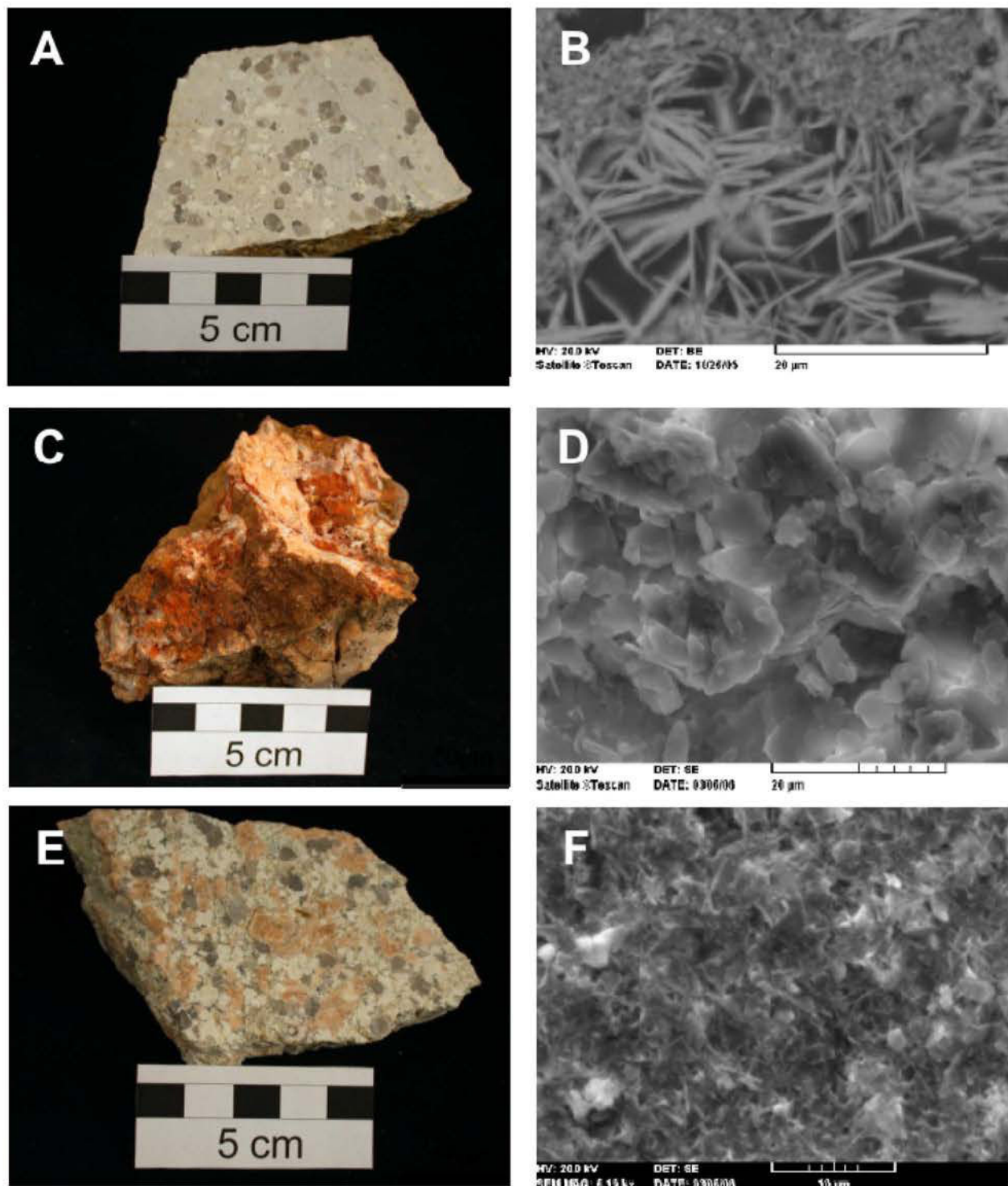
Appendix 5/B.



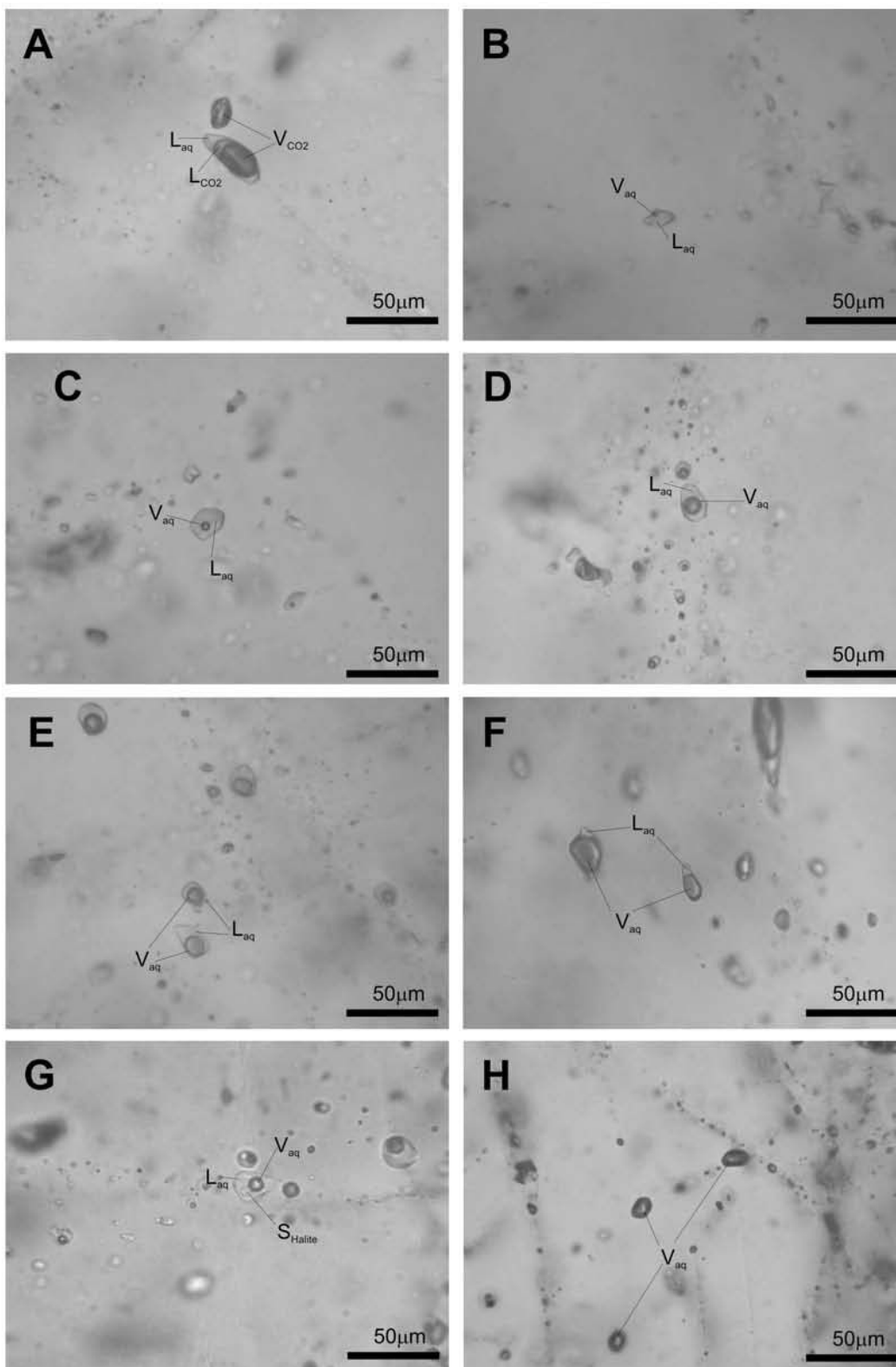
Appendix 5/C.



Photoplate 1.



Photoplate 2.



Photoplate 1.

- A. Granite with illite alteration. Except for the rock forming quartz all rock forming minerals are altered to whitish clay minerals
- B. Well crystallized illite crystals on SEM microphoto.
- C. Brecciated granite with yellowish-white illite-dickite alteration.
- D. SEM microphoto of separated illite-dickite mineral assemblage.
- E. Illite-kaolinite-smectite alteration of the granite. Plagioclase and biotite are altered to greenish-white clay minerals, K-feldspar are macroscopically fresh.
- F. SEM microphoto of the illite-kaolinite-smectite clay mineral assemblage. The size of the clay minerals is smaller than in the case of the illite and illite-dickite assemblages.

Photoplate 2.

- A. Inhomogeneously trapped secondary, Type I/a, three phase carbonic fluid inclusions in the rock forming quartz. The ratio of carbonic vapor, carbonic liquid and aqueous liquid is variable in the same assemblage. L_{CO_2} – carbonic liquid, V_{CO_2} – carbonic vapor, Laq – aqueous liquid
- B. Homogeneously trapped, secondary, Type II. and Type III., two phase aqueous liquid inclusions in rock forming quartz. Volume ratio of the vapor phase is 0.1. Pákozd area. Laq – aqueous liquid, Vaq – aqueous vapor.
- C. Homogeneously trapped, secondary, Type II. and Type III., two phase aqueous inclusions in rock forming quartz. Volume ratio of the vapor phase is 0.3 Nadap-Sukoró area. Laq – aqueous liquid, Vaq – aqueous vapor
- D. Inhomogeneously trapped, Type IV/a, secondary aqueous fluid inclusions with boiling texture in the rock forming quartz of the granite. The vapor/liquid ratio varies between 0.4 and 0.95. Nadap area. Laq – aqueous liquid, Vaq – aqueous vapor
- E. Inhomogeneously trapped, two phase, secondary Type IV/a. aqueous fluid inclusions with boiling texture in the rock forming quartz of the granite. The vapor/liquid ratio varies between 0.5 and 0.95. Nadap area. Laq – aqueous liquid, Vaq – aqueous vapor
- F. Inhomogeneously trapped, two phase, secondary Type IV/a. aqueous fluid inclusions with boiling texture in the rock forming quartz of the granite. The vapor/liquid ratio varies between 0.5 and 0.95. Nadap area. Laq – aqueous liquid, Vaq – aqueous vapor
- G. Inhomogeneously trapped, three phase, Type IV/c. aqueous, halite containing secondary fluid inclusions with boiling texture. The phase ratio of the halite is 0.1, the liquid/vapor ratio varies between 0.3-1. Nadap area. Laq – aqueous liquid, Vaq – aqueous vapor.
- H. Inhomogeneously trapped, Type IV almost only vapor containing fluid inclusions in the rock forming quartz, in fluid inclusion planes. Nadap area. Vaq – aqueous vapor